General Disclaimer

One or more of the Following Statements may affect this Document

- This document has been reproduced from the best copy furnished by the organizational source. It is being released in the interest of making available as much information as possible.

- This document may contain data, which exceeds the sheet parameters. It was furnished in this condition by the organizational source and is the best copy available.

- This document may contain tone-on-tone or color graphs, charts and/or pictures, which have been reproduced in black and white.

- This document is paginated as submitted by the original source.

- Portions of this document are not fully legible due to the historical nature of some of the material. However, it is the best reproduction available from the original submission.

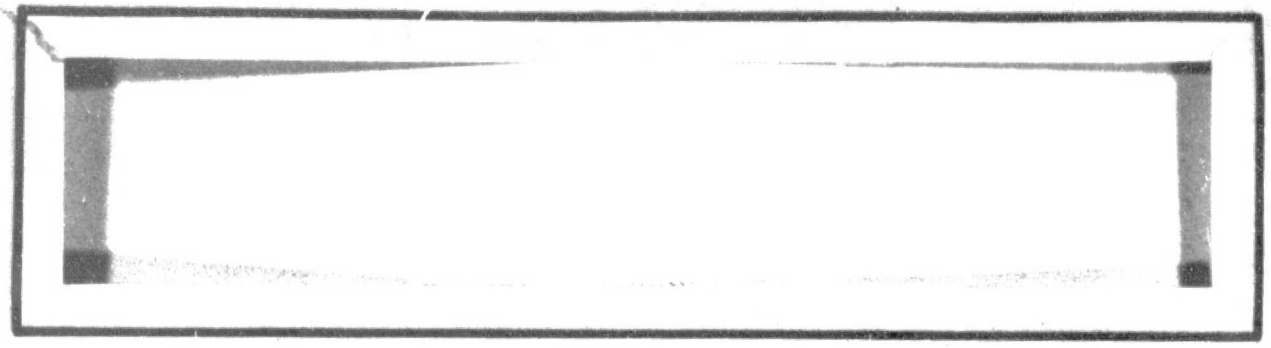

Axiomatix

(NASA-CR-160136) SHUTTLE PAYLOAD S-BAND COMMUNICATIONS STUDY Final Report (Axiomatix, Los Angeles, Calif.) 196 p HC A09/MF A01 CSCL 17E

N79-19190

Unclas
G3/32 16397

SHUTTLE PAYLOAD S-BAND COMMUNICATIONS STUDY

FINAL REPORT

Contract No. NAS 9-15240D

Prepared for

NASA Lyndon B. Johnson Space Center
Houston, Texas 77058

Prepared by

J. C. Springett

Contributions by

T. Nessibou
M. K. Simon
S. Udalov

Axiomatix
9841 Airport Boulevard, Suite 912
Los Angeles, California 90045

Axiomatix Report No. R7903-1
March 9, 1979

TABLE OF CONTENTS

LIST OF TABLES

LIST OF FIGURES

Page

1.0 EXECUTIVE SUMMARY

1.1 Purpose of Effort and Degree of Performance

The overall objectives of the work have been to identify, evaluate, and make recommendations concerning the functions and interfaces of those Orbiter avionic subsystems which are dedicated to, or play some part in, handling communication signals (telemetry and command) to/from payloads (spacecraft) that will be carried into orbit by the Shuttle. Some principal directions taken by the efforts have been:

(1) Analysis of the ability of the various avionic equipment to interface with and appropriately process payload signals.

(2) Development of criteria which will foster equipment compatibility with diverse types of payloads and signals.

(3) Study of operational procedures, especially those affecting signal acquisition.

(4) Trade-off analysis for end-to-end data link performance optimization.

(5) Identification of possible hardware design weaknesses which might degrade signal processing performance.

The contract Statement of Work identifies the following specific tasks that were to be performed:

> Task #1 - Evaluation of Orbiter Payload S-Band Communications Link Hardware Implementation
>
> Task #2 - Evaluation of Payload Data Interleaver (PDI) Implementation
>
> Task #3 - Test Definition and Analysis.

During the contract period (March 1978 through February 1979), probably 90% of the activity was directed toward various aspects of Task #1.

Because of the developing nature of the payload supporting communication system, certain tasks not specifically identified in the Statement of Work naturally grew out of various problems and issues. The most prominent of these may be summarized as follows.

> Task A - Specification of Payload Modulation Parameters - Axiomatix investigated the possible sets of carrier modulating waveforms as a function of data rates, subcarrier frequencies, and modulation indices.

Task B - Bent-Pipe Throughput Performance - Axiomatix analyzed the end-to-end (payload-to-ground) performance of the wideband (4.5 MHz) bent-pipe link.

Task C - Payload Nonstandard Modulation Restrictions - Axiomatix developed a set of rationales upon which a user's guidelines may be generated.

Task D - Minimization of PI False Lock - Axiomatix investigated methods by which the PI receiver may be made essentially immune to lock onto carrier sideband components.

Task E - Wideband Bent-Pipe Signal Drive Regulation Within the Ku-Band Signal Processor - Axiomatix designed a signal peak voltage regulating circuit which optimally establishes the Ku-band transmitter frequency modulation index.

In addition to the foregoing, Axiomatix also acted to disseminate system information regarding the Orbiter's ability to accommodate payload communications by providing a paper to the IEEE Transactions on Communications (special issue on Space Shuttle Communications and Tracking) and a second paper to the 1978 International Telemetering Conference (ITC).

1.2 General Approach to the Activity

Development of the payload avionic equipment was a new activity beginning in CY78. The general approach has been to work with cognizant NASA personnel and individuals at the principal prime contractor (Rockwell International) and equipment subcontractors (TRW and Hughes Aircraft Co.) to ascertain directions taken. A vital part of this activity has involved Axiomatix attendance and participation in the regular monthly program reviews and all special meetings. These latter gatherings usually involved detailed discussions on design and specification issues that surfaced at the regular monthly reviews.

Each month, Axiomatix prepared a Monthly Technical Report which contained a brief summary of all relevant technical activity, including design reviews, technical conferences, design and analysis efforts and results, critical problem areas, and a forecast of effort for the next monthly reporting period. Many of the Axiomatix in-process analysis activities and results were appended to these reports.

Apart from attendance at meetings, monthly reporting, and analysis activities, Axiomatix also acted in a technical consulting role to both NASA and the contractors. Most of the in-depth discussions were conducted at TRW or with various engineers over the phone.

The work performed under the subject contract was strongly interrelated to parallel efforts. Companion contract NAS 9-15514A, "Shuttle Orbiter S-Band Communications Equipment Design Evaluation," provided support to critique the design and assess the performance of the individual Orbiter S-band communication equipment. Additional related work was conducted under contract NAS 9-15604B which provided a handbook, entitled "Users' Handbook for Payload-Shuttle Data Communication." Also, the report "Guidelines for Choosing and Evaluating Payload RF Frequencies," produced under contract NAS 9-15604A, was related to this effort.

1.3 Contents of the Final Report

There are four sections following which address various aspects and details of the work.

Section 3.0 contains functional descriptions of the various S-band equipment and their payload link configurations. This section is primarily intended for orientation of the reader.

Section 4.0 summarizes the year history and highlights of important issues. Problem solutions are stated, and open or continuing actions are outlined.

In Section 5.0, specific supporting Axiomatix studies and analysis are presented. Some of this work is finished, while other parts are ongoing.

Finally, in Section 6.0, design and performance assessments of the payload links are provided.

1.4 Principal Activities, Studies, Results and Assessments

The overall payload communication system is still evolving. Direct payload interfacing avionic subsystems such as the PI and PSP are only in their conceptual design stages. Other hardware, such as that which makes up the Orbiter-ground S-band and Ku-band links is more fully developed, but is just entering its performance verification testing phase. Thus, it will be some time before all developmental problems are solved and reliable, well understood performance can be documented.

The following recounts the major issues with which Axiomatix had some degree of involvement and which appeared in the Monthly Technical Reports. Table 1 summarizes the major issues by addressing the nature of

Table 1. Major Payload System Issues Summary

Issue	Issue Nature	Effort Toward Resolution	Resolution
PI Receiver Wideband Output Regulation to KuSP	1. Incompatibility between PI and KuSP specifications 2. Proposed PI RMS AGC regulator does not optimize FM bent-pipe link performance	1. Assess bent-pipe performance using various types of regulation characteristics (Axiomatix) 2. Propose a signal peak regulation circuit (Axiomatix)	Change PI output to KuSP to be unregulated (no AGC). Place regulation circuit in KuSP (NASA and Rockwell)
PI Received Carrier Modulation Index Limits	1. Undetermined PI receiver performance for payload subcarrier modulation. index larger than 1 rad 2. Undetermined PI receiver performance with two or more payload subcarriers.	Complete parametric analysis of the PI carrier and subcarrier levels as a function of modulation index and waveform types (Axiomatix)	Results of analysis made known to TRW (Axiomatix)
PI Input Sensitivity Ranges	Exact requirement of Rockwell specification on three receiver sensitivity levels needs further definition	1. Meet the requirement by using RF signal level limiting (TRW) 2. Use manual signal level attenuators (TRW and NASA)	Manual attenuator approach selected. Preamplifier overload diodes as alternate under investigation (TRW)
PI Transmitter Phase Noise	1. Incomplete specification on transmitter phase noise with respect to DSN payloads 2. Possible excessive phase noise due to TRW frequency synthesizer design	1. Analysis of synthesizer phase noise (TRW) 2. Phase noise measurements of synthesizer breadboard (TRW)	In process. Preliminary measurements show phase noise to be within spec
PI Wideband Output HPF	The PI wideband output to all interfaces is AC coupled. For nonstandard modulations (e.g., NRZ and no subcarrier), excessive waveform distortion may result	1. Establishment of nonstandard NRZ lower data rate limits (Axiomatix) 2. Analysis of HPF effects (Axiomatix)	Current TRW design acceptable but close to marginal. Recommended changes suggested (Axiomatix)

Table 1. (Continued)

Issue	Issue Nature	Effort Toward Resolution	Resolution
PI Interference Susceptibility	Rockwell specification that the PI receiver should work with an out-of-band interference signal level as large as -25 dBm	Analysis showed that, with the expected receiver first LO noise characteristics, only a -65 dBm interference signal level can be tolerated (TRW and Axiomatix)	Specification amended to the -65 dBm signal level (Rockwell)
PI False Lock Susceptibility	1. PI receiver false lock discrimination with respect to standard and nonstandard payload modulations 2. Degree to which basic PI design should be augmented to include anti-false-lock circuits	1. Analysis of PI susceptibility to standard modulations (TRW) 2. Survey of anti-false lock methods (TRW and Axiomatix) 3. Analysis of strong signal phase demodulation discriminator (Axiomatix)	In process. Protection only against standard modulations is currently being considered. Methods still under review
PI Receiver Frequency Sweep Acquisition Strategy	1. Methods of initiating and stopping sweep not fully analyzed 2. Sweep range and rates may be inadequate for all postulated conditions	1. Sweep on and off strategy under study (Axiomatix). 2. Sweep range and rates are being reevaluated (TRW)	In process. Lower sweep rate for DSN payloads required. Wider PI receiver sweep range needed (Axiomatix)
PI RMS Regulator Performance and Wideband Interface to PSP and CIU	Current specification calls for 2V RMS and 6V p-p range above which amplitude clipping occurs.	Specification should be 2V RMS and 12V p-p above which amplitude clipping is O.K. (Axiomatix)	Recommendation to be made
PSP Data Transition Characteristics	1. Lack of consideration in PSP design for data formats 2. Unspecified transition requirements for minimum performance	1. Evolving TRW design has incorporated provisions for formats 2. Transition characteristics require definition by NASA/Rockwell	Use NASA Data Standards

Table 1. (Continued)

Issue	Issue Nature	Effort Toward Resolution	Resolution
PSP Performance Losses	Overall PSP degradation is specified at 1.5 dB. No partitioning between subcarrier loop and bit synchronizer is given	1. Analysis indicates bit synchronizer will contribute majority of loss (TRW) 2. Bit synchronizer performance will depend on data transition density (Axiomatix)	In process
Bent-Pipe Modulation Characteristics	No definition of bent-pipe modulations exists	1. Rationale for modulation restrictions developed (Axiomatix) 2. Some specific modulation types and forms suggested (Rockwell and NASA)	Further study required to reach agreement on characteristics and their impact on payload equipment
CIU Interfaces	CIU compatibility with PI and MDM interfaces	Specification and interface review identified incompatibilities (Axiomatix, NASA, SAMSO & TRW)	Appropriate agencies taking action
Possible Payload Receiver (Transponder) False Lock	When command modulation is "on" and the PI transmitter is frequency swept, the payload receiver could lock to a carrier sideband	Study of possible conditions (Axiomatix)	Recommendation that modulation be "off" during acquisition (Axiomatix)
Payload Communications Turn-Around Characteristics	Possible effects of turn-around phase noise	Analysis to predict performance available. PI phase noise characteristics need to be known	Assessment awaits TRW PI phase noise data

the issue and the effort expended by all concerned (TRW, Rockwell, NASA and Axiomatix) toward its resolution. Specifically, some of the problems involving the payload avionic equipment capabilities and operating parameters (especially for the PI) that have been given in-depth study under this contract are:

(1) PI Transmitter Sweep Rates
(2) PI Receiver Sweep Range
(3) PI Receiver Sweep Methodology
(4) PI Receiver Maximum Allowable SPE
(5) PI Transmitter Phase Noise
(6) PI Receiver Wideband Output Characteristics
(7) KuSP Bent-Pipe FM Drive Regulation
(8) PI Receiver Lock Detector Statistics.

Well over one-half of the activity has been concerned with the problems of PI receiver false lock. Rockwell's specification most generally states: "The receiver shall not lock-on to sidebands." It was found that TRW's initial conceptual design of the receiver was such that certain standard modulation conditions could produce false states of in-lock. Axiomatix determined that the problem was a function of lack of receiver out-of-lock IFA gain control and the setting of the lock detector threshold voltage according to a minimum operating point some 6 dB below that required by the Rockwell specification. Axiomatix therefore recommended use of a noncoherent receiver AGC during periods prior to acquisition. This recommendation was acted upon by TRW to the effect that false states of in-lock for standard modulations have been virtually eliminated.

A second aspect of the false lock problem concerns nonstandard modulations and the propensity of their characteristics to give rise to potential PI receiver false lock. It is clear that definitions of "nonstandard" payload modulation characteristics are required if the receiver design is to realistically preclude false lock to "bent-pipe" signals. Further, the methods for antisideband false lock require detailed analysis if such circuits are to be effectively incorporated into the PI receiver. Thus, trade-offs have been studied between augmented PI anti-false-lock capability and payload modulation restrictions.

Presently, the capability of the PI receiver to preclude false lock is based upon the operation of the PLL lock detector and its discrimination against inhibiting receiver sweep frequency acquisition with respect to small discrete sideband levels as compared to that of the true carrier component. Since the ability of the lock detector as an antisideband false lock device is limited due to its inherent characteristics, additional means must be incorporated if the lock detector performance alone proves inadequate. Suggestions for augmented anti-false-lock capability have all included some form of frequency spectrum discrimination which can be used to determine whether the receiver tracking loop is truly centered on the proper discrete carrier. No AFC loop techniques are currently being given serious consideration for implementation within the PI. Axiomatix has, however, begun detailed investigations of several discriminator antilock circuits; details appear in Section 5.0.

One method of precluding PI receiver false lock is to restrict the payload modulation such that carrier sideband components which give rise to the potential of false lock are not allowed. The task of generating such restrictions is not an easy one because: (1) theoretical acquisition performance of PLL receivers with respect to many of the possible modulation forms is unknown, and (2) there are many parameters that must be taken into consideration. However, Axiomatix has made an attempt to develop a rationale upon which a set of restrictions might be based. The rationale has, in turn, led to the generation of a set of user's guidelines and restrictions. Currently under review by all concerned, it is expected that the user's guidelines will eventually be adopted as the governing payload modulation restrictions for the PI.

The second major effort during the contract period has involved the bent-pipe and the interface between the PI and KuSP. The PI employs an RMS regulator as an AGC on the wideband demodulated signal, and Axiomatix analyzed the implications of using the RMS regulating loop for FM bent-pipe signals. Analysis which fully accounted for both noise sources in the Ku-band bent-pipe link model showed that a peak-type regulator would outperform the RMS-type regulator under all conditions and would provide a minimum overall link improvement of 1.1 dB and a maximum improvement of 9.4 dB for high data rate NRZ data. Axiomatix therefore recommended that the regulator be changed from an RMS type to a peak type.

Following several round-table technical discussions between NASA, Axiomatix and Rockwell personnel, it was concluded that any necessary signal waveform conditioning required to optimize the Ku-band FM bent-pipe link is properly a function of the KuSP rather than the PI. This conclusion was based primarily upon the fact that attached, as well as detached, payload signals must be regulated and properly scaled within the KuSP.

Because of some expressed concern over a peak regulator to the effect that such a regulating loop may be complex to implement and that proper response time/conditions may be difficult to achieve, Axiomatix initiated a program to assess what is functionally required of a signal peak regulating loop, to generate a detailed design for a peak regulating circuit, and to functionally breadboard and evaluate the peak regulator's performance relative to the types of anticipated waveforms with which it must operate. A complete design has been established, and only the circuit performance evaluation remains.

2.0 INTRODUCTION

2.1 Statement of Work

2.1.1 Objectives

The overall objectives of the work have been to identify, evaluate, and make recommendations concerning the functions and interfaces of those Orbiter avionic subsystems which are dedicated to, or play some part in, handling communication signals (telemetry and command) to/from payloads (spacecraft) that will be carried into orbit by the Shuttle. Some principal directions taken by the efforts have been:

(1) Analysis of the ability of the various avionic equipment to interface with and appropriately process payload signals.

(2) Development of criteria which will foster equipment compatibility with diverse types of payloads and signals.

(3) Study of operational procedures, especially those affecting signal acquisition.

(4) Trade-off analysis for end-to-end data link performance optimization.

(5) Identification of possible hardware design weaknesses which might degrade signal processing performance.

2.1.2 Stipulated Tasks

The contract Statement of Work identifies the following specific tasks that were to be performed.

> Task #1 - Evaluation of Orbiter Payload S-Band Communications Link Hardware Implementation - The contractor shall conduct a detailed evaluation and assessment of the Orbiter payload S-band communications system hardware element designs (i.e., the payload interrogator, the payload signal processor and payload antenna) to determine the adequacy of the overall system design to support payload user requirements. Constraints that must be imposed on attached and deployed payloads desiring to interface with these hardware elements shall be defined.
>
> Task #2 - Evaluation of Payload Data Interleaver (PDI) Implementation - The contractor shall conduct a detailed evaluation and assessment of the upgraded Orbiter PDI design and integration into the PSP (payload signal processor) and PCMMU (PCM master unit) data interfaces. The capability of this hardware element and its associated interfaces to support on-board payload data processing/data display shall be evaluated.

Task #3 - Test Definition and Analysis - The contractor shall formulate recommendations for laboratory breadboard fabrication and testing to support Orbiter/payload communication/data system integration and performance evaluation. Test results shall be analyzed and payload interface specifications suitable for documentation as payload user contraints in Orbiter/payload interface control documents (ICDs) shall be generated.

During the contract period (March 1978 through February 1979), probably 90% of the activity was directed toward various aspects of Task #1. Concentrated effort was given the evolving development of the Payload Interrogator (PI) and Payload Signal Processor (PSP) and, to a somewhat lesser extent, the USAF Communications Interface Unit (CIU), the design of all three being initiated in CY78 by the subsystem contractor, TRW. The PDI (Task #2), being developed by Harris, was principally reviewed by NASA and Rockwell engineers, and Axiomatix did not participate on a first-hand basis in the detailed evaluation and assessment. Some test definition and analysis work (Task #3) was begun, but further work remains as the PI, PSP, and CIU are all still in their conceptual design phases, thus precluding the generation of specific test details until the latter part of CY79.

Because of the developing nature of the payload supporting communication system, certain tasks not specifically identified in the Statement of Work naturally grew out of various problems and issues. The most prominent of these may be summarized as follows.

Task A - Specification of Payload Modulation Parameters - Axiomatix investigated the possible sets of carrier modulating waveforms as a function of data rates, subcarrier frequencies, and modulation indices.

Task B - Bent-Pipe Throughput Performance - Axiomatix analyzed the end-to-end (payload-to-ground) performance of the wideband (4.5 MHz) bent-pipe link.

Task C - Payload Nonstandard Modulation Restrictions - Axiomatix developed a set of rationales upon which a user's guidelines may be generated.

Task D - Minimization of PI False Lock - Axiomatix investigated methods by which the PI receiver may be made essentially immune to lock onto carrier sideband components.

Task E - Wideband Bent-Pipe Signal Drive Regulation Within the Ku-Band Signal Processor - Axiomatix designed a signal peak voltage regulating circuit which optimally establishes the Ku-band transmitter frequency modulation index.

In addition to the foregoing, Axiomatix also acted to disseminate system information regarding the Orbiter's ability to accommodate payload communications by providing a paper to the IEEE Transactions on Communications (special issue on Space Shuttle Communications and Tracking) and a second paper to the 1978 International Telemetering Conference (ITC). The IEEE paper appears as Appendix A of this report, and the ITC presentation viewgraphs are found in Appendix B.

2.1.3 General Approach

The general approach has been to work with cognizant NASA personnel and individuals at the principal prime contractor (Rockwell International) and equipment subcontractors (TRW and Hughes Aircraft Company) to ascertain directions taken. A vital part of this activity has involved Axiomatix attendance and participation in the regular monthly program reviews and all special meetings. These latter gatherings usually involved detailed discussions on design and specification issues that surfaced at the regular monthly reviews.

Each month, Axiomatix prepared a Monthly Technical Report which contained a brief summary of all relevant technical activity, including design reviews, technical conferences, design and analysis efforts and results, critical problem areas, and a forecast of effort for the next monthly reporting period. Many of the Axiomatix in-process analysis activities and results were appended to these reports.

Apart from attendance at meetings, monthly reporting, and analysis activities, Axiomatix also acted in a technical consulting role to both NASA and the contractors. Most of the in-depth discussions were conducted at TRW or with various engineers over the phone.

2.1.4 Continuity with Previous Work

Development of the payload avionic equipment was a new activity beginning in CY78. Since the PI and PSP interface with other S-band and Ku-band hardware, some previous activity associated with the network equipment, carried out under contracts NAS 9-14614C, "Study to Investigate and Evaluate Means of Optimizing the Communications Functions," and NAS 9-13467, "Integrated Source and Channel Encoded Digital Communication System Design Study," was applicable.

2.1.5 Relationship to Parallel Work

The work performed under the subject contract was strongly interrelated to parallel efforts. Companion contract NAS 9-15514A, "Shuttle Orbiter S-Band Communications Equipment Design Evaluation," provided support to critique the design and assess the performance of the individual Orbiter S-band communication equipment. The work had three principal aspects/goals:

(1) Review and analysis of the ability of the various subsystem avionic equipment designs to interface with, and operate on, signals from/to adjoining equipment.

(2) Assessment of the performance peculiarities of the hardware against the overall specified system requirements.

(3) Evaluation of EMC/EMI test results of the various equipment with respect to the possibility of mutual interference.

Additional related work was conducted under contract NAS 9-15604B which provided a handbook, entitled "Users' Handbook for Payload-Shuttle Data Communication." Also, the report "Guidelines for Choosing and Evaluating Payload RF Frequencies," produced under contract NAS 9-15604A, was related to this effort.

2.2 Scope of the Final Report

There are four sections following which address various aspects and details of the work.

Section 3.0 contains functional descriptions of the various S-band equipment and their payload link configurations. This section is primarily intended for orientation of the reader.

Section 4.0 summarizes the year history and highlights of important issues. Problem solutions are stated, and open or continuing actions are outlined.

In Section 5.0, specific supporting Axiomatix studies and analysis are presented. Some of this work is finished, while other parts are ongoing.

Finally, in Section 6.0, design and performance assessments of the payload links are provided.

3.0 BRIEF DESCRIPTIONS OF THE PRINCIPAL AVIONIC EQUIPMENT

The following subsections are functional descriptions of the Orbiter avionic and payload systems and subsystems with which this contract has dealt (at least in some sense) during the past year.

This material is included in the report primarily as a primer for those readers not routinely familiar with the payload links and associated equipment. As such, the texts are simply summaries of the principal operating functions and capabilities. Functional block diagrams are provided.

Additional information may be found in Appendix A and in Reference [1].

3.1 Payload Systems Overview

A user of the Shuttle Orbiter system will have need to communicate with the Orbiter and with the ground. To implement such communications, the Orbiter contains a versatile set of payload-oriented avionic hardware and provides several communication links to various ground stations. A user that wishes to communicate may make use of the Shuttle communication systems in either a standard or nonstandard manner. Standard accommodations will usually meet the majority of user requirements with maximum flexibility and reliability and with minimum concern and cost. Nonstandard capabilities, however, are provided so that special or unique user needs may be met. In the nonstandard situation, the user bears a much greater responsibility for the design, implementation, and operation of the communication link.

A user/payload may be defined as any system which is carried by the Shuttle into orbit but which is not in any way a functional part of the Orbiter itself. Payloads may be divided into two distinct classes: (1) those which will be separated or become "detached" from the Orbiter and (2) those which will remain "attached" to the Shuttle in the associative surroundings of the cargo bay. Many detached payloads will be transported into geosynchronous or other Earth orbits or placed on deep space trajectories by the Inertial Upper Stage (IUS). Certain detached payloads (known as free-flyers) will simply operate away from the Orbiter in co-orbit, and some of these will be subsequently recovered by the

Shuttle for return to the ground. Usually, attached payloads will be serviced via hardwire links while communications with detached payloads must use RF channels.

NASA and DOD payload requirements and subsystem capabilities have predominantly driven the design of the avionic subsystems (especially in terms of the detached payload communication links). Thus, "standard" capabilities have evolved to serve NASA and DOD. Nonstandard conditions have also been provided for but with generally less operational capability (especially aboard the Orbiter).

The Orbiter communications and tracking subsystem provides links between the Orbiter and the payload. It also transfers payload telemetry and uplink data commands to and from the space networks.

The Orbiter can communicate with ground stations directly or through the Tracking and Data Relay Satellite System (TDRSS). Payloads communicate with the Orbiter through hardline cables (attached payloads) or the payload radio frequency link (detached payloads). Table 2 lists the major unmanned payload functions and the communication links over which they are handled.

Figure 1 shows a pictorial representation of the Shuttle and the various RF channels which comprise the communication links between the Shuttle, payloads and ground. The links between the Shuttle and payloads are at S-band (L-band forward frequency for DOD/SGLS), and the Shuttle/ground direct links are also S-band. Relay links through the TDRS are at S-band and Ku-band.

Generally, only one detached payload may be communicated with at any time. Similarly, only one coherent Shuttle/ground direct link is available. Since, however, the FM direct link utilizes separate equipment, it may be worked simultaneously with the coherent direct link. TDRSS relay can make use of the S-band and Ku-band capabilities concurrently. Since the Shuttle operates in low orbit (100 to 500 nmi), the time that it may communicate with any direct ground station is limited while nearly continuous contact using the TDRS may be maintained.

Aboard the Orbiter, a number of avionic subsystems perform various operations on the communication signals to and from payloads. Table 3 indicates the subsystems, the acronyms by which they are commonly referred, and the various internal functions. Detailed descriptions

Table 2. Orbiter Avionics Services to Payloads

Function	Payload/Ground Direct or Through Tracking and Data Relay Satellite		Payload/Orbiter Hardline		Payload/Orbiter Radio Frequency Link	
	Payload to Ground via Orbiter	Ground to Payload via Orbiter	Orbiter to Attached Payload	Attached Payload to Orbiter	Orbiter to Detached Payload	Detached Payload to Orbiter
Scientific Data	X			X		
Engineering Data	X	X		X		X
Command		X	X		X	
Guidance, Navigation and Control		X	X	X	X	
Caution & Warning	X			X		X
Master Timing			X			
Uplink Data		X	X			

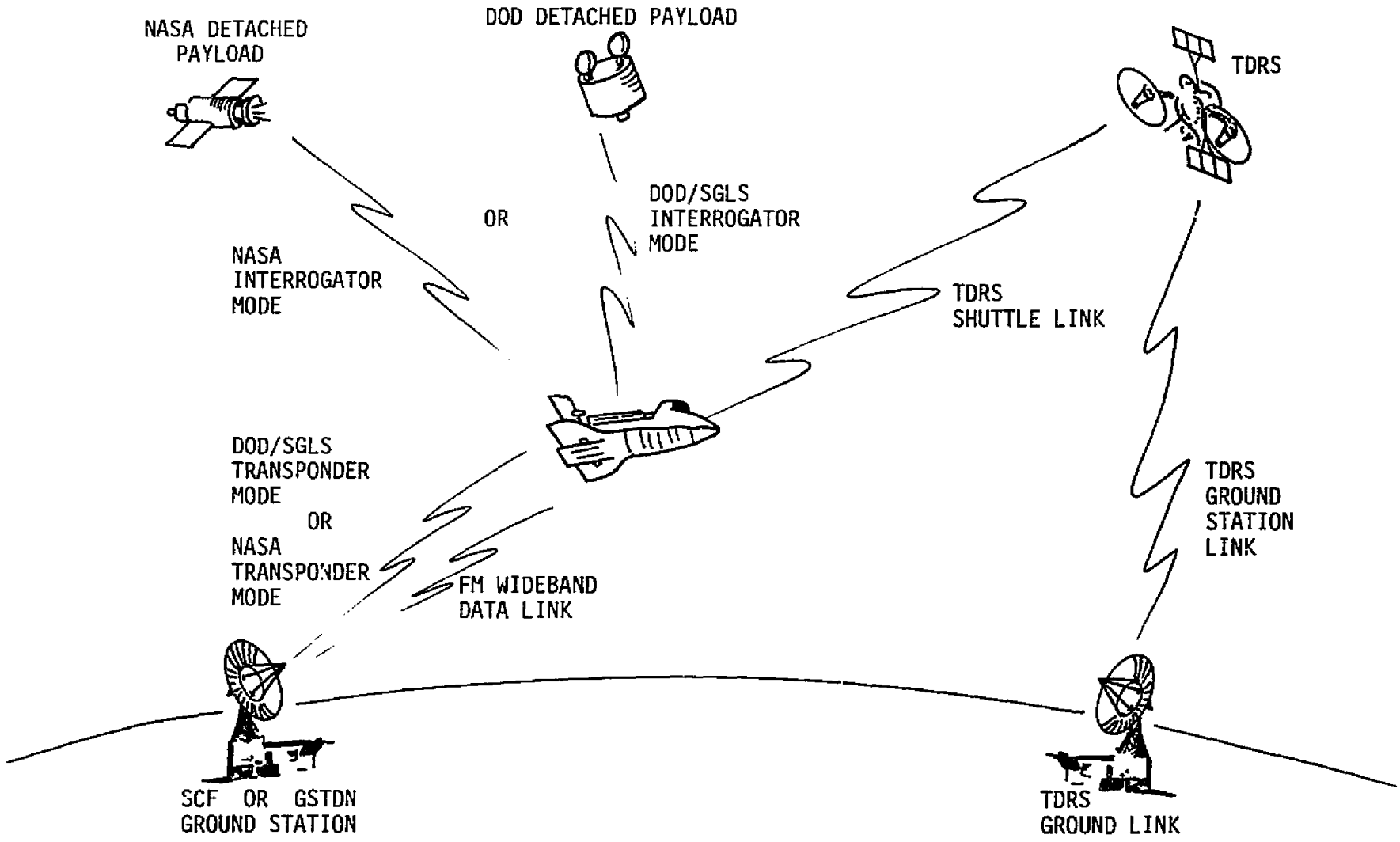

Figure 1. Payload Communication Links Overview

Table 3. Orbiter Avionic Subsystems and Functions

Subsystem Name	Acronym	INTERNAL FUNCTIONS									
		Carrier Modulation	Carrier Tracking & Demodulation	Subcarrier Demodulation	Data Synchronization & Detection	Command Modulation Generation	Data Stream Multiplexing	Data Stream Demultiplexing	Data Validity Check	Data Buffering & Rate Change	Data Decoding
Payload Interrogator	PI	X	X								
NASA Payload Signal Processor	PSP			X	X	X			X	X	X
DOD Communication Interface Unit	CIU			X	X	X	X		X	X	X
S-Band Network Transponder	-	X	X								
Payload Data Interleaver	PDI						X				
Network Signal Processor	NSP				X		X	X		X	X
Ku-Band Transmitter & Receiver	-	X	X								
Ku-Band Signal Processor	KuSP				X		X	X		X	X
Multiplexer/ Demultiplexer General Purpose Computer	MDM GPC						X	X	X		X

of most of these subsystems are given in Subsections 3.3 through 3.7 following.

The number of possible end-to-end payload communication link configurations is considerable; thus, only a few will be given here so that the reader may appreciate their generic nature. Figure 2 shows a block diagram of the detached payload standard telemetry S-band direct link. Standard telemetry for NASA and DOD payloads involves the transmission of digitally encoded data at specified bit rates. Within the payload itself, the digital data must be modulated onto subcarriers of specified frequency and with an NRZ-type format. Table 4 summarizes the standard digital tel... requirements. In addition, for DOD payloads, certain FM/FM analog telemetry on a subcarrier is allowed, as indicated in Table 4.

Table 4. Payload Standard Telemetry Requirements

Parameter	Parameter/Range	
	PSK Modulation	Frequency Modulation
Subcarrier Frequencies	1.024 MHz or 1.7* MHz	1.7* MHz
Bit Rates or Modulation Response	256,*† 128,*† 64,* 32,* 16, 10, 8, 4, 2, 1, 0.5,* 0.25* kbps	100 Hz to 200 kHz

*DOD only
†1.7 MHz subcarrier only

The standard telemetry is transmitted via the payload transponder and received and demodulated aboard the Orbiter in the Payload Interrogator (PI). For NASA payloads, the Payload Signal Processor (PSP) demodulates the subcarrier and detects the data while, for DOD payloads, the Communications Interface Unit (CIU) performs the like function. (Note that the DOD CIU in Figure 2 is shown as an alternate path to the NASA PSP; these subsystems do not operate simultaneously on payload signals.)

The Payload Data Interleaver (PDI) and the Network Signal Processor (NSP) function to multiplex the detected detached payload data from

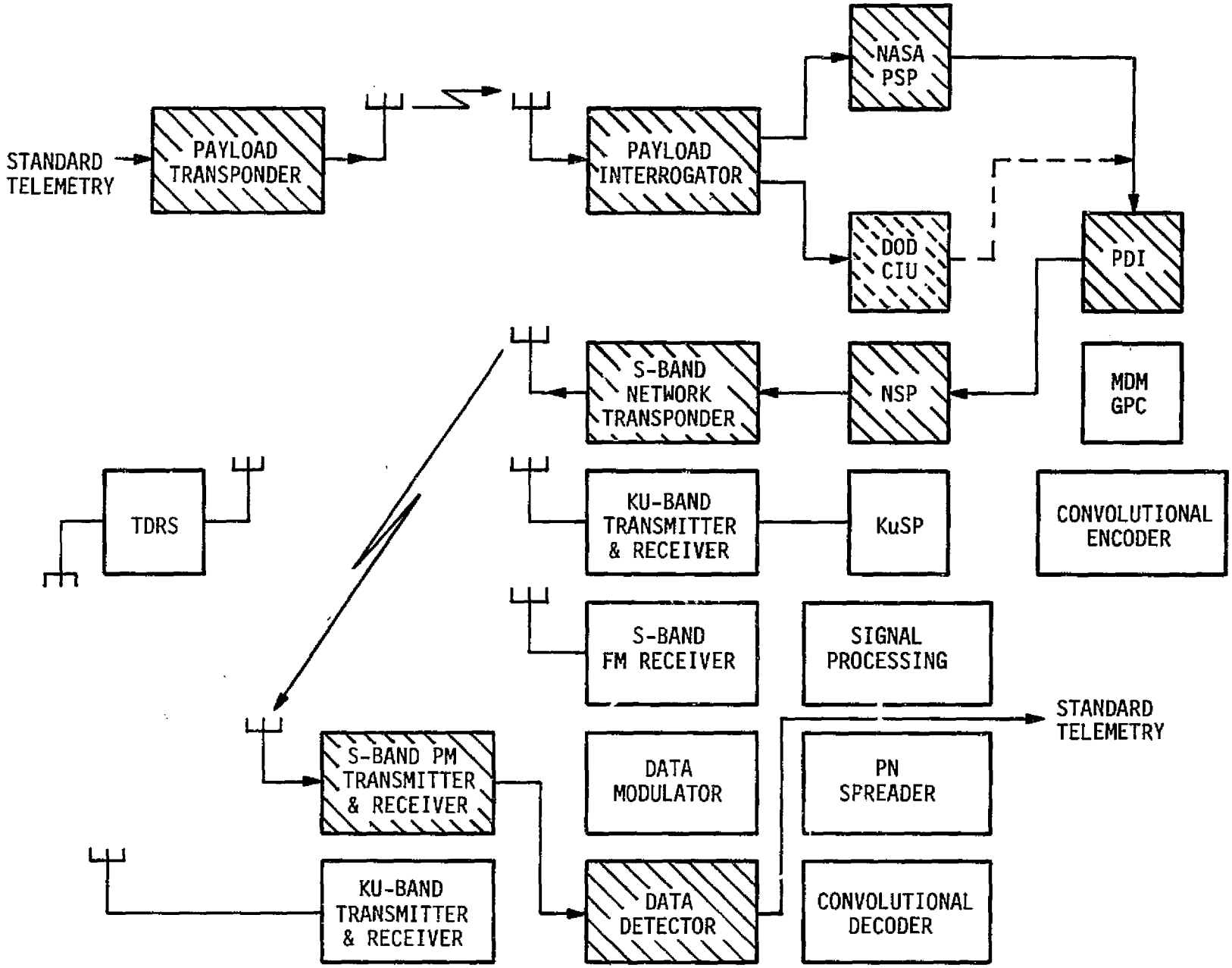

Figure 2. Detached Payload Standard Telemetry S-Band Direct Link

the PSP (or CIU) with other attached payload and Orbiter data. A composite digital data stream is then transmitted directly to the ground station via the S-Band Network Transponder.

At the ground station, the telemetry signal is received, demodulated and detected. It is also demultiplexed (not shown functionally in Figure 2) so that the standard telemetry data stream, as it appeared at the input to the payload transponder, is delivered to the appropriate payload/user facility. Because of the noisy detection operations that take place in the PSP (or CIU) and in the ground data detector, some bits of information in the telemetry data stream are in error.

The standard telemetry data capability available for detached payloads provides for a reasonable degree of flexible operation. It may happen, however, that certain payloads are not able to avail themselves of the standard system. To accommodate payloads whose telemetry formats are not compatible with standard data rates and subcarrier frequencies, "bent-pipe" modes of operation are provided within the Shuttle's avionic equipment. Several signal paths acting as "transparent throughputs" are available for both digital and analog signals.

Digital data streams at rates higher than 64 kbps (which therefore cannot be handled by the PDI) may directly enter the Ku-Band Signal Processor (KuSP) where they may be (1) QPSK modulated onto an 8.5 MHz subcarrier, (2) QPSK modulated onto the Ku-band carrier, or (3) frequency modulated onto the Ku-band carrier. Detection and processing of all such data occur at the ground stations.

Analog signals may take one of two paths. If they are in the form of a modulated subcarrier and do not have significant frequency components above 2 MHz, they may be hard-limited (i.e., a two-level or one-bit-quantized waveform produced) and treated as "digital" signals by the 8.5 MHz subcarrier QPSK modulator. On the other hand, if the analog signal is baseband in nature on a frequency range up to 4.5 MHz, it may be transmitted via the Ku-band link utilizing FM. Again, all processing is accomplished on the ground. Figure 3 shows the subsystems that would be employed in an FM bent-pipe link.

Commands from the ground to detached payloads may be transmitted from the ground to the Orbiter by any one of three links: (1) S-band direct link, (2) S-band TDRS relay link, and (3) Ku-band TDRS relay link.

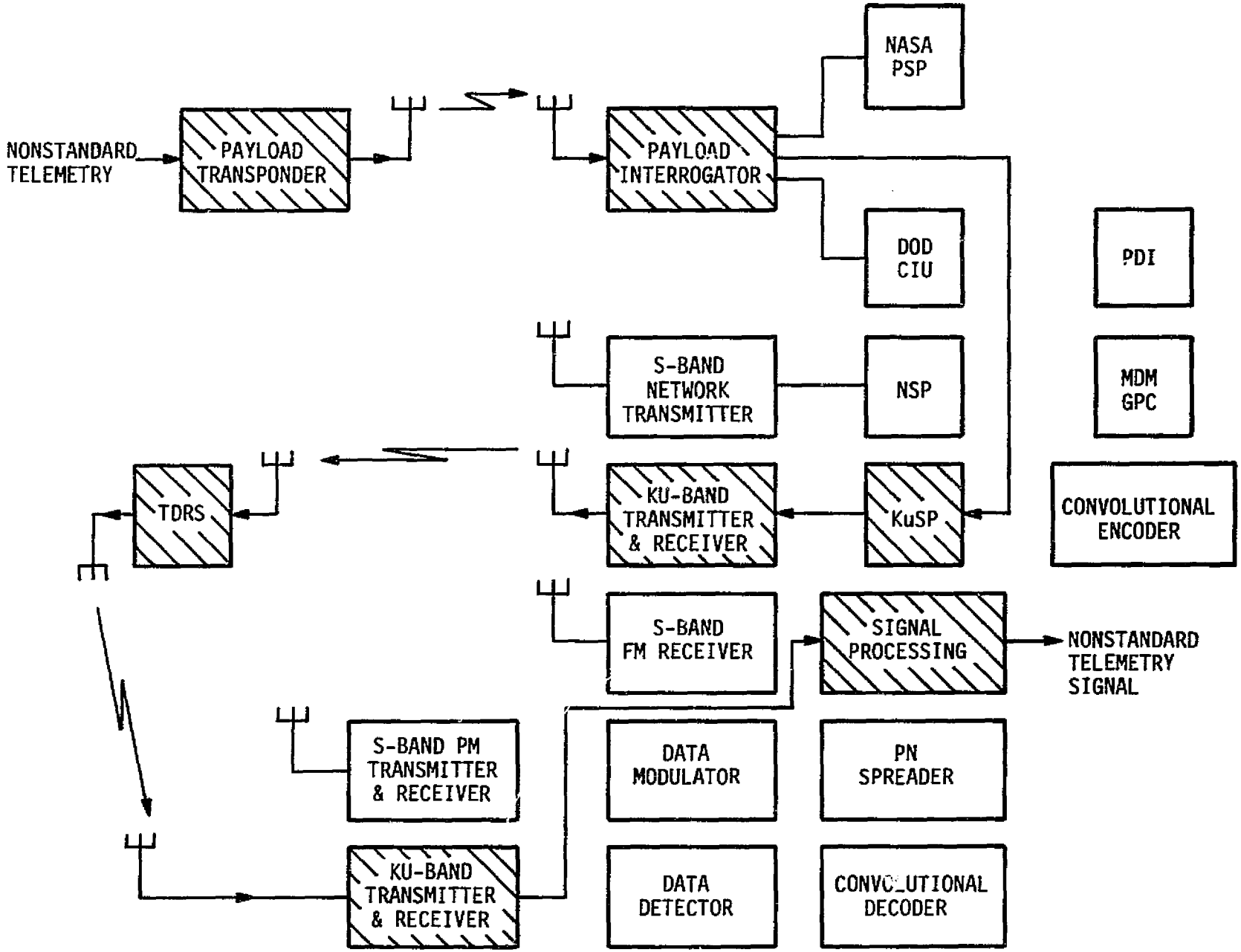

Figure 3. Detached Payload Nonstandard Telemetry Bent-Pipe Link

Irrespective of which link is used, detected command data onboard the Orbiter is thoroughly checked for validity and errors before it is transmitted to the payload.

Figure 4 shows the end-to-end subsystems employed in an S-band relay command link. Encoded (i.e., structured) payload command data bits at the ground station are multiplexed with Orbiter commands and data and PN code-modulated in order to spread the data frequency spectrum. (This is a requirement of the TDRS forward link in order to satisfy transmitted power versus frequency flux density limitations.) The resultant signal is then carrier-modulated and transmitted to the Orbiter through the TDRS.

At the Orbiter, the S-Band Network Transponder acquires, tracks, despreads (removes the PN codes), and demodulates the composite command data stream. In turn, the NSP bit synchronizes and detects the command bits, while the MDM/GPC performs demultiplexing and validation.

The payload command bit stream is input to the NASA PSP (or DOD CIU as the alternate path) where it is transformed into the proper payload subcarrier signal structure. Transmitted to the payload via the PI and received, demodulated and detected by the payload transponder, the command data is sent to the payload decoder (not shown in Figure 4) for final decoding and disposition.

Commands to detached payloads are always in a standard form; there is no nonstandard command equivalent to the nonstandard telemetry capability. Table 5 indicates the standard command conditions.

Table 5. NASA and DOD Command System Parameters

NASA	
Subcarrier Frequency	16 kHz, sinewave
Bit Rates	$2000 \div 2^N$ bps, N = 0,1,2,...,8
DOD	
Signal Tone Frequencies	65 kHz, 76 kHz, 95 kHz
Symbol Rates	1000 or 2000 sps

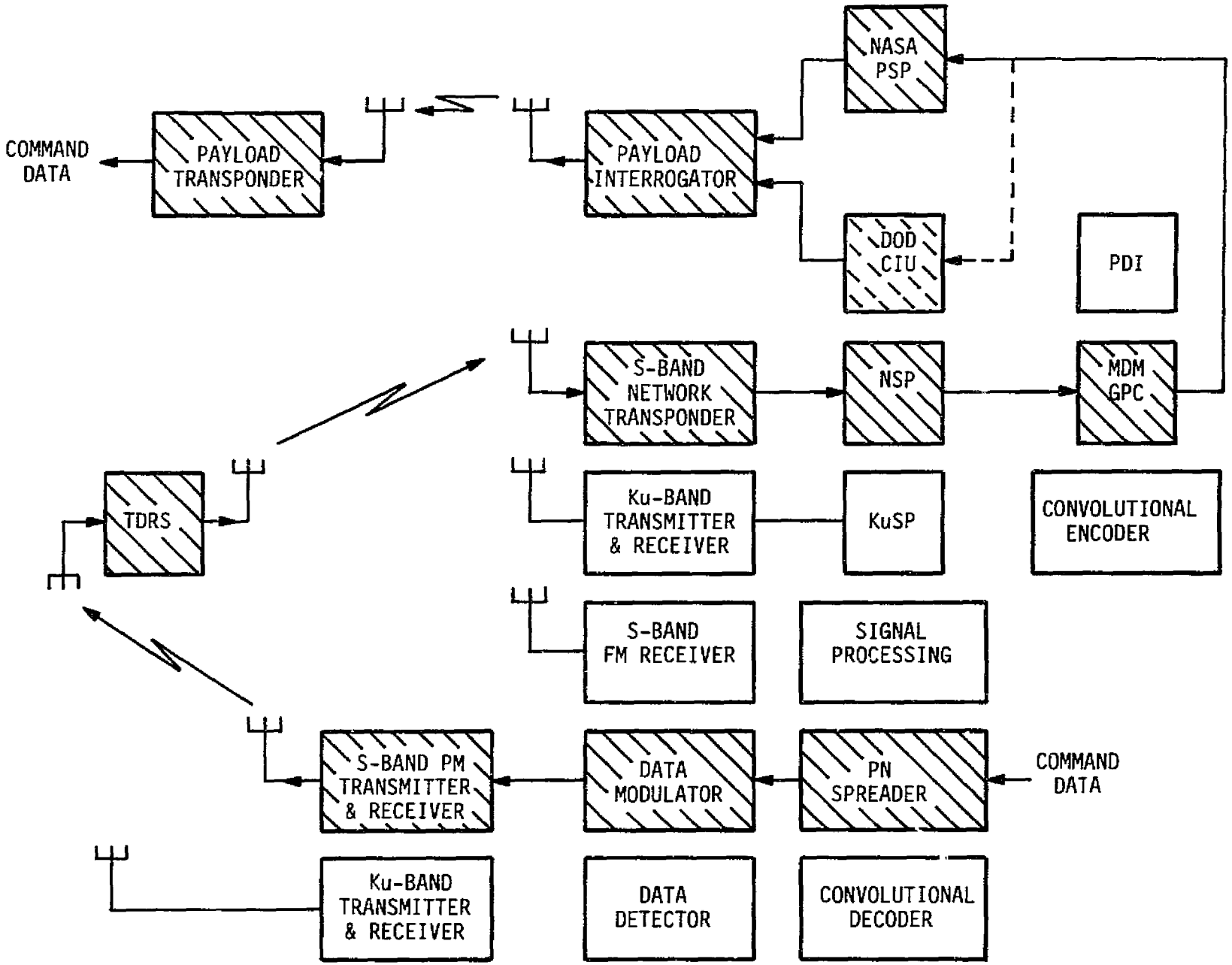

Figure 4. Detached Payload Command S-Band Relay Link

3.2 Typical Payload Transponders

NASA and DOD payload transponders are generically quite similar in terms of their functions and architectures. NASA transponders are standardized, with three mission-oriented types available--deep space transponders [for use with the Deep Space Network (DSN)], near-Earth transponders [for use with the Space Tracking and Data Network Ground stations (GSTDN)], and TDRSS transponders (for use with the TDRSS or GSTDN). DOD transponders interface with the USAF Satellite Control Facility (SCF).

Conspicuous differences between NASA and DOD transponders are the forward link frequency bands and transponding ratios. The NASA receive frequency range is S-band (2025 MHz to 2120 MHz), while the DOD receive frequency range is L-band (1760 MHz to 1840 MHz). The transmitter frequency is related to the receiver frequency by a ratio of integers, called the coherency (or turn-around) ratio. Both the NASA and DOD transmitter frequency ranges are S-band (2200 MHz to 2300 MHz). The corresponding coherency ratios are, for NASA, 240/221, and for DOD, 256/205.

Figure 5 is a block diagram of the typical payload transponder. The forward link RF input is preselected, filtered for the frequency band utilized [S-band for NASA and L-band for Inertial Upper Stage (IUS) and DOD], and the input is then mixed down to the first IF. Further mixing translates the first IF signal to the second IF, where the output from the second IF amplifier is distributed to four phase detector/demodulator functions.

The carrier tracking loop functions to acquire and track the residual carrier component of the input signal. A second-order tracking loop is employed. Frequency and phase coherence are supplied from the VCO to the synthesizer/exciter where the coherent reference frequencies are derived for the demodulation functions.

AGC is obtained through in-phase demodulation of the residual carrier. The AGC voltage is filtered and applied to the first IF amplifier to control the gain of the receiver. The AGC voltage is also filtered and compared with a threshold to determine whether the carrier tracking loop is in or out of lock.

The command demodulator coherently recovers the command phase modulation from the carrier. Spectral conditioning (in most cases,

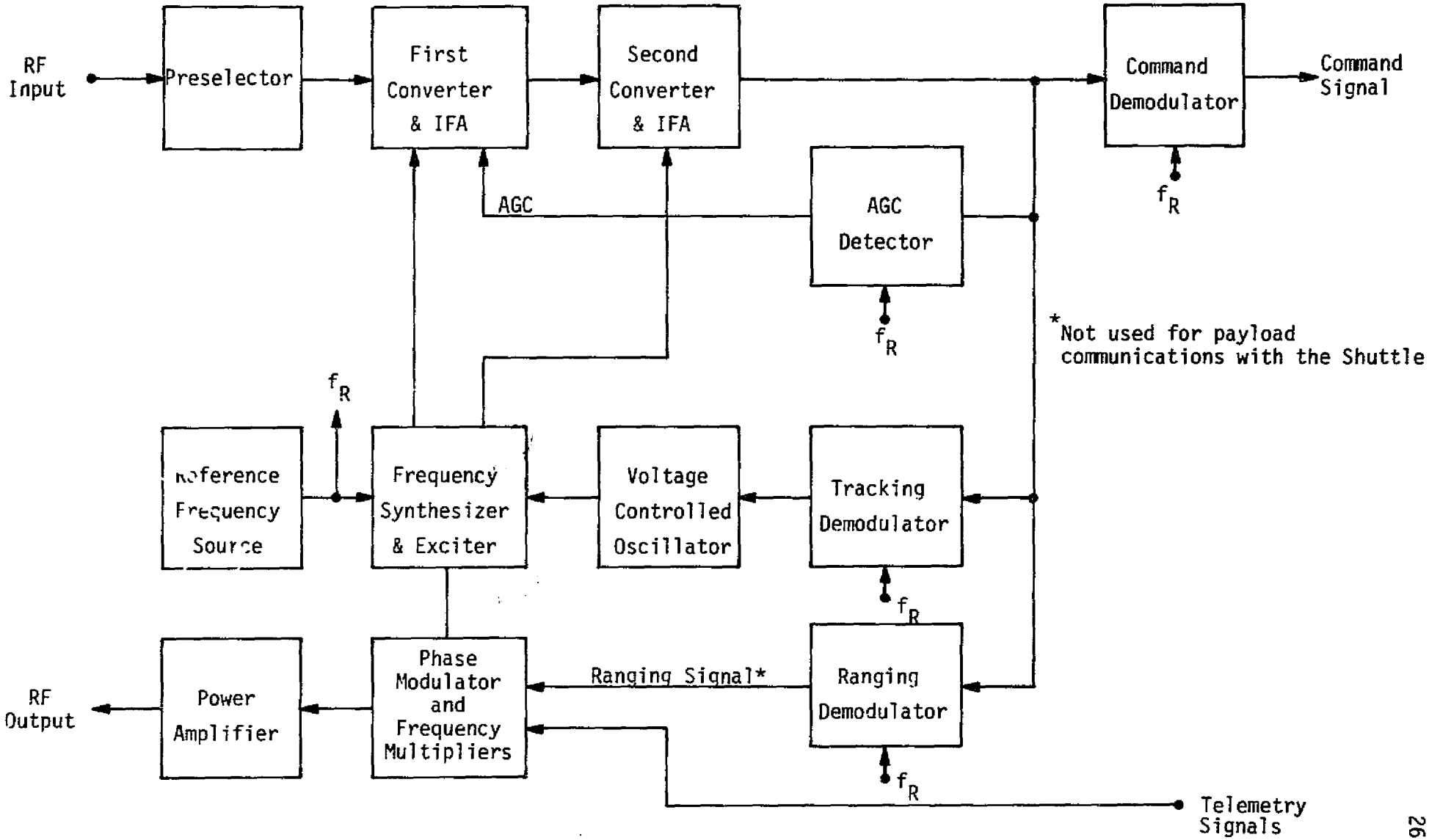

Figure 5. Typical Payload Transponder Diagram

limited to lowpass filtering) is usually provided in the output to the command detector.

Most transponders also have a turn-around ranging capability; there is, however, no plan to make use of such ranging capability with the payload/Shuttle link.

The synthesizer/exciter provides all reference frequencies to the transponder. A reference oscillator supplies standard frequencies to the receiver synthesizer, and coherence is provided by the receiver VCO. Synthesized frequencies are distributed to the receiver mixers and phase detectors and to the transmitter phase modulator through a frequency multiplier.

The phase modulator provides the means of modulating the return link carrier with telemetry and ranging signals. Its output drives the transmitter frequency multiplier, producing the required modulated carrier signal in the S-band frequency range.

Finally, the power amplifier raises the modulated S-band transmitter signal to the level required by the return link. For near-Earth spacecraft, the power levels may range from a few hundred milliwatts to several watts, while deep-space vehicles employ power levels on the order of 100 W.

Typical transponder operating and performance parameters are indicated in Table 6.

3.3 Payload Interrogator

The function of the Payload Interrogator (PI) is to provide the RF communication link between the Orbiter and detached payloads. For communication with the NASA payloads, the PI operates in conjunction with the Payload Signal Processor (PSP). During DOD missions, the PI is interfaced with the Communication Interface Unit (CIU). Nonstandard (bent-pipe) data received by the PI from either NASA or DOD payloads is delivered to the Ku-Band Processor, where it is processed for transmission to the ground via the Shuttle/TDRSS link.

Simultaneous RF transmission and reception is the primary mode of PI operation with both NASA and DOD payloads. The Orbiter-to-payload link carries the commands, while the payload-to-Orbiter link communicates the telemetry data. In addition to this duplex operation, the PI provides

Table 6. Typical Payload Transponder Characteristics

Item	Parameter and Range
Receive Frequency Range	
L-Band Frequency (DOD)	1760-1840 MHz
S-Band Frequency (NASA)	2025-2120 MHz
Transmitter Frequency Range	2200-2300 MHz
Tracking Loop Bandwidth	18, 60, 200 or 2000 Hz
Tracking Loop Order	Second
AGC Dynamic Range	100 dB
Command Channel Frequency Response	1 kHz to 130 kHz
Ranging Channel Frequency Response	1 kHz to 1.2 MHz
Noise Figure	5 dB to 8 dB
Transmitter Phase Deviation	Up to 2.5 radians
Transmitter Output Power	200 mW to 5W*

*Up to 200 watts with external power amplifiers.

for "transmit only" and "receive only" modes of communication with some payloads.

Figure 6 shows the functional block diagram for the Payload Interrogator. The antenna connects to an input/output RF port which is common to the receiver and transmitter of the PI unit. Because of a requirement to operate the PI simultaneously with the Shuttle-ground S-band network transponder which radiates and receives on the same frequency bands, a dual triplexer is employed. The S-band network transponder emits a signal at either 2217.5 MHz or 2287.5 MHz; both frequencies thus fall directly into the PI receive band of 2200-2300 MHz. Conversely, the payload transmitter, operating either in the 2025-2120 MHz (NASA) or in the 1764-1840 MHz (DOD) bands, can interfere with uplink signal reception by the S-band network transponder receiver. Therefore, by use of the triplexer and by simultaneously operating the PI and network transponder in the mutually exclusive subbands, the interference problem is effectively eliminated.

When detached payloads are in the immediate vicinity of the Orbiter, excessive RF power levels may impinge on the interrogator antenna. Thus, the RF preamplifier of the receiver is protected by a set of manually operated sensitivity control attenuators. The output of the preamplifier is applied to the first mixer, where it is converted to the first IF for amplification and level control. The first local oscillator frequency, f_{LO1}, is tunable, and its frequency corresponds with the desired PI receive channel frequency. Except for channel selection, however, f_{LO1} is fixed. Consequently, an unspecified frequency difference between the received payload signal and f_{LO1} will appear within the first IF amplifier and at the input to the second mixer.

The receiver frequency and phase tracking loop begins at the second mixer. As shown in Figure 6, the output of the first IF amplifier is down-converted to the second IF as a result of mixing with a variable second LO frequency, f_{LO2}. The portion of the second IF which involves only the carrier tracking function is narrowband, passing the received signal residual carrier component and excluding the bulk of the sideband frequencies. Demodulation to baseband of the second IF signal is accomplished by mixing with a reference frequency, f_R. The output of the

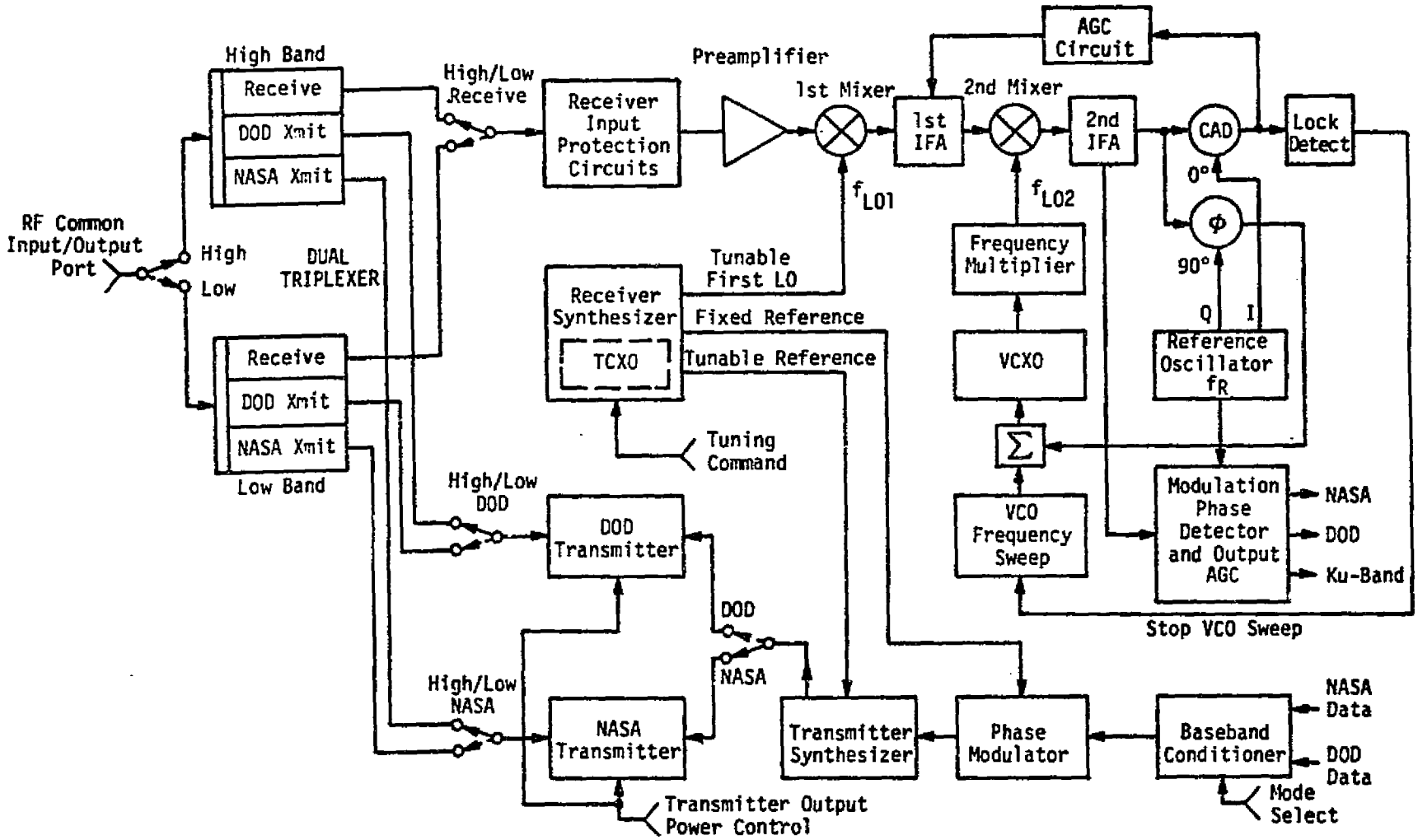

Figure 6. Payload Interrogator Functional Block Diagram

tracking phase detector, after proper filtering, is applied to the control terminals of a VCO which provides the second local oscillator signal, thereby closing the tracking loop. Thus, when phase track is established, f_{LO2} follows frequency changes of the received payload signal.

For the purpose of frequency acquisition, the f_{LO2} may be swept over a ±85 kHz uncertainty region. Sweep is terminated when the output of the coherent amplitude detector (CAD) exceeds a preset threshold, indicating that the carrier tracking loop has attained lock. The output of the CAD also provides the AGC to the first IF amplifier. To accommodate payload-to-Orbiter received signal level changes due to range variation from about a few feet to 10 nautical miles, 110 dB of AGC is provided in the first IFA.

A wideband phase detector is used to demodulate the telemetry signals from the carrier. The output of this detector is filtered, envelope level controlled, and buffered for delivery to the PSP, CIU and Ku-Band Processor units.

The PI receiver frequency synthesizer provides the tunable first LO frequency and the corresponding exciter frequency to the transmitter synthesizer. It also delivers a reference signal to the transmitter phase modulator. Baseband NASA or DOD command signals modulate the phase of this reference signal which, in turn, is supplied to the transmitter where it is upconverted to either the NASA or DOD transmit frequency and applied to the power amplifiers.

For transmitter efficiency optimization, separate NASA and DOD RF power amplifier units are used. Depending on the operating band selected, transmitter output is applied to either the high- or low-band triplexer. To compensate for varying distances to payloads, each transmitter has three selectable output power levels.

3.4 Payload Signal Processor

The Payload Signal Processor (PSP) performs the following functions: (1) it modulates NASA payload commands onto a 16 kHz sinusoidal subcarrier and delivers the resultant signal to the PI and the attached payload umbilical, (2) it demodulates the payload telemetry data from the 1.024 MHz subcarrier signal provided by the PI, and (3) it performs bit and frame synchronization of demodulated telemetry data and delivers this

data and its clock to the Payload Data Interleaver (PDI).

The PSP also transmits status messages to the Orbiter's general purpose computer (GPC); the status messages allow the GPC to control and configure the PSP and validate command messages prior to transmission.

The functional block diagram for the PSP is shown in Figure 7. The PSP configuration and payload command data are input to the PSP via a bidirectional serial interface. Transfer of data in either direction is initiated by discrete control signals. Data words 20 bits in length (16 information, 1 parity, 3 synchronization) are transferred across the bidirectional interface at a burst rate of 1 Mbps, and the serial words received by the PSP are applied to word validation logic which examines their structure. Failure of the incoming message to pass a validation test results in a request for a repeat of the message from the GPC.

Command data is further processed and validated as to content and the number of command words. The function of the command buffers is to perform data rate conversion from the 1 Mbps bursts to one of the selected standard command rates. Command rate and format are specified through the configuration message control subunit.

From the message buffers, the command bits are fed via the idle pattern selector and generator to the 16 kHz subcarrier biphase modulator. The idle pattern (which, in many cases, consists of alternating "ones" and "zeros") precedes the actual command word and is usually also transmitted in lieu of command messages. Subcarrier modulation is biphase NRZ only.

The 1.024 MHz telemetry subcarrier from the PI is applied to the PSK subcarrier demodulator. Since the subcarrier is biphase modulated, a Costas-type loop is used to lock onto and track the subcarrier. The resulting demodulated bit stream is input to the bit synchronizer subunit, where a DTTL bit synchronizer provides timing to an integrate-and-dump matched filter which optimally detects and reclocks the telemetry data.

Detected telemetry bits, together with clock, are input to the frame synchronizer where frame synchronization is obtained for any one of the four NASA standard synchronization words. The frame synchronizer also detects and corrects the data polarity ambiguity caused by the PSK demodulator Costas loop.

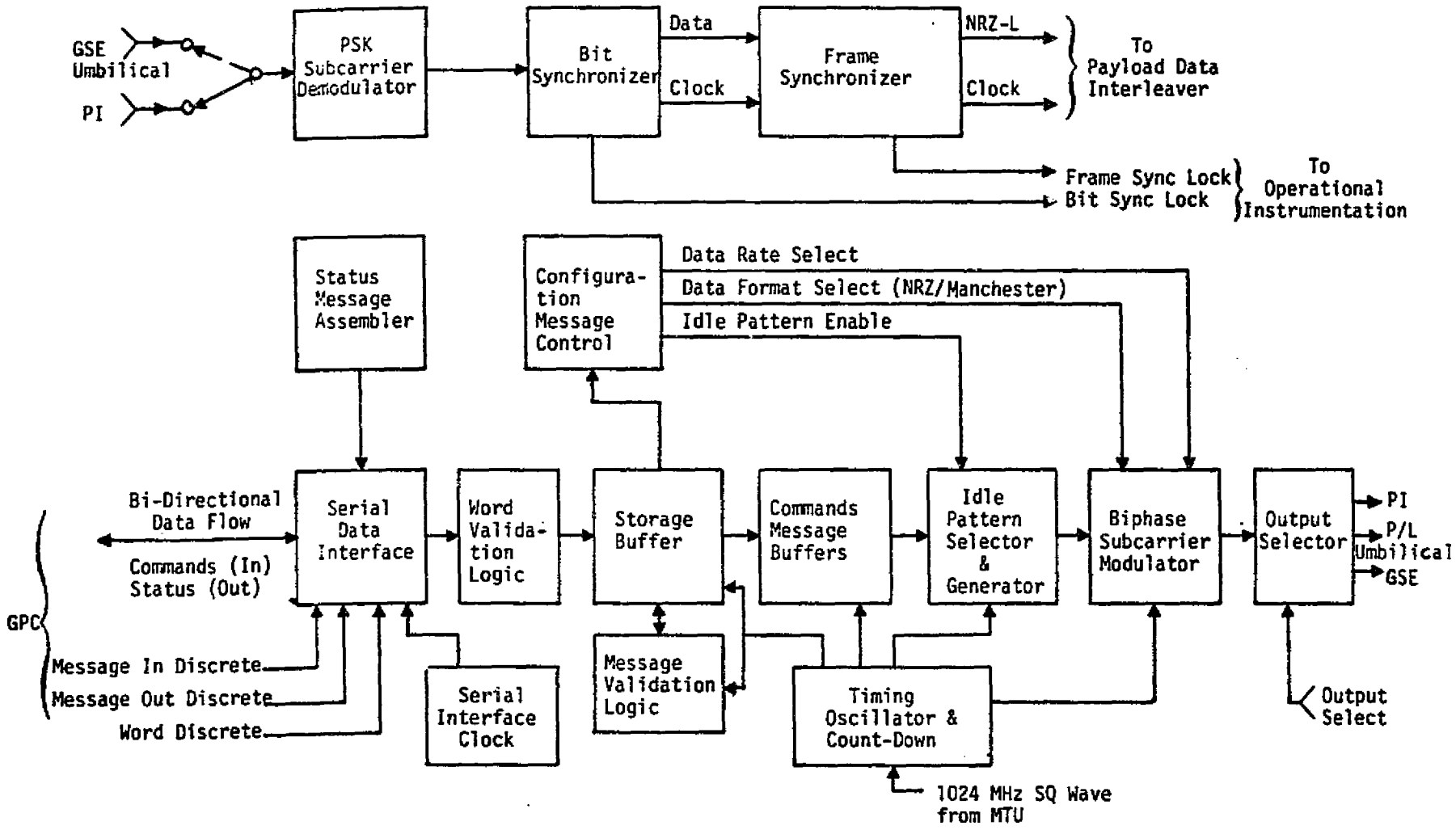

Figure 7. NASA Payload Signal Processor Functional Block Diagram

From the frame synchronizer, the telemetry data with corrected frame synchronization words and clock are fed to the PDI. The telemetry detection units also supply appropriate lock signals to the Orbiter's operational instructional equipment, thus acting to indicate the presence of valid telemetry.

3.5 Communication Interface Unit

The CIU, shown in Figure 8, is the DOD equivalent of the NASA PSP. The major differences are that the CIU (1) handles ternary commands in both baseband and FSK tone formats, (2) accepts Orbiter crew-generated commands, (3) permits a larger range of standard telemetry data rates, and (4) is capable of simultaneously handling two subcarrier frequencies.

Ground-generated commands may be received from either the KuSP or the NSP (through the GPC/MDM interface). Received as a continuous binary data stream at 128 kbps from the KuSP and 1 Mbps bursts from the GPC/MDM, they must be detected and buffered. The binary outputs of the buffers are either 4 kbps or 2 kbps which, when converted to the ternary format, become symbol rates of 2 ksps and 1 ksps, respectively. The input to the binary-to-ternary converter consists of serial data plus clock (two lines), and the output consists of the "S," "0," and "1" symbols plus clock (four lines).

Crew-generated commands are input through the command generator and verification unit which outputs them in the proper ternary format. A priority selection switch determines whether ground or Orbiter originated commands will be transmitted to the payload. The FSK/AM generator encodes the ternary commands into the proper signal for transmission to the payload. Three subcarrier tones of 65 kHz, 76 kHz and 95 kHz (corresponding respectively to the "S," "0," and "1" symbols) are employed in a time-serial manner. The command rate clock, at one-half the symbol rate and in the form of a triangular wave, is amplitude modulated onto the composite tone stream. Attached payloads may receive either the ternary baseband or tone command signals from the CIU.

Figure 8 shows that there are one PI and four hardline telemetry inputs to the CIU. All subcarrier inputs are routed through an input selector to the two PSK demodulators. These PSK demodulators are similar to that used in the PSP. The FM discriminator demodulates the analog

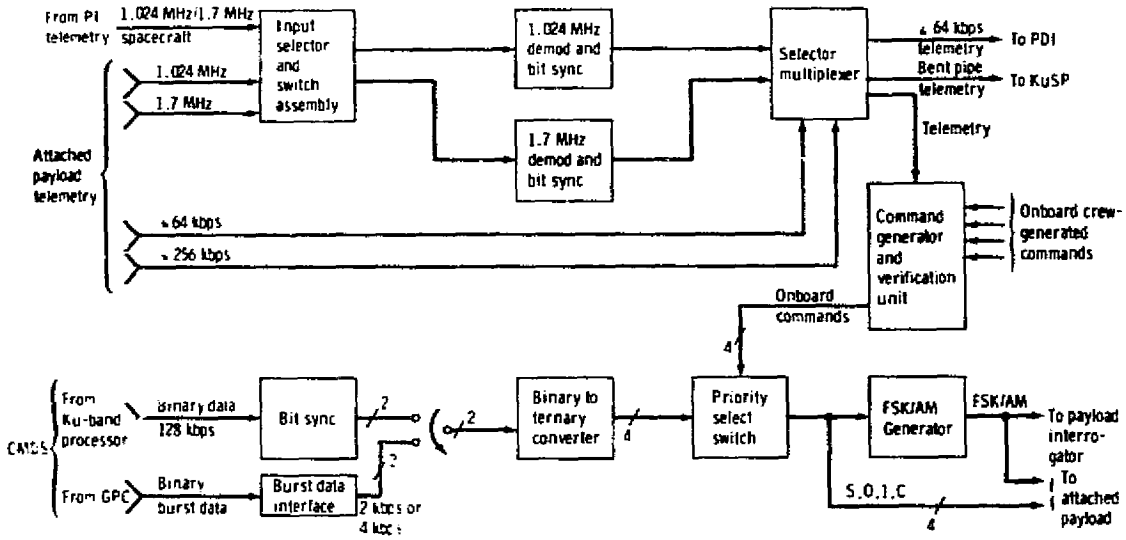

Figure 8. Communication Interface Unit for DOD Payloads

baseband signal from its 1.7 MHz subcarrier which is, in turn, sent to the KuSP to be handled as bent-pipe telemetry. All demodulated/detected and hardline telemetry is routed to the selector/multiplexer where it is partially demultiplexed and sorted for reformatting to the PDI and where the command verification data from the payload is extracted for the command generator and verification unit.

3.6 Payload Data Interleaver

A block diagram of the Payload Data Interleaver (PDI) is shown in Figure 9. It is basically a multiplexer capable of combining various asynchronous data streams into a single serial data stream. The PDI provides for reception of up to six asynchronous payload PCM streams, five from attached payloads and one from the PSP that is active (detached payload). An input switch matrix selects four of the inputs for the bit synchronizers. The "chain" functions of bit synchronization, decommutation, and word selection are provided for up to four simultaneous PCM streams in two possible modes:

Mode 1: In this mode, a chain bit synchronizes, master-frame synchronizes, minor-frame synchronizes, and word synchronizes to the incoming data stream. The word selector blocks data into proper words for storage in the data RAM and/or toggle buffer. PCM code type, bit rate, PCM format, synchronization codes, and word selection are programmable under control of the decommutator format memories. Two word selection capabilities for this mode of operation are as follows:

Type I: The first type selects all, or a subset of, the words in a payload PCM format minor frame (or master frame for formats without minor frames) for storage in the toggle buffer.

Type II: The second type of word selection is by parameter. The specification of a parameter consists of its word location within a minor frame, the first minor frame in which it appears, and its sample rate. The specification is provided as part of the decommutator control memory format load.

Mode 2: In this mode, a chain bit synchronizes to the incoming data, blocks it into 8-bit words, blocks the 8-bit words into frames, supplies synchronization pattern at the start of each frame, and includes the status register as the last three 16-bit words of each frame. A

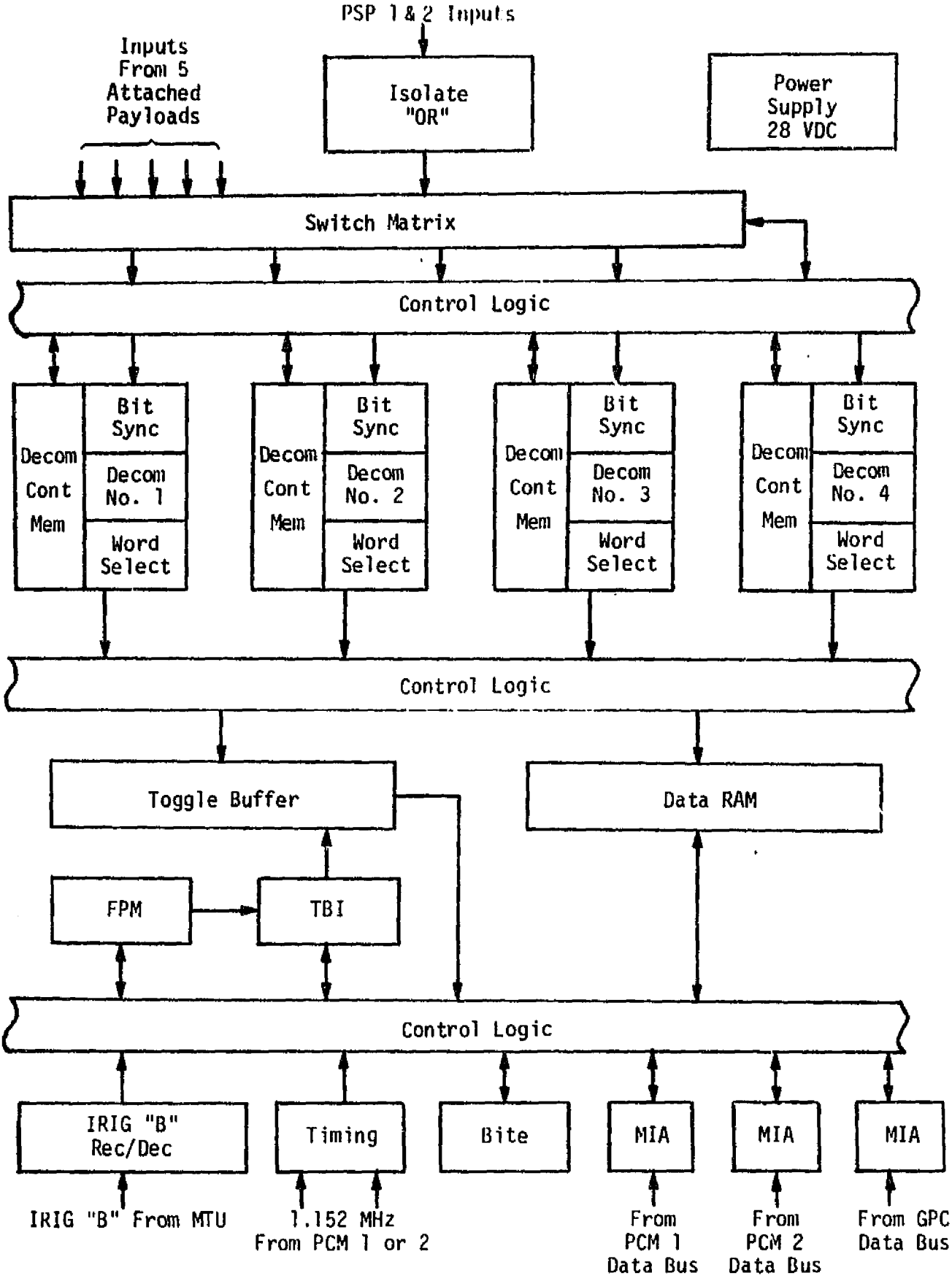

Figure 9. PDI Block Diagram

homogeneous data set for this mode of operation is defined as all information within this PDI-created frame. Code type, bit rate, frame length, and synchronization pattern are programmable under control of the decommutator format memories. The frames are supplied to the toggle buffer for storage as homogeneous data sets. No data is supplied to the data RAM in this mode of operation.

A status register containing the status and time for a given chain operation is provided by the word selector to the Toggle Buffer (TB) control logic. This logic regulates access to and from the half buffers by the word selectors and the data buses. All requests for TB data by the data bus ports are processed through the Fetch Pointer Memory (FPM) and the Toggle Buffer Identifier (TBI). The TB control logic also partitions data from the word selector into homogeneous data sets for access by the data bus ports.

The FPM is used to identify which TB is to be accessed by a data bus port. It also allows access to any location in the data RAM by any of the PDI data bus ports at any time. FPM control logic routes all requests for TB data to the location in the FPM identified by the data bus command word. It further provides for loading and reading of formats to and from the FPM at any time by the data bus ports.

A data RAM for storage of data from the word selector by parameter is provided. The data RAM control logic steers data provided by the word selector into addresses in the data RAM specified by the decommutator control memory.

There are three data bus ports for interface with the Orbiter's GPC that have read and write access into the switch matrix, the decommutator control memory, the FPM, the PDI, and the data RAM.

An IRIG "B" receiver/decoder accepts an IRIG "B" code from an external source, decodes time, and supplies it to the four status registers.

3.7 Ku-Band Signal Processor

The Ku-Band Signal Processor (KuSP) shown in Figure 10 performs the functions of data and signal processing for the Ku-band forward and return links. For the forward link, two modes are available:

(1) A special mode for amplification and impedance matching of

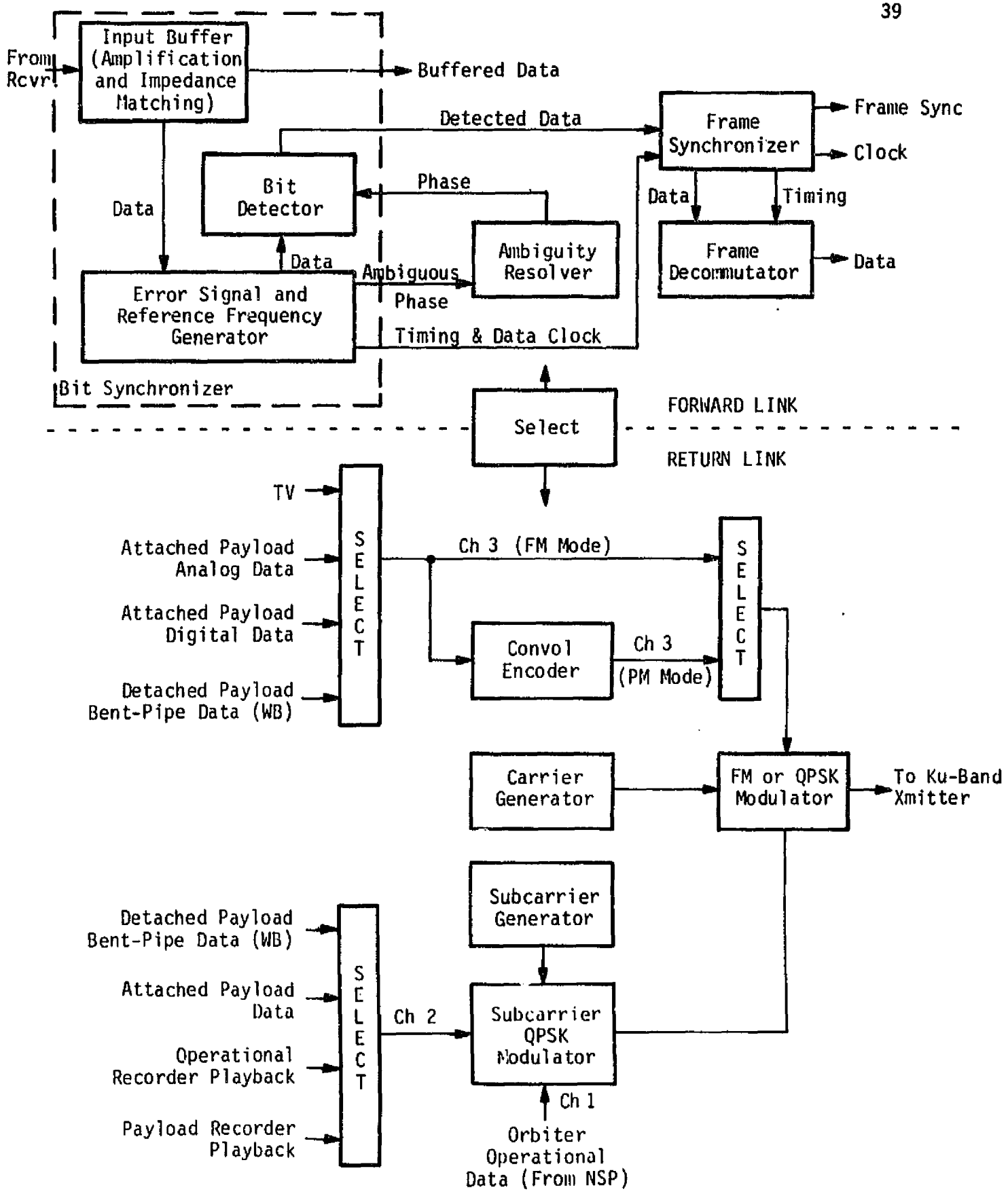

Figure 10. Ku-Band Signal Processor Block Diagram

data from the Ku-band receiver and communication processor assemblies for delivery to the NSP.

(2) A normal mode which performs the operations of bit synchronization, clock generation, ambiguity resolution (data and clock), bit detection, frame synchronization, and data decommutation of Ku-band received data.

Return link signals are handled in the KuSP by modulating the data in one of two modes before upconversion to Ku-band frequencies. The two selectable modes multiplex three channels carrying a wide variety of data. In mode 1, the PM mode, the high rate data channel is convolutionally encoded before modulation onto the carrier. The lower rate data channels 1 and 2 are QPSK modulated onto a square-wave subcarrier which is, in turn, PSK modulated in quadrature with channel 3 onto the carrier.

In mode 2, the FM mode, the two lower rate channels are QPSK modulated onto a square-wave subcarrier as in mode 1. The resulting signal is then summed with the third wideband channel, and the composite signal is then frequency modulated (FM) onto the carrier.

4.0 PAYLOAD COMMUNICATION SYSTEM ISSUES

Each month (with the exception of November), scheduled program reviews were held at the equipment subcontractors (TRW and Hughes). Axiomatix was represented at these reviews. The formal presentations of the hardware development status, schedules and problems usually required one complete day. At times, a second day following was used for splinter meetings wherein technical and specification issues were addressed. The results of the monthly reviews as seen from Axiomatix's perspective and involvement have been summarized in regular Monthly Technical Reports prepared by Axiomatix.

A number of informal engineering discussions were held between Axiomatix and TRW personnel during the year. The subjects most frequently addressed dealt with various aspects of the evolving PI and PSP designs. The information gained generally formed the basis for, or aided in, the analysis of specific problem areas by both TRW and Axiomatix.

4.1 Summary of Important Issues/Problems and Their Resolution/Status

The following recounts the major issues with which Axiomatix had some degree of involvement and which appeared in the Monthly Technical Reports. Table 7 summarizes the major issues by addressing the nature of the issue and the effort expended by all concerned (TRW, Rockwell, NASA and Axiomatix) toward its resolution.

Where the issue impacted the hardware design of the system, the progress toward resolution has been delineated in the final report of Contract NAS 9-15514A (Axiomatix Report No. R7901-3, January 20, 1979). The following subsections outline a number of system-oriented topics that have been given impetus by the issues and related system studies.

4.2 Signal Acquisition

Signal acquisition is defined as the process of achieving the necessary steady-state synchronization of the equipment in order that digital data may be properly demodulated and detected. For the PI, it involves obtaining phase lock onto the discrete carrier component of the received signal and establishment of carrier AGC and output interface (to the PSP or CIU) AGC. For the PSP or CIU, signal acquisition consists of locking the Costas subcarrier loop(s) and the bit synchronizer(s). Once

Table 7. Major Payload System Issues Summary

Issue	Issue Nature	Effort Toward Resolution	Resolution
PI Receiver Wideband Output Regulation to KuSP	1. Incompatibility between PI and KuSP specifications 2. Proposed PI RMS AGC regulator does not optimize FM bent-pipe link performance	1. Assess bent-pipe performance using various types of regulation characteristics (Axiomatix) 2. Propose a signal peak regulation circuit (Axiomatix)	Change PI output to KuSP to be unregulated (no AGC). Place regulation circuit in KuSP (NASA and Rockwell)
PI Received Carrier Modulation Index Limits	1. Undetermined PI receiver performance for payload subcarrier modulation. index larger than 1 rad 2. Undetermined PI receiver performance with two or more payload subcarriers.	Complete parametric analysis of the PI carrier and subcarrier levels as a function of modulation index and waveform types (Axiomatix)	Results of analysis made known to TRW (Axiomatix)
PI Input Sensitivity Ranges	Exact requirement of Rockwell specification on three receiver sensitivity levels needs further definition	1. Meet the requirement by using RF signal level limiting (TRW) 2. Use manual signal level attenuators (TRW and NASA)	Manual attenuator approach selected. Preamplifier overload diodes as alternate under investigation (TRW)
PI Transmitter Phase Noise	1. Incomplete specification on transmitter phase noise with respect to DSN payloads 2. Possible excessive phase noise due to TRW frequency synthesizer design	1. Analysis of synthesizer phase noise (TRW) 2. Phase noise measurements of synthesizer breadboard (TRW)	In process. Preliminary measurements show phase noise to be within spec
PI Wideband Output HPF	The PI wideband output to all interfaces is AC coupled. For nonstandard modulations (e.g., NRZ and no subcarrier), excessive waveform distortion may result	1. Establishment of nonstandard NRZ lower data rate limits (Axiomatix) 2. Analysis of HPF effects (Axiomatix)	Current TRW design acceptable but close to marginal. Recommended changes suggested (Axiomatix)

Table 7. (Continued)

Issue	Issue Nature	Effort Toward Resolution	Resolution
PI Interference Susceptibility	Rockwell specification that the PI receiver should work with an out-of-band interference signal level as large as -25 dBm	Analysis showed that, with the expected receiver first LO noise characteristics, only a -65 dBm interference signal level can be tolerated (TRW and Axiomatix)	Specification amended to the -65 dBm signal level (Rockwell)
PI False Lock Susceptibility	1. PI receiver false lock discrimination with respect to standard and nonstandard payload modulations 2. Degree to which basic PI design should be augmented to include anti-false-lock circuits	1. Analysis of PI susceptibility to standard modulations (TRW) 2. Survey of anti-false-lock methods (TRW and Axiomatix) 3. Analysis of strong signal phase demodulation discriminator (Axiomatix)	In process. Protection only against standard modulations is currently being considered. Methods still under review
PI Receiver Frequency Sweep Acquisition Strategy	1. Methods of initiating and stopping sweep not fully analyzed 2. Sweep range and rates may be inadequate for all postulated conditions.	1. Sweep on and off strategy under study (Axiomatix). 2. Sweep range and rates are being reevaluated (TRW)	In process. Lower sweep rate for DSN payloads required. Wider PI receiver sweep range needed (Axiomatix)
PI RMS Regulator Performance and Wideband Interface to PSP and CIU	Current specification calls for 2V RMS and 6V p-p range above which amplitude clipping occurs.	Specification should be 2V RMS and 12V p-p above which amplitude clipping is OK (Axiomatix)	Recommendation to be made
PSP Data Transition Characteristics	1. Lack of consideration in PSP design for data formats 2. Unspecified transition requirements for minimum performance	1. Evolving TRW design has incorporated provisions for formats 2. Transition characteristics require definition by NASA/Rockwell	Use NASA Data Standards.

Table 7. (Continued)

Issue	Issue Nature	Effort Toward Resolution	Resolution
PSP Performance Losses	Overall PSP degradation is specified at 1.5 dB. No partitioning between subcarrier loop and bit synchronizer is given	1. Analysis indicates bit synchronizer will contribute majority of loss (TRW) 2. Bit synchronizer performance will depend on data transition density (Axiomatix)	In process
Bent-Pipe Modulation Characteristics	No definition of bent-pipe modulations exists	1. Rationale for modulation restrictions developed (Axiomatix) 2. Some specific modulation types and forms suggested (Rockwell and NASA).	Further study required to reach agreement on characteristics and their impact on payload equipment.
CIU Interfaces	CIU compatibility with PI and MDM interfaces	Specification and interface review identified incompatibilities (Axiomatix, NASA, SAMSO & TRW)	Appropriate agencies taking action
Possible Payload Receiver (Transponder) False Lock	When command modulation is "on" and the PI transmitter is frequency swept, the payload receiver could lock to a carrier sideband	Study of possible conditions (Axiomatix)	Recommendation that modulation be "off" during acquisition (Axiomatix)
Payload Communications Turn-Around Characteristics	Possible effects of turn-around phase noise	Analysis to predict performance available. PI phase noise characteristics need to be known	Assessment awaits TRW PI phase noise data

data has been detected (i.e., hard decisions are made as to whether a "one" or a "zero" has been received), other circuits must recognize fixed patterns or codes within the data stream before the data can be declared as valid or some other action can take place.

During the reporting period, the PI has been the focus of signal acquisition strategies and problems. Several aspects are discussed in the following subsections.

4.2.1 Swept Acquisition Methodology

The PI has the capability of acquiring both the forward link (to the payload) and the return link (from the payload) by means of linear frequency sweeps of the transmitter and receiver over some nominal ranges. Tables 8 and 9 list, respectively, the TRW-proposed transmitter and receiver frequency parameters. All of the transmitter frequency control, including sweep, is resident in the PI frequency synthesizer. Receiver frequency control insofar as channel selection is concerned is also part of the frequency synthesizer. However, frequency sweep is generated by applying an analog sawtooth waveform to the receiver's PLL VCO.

In order for a PLL to reliably acquire and track a linear sweep frequency, the relationship between the sweep rate and the PLL natural frequency is [2]

$$\omega_{sweep} \leq \frac{1}{2} \omega_n^2 \tag{1}$$

where ω_n is the PLL natural frequency (rad/sec) which is nominally related to the PLL two-sided loop noise bandwidth, $2B_L$, by

$$\omega_n = 2B_L/1.06 \tag{2}$$

For the payload receiver tracking loop bandwidths indicated in Table 6, the maximum sweep rates have been calculated and are shown in Table 10. Comparing the sweep rates shown in Table 10 with the PI transmitter capabilities indicated in Table 7 shows that the narrow sweep rate is too fast for payload transponders that have either 60 Hz or 18 Hz tracking bandwidths. It therefore appears that the slow sweep rate should be lowered to, say, nominally 20 Hz/sec. In fact, for optimum acquisition

Table 8. PI Transmitter Frequency Parameters

Mode	Channel	Frequency Range	Frequency Step Size	Frequency Sweep Range	Frequency Sweep Rate
STDN (NASA)	1 to 808	2025.8-2118.7 MHz	115 kHz	±55 kHz	30 kHz/sec
DSN (NASA)	850 to 882	2108.8-2119.8 MHz	341.05 kHz	±33 kHz	540 Hz/sec
SGLS (DOD)	900 to 919	1763.7-1839.8 MHz	4.004 MHz	±55 kHz	30 kHz/sec

Nominal Carrier Frequency Tolerance = ±0.001%

Wide Sweep Tolerances: Range = ±5 kHz
Sweep Rate = ±5 kHz/sec

Narrow Sweep Tolerances: Range = ±3 kHz
Sweep Rate = ±60 Hz/sec

Table 9. PI Receiver Frequency Parameters

Mode	Channel	Frequency Range	Frequency Step Size	Frequency Sweep Range	Frequency Sweep Rate
STDN (NASA)	1 to 808	1985-2085.875 MHz	125 kHz	±85 kHz	10 kHz/sec
DSN (NASA)	850 to 882	2075.2-2087.1 MHz	370.37 kHz		
SGLS (DOD)	900 to 919	1987.5-2082.5 MHz	5.0 MHz		

Nominal Frequency Tolerance = ±0.001%

Sweep tolerances are not specified. The absolute maximum frequency deviation of the receiver VCO is ±100 kHz.

Table 10. Maximum Allowable Acquisition Sweep Rates for Various Payload Tracking Bandwidths

Two-Sided Tracking Loop Bandwidth	Maximum Acquisition Sweep Rate
2000	283 kHz/sec
1000	71 kHz/sec
200	2.83 kHz/sec
60	255 Hz/sec
18	23 Hz/sec

over the large range of possible tracking loop bandwidths, three, rather than two, sweep rates appear to be in order. These rates might best be:

Fast Sweep Rate = 30 kHz/sec
Medium Sweep Rate = 800 Hz/sec
Slow Sweep Rate = 20 Hz/sec

At the lower sweep rates, the probable acquisition time can be very long. For example, it takes 55 seconds to sweep the 66 kHz range at 20 Hz/sec. Thus, it seems that some a priori knowledge should be employed to start the sweep in the vicinity of the expected nominal receiver frequency (determined by past history) rather than beginning the sweep at the nominal PI transmitter channel frequency. The current PI design, however, does not allow for initialization of this type. Such capability should therefore be subject to review as to design and cost impact.

The frequency turn-around ratio for NASA payload transponders is 240/221 and for DOD transponders is 256/205. This means that, whatever the forward link frequency sweep range and rate, the return link signal is modulated by the forward link parameters increased by the turn-around ratio factors when the payload transponder is in its two-way mode. Thus, the DOD forward link sweep of ±55 kHz at 30 kHz/sec is seen on the return link signal as ±69 kHz at 37 kHz/sec. Taking into account worst-case tolerances, the return link carrier could be swept ±75 kHz at a rate of 44 kHz/sec.

Now, from Table 9, the receiver sweep rate, which is totally independent of the transmitter sweep process, is 10 kHz/sec. Assuming a worst-case tolerance on this rate to be 10%, it is seen that, if the turned-around transmitter rate and receiver rate are such that they add, the net receiver acquisition rate could be as large as 48 kHz/sec. Using (1) and (2), the minimum receiver two-sided tracking loop bandwidth would have to be 823 Hz in order to insure reliable acquisition. The current (January 1979) TRW design value for this bandwidth is 1200 Hz.

When the forward link is in the unacquired state, the payload transmitter usually derives its frequency from an auxiliary oscillator. For NASA standard transponders, the overall stability of this frequency source is on the order of $\pm 5 \times 10^{-6}$ which, at the high end of the transmitter band (2300 MHz), gives a maximum frequency error of ±12 kHz.

If the receiver frequency synthesizer and VCO each have a maximum error of 0.001%, the frequency uncertainty range which the receiver must accommodate in the one-way mode is ±58 kHz. Current TRW PI design allows the receiver to sweep ±85 kHz about the nominal receive frequency; thus, the design appears to be adequate for the one-way situation.

For two-way operation, the total frequency uncertainty could be as great as ±70 kHz due to maximum tolerances on all frequency sources. However, the way in which the combined uncertainties and sweep ranges might misalign portends a certain degree of incompatibility. Figure 11 shows such an extreme case. Here the swept carrier from the payload is offset to its maximum positive limit while the PI receiver swept range is offset to its negative limit. Clearly, the receiver range cannot cover the relative frequency range between +39 kHz and +98 kHz. Further, even if acquisition is achieved on the overlap range, the PI VCO cannot track more than ±100 kHz from its nominal frequency. Thus, lock would be lost whenever the received signal sweep exceeds +54 kHz [f_{VCO} (max)]. Only if the PI transmitter sweep were discontinued during an in-lock frequency overlap period, wherein the received frequency would rest at its nominal value (f_0 = +23 kHz), could lock be maintained. The conclusion, therefore, is that a ±65 kHz sweep range for the PI receiver is inadequate and that a sweep range on the order of ±145 kHz is needed, all other operating parameters remaining unchanged.

The method and manner of initiating and stopping the receiver sweep is controlled by the receiver lock detector. When the receiver is out of lock for a period of time exceeding 0.5 sec, the sweep is automatically applied to the VCO. Sweep voltage is generated by means of an operational integrator which is an inherent part of the loop filter. The loop filter capacitor serves as the integrator storage element. Sweeping is accomplished closed-loop such that the VCO responds to the sum of the loop phase detector and sweep voltages. When the sweep frequency reaches its upper maximum value as determined by sensing the value of the VCO input voltage, the capacitor voltage is initialized to the maximum negative value (corresponding to the minimum frequency) and the integration process continues. Thus, a sawtooth type of sweep waveform is generated.

Whenever the lock detector indicates a state of in-lock, the

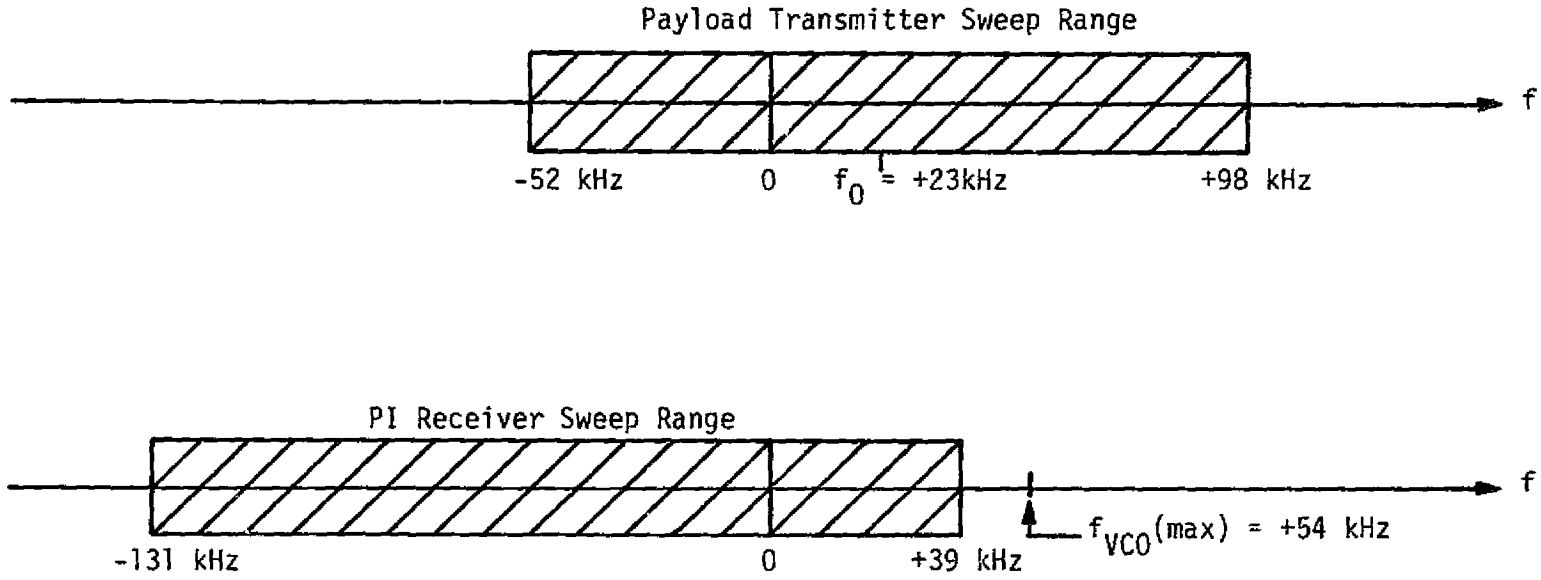

Frequencies are relative. f=0 represents the channel true center frequency.

Figure 11. Transmitter/Receiver Extreme Frequency Offset

sweep is instantly removed by switching off the steady current into the operational integrator. If lock has truly occurred, there will be a settling period wherein the loop phase detector output changes to produce the necessary drive voltage to keep the VCO at the correct frequency and phase. Therefore, since the sweep is not designed to retain frequency "memory" at the point of acquisition, loop stress or static phase error must result whenever there is frequency error between the received signal and the receiver frequency synthesizer and VCO. The problem with this mechanization is that very large loop gains are required if the maximum static phase error is to be kept small. Axiomatix believes that such static phase error should be held to less than 10° so that (1) data demodulation efficiency is high (less than 0.2 dB power loss) and (2) the combined effects of additive noise, data modulation, and oscillator instability produced phase jitter do not cause the loop to slip cycles or lose lock.

In conclusion, it is noted that the current PI design has no means for disabling the receiver sweep or otherwise starting or stopping it apart from the lock detector control. There also exist some potential problems of premature sweep disable due to false states of in-lock indicated by the lock detector; see [3, Subsections 4.2.1.5 and 5.3.2] for details.

4.2.2 Receiver False Lock

Rockwell's specification most generally states: "The receiver shall not lock-on to sidebands." TRW's initial assessment was that they would comply with the false lock specification by "precluding sideband false lock as a design goal." TRW held that there probably would be no problem in meeting the intent of this specification for normal modulations by the 1.024 MHz and 1.7 MHz subcarriers. Their concern was with "bent-pipe" modulations, which still remain undefined.

It was found that TRW's initial conceptual design of the receiver was such that certain standard modulation conditions could produce false states of in-lock. Axiomatix determined that the problem was a function of lack of receiver out-of-lock IFA gain control and the setting of the lock detector threshold voltage according to a minimum operating point some 6 dB below that required by the Rockwell specification. Axiomatix

therefore recommended use of a noncoherent receiver AGC during periods prior to acquisition. This recommendation was acted upon by TRW to the effect that false states of in-lock for standard modulations have been virtually eliminated. See [3, subsections 4.2.1.5 and 6.1] for details regarding the standard modulation false lock problem.

Nonstandard modulations, and the propensity of their characteristics to give rise to potential PI receiver false lock, remain as a major issue requiring resolution. It is clear that definitions of "nonstandard" payload modulation characteristics are required if the receiver design is to realistically preclude false lock to "bent-pipe" signals. Further, the methods for antisideband false lock require detailed study and analysis if such circuits are to be effectively incorporated into the PI receiver.

Presently, the capability of the PI receiver to preclude false lock is based upon the operation of the PLL lock detector and its discrimination against inhibiting receiver sweep frequency acquisition with respect to small discrete sideband levels as compared to that of the true carrier component. Since the ability of the lock detector as an antisideband false lock device is limited due to its inherent characteristics, additional means must be incorporated if the lock detector performance alone proves inadequate. Suggestions for augmented anti-false-lock capability have all included some form of frequency spectrum discrimination which can be used to determine whether the receiver tracking loop is truly centered on the proper discrete carrier. The principal ideas that have been given some consideration are:

(1) Employ an AFC loop and discriminator-based lock detector in conjunction with the APC loop and coherent lock detector in the PI receiver.

(2) Eliminate receiver swept acquisition in favor of frequency-discriminator centering of the VCO frequency.

(3) Use a noncoherent (discriminator-type) receiver for strong signals, relegating the PI to weak signal conditions only, thus avoiding the strong signal false lock problems.

(4) Determine via ground-based observations whether bent-pipe signals are proper, i.e., whether the PI receiver may be tracking a sideband

rather than the carrier, and command the PI into a reacquisition mode if needed.

(5) Employ several receiver swept acquisition frequency sweep rates as a function of received signal level. Faster rates at strong signal levels preclude false lock to sidebands.

Of the above, after much discussion between Axiomatix, NASA, and TRW engineers, only approaches (1) and (3) appear to be the most viable.

Axiomatix has surveyed four discriminator antilock circuits that have been used in other receiver designs (see subsection 5.3.3 of [3] for details). Additional analyses have been performed and are reported in subsection 5.1.3 of this report to show how a closed-loop frequency discriminator may be used to decrease PLL false lock sensitivity. From the results, one may make the necessary trade-off between improving acquisition performance (as measured by false lock sensitivity for a given sweep rate) and deteriorating tracking performance (as measured by mean-squared phase jitter due to additive noise). No AFC loop techniques are, however, currently being given serious consideration for implementation within the PI.

Axiomatix has also given conceptual consideration to a discriminator-based lock detector. This would work in conjunction with the coherent lock detector in order to continue or discontinue the sweep acquisition process within the receiver. Detailed work and analysis will be performed during CY79.

Both TRW and Axiomatix have analyzed the use of a discriminator for strong signal phase demodulation. The analysis and results, which are summarized in subsection 5.2.1 of this report, indicate that this method might be useful for signal levels as low as -100 dBm for various types of bent-pipe modulations. Optimum performance would be dependent upon a discriminator receiver that can be adjusted to match the received signal bandwidth characteristics.

4.2.3 Modulation Characteristics and Restrictions

One method of precluding PI receiver false lock is to restrict the payload modulation such that carrier sideband components which give rise to the potential of false lock are not allowed. The task of generating such restrictions is not an easy one because: (1) theoretical acquisition

performance of PLL receivers with respect to many of the possible modulation forms is unknown, and (2) there are many parameters that must be taken into consideration. However, Axiomatix has made an attempt to develop a rationale upon which a set of restrictions might be based. The rationale is developed in subsection 5.2.2, and a set of restrictions in the form of a Strawman User's Guideline appears in Appendix C.

4.3 Tracking and Detection

Tracking is defined as the process of following the phase or epoch of a given signal (carrier, subcarrier, data stream, etc.) in the presence of additive and multiplicative noise. Detection involves the clean-up or recovery of demodulated intelligence signals by means of filtering and decision-making processes. Carrier and subcarrier demodulation are an inherent part of the tracking function.

In the PI, the receiver coherently tracks the received signal discrete carrier component and simultaneously demodulates the modulation that was placed on the carrier within the payload. The PSP and CIU function to track and demodulate subcarriers that have been biphase modulated with digital data streams, perform bit synchronization of the demodulated data streams, and make matched filter decisions on the state of the received bits.

Since all aspects of the additive and multiplicative noise, as well as certain signal characteristics, combine to cause imperfections in tracking and detection, they are very important from a system point of view as to their effects on overall performance degradation. Several topics within this category that have been addressed during the reporting period are outlined in the following subsections.

4.3.1 PI Phase Noise

Phase noise will arise in the PI frequency synthesizer and the receiver tracking loop VCO. Since the PI is not a transponder, there is no problem with turn-around phase noise. However, the phase noise specifications, especially on the transmitter, are incomplete, and there is some concern as to whether the phase noise characteristics of the forward link will be adequate to payload transponders which have narrow tracking loop bandwidths (e.g., a DSN transponder with $2B_L$ = 18 Hz).

The PI transmitter S-band output phase noise has been simply specified by Rockwell at 4° RMS in a 300 Hz test bandwidth. Axiomatix has made the point that this does not necessarily guarantee that a 10° RMS error in a 10 Hz test bandwidth will be obtained. This latter requirement stems from the need to properly communicate with DSN-type payload transponders.

TRW's conceptual transmitter frequency synthesizer design employs one TCXO, two VCXOs and two VCOs, all of which interact in generating reference and output frequencies. Two potential problems have been noted by Axiomatix:

(1) Incomplete performance parameters preclude analysis to predict internal PLL acquisition and tracking characteristics or whether frequency-divider induced noise will be prevalent.

(2) There is no indication whether the S-band phase noise will be sufficiently small to achieve a 10° RMS error in a 10 Hz test bandwidth.

TRW has made available a two-year-old analysis from a previous program for a similar synthesizer which shows the phase noise should be between 6° RMS and 10° RMS in a 10 Hz bandwidth. It is concluded, however, that the final assessment will have to await breadboard tests. Such testing, originally scheduled for the summer months of 1978, was delayed due to fiscal year funding problems and manpower diversion. No definitive test results have been produced, as of the writing of this report, which convince Axiomatix that the requirement will be met by the TRW design.

This potential problem will be closely followed by Axiomatix during the CY79 design detail and breadboard testing activities. It may prove necessary to test the breadboard with an actual DSN flight transponder in order to obtain a quantitative assessment of phase noise performance.

An additional effort that should be accomplished in terms of payload system performance evaluation is an accounting for the turn-around phase noise. Axiomatix has previously addressed this problem [4] in terms of the model and mathematical formulation. A review of overall performance (taking into consideration the latest PI capabilities status) is therefore appropriate once good phase noise test data becomes available.

4.3.2 Payload Interrogator and Payload Signal Processor Interface

The wideband signal delivered to the PSP from the PI is to be regulated and held constant to a 2V RMS value. The current Rockwell specification adds, in addition, that a 6V peak-to-peak (3V zero-to-peak) linear transfer capability shall exist, outside of which amplitude clipping will take place. This means that any waveform having a peak-to-RMS ratio larger than 1.5 will experience amplitude limiting and will cause SNR performance loss.

Table 11 lists the peak-to-RMS values for typical complex waveforms that may be present at the PI/PSP interface. As can be seen, only the first two entries will be transferred without clipping. Since, for all possible modulations, the output of the PI for weak received signals (< -100 dBm) is essentially Gaussian in character, the output will be clipped.

As it is undesirable to clip Gaussian noise peaks below the 3σ level, a 12V peak-to-peak output amplifier range is required. This capability will also accommodate up to four simultaneous subcarriers without clipping, and five subcarriers with only occasional clipping. It is recommended, therefore, that the requirement be changed to provide a 12V peak-to-peak linear transfer capability.

The PI receiver PLL can be viewed as a highpass filter insofar as the demodulation of the sidebands is concerned. This can be particularly important for direct carrier (no subcarrier) data modulations of the NRZ form. Such conditions could exist for the nonstandard bent-pipe link. The requirement is that the highpass characteristics do not adversely affect the demodulated data waveform by filtering out significant waveform frequency components, nor should the data waveform introduce large tracking jitter within the PLL. This requirement must, therefore, impose specifications on minimum NRZ data rate and the maximum period of transitionless bits.

It is also desirable that the video amplifier which provides the PI receiver wideband output signal to the KuSP have a dc blocking capacitor between its output and the KuSP input. Requirement for this stems from the fact that all the circuits within the KuSP, including those of the FM transmitter, are direct coupled. Thus, any direct voltage offsets

Table 11. Peak-To-RMS Values of Various Waveforms

Waveform Type	Peak/RMS Value
Square-Wave; Binary Data	1.0
Single Sinewave Subcarrier	1.4
Two Equal Amplitude Incoherent Subcarriers	2.0
Three Equal Amplitude Incoherent Subcarriers	2.5
Four Equal Amplitude Incoherent Subcarriers	2.8
Gaussian Noise	3.0
Five Equal Amplitude Incoherent Subcarriers	3.2

arising within the PI receiver output circuits could, without the use of ac coupling, "detune" the FM transmitter. Given that an output coupling capacitor is to be used, it is also desirable to utilize additional capacitive coupling within the PI circuits themselves. The overall net effect is to place a two-pole highpass filter between the PI receiver's wideband phase demodulator and the input to the KuSP.

Subsection 5.4 of [3] contains an analysis which establishes the proper data stream and highpass filter specifications. Direct modulation of the carrier by NRZ data should not introduce more than 10° RMS phase jitter in the PI receiver PLL, and the maximum phase reference slewing due to periods of transitionless data should not exceed 18°. For the TRW maximum* PLL noise bandwidth design value of 1460 Hz, the data stream restrictions are:

(1) $R_b > 185$ kbps, and

(2) Maximum string of no-transition bits = 30 for the bit rate of 185 kbps.

Additionally, the HPF following the PLL should not introduce any more than -0.1 dB of data power loss; therefore, the 3 dB frequency of each of the two cascaded HPFs should be less than 678 Hz. Axiomatix recommends that each of the HPF sections have a 3 dB frequency of 200 Hz.

4.3.3 Payload Modulation Index Limits

From the beginning of the PI development activity, TRW consistently commented on the fact that the PI carrier tracking loop operation would be TBS for phase deviation β on the range of $1.0 < \beta \leq 2.5$ rad. They further recommended that PI receiver performance be specified only for the range $0.3 \leq \beta \leq 1.0$ rad.

The major problem appeared to be one of interpretation of intent on the part of the PI specification. Rockwell had established the minimum PI residual carrier level which, in effect, bounds the modulation index insofar as carrier suppression is concerned (given maximum range and worst-case performance conditions). The modulation indices for standard 1.024 MHz and 1.7 MHz subcarriers are set at 0.3 or 1.0 rad peak. No specific characteristics were established, however, for nonstandard

*Strong received signal conditions.

bent-pipe modulations. All that was specified is:

> "Information (modulations) with indices of up to 2.5 radians will be detected, provided a minimum of -122.5 dBm for acquisition and -124 dBm for tracking residual carrier is present."

This is the proper general way to specify the relationship of modulation index to receiver acquisition and demodulation performance.

The β range ($0.3 < \beta < 2.5$ rad) is, in reality, on the payload transmitter capability and not on the PI receiver. The receiver need only work with received signals whose characteristics are such that a residual carrier is present with sufficient power. It should also be noted that there may be payload signal formats where three or more subcarriers could simultaneously modulate the transmitter, each with a $\beta < 1.0$ rad but with a combined peak deviation on the order of 2.5 rad (thus, the need for the β range specification).

As a result of all these considerations, Axiomatix proceeded to perform an analysis intended to:

(1) Determine PI output component levels for the mixed subcarrier cases.

(2) Show when various combinations of individual bent-pipe signal modulation index violate the residual carrier requirements or otherwise degrade PI performance.

The analysis and results appear in subsection 5.3. Three specific cases of modulation are considered.

Case I: A single sinusoidal modulation, with application to either a 1.024 MHz or a 1.7 MHz subcarrier phase modulating the carrier.
Case II: Two sinusoidal modulations, with application to simultaneous 1.024 MHz and 1.7 MHz subcarriers phase modulating the carrier.
Case III: A sinusoidal plus a "square" type modulation, with application to a sinusoidal subcarrier and a lowpass digital data signal simultaneously phase modulating the carrier. (This case could be typical of a nonstandard bent-pipe class of modulation.)

For each of these cases, plots of the normalized carrier and sideband power levels as a function of modulation index are provided, and conclusions are made with respect to residual carrier suppression and modulation index limits. Within these limits, the PI receiver tracking and demodulation performance is in no way compromised.

4.4 Bent-Pipe Characteristics

4.4.1 General Description

The standard telemetry data capability available for attached and detached payloads provides for a reasonable degree of flexible operation. It may happen, however, that certain payloads are not able to avail themselves of the standard system. To accommodate payloads whose telemetry formats are not compatible with standard data rates and subcarrier frequencies, bent-pipe modes of operation are provided within the Shuttle's avionic equipment. Several signal paths acting as "transparent throughputs" are available for both digital and analog signals.

Nonstandard telemetry forms (e.g., data rate, coding) and modulations (e.g., nonstandard subcarrier frequencies, direct carrier modulation by data) are allowed on the return link provided that they are compatible with the PI. Specifically, they must have a residual carrier component and sideband characteristics that do not promote PI receiver false lock or in any way compromise PI operation. It must also be understood that, beyond acting as a bent-pipe to nonstandard modulations, the Orbiter's avionic subsystems cannot be used to demodulate, detect, decode, or otherwise process such signals.

When the Ku-band relay link is operating in its QPSK mode, digital data streams at rates higher than 64 kbps (which therefore cannot be handled by the PDI) may directly enter the KuSP where they may be (1) QPSK modulated onto an 8.5 MHz subcarrier or (2) QPSK modulated onto the Ku-band carrier. Detection and processing of all such data occur at the ground stations.

When the Ku-band relay link is operating in its FM mode, digital and analog signals may take one of two modulation paths. (The Ku-band FM bent-pipe link functional block diagram is shown in Figure 12.) If the signal is in the form of a modulated subcarrier and does not have significant frequency components above 2 MHz (i.e., narrowband), it may be hard-limited (i.e., a two-level or one-bit-quantized waveform produced) and treated as a "digital" signal by the 8.5 MHz subcarrier QPSK modulator. On the other hand, if the signal is baseband in nature on a frequency range up to 4.5 MHz (i.e., wideband), it may be transmitted via the Ku-band link utilizing direct FM. Again, all processing is accomplished on the ground.

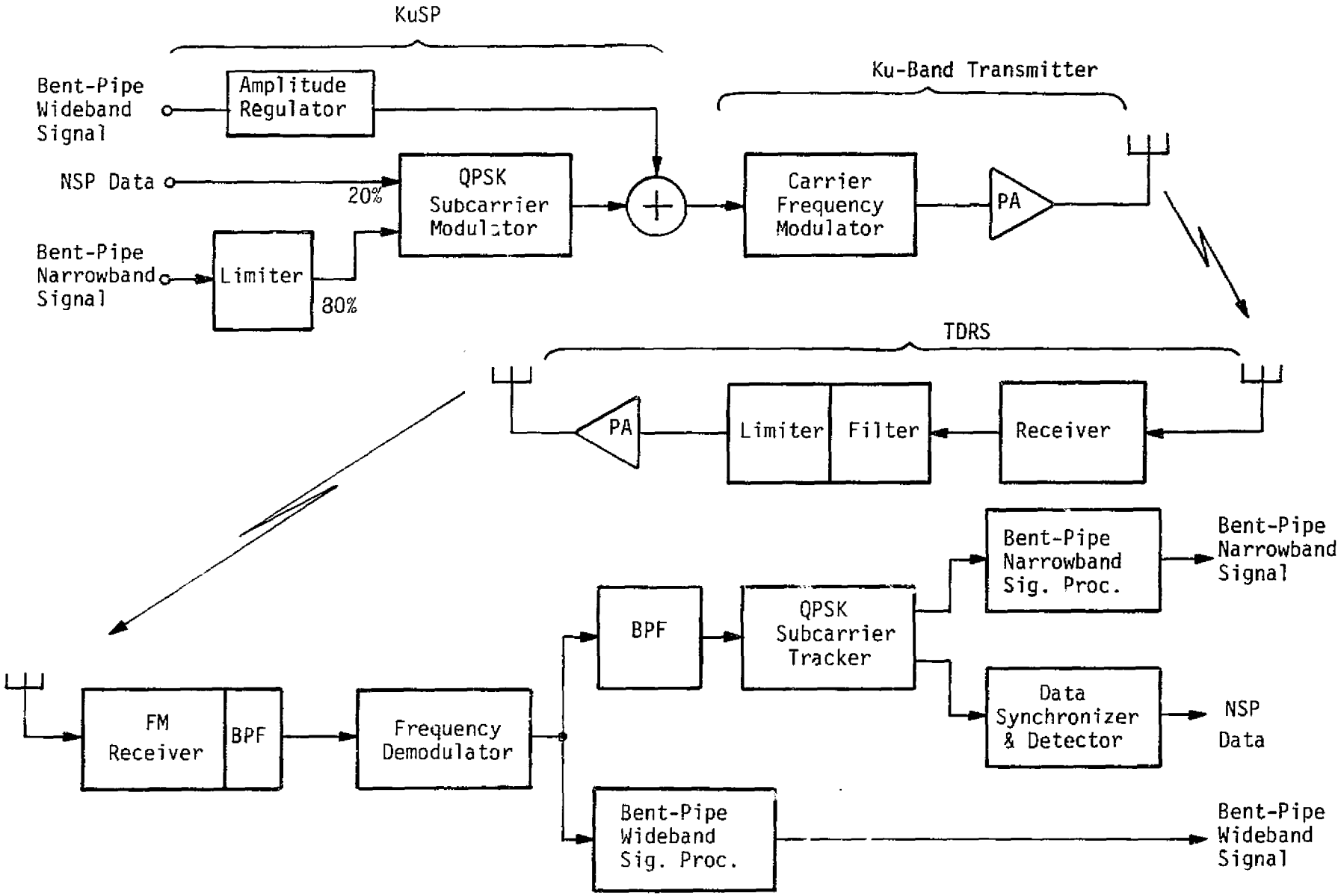

Figure 12. Ku-Band Bent-Pipe FM Link

4.4.2 Payload Interrogator and Ku-Band Signal Processor Interface

As discussed in subsection 4.3.2, the PI employs an RMS regulator as an AGC on the wideband demodulated signal. Originally, this RMS scaled signal was to be output in like manner to the PSP, CIU, and KuSP. This meant that the drive signal into the Ku-band frequency modulator would always be set in proportion to its RMS value, irrespective of its waveform. Axiomatix proceeded to analyze the implications of using the RMS regulating loop for FM bent-pipe signals. Analysis which fully accounted for both noise sources in the Ku-band bent-pipe link model showed that a peak-type regulator would outperform the RMS-type regulator under all conditions and would provide a minimum overall link improvement of 1.1 dB for high data rate NRZ data. Significantly larger improvements can be expected for other qualifications (see subsection 5.4.1).

Following several round-table technical discussions between NASA, Axiomatix and Rockwell personnel, it was concluded that any necessary signal waveform conditioning required to optimize the Ku-band FM bent-pipe link is properly a function of the KuSP rather than the PI. This conclusion was based primarily upon the fact that attached, as well as detached, payload signals must be regulated and properly scaled within the KuSP. Since the PI is not employed in the attached payload configuration, consigning such regulation to the PI for its signals would also mean that every payload would have to provide similar capability at the payload/KuSP interface. This burden, it was concluded, should not be placed on the user, and it therefore became universally agreed that such regulation and its necessary circuits should be incorporated into the KuSP. The location of the regulator in the wideband FM channel is shown on Figure 12. The nature of such regulation capability, however, was left open, and Axiomatix was requested by Rockwell to further review the requirements and necessary circuit designs and make recommendations. In order to avoid potential problems with tandem regulator circuits (one in the PI and the other in the KuSP), TRW was requested to review the PI receiver wideband output design so that the signal interface to the KuSP circumvents the RMS AGC circuits. The RMS regulator will therefore be used only for the PSP and CIU interfaces.

The results of Axiomatix's analysis and design assessment, as it

has progressed to the writing of this report, are delineated in subsection 5.4. The conclusion reached by Axiomatix is that a peak-to-peak type of regulator always gives equal or superior performance compared to an RMS type regulator for all of the types of waveforms and SNR conditions that were considered.

One expressed concern over a peak regulator is that such a regulating loop may be complex to implement and that proper response time/conditions may be difficult to achieve. Axiomatix has therefore initiated a program to assess what is functionally required of a signal peak regulating loop, to generate a detailed design for a peak regulating circuit, and to functionally breadboard and evaluate the peak regulator's performance relative to the types of anticipated waveforms with which it must operate. Some of the performance goals that the peak regulator is expected to attain are:

Throughput Lowpass BW	= 4.5 MHz
Regulation Range	= >40 dB
Signal Peak Sampling Period	= 1 ms (alterable)
Regulation Loop Time Constant	= 1 sec (alterable)

Details of all this activity may be found in subsection 5.4.2.

4.5 Commonality of Payload Signal Processor and Communication Interface Unit Functions

Functional descriptions of the PSP and CIU appear in subsections 3.4 and 3.5, respectively. As can be seen, each unit interfaces with essentially the same avionic equipment in nearly identical fashion, and internally, very similar (and some identical) functions are performed.

A review in August 1978 of the CIU interface requirements disclosed several CIU specification incompatibilities with respect to the CIU/MDM interface. Digital command data buffering and decoding by the CIU of burst inputs from the MDM proved to be the central problem. It was then suggested that, since the PSP is already designed to perform these functions, a simpler interface could be obtained between the CIU and the PSP, rather than the CIU and the MDM, and that CIU design would be simplified.

Axiomatix believes that such a change of the interface is reasonable and desirable, especially since TRW is the design and production contractor for both units. Whether this can be accomplished without significantly impacting the cost and schedule of either or both units is not clear. Some formal study by TRW should make such an assessment.

5.0 AXIOMATIX SUPPORTING STUDIES AND ANALYSIS

5.1 Payload Interrogator False Lock Avoidance

5.1.1 Problem Definition

Receivers employing a discrete carrier PLL plus an attendant coherent lock detector are capable of locking or indicating a state of lock when the receiver frequency is centered on sideband frequencies relative to the frequency of the true discrete carrier. Whether an actual and/or indicated state of lock can exist is directly related to the spectral characteristics of the carrier sidebands, the PLL subsidiary acquisition method, the PLL natural frequency, and the lock detector performance parameters.

Three false lock types may be postulated, as indicated in Table 12. Type I might occur for a set of conditions wherein the sideband spectral components that fall within the PLL and lock detector bandwidths are sufficiently random in nature to preclude the generation of an "S-curve" which can force the PLL to lock but are of sufficient intensity to cause the lock detector threshold to be exceeded. False lock Type II is likely when the sideband components are discrete (or nearly discrete) but sufficiently small that the lock detector cannot respond. Type III is obviously a total lock state, but it is classified as false because it does not occur at the frequency of the discrete carrier.

Table 12. False Lock Types

False Lock Type	PLL State	Lock Detector State
I	Out-of-lock	True
II	In-lock	False
III	In-lock	True

False lock Types I and III are of greatest importance to receivers that employ a swept frequency acquisition algorithm, as does the PI. Whenever the lock detector state becomes true, the sweep is terminated,

meaning that the receiver is left to "hang" in frequency at some point from the discrete carrier frequency. It makes no difference whether the loop is, in fact, out-of-lock or in-lock as the lock detector has stopped the sweep acquisition process, and, unless the lock detector subsequently returns to the false state (and it may if the sideband characteristics are changing as a function of time), there is little chance that proper acquisition will be attained.

The problem of avoiding receiver false lock, especially for Type III conditions, has no easy solution. For this reason, the potential of a number of methods which might be applied to the PI has been investigated, but no approach has yet been selected in lieu of, or in addition to, the basic PI receiver lock detector threshold discrimination technique.

It is important to define several aspects of the problem so that the various methods are properly categorized. First, there are two distinct false lock classes or levels to be considered. The first, and most fundamental or theoretical, is the false lock susceptibility of an "ideal" swept acquisition phase-lock type receiver to sidebands of the carrier (whether they may be caused by "standard" or "nonstandard" modulation forms). This may be defined as Fundamental False Lock Susceptibility (FFLS). The second is more realistic and is concerned with the false lock state (however manifested) of a practical receiver implementation to situations that would not give rise to false lock conditions in the ideal receiver. This problem will be referred to as Implementation False Lock Susceptibility (IFLS).

Now, regarding anti-false-lock techniques, there are also two distinctions. First, there is False Lock Avoidance (FLA) wherein the basic premise is that some direct means are provided to preclude the actual state of false phase lock by the tracking loop. FLA is an absolute technique, i.e., false lock is precluded within some set of requirements and restrictions whether the susceptibility is fundamental or a function of implementation. FLA does not necessarily solve the attendant problem associated with the lock detector issuing a true state (false lock Type I). Some methods which have been proposed for FLA are: (1) use of optimized frequency sweep rates, (2) closed-loop AFC aiding, and (3) phase feedback (antimodulation).

The second anti-false-lock technique is defined as False Lock Detection (FLD). Here the premise is that of providing subsidiary means for detecting a possible state of false lock or, alternately, mechanizing the receiver's lock detector in such a way that it will not indicate lock for a specific set of potential false lock conditions even though the tracking loop may have indeed achieved a state of valid lock to a carrier sideband component (false lock Type II). Thus, FLD is a relative technique in that it allows false lock to occur but acts (in some way) to negate such lock and continue the acquisition process until valid carrier lock is obtained. Some methods that have been investigated for FLD include (1) high-biased lock detectors, (2) frequency error detection, and (3) spectrum analyzer.

There is a third method that could be employed to avoid the total problem of coherent receiver false lock. A noncoherent demodulator (e.g., a frequency discriminator followed by an integrator) could be used to recover the carrier phase modulation. If its bandwidth is sufficiently wide to embrace all modulation and frequency uncertainty limits, it requires no acquisition or tuning. The penalty paid for such simplicity of operation, however, is great in terms of demodulated signal waveform distortion and SNR performance. Details regarding the operation of a noncoherent receiver for some potential nonstandard payload modulations are covered in subsection 5.2.1.

Studies of the usefulness and performance of the FLA and FLD techniques are in process. FLA technique (2) has been evaluated as to its ability to reduce the FFLS of a swept acquisition PLL; the analysis and results appear in subsection 5.1.3. FLD technique (1) as applied to the current PI lock detector design proposed by TRW has been evaluated and details are presented in subsection 5.1.2. FLA technique (3) and FLD technique (2) are presently being considered; substantive results, however, await additional effort. Finally, some rationale for avoiding phase lock to specific sideband conditions is developed in subsection 5.2.2 and is used to justify certain payload modulation restrictions which are known to produce a high susceptibility to false lock (especially Type III).

5.1.2 Payload Interrogator Current Design False Lock Discriminator Capability

Figure 13 is a functional block diagram of the PI receiver sweep acquisition and lock detector circuits. (See subsection 3.3 for the overall PI functional description.) The in-phase detector, known as the coherent amplitude detector (CAD), produces the signal used to derive both the receiver's AGC and lock detector voltages. The quadrature phase detector generates the loop error signal which is processed by the loop filter and input to the VCO. An acquisition sweep voltage is also generated through the loop filter and applied to the VCO in order that the receiver frequency may be swept over a ±85 kHz* input signal frequency range uncertainty. Enabling of the sweep function is initiated by an out-of-lock state (after some delay), while the disable signal is generated when the lock detector attains its in-lock state.

For the purpose of analysis, the signal appearing at the input to the phase detectors is taken as a sinusoid of frequency f_0, phase modulated by a second sinusoid of frequency, f_m, viz.,

$$S(t) = \sqrt{2P} \cos \left[\omega_0 t + \beta \cos (\omega_m t)\right] \qquad (3)$$

where β is the phase modulation index. This is a good signal model for predicting worst-case lock detector performance. When β is small, as it must be in order to have sidebands with relatively low power content (less than -20 dBc), (3) may be approximated by:

$$S(t) \cong \sqrt{2P_0} \cos \omega_0 t - \sqrt{2P_1} \sin (\omega_0 - \omega_m)t - \sqrt{2P_1} \sin (\omega_0 + \omega_m)t \qquad (4)$$

with $P_0 = J_0^2(\beta)P$ and $P_1 = J_1^2(\beta)P$. Thus, the input signal may simply be considered as a carrier with power P_0 and a pair of sidebands f_m Hz away from the carrier, each with power P_1.

Now, when the loop is attempting acquisition, a frequency sweep linearly changes the frequency of the reference signals to the phase detectors. Assume for this scenario that the sweep is from above f_0+f_m and downward in frequency. Then, when the reference frequency becomes

*Current design, subject to change. See Subsection 4.2.1.

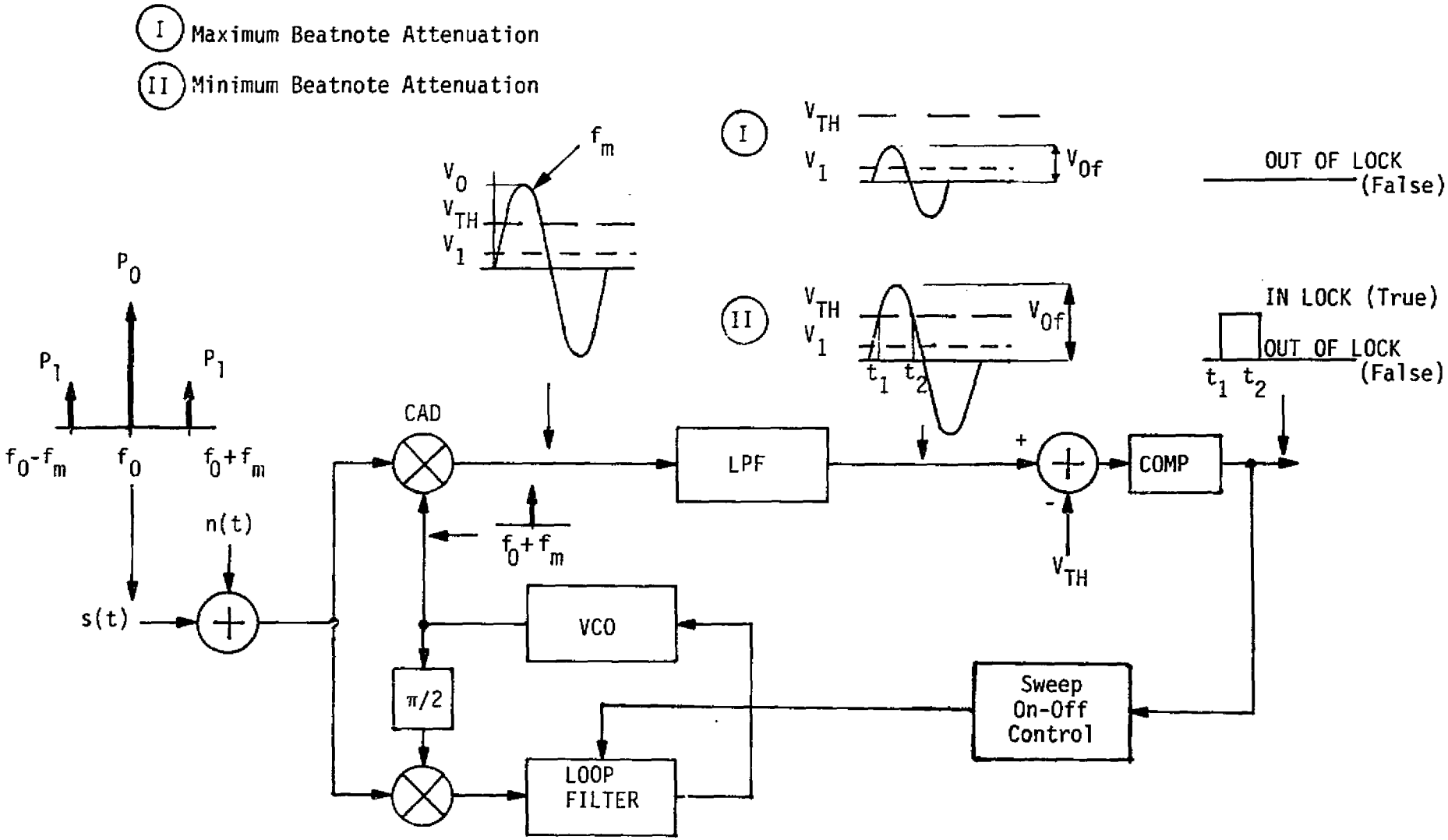

Figure 13. PI Receiver Simplified Block Diagram With Waveforms at Different Points of CAD Channel

on the order of (nearly identical to) f_0+f_m, there is a possibility that the loop may false lock to the f_0+f_m sideband provided the conditions are right. Given that a state of false lock occurs, it is then desired to determine the lock detector requirements such that the lock detector will not declare an in-lock state. The pertinent situation is depicted in Figure 13. The multiplication of the f_0+f_m reference with the f_0+f_m input component produces a direct voltage* designated V_1. By contrast, the input f_0 carrier component results in a beat note of frequency f_m at the CAD output. The peak value, V_0, of the beat note is very large, i.e., $V_0 >> V_1$ (see Figure 13). A second beat note at frequency $2f_m$ is also produced by the phase detection process, but this can be neglected as will become apparent when the desired effects of the LPF following the CAD are considered.

Referring to Figure 13, it can be seen from the graphical inset above the CAD that the maximum positive voltage swing of the combined direct voltage and beat note voltage will be V_1+V_0 and that this can be much greater than the comparator threshold voltage V_{TH}. However, the LPF between the CAD and comparator should have a significant attenuating effect on the beat note depending upon (a) the relationship between the beat note frequency, f_m, and the filter 3 dB frequency, f_c, and (b) the order of the LPF. Two possible results may thus be obtained as depicted on Figure 13 following the LPF: Case I, where the beat note is sufficiently attenuated so that the threshold voltage is not exceeded and the detector indicates out-of-lock all of the time, and Case II, where the beat note is insufficiently attenuated so that the lock detector has an in-lock state for some fraction of the beat note cycle.

Clearly, only Case I is acceptable for all situations conducive to false lock.** Therefore, the designer of the lock detector must specify f_c and the order of the LPF to meet the requirement. Axiomatix recommends that a third-order filter be used so that the beat note component

---

*All RF second harmonic terms are ignored.

**It should be noted that, if f_m is small and on the order of the PLL bandwidth, false lock is not likely to occur as the presence of the beat note within the loop should cause the loop to lock to the true carrier, the desired condition.

produces a minimum contribution to the conditions which may cause the lock detector to issue a valid lock indication for a state of false lock.

Typically, the threshold voltage, V_{TH}, will be four to five times greater than V_1 and about one-half of the direct voltage value, V_0, for the true lock situation. (This result stems from noise and the false alarm probabilities as discussed below.) Therefore, the filter attenuated sinusoid peak value, V_{0f}, should be no more than about two times V_1 (this allows some margin for noise peaks). Clearly, the first-order filter is not very effective in attenuating V_0 for values of f_m/f_c greater than 2. Furthermore, f_c certainly should be no larger than the one-sided tracking loop noise bandwidth, B_L, and probably a good deal less.

Once the order and 3 dB frequency of the LPF are selected, the only remaining lock detector parameter available for optimization of the overall lock detector performance is the threshold voltage, V_{TH}. Two operational performance probabilities provide the basis for setting V_{TH}: (a) the probability of erroneously indicating a state of in-lock for all conditions apart from true carrier lock, and (b) the probability of indicating a state of out-of-lock when the PLL is in fact locked onto the true carrier. (Neither of these values has been specified as of the writing of this report.)

An additional factor which complicates the selection of V_{TH} is the dynamic range of the receiver from strong to weak received signals. When the tracking loop is out-of-lock, coherent AGC is not available. Thus, a noncoherent AGC loop is employed. In subsection 6.1.1 of [3], it has been shown that such a loop, operating in conjunction with the other current PI design parameters, can compress the strong to weak signal dynamic gain range to about 9 dB. (Open loop, the range is 100 dB.) The decrease in gain from strong to weak signal conditions is assigned the symbol α. If, equivalently, the receiver is said to have a normalized gain of unity for strong signals, then the receiver has relative gain α, with $\alpha < 1$, when weak signals prevail.

Consider, now, that noise as well as signal appears at the input to the lock detector model shown in Figure 13. The noise is assumed to have the usual Gaussian and wideband characteristics. Taking all variables as they appear at the output of the lock detector LPF, the probability of

erroneously indicating a state of in-lock (also known as the false alarm probability) when the loop becomes locked to the f_0+f_m sideband at relatively strong signal levels is:

$$P_{FL} = \text{Prob}\left[1 + \frac{V_{0f}}{V_1}\sin(2\pi f_m t) - \frac{V_{TH}}{V_1} + \frac{1}{V_1} n_{fs}(t)\right] > 0, \quad (5)$$

where $n_{fs}(t)$ is the strong-signal noise appearing at the LPF output and V_{0f} is the peak value of the beat note term attenuated by the LPF. The subscript "FL" stands for "false lock." The term $n_{fs}(t)/V_1$ is proportional to the sideband noise-to-signal ratio which may be calculated from the total received signal-to-noise ratio and the specified relative sideband level, P_1/P_0. Note that (5) contains two time variables: beat note and noise. In order to calculate P_{FL}, the convolution of sinusoidal and Gaussian probability densities is required.

For the situation of true carrier lock, the probability of indicating out-of-lock given the in-lock state for a weak carrier signal is:

$$P_{OL/IL} = \text{Prob}\left[\alpha V_0 - V_{TH} + n_{fw}(t)\right] < 0, \quad (6)$$

where α is the weak-signal gain factor (suppression) and n_{fw} is the weak-signal lowpass noise.

The two dependent variables that will likely be determined by (5) and (6) are V_{TH} and $P_{OL/IL}$. Since a false-lock indication will stop the sweep acquisition process prematurely, P_{FL} needs to be relatively small, say, on the order of 10^{-4}.

TRW estimates that a properly designed lock detector (i.e., parameters optimized) should be capable, at strong signals, of discriminating against false lock indications for discrete sideband power levels of -26 dBc and less. Axiomatix believes that a -20 dBc capability can be achieved if the sweep dynamics are taken fully into account. It must be remembered, however, that even though the lock detector does not indicate a state of lock, the PLL itself could be locked and tracking.

5.1.3 Reduction of False Lock Sensitivity of the Payload Interrogator Receiver by Discriminator Aiding

Swept acquisition of the payload interrogator (PI) receiver over

the received signal frequency uncertainty range about the nominal carrier frequency (ω_0) brings with it the potential problem of falsely locking the receiver to a frequency other than that of the incoming phase modulated (PM) carrier, as has been explained in subsection 5.1.1. This false lock mode comes about because of the presence of modulation sidebands with significant power residing in the sweep frequency range. The modulation sidebands are due either to intentional phase modulation of the carrier by information-carrying signals or unintentional phase modulation by spurious signals.

The receiver model under consideration is one wherein the receiver VCO is linearly frequency swept by an analog sweep voltage. The sweep rate is sufficiently low to virtually guarantee that the receiver will lock on the carrier for the worst-case combined effects of the local frequency sweep and the input signal maximum doppler rate. As a result, for other than worst-case conditions, there is the likelihood that the receiver could false lock to a carrier sideband of sufficient power level. Since it is essentially impossible to control all the conditions which might give rise to a false lock situation, it is of interest to investigate means by which the receiver may be false lock desensitized.

This section analyzes the effects of frequency discriminator aiding on the false lock sensitivity of a PLL receiver. Also included is the companion analysis of the true lock and false lock tracking performance of the discriminator-aided loop. From these two analyses, one may make the necessary trade-off between improving acquisition performance (as measured by false lock sensitivity for a given sweep rate) and deteriorating tracking performance (as measured by mean-squared phase jitter due to additive noise).

As will be seen, the frequency discriminator is capable of significantly decreasing the false lock sensitivity of the PLL. The price paid is a correspondingly higher threshold with respect to additive noise performance. Quantitative assessments of such operation relative to required threshold capability and alternate methods (yet to be evaluated) have not been made. It is Axiomatix's belief, however, that frequency error detection methods for determining false lock states may ultimately give an equivalent sensitivity decrease without the corresponding SNR penalty. Future analysis will seek to prove this supposition.

5.1.3.1 A Brief Review of False Lock Considerations for a Conventional PLL Receiver

Probably the greatest cause of false lock to a modulation sideband is the situation where the sideband corresponds to a discrete spectral line. An example of such a situation is a carrier at frequency ω_0 that is phase modulated by a sinusoidal waveform of frequency ω_m, viz.,

$$\begin{aligned} s(t) &= \sqrt{2P}\cos\left[\omega_0 t + \beta \sin \omega_m t\right] \\ &= \underbrace{\sqrt{2P}\, J_0(\beta)\cos \omega_0 t}_{\text{carrier component}} \\ &\quad \underbrace{-\sqrt{2P}\, J_1(\beta)\left\{\sin\left[(\omega_0-\omega_m)t\right]+\sin\left[(\omega_0+\omega_m)t\right]\right\}}_{\text{First Sideband Pair}} \\ &\quad \underbrace{-\sqrt{2P}\, J_2(\beta)\left\{\cos\left[(\omega_0-2\omega_m)t\right]+\cos\left[(\omega_0+2\omega_m)t\right]\right\}}_{\text{Second Sideband Pair}} \\ &\quad + \cdots \end{aligned} \tag{7}$$

Assuming the phase modulation index $\beta \leq 1$, the first sideband pair has the largest power of all the sideband pairs and, provided that $\omega_0 - \omega_m$ and/or $\omega_0 + \omega_m$ fall within the receiver sweep frequency range, is the most likely to cause false lock.

Since for a second-order PLL with perfect integrating loop filter, the maximum sweep rate to achieve lock with any probability is determined solely by the loop's natural frequency [5], one can determine a maximum value of β, say β_{max}, which if exceeded will false lock the receiver to either $\omega_0 - \omega_m$ or $\omega_0 + \omega_m$. In particular, it may be shown that β_{max} satisfies the relation

$$\frac{J_1(\beta_{max})}{J_0(\beta_{max})} = \frac{\omega_{sw}}{\omega_n^2(max)}, \tag{8}$$

where ω_{sw} is the sweep rate in rad/sec^2 and $\omega_n(max)$ is the natural

frequency of the loop when true locked to the discrete carrier component at ω_0.

Our first purpose then is to consider the modification of (8) when discriminator aiding is applied to the conventional PLL receiver.

5.1.3.2 System Model of Discriminator-Aided PLL

Discriminator aiding of a PLL implies the addition of circuitry which generates a signal component input to the loop filter which ideally is directly proportional to the frequency difference between the incoming carrier and the loop's VCO reference. One way to accomplish this purpose is illustrated in Figure 14. Such a discriminator aid has previously been considered [6-7] with regard to improving the acquisition performance of suppressed carrier receivers such as those which employ a Costas loop for carrier synchronization. Indeed, many of the notions and results to be derived and presented here follow directly from the approaches taken in the above-cited references.

The discriminator aid of Figure 14 by itself has the advantage of being a balanced configuration and is thus relatively insensitive to gain imbalances in its two arms. When combined with the conventional PLL, it allows a continuously variable degree of trade-off between tracking performance degradation and false lock sensitivity improvement, depending on the relative gains of the two error signal components.

When the input signal of (7) is demodulated by the in-phase and quadrature reference signals

$$\begin{aligned} r_c(t) &= \sqrt{2}\, K_1 \cos\left[(\omega_0 - \Delta\omega)t - \phi(t)\right] \\ r_s(t) &= -\sqrt{2}\, K_1 \sin\left[(\omega_0 - \Delta\omega)t - \phi(t)\right], \end{aligned} \tag{9}$$

one obtains the in-phase and quadrature phase detector outputs:

$$\begin{aligned} \varepsilon_c(t) &= K_m s(t)\, r_c(t) \\ &= \frac{1}{2}\sqrt{P}\, K_1 K_m \sum_{n=0}^{\infty} \varepsilon_n (-1)^n J_{2n}(\beta) \{\cos\left[(2n\omega_m + \Delta\omega)t + \phi(t)\right] \\ &\qquad + \cos\left[(-2n\omega_m + \Delta\omega)t + \phi(t)\right]\} \\ &\quad - \sqrt{P}\, K_1 K_m \sum_{n=0}^{\infty} (-1)^n J_{2n+1}(\beta) \{\sin\left[(2n\omega_m + \Delta\omega)t + \phi(t)\right] \\ &\qquad + \sin\left[(-2n\omega_m + \Delta\omega)t + \phi(t)\right]\} \end{aligned} \tag{10}$$

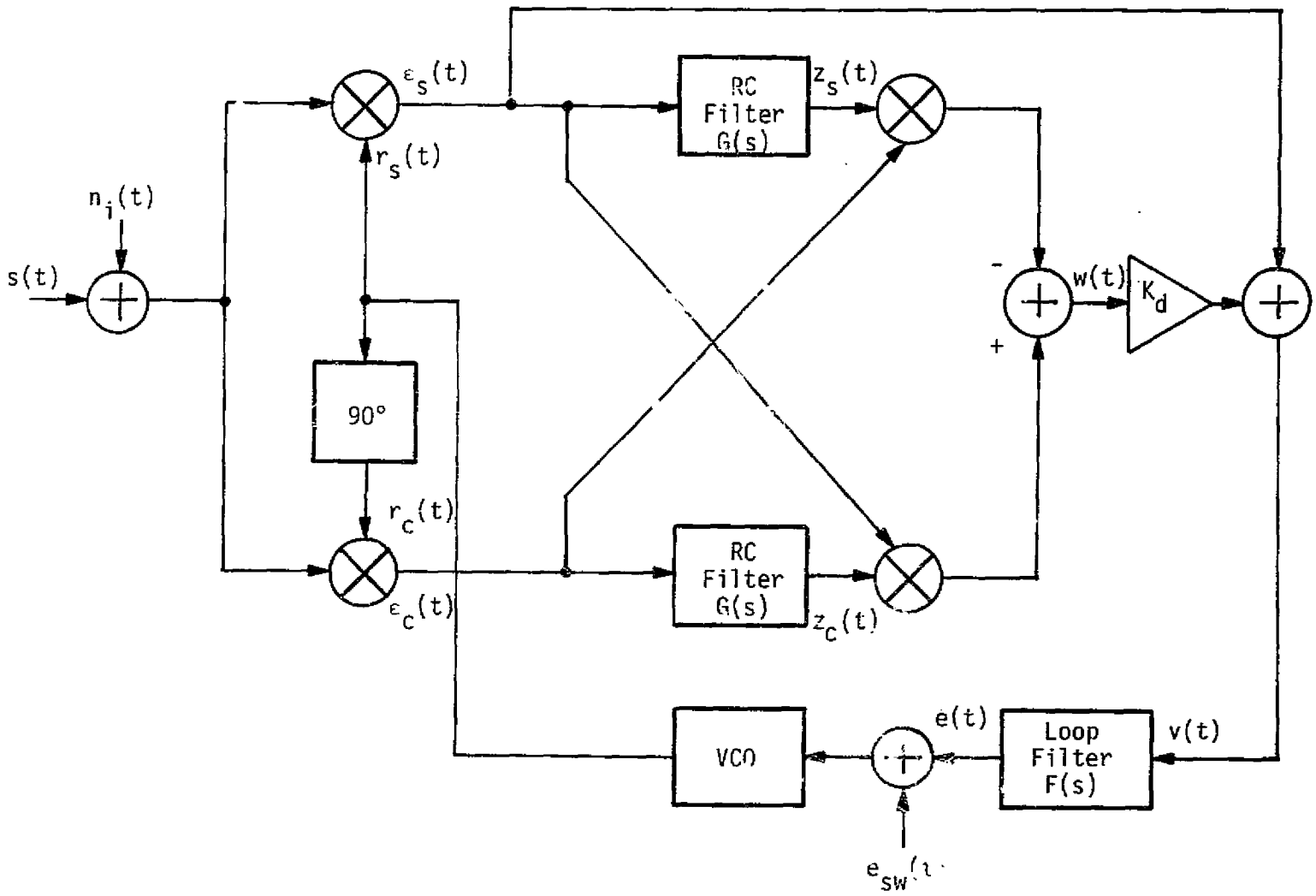

Figure 14. A Discriminator-Aided PLL

and

$$\varepsilon_s(t) = K_m s(t) r_s(t)$$

$$= \frac{1}{2}\sqrt{P}\, K_1 K_m \sum_{n=0}^{\infty} \varepsilon_n (-1)^n J_{2n}(\beta) \{\sin[(2n\omega_m + \Delta\omega)t + \phi(t)] + \sin[(-2n\omega_m + \Delta\omega)t + \phi(t)]\}$$

$$- \sqrt{P}\, K_1 K_m \sum_{n=0}^{\infty} (-1)^n J_{2n+1}(\beta) \{\cos[(2n\omega_m + \Delta\omega)t + \phi(t)] + \cos[(-2n\omega_m + \Delta\omega)t + \phi(t)]\}. \quad (11)$$

In the above, $\Delta\omega = 0$ for true lock on the discrete carrier at ω_0, or $\Delta\omega = n\omega_m$, $n = \pm 1, \pm 2, \ldots$ for false lock on the nth sideband at $n\omega_m$. Also, $\phi(t)$ denotes the loop phase error which includes a frequency dependent term $[\dot{\phi}(t) = \Omega]$ representative of the frequency offset relative to the true or false lock frequency, whichever the case may be.

Assuming that the acquisition loop bandwidth is narrow relative to the discriminator arm filter bandwidth, then it is reasonable to approximate $\phi(t)$ by $\phi_0 + \Omega t$ and consider only the sinusoidal response of the arm filters at the frequencies $n\omega_m + \Delta\omega + \Omega$; $n = 0, \pm 1, \pm 2, \ldots$. Representing the arm filter transfer function $G(\omega)$ by its magnitude and phase characteristics, i.e.,

$$G(\omega) = |G(\omega)|\, e^{j\theta_G(\omega)} \quad (12)$$

which, for an RC filter with 3 dB cutoff frequency ω_c, becomes

$$G(\omega) = \frac{1}{1 + j\frac{\omega}{\omega_c}}; \qquad |G(\omega)| = \sqrt{\frac{1}{1 + \left(\frac{\omega}{\omega_c}\right)^2}}$$

$$\theta_G(\omega) = -\tan^{-1}\frac{\omega}{\omega_c}, \quad (13)$$

then the in-phase and quadrature filter outputs can be written as

$$z_c(t) =$$

$$\frac{1}{2}\sqrt{P}\,K_1 K_m \sum_{n=0}^{\infty} \varepsilon_n (-1)^n J_{2n}(\beta)\,\{|G(\omega_{2n+})|\cos[\omega_{2n+}t + \phi_0 + \theta_G(\omega_{2n+})]$$

$$+ |G(\omega_{2n-})|\cos[\omega_{2n-}t + \phi_0 + \theta_G(\omega_{2n-})]\}$$

$$- \sqrt{P}\,K_1 K_m \sum_{n=0}^{\infty} (-1)^n J_{2n+1}(\beta)\,\{|G(\omega_{2n+})|\sin[\omega_{2n+}t + \phi_0 + \theta_G(\omega_{2n+})]$$

$$+ |G(\omega_{2n-})|\sin[\omega_{2n-}t + \phi_0 + \theta_G(\omega_{2n-})]\} \quad (14)$$

and

$$z_s(t) =$$

$$\frac{1}{2}\sqrt{P}\,K_1 K_m \sum_{n=0}^{\infty} \varepsilon_n (-1)^n J_{2n}(\beta)\,\{|G(\omega_{2n+})|\sin[\omega_{2n+}t + \phi_0 + \theta_G(\omega_{2n+})]$$

$$+ |G(\omega_{2n-})|\sin[\omega_{2n-}t + \phi_0 + \theta_G(\omega_{2n-})]\}$$

$$+ \sqrt{P}\,K_1 K_m \sum_{n=0}^{\infty} (-1)^n J_{2n+1}(\beta)\,\{|G(\omega_{2n+})|\cos[\omega_{2n+}t + \phi_0 + \theta_G(\omega_{2n+})]$$

$$+ |G(\omega_{2n-})|\cos[\omega_{2n-}t + \phi_0 + \theta_G(\omega_{2n-})]\}\,, \quad (15)$$

where

$$\omega_{2n+} \triangleq 2n\omega_m + \Delta\omega + \dot{\phi}$$

$$\omega_{2n-} \triangleq -2n\omega_m + \Delta\omega + \dot{\phi}$$

$$\varepsilon_n = \begin{cases} 1\,; & n = 0 \\ 2\,; & n > 0 \end{cases}. \quad (16)$$

The discriminator error signal $w(t)$ is then formed by cross-multiplying the in-phase and quadrature arm filter inputs and outputs and differencing the result, namely,

$$w(t) = K_1^2 K_m^2 P\,[z_c(t)\,\varepsilon_s(t) - z_s(t)\,\varepsilon_c(t)]\,. \quad (17)$$

From (10), (11), (14), and (15), we observe that w(t) will contain a dc component plus sinusoidal terms with frequencies which are integer multiples of ω_m. Recognizing that the loop filter is narrow band with respect to ω_m, it is sufficient to consider only the dc term in w(t) insofar as computing loop performance. Thus, letting $\langle w(t) \rangle$ denote the dc component of w(t), we find from (10), (11), (14), (15), and (17) that

$$\frac{\langle w(t) \rangle}{K_1^2 K_m^2 p} = -\frac{1}{2} \sum_{k=0}^{\infty} \varepsilon_k J_k^2(\beta) \left\{ |G(\omega_{k+})| \sin \theta_G(\omega_{k+}) + |G(\omega_{k-})| \sin \theta_G(\omega_{k-}) \right\} \quad (18)$$

Using (13) and (16) in (18) produces the result

$$\frac{\langle w(t) \rangle}{K_1^2 K_m^2 p} = \frac{1}{2} \sum_{k=0}^{\infty} \varepsilon_k J_k^2(\beta) \left[\frac{\left(\frac{\omega_{k+}}{\omega_c}\right)}{1 + \left(\frac{\omega_{k+}}{\omega_c}\right)^2} + \frac{\left(\frac{\omega_{k-}}{\omega_c}\right)}{1 + \left(\frac{\omega_{k-}}{\omega_c}\right)^2} \right] \quad (19)$$

If we further assume that $\omega_m/\omega_c \ll 1$, then for k less than some value k_0, we can ignore the squared terms in the denominator of (19) and, using (16), arrive at the approximation

$$\frac{\left(\frac{\omega_{k+}}{\omega_c}\right)}{1 + \left(\frac{\omega_{k+}}{\omega_c}\right)^2} + \frac{\left(\frac{\omega_{k-}}{\omega_c}\right)}{1 + \left(\frac{\omega_{k-}}{\omega_c}\right)^2} \cong \frac{\omega_{k+} + \omega_{k-}}{\omega_c} = \frac{2(\Delta\omega + \dot{\phi})}{\omega_c} \quad (20)$$

For large values of k (e.g., $k > k_0$), $J_k^2(\beta)$ is quite small and thus, as a further approximation, we assume (20) holds for all k insofar as evaluating (19). Thus, we obtain the final approximate result

$$\frac{\langle w(t) \rangle}{K_1^2 K_m^2 p} \cong \frac{1}{2} \sum_{k=0}^{\infty} \varepsilon_k J_k^2(\beta) \left[\frac{2(\Delta\omega + \dot{\phi})}{\omega_c} \right] = \frac{(\Delta\omega + \dot{\phi})}{\omega_c} \quad (21)$$

which clearly indicates the desired discriminator action, i.e., the average discriminator output is approximately a linear function of the frequency difference between the incoming signal and the VCO reference.

5.1.3.3 Swept Acquisition Performance for False Lock on the First Lower Sideband

We are interested now in applying the discriminator characteristics derived in the previous section to the characterization of the false lock acquisition behavior of the aided PLL. Since, as previously mentioned, the first sidebands produce the strongest false lock, we shall consider first characterizing the loop differential equation of operation (in the absence of noise) for a positive going sweep acquisition voltage attempting to lock the loop at $\omega = \omega_0 - \omega_m$. Letting $\Delta\omega = -\omega_m$, the VCO output frequency $\hat{\omega}(t)$ is related to its input voltage e(t) by

$$\hat{\omega}(t) = \omega_0 - \omega_m - \dot{\phi}(t) = K_v F(p)\, e(t) + \omega_0 + K_v\, e_{sw}(t) \tag{22}$$

where K_v is the VCO gain in rad/sec/v and p is the Heaviside operator. Since the loop filter will respond only to the low frequency components of its input, we can, as was done for the discriminator output, consider only the dc component of the quadrature phase detector output $\epsilon_s(t)$. Denoting this component by $\langle\epsilon_s(t)\rangle$, we have, from (11), that

$$\langle\epsilon_s(t)\rangle = K_1 K_m \sqrt{P}\, J_1(\beta) \cos\phi(t) \tag{23}$$

Since $\langle e(t)\rangle = \langle\epsilon_s(t)\rangle + K_d \langle w(t)\rangle$, substituting (21) and (23) into (22) gives

$$\left[1 + \frac{P K_B}{\omega_c} F(p)\right] \dot{\phi}(t) = -\omega_m - F(p)\left\{\sqrt{P} K_A J_1(\beta) \cos\phi(t) + P K_B \frac{\omega_m}{\omega_c}\right\} - K_v\, e_{sw}(t) \tag{24}$$

where

$$K_A = K_1 K_m K_v$$
$$K_B = K_1^2 K_m^2 K_d K_v \tag{25}$$

For a second-order loop with perfect integrating loop filter,

$$F(s) = \frac{1 + s\tau_2}{\tau_1 s} \quad ; \quad F_0 \triangleq \frac{\tau_2}{\tau_1} << 1 \tag{26}$$

and a linear sweep voltage $e_{sw}(t) = K_f t$, the differential equation of (24) becomes

$$\left(\tau_1 + \frac{PK_B}{\omega_c}\tau_2\right)\ddot{\phi}(t) + \left[\frac{PK_B}{\omega_c} - \tau_2\sqrt{P}\,K_A\,J_1(\beta)\sin\phi(t)\right]\dot{\phi}(t)$$

$$+ \sqrt{P}\,K_A\,J_1(\beta)\cos\phi(t) + PK_B\left(\frac{\omega_m}{\omega_c}\right) + \tau_1\,\omega_{sw} = 0 \qquad (27)$$

where $\omega_{sw} \triangleq K_f K_v$ is the sweep rate in rad/sec^2. Letting $\varphi(t) = \phi(t) + \frac{\pi}{2}$ then (27) takes on the more conventional form

$$\left(\tau_1 + \frac{PK_B}{\omega_c}\tau_2\right)\ddot{\varphi}(t) + \left[\frac{PK_B}{\omega_c} + \tau_2\sqrt{P}\,K_A\,J_1(\beta)\cos\varphi(t)\right]\dot{\varphi}(t)$$

$$+ \sqrt{P}\,K_A\,J_1(\beta)\sin\varphi(t) + PK_B\left(\frac{\omega_m}{\omega_c}\right) + \tau_1\omega_{sw} = 0 \qquad (28)$$

In the absence of the discriminator (or, equivalently, let $K_d(\gamma_B) = 0$), (28) becomes the well-known result

$$\tau_1\,\ddot{\varphi}(t) + \left[\tau_2\sqrt{P}\,K_A\,J_1(\beta)\cos\varphi(t)\right]\dot{\varphi}(t)$$

$$+ \sqrt{P}\,K_A\,J_1(\beta)\sin\varphi(t) + \tau_1\omega_{sw} = 0 \qquad (29)$$

In terms of the unaided false lock natural frequency $\omega_n = \left(\sqrt{P}\,K_A\,J_1(\beta)/\tau_1\right)^{1/2}$ and damping factor $\zeta = \omega_n\tau_2/2$, (28) becomes

$$\ddot{\varphi}(t) + \left[\frac{\delta}{\tau_2(1+\delta)} + \frac{2\zeta\omega_n}{1+\delta}\cos\varphi(t)\right]\dot{\varphi}(t) + \frac{\omega_n^2}{1+\delta}\sin\varphi(t) + \frac{\omega_m\delta}{\tau_2(1+\delta)}$$

$$+ \frac{\omega_{sw}}{(1+\delta)} = 0 \qquad (30)$$

where we have further introduced the notation

$$\delta = \frac{PK_BF_0}{\omega_c} \qquad (31)$$

In order for the loop to false lock and remain locked in the presence of the sweep, the sweep rate must be below a critical value such that a steady-state phase error exists. This critical value is determined by noting that, in the steady state, i.e., $\ddot{\varphi}(t) = \dot{\varphi}(t) = 0$, we have, from (30), that

$$\omega_n^2 \sin \varphi_{ss} + \frac{\omega_m \delta}{\tau_2} + \omega_{sw} = 0 \tag{32}$$

where φ_{ss} is the steady-state value of φ. In order for (32) to have a solution for φ_{ss}, we must require that

$$|\sin \varphi_{ss}| = \frac{\omega_m \delta}{\omega_n^2 \tau_2} + \frac{\omega_{sw}}{\omega_n^2} < 1 \tag{33}$$

or

$$\omega_{sw} < \omega_n^2 \left[1 - \frac{\omega_m \delta}{\omega_n^2 \tau_2}\right] = \omega_n^2 \left[1 - f(\beta)\right] \tag{34}$$

where, from (25) and (31),

$$f(\beta) = \frac{\omega_m \delta}{\omega_n^2 \tau_2} = \left(\frac{\omega_m}{\omega_{c'}}\right) \frac{\sqrt{P}\, K_1 K_m K_d}{J_1(\beta)} \tag{35}$$

Now, as previously stated, it is desired that no discrete sideband component (in particular, the first lower sideband) produce a false lock natural frequency ω_n which violates the inequality

$$\omega_n \sqrt{1 - f(\beta)} < \sqrt{\omega_{sw}} \tag{36}$$

Thus, it is clear that, if the discrete carrier component at ω_0 whose amplitude is proportional to $J_0(\beta)$ gives rise to $\omega_n(\max)$, the sideband component whose amplitude is proportional to $J_1(\beta)$ must be sufficiently small so that (36) is not violated. As a result, the following relationship can be established

$$\frac{\omega_n}{\omega_{n(\max)}} = \sqrt{\frac{J_1(\beta)}{J_0(\beta)}} \tag{37}$$

Combining (36) and (37) gives the desired modification of (8) for the discriminator-aided PLL, namely,

$$\frac{J_1(\beta)}{J_0(\beta)}\,[1-f(\beta)] < \frac{\omega_{sw}}{\omega_n^{\,2}(max)} \tag{38}$$

which, since $f(\beta) < 1$, clearly renders an improvement in false lock sensitivity relative to the unaided loop, i.e., a larger value of β [and thus $J_1(\beta)$] is needed to satisfy (38) than (8).

The amount of false lock sensitivity improvement is from (35) clearly dependent on the selection of the multiplicative gain $\sqrt{P}K_1K_mK_d$. Indeed, it would seem, at first glance, that continued increase of this gain would produce continued reduction of false lock sensitivity. However, one must remember that the result of (38) was obtained assuming no additive noise. When the effects of noise are taken into account, the maximum sweep rate expression of (34) must be modified to include a dependence on loop signal-to-noise ratio. This, in turn, would lead to a modification of (38) to reflect this same dependence and allow the selection of the loop gain to achieve a given level of false lock sensitivity depending on the input total power-to-noise ratio.

As exact expressions for maximum sweep rate as a function of loop signal-to-noise ratio are not presently available even for conventional PLL receivers, we are clearly faced with the same limitation for the discriminator-aided loop. Nevertheless, we shall proceed to derive expressions for the effective loop signal-to-noise ratio of the loop in Figure 14 as a function of input total power-to-noise ratio and loop gain for both the true lock and false lock modes. This, in turn, will allow determination of the steady-state tracking performance of the loop under these two conditions which can be used to trade off with false lock acquisition performance as a function of loop gain.

5.1.3.4 True Lock Tracking Performance ($\Delta\omega$ = 0, Sweep Disabled)

When the loop is locked to the true carrier component in (7), the additive noise can be written in the familiar bandpass expansion around the carrier frequency ω_0, namely,

$$n_i(t) = \sqrt{2}\left\{N_c(t)\cos\omega_0 t - N_s(t)\sin\omega_0 t\right\} \tag{39}$$

where $N_s(t)$ and $N_c(t)$ are lowpass Gaussian noise processes with flat spectral density N_0 W/Hz and bandwidth $B_H < \omega_0/2\pi$. After demodulation by the in-phase and quadrature reference signals of (9), the corresponding phase detector outputs due to noise only become

$$\begin{aligned}\varepsilon_c(t) &= K_m n_i(t)\, r_c(t) = K_1 K_m\left[N_c(t)\cos\phi(t) - N_s(t)\sin\phi(t)\right]\\ \varepsilon_s(t) &= K_m n_i(t)\, r_s(t) = K_1 K_m\left[N_c(t)\sin\phi(t) + N_s(t)\cos\phi(t)\right]\end{aligned} \tag{40}$$

Passing $\varepsilon_c(t)$ and $\varepsilon_s(t)$ through the in-phase and quadrature arm filters and performing the required cross multiplications and differencing gives the noise component at the discriminator output, namely [using (17)],

$$w(t) = K_1^2\, K_m^2\left[\hat{N}_c(t)\, N_s(t) - N_c(t)\,\hat{N}_s(t)\right] \tag{41}$$

where the "hat" denotes filtering by $G(s)$, e.g., $\hat{N}_c(t) = G(p)\, N_c(t)$. For the ideal discriminator as defined by the assumptions leading up to (21), we note that, for steady-state ($\dot{\phi}=0$) lock on the desired carrier ($\Delta\omega=0$), the signal component of the discriminator output is zero. Furthermore, the signal × noise components would also be zero. Thus, to determine the effect of the discriminator on overall loop tracking performance, we merely have to find the equivalent noise spectral density of the noise process in (41) and add it to that of $\varepsilon_s(t)$, which is due to the PLL acting alone*.

The correlation function of the noise component of $w(t)$ as specified by (41) is given by

$$R_{n_w}(\tau) = K_1^4\, K_m^4\,\overline{\left[\hat{N}_c(t)N_s(t) - N_c(t)\hat{N}_s(t)\right]\left[\hat{N}_c(t+\tau)N_s(t+\tau) - N_c(t+\tau)\hat{N}_s(t+\tau)\right]} \tag{42}$$

where the overbar denotes statistical expectation. Carrying out the various expectations required in (42), we obtain

---

*Note that $\varepsilon_s(t)$ of (40) and $w(t)$ of (41) are uncorrelated and thus no cross-noise coupling exists insofar as determining the total noise power perturbing the aided loop.

$$R_{n_w}(\tau) = 2K_1^4K_m^4 \left[R_N(\tau)\, R_{\hat{N}}(\tau) - R_{N\hat{N}}(\tau)R_{N\hat{N}}(-\tau)\right] \tag{43}$$

where

$$R_N(\tau) = \frac{N_0}{2}\,\delta(\tau)$$

$$R_{\hat{N}}(\tau) = \frac{N_0}{2}\int_{-\infty}^{\infty} |G(j2\pi f|^2\, e^{j2\pi f\tau}\, df$$

$$R_{N\hat{N}}(\tau) = \frac{N_0}{2}\int_{-\infty}^{\infty} G(j2\pi f)\, e^{j2\pi f\tau}\, df$$

$$R_{N\hat{N}}(-\tau) = \frac{N_0}{2}\int_{-\infty}^{\infty} G^*(j2\pi f)\, e^{j2\pi f\tau}\, df \tag{44}$$

The equivalent noise spectral density corresponding to $R_{n_w}(\tau)$ of (43) is then (applying Parseval's theorem)

$$N_{0_w} \triangleq 2\int_{-\infty}^{\infty} R_{n_w}(\tau)\, d\tau = 4\, K_1^4K_m^4\left\{\left(\frac{N_0}{2}\right)^2\int_{\infty}^{\infty} |G(j2\pi f)|^2\, df - \left(\frac{N_0}{2}\right)^2\int_{-\infty}^{\infty} G^2(j2\pi f)\, df\right\} \tag{45}$$

Recognizing that

$$|G(j2\pi f)|^2 = \overbrace{\left[\mathrm{Re}\left\{G(j2\pi f)\right\}\right]^2}^{\text{even function of f}} + \overbrace{\left[\mathrm{Im}\left\{G(j2\pi f)\right\}\right]^2}^{\text{even function of f}}$$

$$G^2(j2\pi f) = \left[\mathrm{Re}\left\{G(j2\pi f)\right\}\right]^2 - \left[\mathrm{Im}\left\{G(j2\pi f)\right\}\right]^2 + 2j\underbrace{\mathrm{Re}\left\{G(j2\pi f)\right\}\,\mathrm{Im}\left\{G(j2\pi f)\right\}}_{\text{odd function of f}} \tag{46}$$

then, the two terms of (45) combine to give

$$N_{0_w} = 2\, K_1^4K_m^4N_0^2\int_{-\infty}^{\infty}\left[\mathrm{Im}\left\{G(j2\pi f)\right\}\right]^2 df \tag{47}$$

Since, from (40), the correlation function of the noise component of $\varepsilon_s(t)$ is

$$R_{N_\varepsilon}(\tau) = K_1^2 K_m^2 R_N(\tau) = K_1^2 K_m^2 \frac{N_0}{2} \delta(\tau) \tag{48}$$

with corresponding spectral density

$$N_{0_\varepsilon} = 2 \int_{-\infty}^{\infty} R_N(\tau)\, d\tau = K_1^2 K_m^2 N_0 \tag{49}$$

then the spectral density of the total noise input to the loop filter is

$$N_0' = K_d^2 N_{0_w} + N_{0_\varepsilon} = K_1^2 K_m^2 N_0 \left[1 + 2K_1^2 K_m^2 K_d^2 N_0 \int_{-\infty}^{\infty} \left[\mathrm{Im}\{G(j2\pi f)\} \right]^2 df \right] \tag{50}$$

From (11) and (21), the total <u>signal</u> input to the loop filter when the loop is true locked to ω_0 is

$$\begin{aligned} v(t) &= \langle \varepsilon_s(t) \rangle + K_d \cancel{\langle w(t) \rangle^{=0}} \Big|_{\substack{\Delta\omega=0 \\ \dot{\phi}=0}} \\ &= \sqrt{P}\, K_1 K_m J_0(\beta) \sin\phi \end{aligned} \tag{51}$$

Thus, the equivalent loop signal-to-noise ratio (SNR) ρ' is given by

$$\rho' = \frac{P K_1^2 K_m^2 J_0^2(\beta)}{N_0' B_L} \tag{52}$$

where B_L is the one-sided loop noise bandwidth. For an RC discriminator arm filter as defined by (13),

$$\left[\mathrm{Im}\{G(j2\pi f)\} \right]^2 = \frac{(f/f_c)^2}{\left[1 + (f/f_c)^2 \right]^2} \tag{53}$$

and thus

$$\int_{-\infty}^{\infty} \left[\mathrm{Im}\{G(j2\pi f)\} \right]^2 df = \frac{1}{2} \pi f_c = \frac{\omega_c}{4} \tag{54}$$

Substituting (54) into (50) and the result of this substitution into (52) gives the desired result for loop signal-to-noise ratio, namely,

$$\rho' = \left(\frac{P\, J_0^2(\beta)}{N_0 B_L}\right)\left[1 + PK_1^2K_m^2K_d^2\left(\frac{N_0\omega_c}{2P}\right)\right]^{-1} \tag{55}$$

Since, for high loop SNR, the mean square phase jitter is inversely related to ρ' and, since the first factor in (55) represents the loop SNR in the absence of the discriminator aid, the increase in tracking phase jitter caused by the presence of the discriminator is represented by the factor

$$\eta = \frac{\sigma_\phi^2\Big|_{\text{aided}}}{\sigma_\phi^2\Big|_{\text{unaided}}} = 1 + PK_1^2K_m^2K_d^2\left(\frac{N_0\omega_c}{2P}\right) \tag{56}$$

5.1.3.5 False Lock Tracking Performance ($\Delta\omega = -\omega_m$, Sweep Disabled)

Here the loop has false locked to a frequency $\omega_0-\omega_m$ and the sweep has become disabled. The additive noise can, in this situation, be expanded around $\omega_0-\omega_m$, giving

$$n_i(t) = \sqrt{2}\left\{N_c(t)\cos\left[(\omega_0-\omega_m)t\right] - N_s(t)\cos\left[(\omega_0-\omega_m)t\right]\right\} \tag{57}$$

where $N_c(t)$ and $N_s(t)$ are again lowpass Gaussian noise processes with flat spectral density N_0 W/Hz. Since the demodulation references of (9) are also now at $\omega_0-\omega_m$, the noise components of $\varepsilon_s(t)$, $\varepsilon_c(t)$, $z_s(t)$, and $z_c(t)$ are identical to their counterparts in the true lock case [see, for example, (40)]. Thus, the spectral density of the total equivalent noise when the loop is false locked to the lower sideband at $\omega_0-\omega_m$ is still given by (50).

The total error signal may once again be found from (11) and (21) with the result

$$v(t) = \langle \varepsilon_s(t) \rangle + K_d \langle w(t) \rangle \Big|_{\substack{\Delta\omega = -\omega_m \\ \dot{\phi} = 0}}$$

$$= \sqrt{P} K_1 K_m J_1(\beta) \cos\phi + P K_1^2 K_m^2 K_d \left(\frac{\omega_m}{\omega_c}\right)$$

$$= \sqrt{P} K_1 K_m J_1(\beta) \sin\varphi + P K_1^2 K_m^2 K_d \left(\frac{\omega_m}{\omega_c}\right) \tag{58}$$

which, at the lock point $\left(v(t) = 0,\ dv(t)/dt > 0\right)$, corresponds to a steady-state phase error

$$\varphi_{ss} \triangleq \phi_{ss} - 90° = -\sin^{-1}\left[\frac{\sqrt{P} K_1 K_m K_d \left(\frac{\omega_m}{\omega_c}\right)}{J_1(\beta)}\right] \tag{59}$$

Thus, the loop SNR for false lock at $\omega_0 - \omega_m$ is given by

$$\rho' = \frac{\left[\sqrt{P} K_1 K_m J_1(\beta) \cos\varphi_{ss}\right]^2}{N_0' B_L} \tag{60}$$

or using (50), (54) and (59)

$$\rho' = \frac{P J_1^2(\beta)}{N_0 B_L} \left\{ \frac{1 - \frac{P K_1^2 K_m^2 K_d^2 \left(\frac{\omega_m}{\omega_c}\right)^2}{J_1^2(\beta)}}{1 + P K_1^2 K_m^2 K_d^2 \left(\frac{N_0 \omega_c}{2P}\right)} \right\} \tag{61}$$

and we observe that the discriminator causes a signal power penalty (due to the steady-state phase error) in addition to the noise penalty previously observed for the true lock case. As before, we can compute the ratio of aided to unaided tracking jitter for the large SNR case with the result

$$\eta = \frac{1 + PK_1^2K_m^2K_d^2\left(\frac{N_0\omega_c}{2P}\right)}{1 - \frac{PK_1^2K_m^2K_d^2\left(\frac{\omega_m}{\omega_c}\right)^2}{J_1^2(\beta)}} \tag{62}$$

The results of (56) and (62) clearly identify the dependence of the tracking performance degradation on the gain $\sqrt{P}K_1K_mK_d$ as promised.

5.2 Payload Nonstandard Modulation Considerations

Payload standard telemetry requirements are given in Table 4 of subsection 3.1. Any payload modulation that does not conform to these standards is classed as nonstandard. Nonstandard modulations may typically be expected to fall into one of four classes: (1) PSK modulations on other than standard subcarrier frequencies (especially subcarrier frequencies less than 500 kHz), (2) FM on other than standard subcarrier frequencies (especially subcarrier frequencies less than 500 kHz), (3) PSK modulations directly on the carrier (no subcarrier), and (4) the simultaneous presence of multiple FM nonstandard subcarrier frequencies (e.g., IRIG type signals).

As discussed in subsection 5.1.1, some nonstandard modulation conditions may cause the PI to false lock. Additionally, there are certain nonstandard modulations that the PI cannot handle at all, for example, suppressed carrier signals (i.e., no discrete carrier component). On the other hand, many nonstandard modulations can be accommodated by the PI without adverse effects, provided a few limiting restrictions are observed.

In subsection 5.1.1, it is mentioned that a noncoherent receiver is one method of handling nonstandard modulations, especially those for which the PI may encounter significant false lock problems or may otherwise be impaired from proper operation. Performance of a discriminator-integrator type of receiver for demodulation of phase modulated carriers is covered in subsection 5.2.1. Some possible modifications to the current PI design which would allow it to acquire, track and demodulate suppressed carrier signals are discussed in subsection 5.2.2. Then, assuming that the PI design and capability will remain essentially the same as its present form, subsection 5.2.3 explores a set of rationales for restrictions that would have to be placed on nonstandard payload modulations in order to insure proper PI functioning. Finally, subsection 5.2.4 presents a preliminary suggestive (strawman) set of user's guidelines based upon the restrictions rationale.

5.2.1 Use of a Noncoherent Discriminator Type Receiver

A frequency discriminator may be used to demodulate a phase-modulated carrier if a good signal integrator is used following the

discriminator proper to restore the discriminator-produced signal to its original phase-modulating waveform. Figure 15 shows a model of this type of receiver. The frequency discriminator itself acts functionally as a differentiator/envelope-demodulator over the frequency range of interest, while the integrator restores the demodulated signal to its proper form from its differentiated equivalent produced by the discriminator. The input BPF has noise bandwidth B_i, which is instrumental in establishing input signal-to-noise ratio, $(SNR)_i$. A lowpass/highpass filter combination follows the discriminator, with the lowpass frequency being dependent upon the highest frequency component of the modulating signal that need be recovered and the highpass frequency being quite low so as to effectively block discriminator direct voltage output (due to received frequency offset, etc.) but not affect the signal itself. Output of the integrator is the desired demodulated signal. If it is a digital data stream, its quality or figure of merit is determined by the energy-per-bit to noise-spectral-density ratio, E_b/N_0, available; for analog signals, output signal-to-noise ratio, $(SNR)_o$, is the measure.

Defining the received bandpass signal by:

$$S(t) = \sqrt{2P} \cos \left[\omega_0 t + \beta\, m(t)\right], \tag{63}$$

where m(t) is defined as a unit peak amplitude phase modulating signal, β is the phase modulation index, and the input noise is identical with (39), the input signal-to-noise ratio is given by:

$$(SNR)_i = \frac{P}{N_0 B_i} . \tag{64}$$

The general performance for discriminators operating with FM and PM signals is the same. Thus, published curves of FM performance may be used (with reasonable accuracy) to obtain the PM performance. For a phase modulation discriminator operating in the full improvement input SNR region, the output SNR, when the modulation is in a sinusoidal subcarrier, is given by

$$(SNR)_o = \frac{\beta^2 B_i}{2B_o} (SNR)_i , \tag{65}$$

C-2

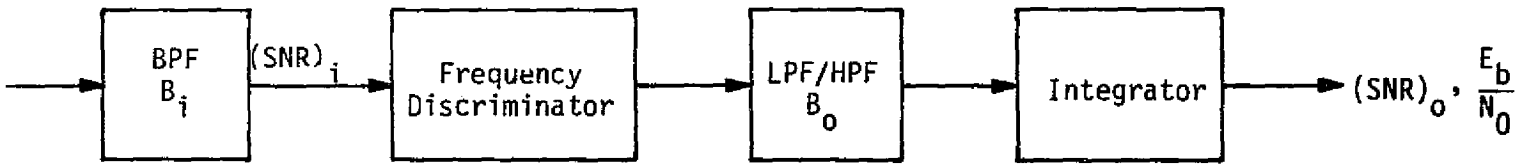

Figure 15. Phase Demodulation Discriminator Model

where B_o is the output LPF/HPF noise bandwidth. When the modulation, m(t), is of a more general nature, the full improvement output SNR is:

$$(SNR)_o = \frac{\beta^2 B_i}{B_o} \langle m^2(t) \rangle (SNR)_i , \qquad (66)$$

where the brackets < > indicate the time average taken on the square of the modulating signal.

If m(t) = d(t), d(t) being a unit amplitude digital data stream, then $\langle m^2(t) \rangle = 1$. However, when m(t) is some random analog signal, say Gaussian in nature, then $\langle m^2(t) \rangle \cong 1/9$. For digital modulations, usually $\beta = 1.1$ or $\beta = \pi/2$; for analog modulations of the Gaussian type, β could be 4 or larger.

It is instructive and useful to produce some graphs of phase demodulation discriminator performance for various modulation types. Since the discriminator receiver is to be an alternate to the PI phase coherent demodulator capability for conditions which preclude proper coherent demodulation, it will be assumed that the discriminator receiver has the same input and output bandwidths as that of the coherent receiver. Therefore, B_i = 12 MHz and B_o = 5 MHz. (These bandwidth values are representative of the current TRW PI receiver wideband phase demodulation channel design.) It will also be assumed that miscellaneous RF and waveform losses plus those associated with the nonideal mechanization of the discriminator and integrator will be 2 dB.

Now, the following cases will be considered:

Modulation Waveform	Subcarrier	β
Digital data	No	$\pi/2$
Digital data	Yes (PSK)	1.0
Analog-Gaussian	No	4.0
Analog-Gaussian	Yes (FM)	1.0

For digital data, where the important output measure is E_b/N_o, operation of the discriminator in the less than full improvement region (i.e., below the knee of the curve) will be allowed; for analog modulations, the minimum $(SNR)_i$ will be taken to be 10 dB in order to avoid thresholding conditions. Figures 16 through 19 present performance curves for each of the

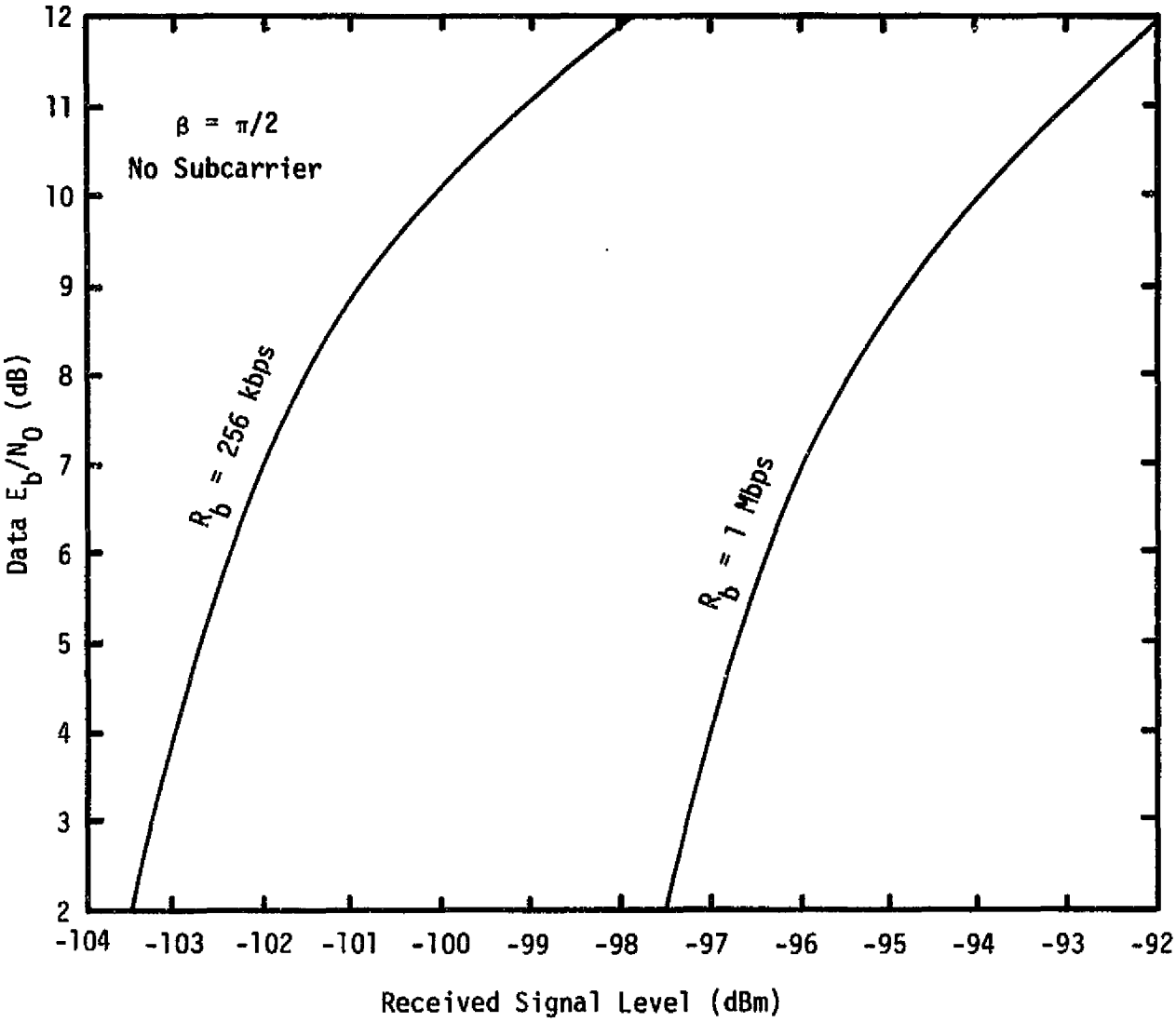

Figure 16. Phase Discriminator Performance for Direct Carrier Modulation by Digital Data

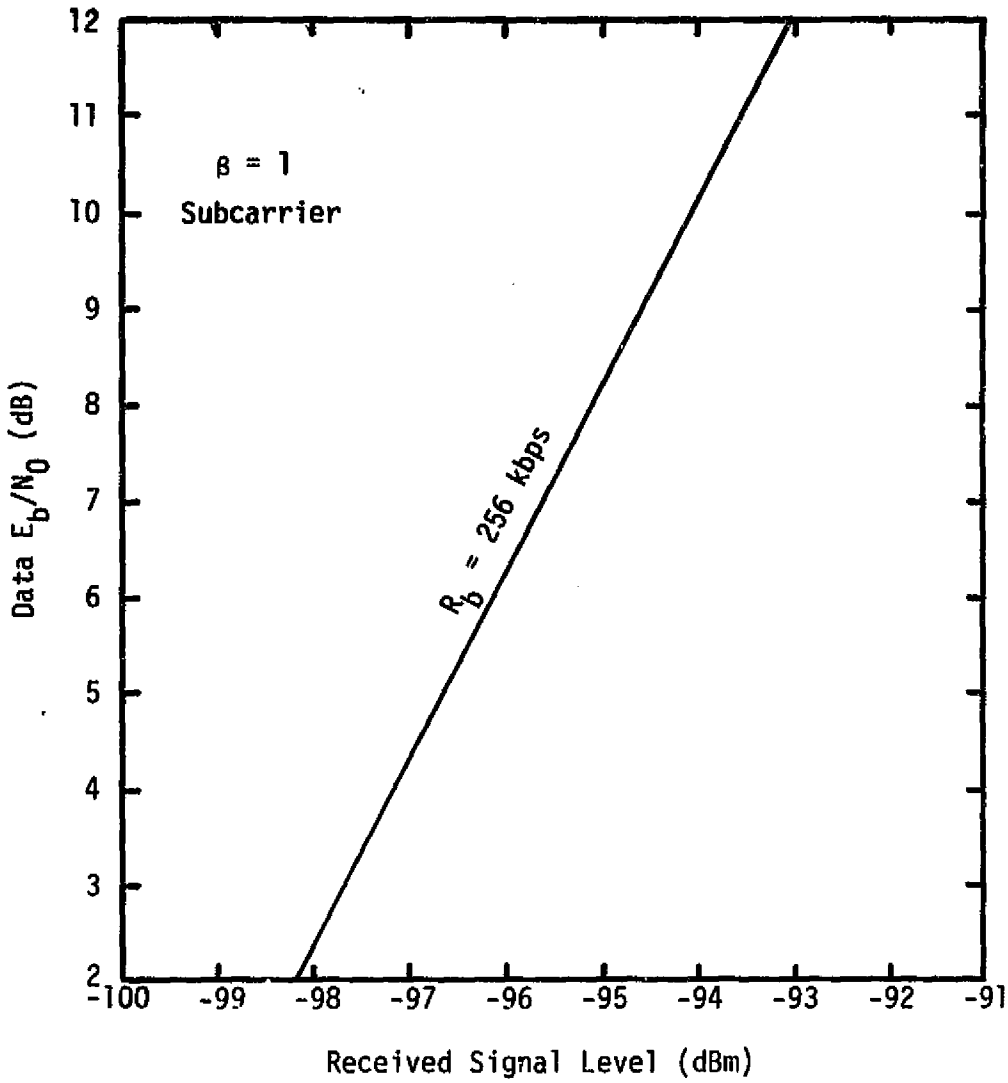

Figure 17. Phase Discriminator Performance for Biphase Data on a Subcarrier

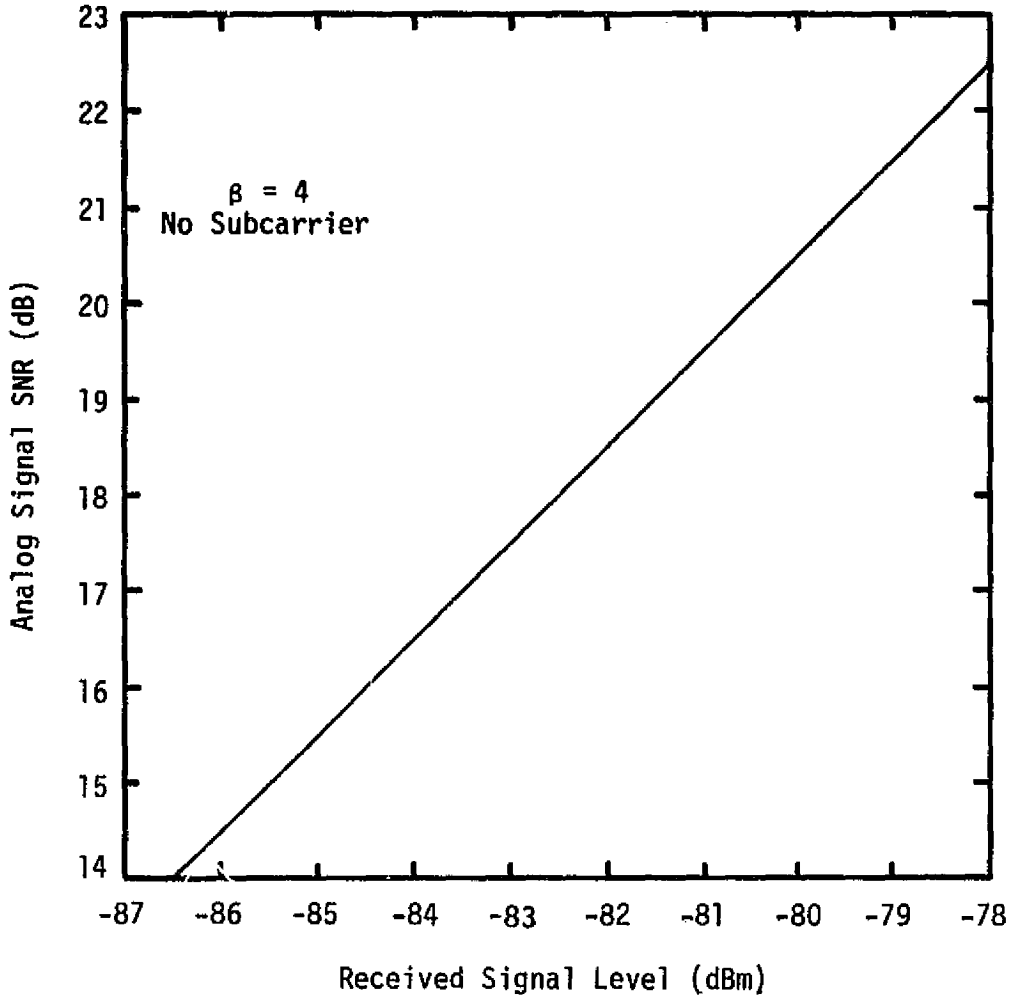

Figure 18. Phase Discriminator Performance for Direct Carrier Modulation by Analog Signal

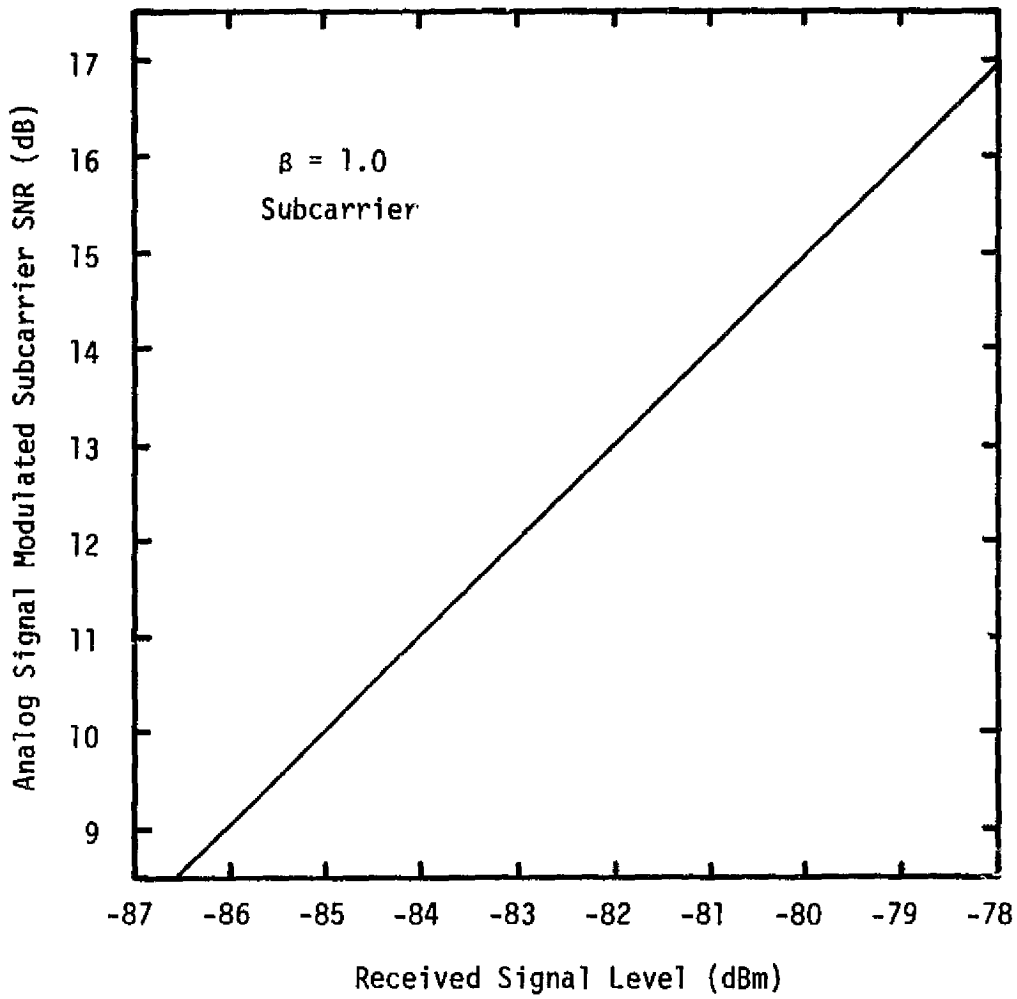

Figure 19. Phase Discriminator Performance for Analog Signal on a Subcarrier

above cases. Additional qualifying parameters are shown on the figures. Note that $(SNR)_1$ has been converted to equivalent received signal level (NF = 7.0 dB).

The performance curves presented in Figures 16 through 19 should be regarded from a general point of view as typical of probable performance. A specific topology and mechanization may have improved or poorer performance. Clearly, if the input and output bandwidths are optimized to a particular set of signal characteristics, generally better performance may be expected.

5.2.2 Modified PI for Suppressed Carrier Signals

As explained in subsection 3.3, the current PI receiver is capable of acquiring and tracking only those RF signals which have a discrete or residual carrier component. It is probable that, in the future, some payloads will incorporate nonstandard modulations for which the carrier is completely suppressed. Some possible suppressed carrier signal types that might be expected are: (1) Biphase PSK, (2) Quadriphase PSK (QPSK), and (3) Spread Spectrum PSK or QPSK. All of these types are already being used for the Shuttle S-band network [types (1) and (3)] and the TDRS [types (2) and (3)] links. Because of their high power and bandwidth efficiency, increased use on the part of payloads is quite likely.

The ability to handle suppressed carrier modulations will be only for a second-generation PI design. The present PI could be modified to accommodate signal types (1) and (2) by the addition of baseband processing circuits following the PLL phase detector and CAD. This would require redesign of the Demodulator and Baseband Module.

The capability of processing spread spectrum signals will necessitate considerable PI receiver redesign, and it is likely that simple modifications to the current PI will not suffice because of both functional and physical limitations.

5.2.3 Rationale for Payload Modulation Restrictions When Using the Payload Interrogator

5.2.3.1 Introduction

The basic problem of false lock avoidance has been delineated in subsection 5.1. Given the current PI design and capability, the present

discussion is intended to explore those specific payload modulation conditions that will produce false lock of any of the three types defined under subsection 5.1.1. False lock Type I can occur if the relative sideband level is larger than -26 dBc (see subsection 5.1.2). Type II may occur if certain discrete sideband components are of sufficient signal strength to foster actual phase-lock but weak enough to fall below the lock detector threshold. False lock Type III can occur for any sideband condition that has a relatively strong power level (greater than -26 dBc) and is reasonably narrowband (i.e., the majority of the spectral power falls within the PLL bandwidth).

In the following subsections, then, some criteria for avoiding false lock Types II and III will be established. The basic goal is to constrain the characteristics of the payload signal such that (a) the PI receiver can acquire and track the carrier component without false locking and undue tracking degradation, and (b) the demodulated baseband signal is recovered without significant modification of its original parameters (power, waveform, etc.).

5.2.3.2 Review of Standard Modulations and PI Receiver Characteristics

Payloads conforming to the payload/Orbiter standard signal formats have their carriers phase modulated by either a 1.024 MHz or 1.7 MHz sinusoidal subcarrier (in some cases, both subcarriers may be simultaneously present). These subcarriers may be biphase modulated by binary NRZ bit streams, or the 1.7 MHz subcarrier may be frequency modulated in an IRIG fashion or by some analog baseband signal. Standard bit rates for the 1.024 MHz subcarrier are 0.25 kbps to 64 kbps in steps of two; for the 1.7 MHz subcarrier, bit rates are 0.25 kbps to 256 kbps in steps of two. The standard modulation index for a single subcarrier is 1 rad (carrier suppression = 2.3 dB). The typical spectral form of a standard single subcarrier signal is shown in Figure 20.

The PI employs a phase coherent discrete carrier tracking receiver to track and demodulate the payload signal. This receiver phase-locks to the discrete carrier component (frequency f_0 of Figure 20), from which the necessary information is obtained to demodulate the sidebands. In order to initially acquire the discrete carrier component, the tracking loop, whose one-sided weak signal bandwidth is 1200 Hz, is swept

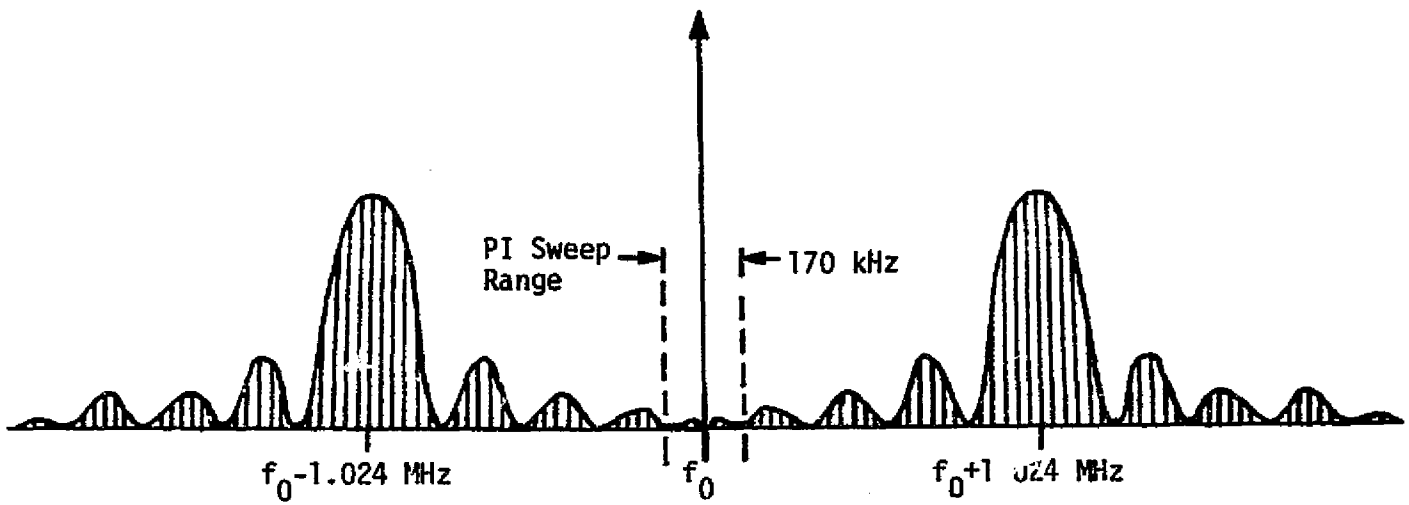

Figure 20. Typical Standard Signal Spectrum

at a rate of ω_{sw} = 10 kHz/sec over a frequency range of $\pm\Delta f$ kHz* about the nominal received carrier frequency. By this action, the discrete carrier at some point on the sweep interval falls within the loop bandwidth, thus allowing the loop to phase synchronize. The key to successful acquisition, apart from the usual bandwidth and sweep rate conditions, is that no significant sideband power resides within the sweep frequency range such that the receiver will false lock to a sideband component. Using standard subcarrier modulation, with the resulting carrier spectrum of the form shown in Figure 20, virtually assures that false lock is not a problem, as the power of the sideband components within the sweep range is quite small compared to the discrete carrier component power.

Nonstandard modulations are any apart from those outlined above. (See subsection 5.2 for detailed class definitions.) Rationale which can lead to nonstandard modulation restrictions and requirements must therefore be established from the perspectives of: (1) modulation waveform types, (2) modulation spectra, (3) modulation index, and (4) PI acquisition, tracking, and demodulation performance.

5.2.3.3 False Lock Onto Discrete Spectral Sidebands

Probably the greatest potential to sideband lock is the discrete spectral line sideband. For a simple and representative model, consider a carrier at frequency ω_0 that is phase modulated by a sinusoidal waveform of frequency ω_m, viz.,

$$S(t) = \sqrt{2P}\cos\left[\omega_0 t + \beta\cos\left(\omega_m t\right)\right] \tag{67}$$

This equation may be expanded into its discrete carrier and sideband components using Bessel function coefficients, i.e.,

$$\begin{aligned} S(t) = {} & \sqrt{2P}\,J_0(\beta)\cos\left[\omega_0 t\right] && \left.\right\} \text{ Carrier} \\ & - \sqrt{2P}\,J_1(\beta)\sin\left[(\omega_0-\omega_m)t\right] && \left.\right\} \text{ First} \\ & - \sqrt{2P}\,J_1(\beta)\sin\left[(\omega_0+\omega_m)t\right] && \left.\right\} \text{ Sideband pair} \\ & - \sqrt{2P}\,J_2(\beta)\sin\left[(\omega_0-2\omega_m)t\right] && \left.\right\} \text{ Second} \\ & - \sqrt{2P}\,J_2(\beta)\sin\left[(\omega_0+2\omega_m)t\right] && \left.\right\} \text{ Sideband pair} \\ & + \cdots. \end{aligned} \tag{68}$$

*For the current PI design, Δf = 85 kHz.

Usually, because $\beta < 2.4$, the first sideband pair is the largest of all sideband pairs and therefore represents those components to which the PLL is most likely to false lock, provided $\omega_0-\omega_m$ and $\omega_0+\omega_m$ fall within the receiver sweep frequency range.

Whether the PLL is able to false lock on either of the sideband pairs depends upon the acquisition frequency sweep rate and the natural frequency of the PLL. The PLL natural frequency is a function of the receiver PLL loop gain, which is, in turn, proportional to the sideband component level. The problem then is to determine the maximum sideband component level allowable without running the risk of false acquisition.

It has been determined [2] that acquisition will not occur if $\omega_n < \sqrt{\omega_{sw}}$, where ω_n is the natural frequency of the PLL. Now, $\omega_n \propto \sqrt{K}$ (where K is the loop gain) which is, in turn, proportional to the effective amplitude level of the input signal component which produces a zero beat frequency within the receiver loop.

For the proper discrete carrier component, the receiver PLL is designed to have a certain maximum natural frequency during acquisition and for strong received signals. With the use of noncoherent AGC, the maximum natural frequency should not exceed about three times the value specified at the PLL minimum weak signal operating point. The strong signal natural frequency is defined by ω_{nm}. Now, as previously stated, it is desired that no discrete sideband component produce a natural frequency, $\omega_n(\text{no acq.})$, which violates the inequality

$$\omega_n(\text{no acq.}) < \sqrt{\omega_{sw}} \ . \tag{69}$$

Thus, it is clear that, if the discrete carrier component whose amplitude is proportional to $J_0(\beta)$ gives rise to ω_{nm}, then the sideband component whose amplitude is proportional to $J_1(\beta)$ must be sufficiently small so that (69) is not violated. As a result, the following relationship can be established.

$$\frac{\omega_n(\text{no acq.})}{\omega_{nm}} = \sqrt{\frac{K(\text{no acq.})}{K_m}} = \sqrt{\frac{J_1(\beta)}{J_0(\beta)}} \ . \tag{70}$$

Taking into account the inequality which determines $\omega_n(\text{no acq.})$ and solving for $J_1(\beta)/J_0(\beta)$,

$$\frac{J_1(\beta)}{J_0(\beta)} < \frac{\omega_{sw}}{\omega_{nm}^2} . \qquad (71)$$

Since $\omega_{sw} < \frac{1}{2}\omega_{nm}^2$, then in order to guarantee proper and reliable acquisition on the discrete carrier component, the ratio $J_1(\beta)/J_0(\beta)$ must be less than 0.5, thereby constraining β to be less than 1. Figure 21 gives a plot of $J_1(\beta)/J_0(\beta)$ from which the critical value of β may be readily determined.

An example for the current design values of the PI is now presented.

$$f_{sw} = 10 \text{ kHz/ sec}$$
$$\omega_{nm} \approx 3800 \text{ rad/sec.}$$

Solving for β [using (71)] results in $\beta < 0.0087$ rad = 0.5°. This is indeed a very small deviation! In fact, it is often quite difficult to maintain incidental modulations below such a level. Expressed in another way, the result states that the allowable discrete frequency sideband level (relative to that of the carrier) can be no greater than -47 dBc.

What has been demonstrated is that a discrete sideband, with relative power level greater than -47 dBc, whose frequency falls within the frequency sweep range of the receiver, can actually be acquired and tracked by the PLL at strong received signal strengths. Yet, as was established in subsection 5.1.2, the PLL frequency sweep function is not removed by the lock detector unless the sideband component relative power level is in excess of -26 dBc. It therefore appears that there is a discrete sideband relative signal level range between -47 dBc and -26 dBc for for which a Type II false lock condition can exist.

Whether lock can be maintained over the entire sweep range, however, is a function of the receiver mechanization. The TRW current design is such that, for sideband levels less than -26 dBc, the phase detector error voltage is incapable of negating the sweep voltage into the VCO over the entire sweep range. The cancelling effect is therefore limited to a subrange in sweep frequency which approaches zero near -47 dBc, but is on the order of $\pm\Delta f$ in the vicinity of -26 dBc. (It should be noted that the receiver nominal gain is controlled by a noncoherent AGC

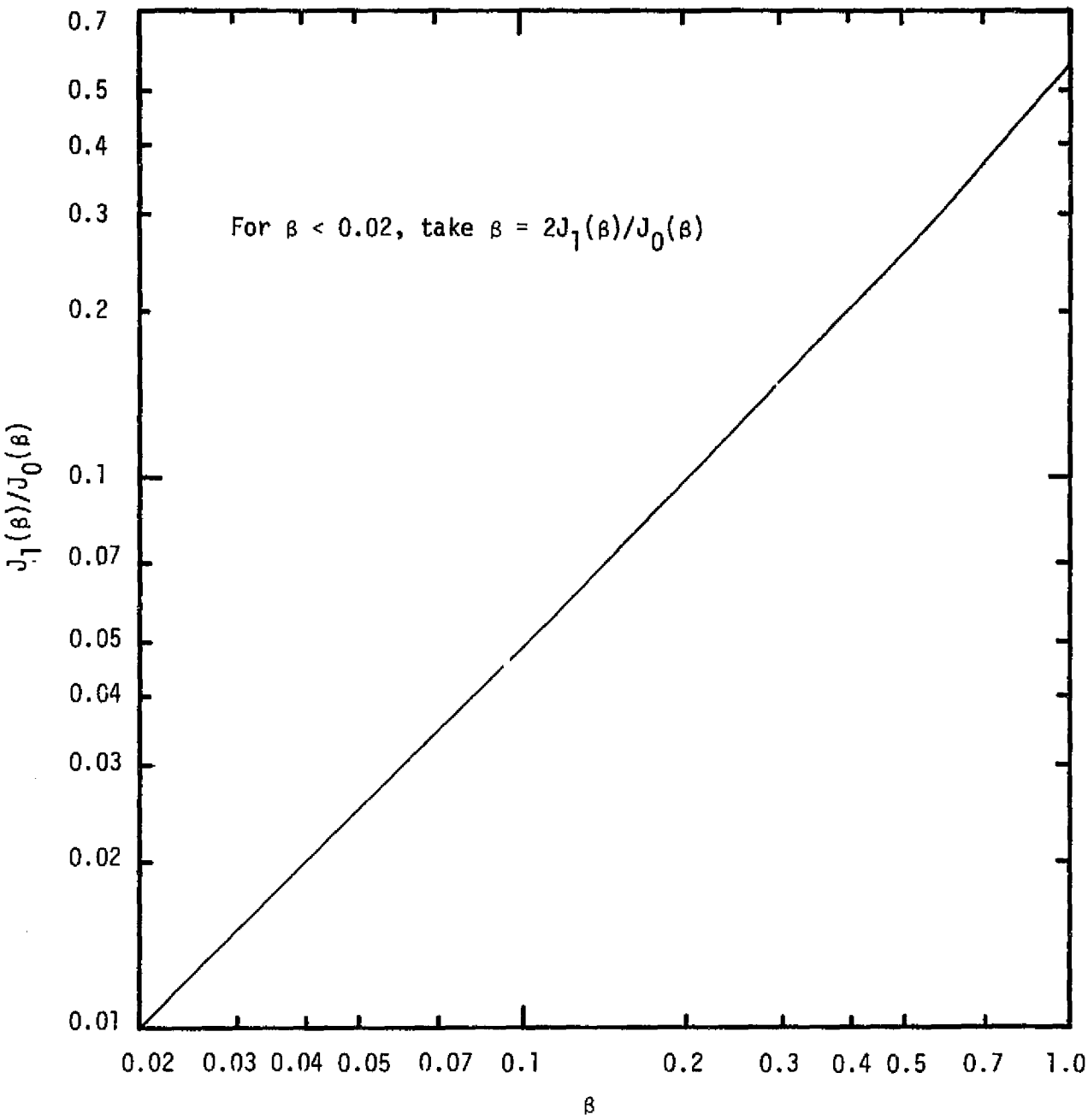

Figure 21. Plot for Determining β From $J_1(\beta)/J_0(\beta)$

which regulates principally to the discrete carrier level and is influenced little by sidebands that are less than -26 dBc.) What is not clear (at this time), however, is exactly what will happen, given a sideband lock condition and the continuance of the sweep, when the phase detector reaches its maximum output, following which the phase-lock state is broken. Because of the integrating effect of the loop filter, it is expected that the sweep acquisition process will continue in such a way as to ultimately attain true carrier lock. This is certainly the present assumption. Thus, it would appear that the sideband lock condition only serves to lengthen the sweep acquisition time (by the period of the lock state) but does not otherwise impair the acquisition process. It then remains to establish some sideband level less than -26 dBc which results in acceptable acquisition performance. This value should be toward the -26 dBc end of the range, however, so that the resulting restriction on payload nonstandard modulations is not overly constraining.

Insufficient detailed design and operating information is currently available about the PI receiver upon which to establish a valid restriction on the maximum allowable discrete frequency relative sideband level. For the sake of the strawman user's guideline in subsection 5.2.4, a restriction of -32 dBc is postulated. This figure is a 6 dB backoff from the -26 dBc upper limit and should therefore be reasonably safe with respect to all implementation tolerances.

The foregoing development was based upon phase-modulating the payload transmitter carrier with a single sinusoid. In reality, periodic type modulations, which produce discrete spectral line sidebands, may be more complex than sinusoids and multiple in nature. Thus, a large number of discrete frequency sidebands may be present. Under such conditions, the simple modulation index criterion developed above will no longer suffice. However, it is imperative that no particular discrete sideband be larger than the critical level which can result in PI receiver false lock. Therefore, the -32 dBc figure obtained as a result of the above reasoning is a valid condition that should not be exceeded by any spectral sideband when the composite modulation phase deviation of the carrier is small.

5.2.3.4 False Lock Onto Subcarrier Narrowband Spectral Sidebands

In the preceding subsection, a maximum allowable discrete frequency sideband level was established. Since discrete frequency sidebands (although they may occur as spurs or as the result of modulation by synchronizing signals) form an almost insignificant subset of the nonstandard modulation possibilities, they do not present the potential false lock problems that information-bearing modulations (random analog or digital) portend. Discrete sidebands manifest themselves as a Type II false lock situation, while false lock Types I and III are the ones that must be precluded for random modulations.

Consider the form of the signal input to the receiver to be:

$$S(t) = \sqrt{2P}\cos\left[\omega_0 t + \beta \sin\left\{\omega_m t + \theta m(t)\right\}\right], \qquad (72)$$

where $\omega_0 \pm \omega_m$ are sideband frequencies within the acquisition swept frequency range, θ is the subcarrier modulation sensitivity, and $m(t)$ is some form of aperiodic modulation. The most likely forms of $m(t)$ are: (a) $m(t) = d(t)$, where $d(t)$ is a binary data stream with bit period T_b; and (b) $m(t) = \int x(t)\,dt$, where $x(t)$ is some lowpass analog (continuous) waveform. Form (a) corresponds to subcarrier phase-shift-keying (PSK) (usually $\theta = \pi/2$), and (b) is subcarrier frequency modulation by $x(t)$. The signal spectrum of (a) is that shown in Figure 20, except now the large spectral peaks fall within the PI sweep range. For (b), the signal spectrum will have its maximum sideband values at or in the vicinity of $\omega_0 \pm \omega_m$ and will fall off about the frequencies $\omega_0 \pm \omega_m$ in accord with the characteristics of $x(t)$. In either situation, it is assumed (in this subsection) that the effective bandwidth of the sidebands is less than the natural frequency of the receiver PLL. As such, the majority of the sideband power will fall within the PLL tracking bandwidth and/or the lock detector bandwidth (as the loop is frequency swept across the maximal sideband regions), giving rise to the potential of false lock.

When a PLL locks onto the sidebands of a signal defined by (72), the operation of the loop becomes that of a modulation tracker (as opposed to a discrete component tracker discussed under 5.2.3.3). Relatively little theoretical or experimental information is available on the acquisition and tracking properties of modulation tracking loops (especially apart from FM

loops) and, as a result, rationale concerning lock onto narrowband non-discrete sidebands will of necessity be somewhat heuristic in nature.

Examining form (a) where $m(t) = d(t)$ with $\theta = \pi/2$, the following observations can be made. A data transition by the waveform d(t) causes the phase of the subcarrier to instantly switch in magnitude by an amount of π radians. Assume for the moment that the PLL is locked at the subcarrier relative frequency and that a data transition has not occurred for some time. The loop phase error will therefore be small (on the order of zero) as the PLL tracks the constant phase (at the moment) subcarrier. Suddenly, a data transition takes place and the phase error in the loop steps by π radians. For a discrete carrier type tracking loop, this is tantamount to moving the loop's operating point from a stable null to an unstable null. The performance of the loop under such conditions is dictated by the nonlinear differential equation describing the operation of the loop. (Here, linear PLL modeling cannot be used.) A small restoring force begins to drive the operating point of the loop back to a stable null. The transient time for this to take place is strongly dependent upon the initial phase error relative to the unstable null point. The smaller this error (and therefore the smaller the initial restoring force), the longer the transient state. Practically speaking, the loop will generally transition to the stable null in less than a data bit period provided $\omega_n T_b > 4$, where ω_n is the loop natural frequency and T_b is the data bit period. Since the data bit rate is $R_b = 1/T_b$, another way of viewing this result is that, if $\omega_n > 4R_b$, the loop will almost certainly track the data modulated subcarrier.

A second question is, what becomes the critical sideband level condition for acquisition? Certainly, the propensity to acquire will be somewhat weaker than the discrete spectral sideband case. However, one can certainly postulate circumstances for which acquisition will occur--for example, the absence of data transitions for a considerable number of bit periods, making the subcarrier appear at the moment of acquisition as if it were discrete. Thus, the most favorable situation for allowing acquisition is identical to the discrete sideband case, and as a result, the same conditions precluding the likelihood of acquisition must be involved. Since the restricting modulation index has already been shown to be (<0.5°) (meaning that no significant power may be represented in the sidebands as

would be required for data communication purposes), then, for all practical purposes, data modulation with bit rates less than $\omega_n/4$ on subcarrier frequencies that fall within the receiver acquisition frequency sweep range should not be allowed.

Subcarrier modulation form (b) is now examined. With narrowband analog FM such that the bandwidth of the resultant modulated subcarrier is less than ω_n, it is well known that a PLL locked onto the subcarrier will track the modulation with little phase error [2]. Allowing for an RMS tracking phase error of 10°, the expression for loop natural frequency is [8]

$$\omega_n = 11.4\sqrt{\sigma_f \cdot f_m} \tag{73}$$

where σ_f is RMS deviation of the subcarrier by the modulation and f_m is the maximum frequency of the modulating signal. As an upper deviation limit for narrowband FM, $\sigma_f = f_m/3$, so that $\omega_n = 6.6\ f_m$. But since the bandwidth, B_{FM}, of a NBFM signal is on the order of 4 f_m, $B_{FM} < \omega_n/1.65$ Hz if good modulation tracking is to occur.

Thus, the FM sideband bandwidth for good tracking, and therefore high false lock probability, is established. Again, the critical sideband level conditions will be on the order of those for the discrete frequency sideband, and the $\beta < 0.5°$ restriction must be invoked if sideband lock-on is to be completely avoided.

5.2.3.5 False Lock Onto Subcarrier Wideband Spectral Sidebands

In this subsection, the problem of acquiring and tracking wideband spectral sidebands is addressed. The approach is to consider what happens to the signal forms discussed in 5.2.3.4 as $\theta m(t)$ increases in intensity and bandwidth so that the effective bandwidth of the sidebands becomes greater than the natural frequency of the PLL. Such conditions should further preclude lock onto the sidebands.

The known relationship between PLL natural frequency, PLL RMS phase error, and the FM parameters is to be investigated as a measure of tracking integrity. Then, based upon a maximum RMS error criterion for the in-lock condition, the no-acquisition and tracking requirements may be extrapolated. From [8],

$$\sigma_\phi = 22.9 \frac{\sigma_f \cdot f_m}{\omega_n^2} \tag{74}$$

where σ_ϕ is the RMS phase error of the PLL arising from its inability to track the modulated subcarrier in a perfect fashion.

Now, the additive noise threshold for discrete carrier PLLs is often taken to occur when $\sigma_\phi = 1$ radian, and, from all practical points of view, the loop is considered to be out-of-lock. For want of a better threshold (in lieu of measured results), this will also be taken as the threshold inability of the loop to track the FM sideband. From (74), the unlock condition becomes:

$$\sigma_f \cdot f_m = 0.0437\ \omega_n^2 \ . \tag{75}$$

Now, in order to make this result more meaningful, consider that $\Delta f = 3\sigma_f$ is the peak frequency deviation of the subcarrier. Further, Carson's rule concerning wideband FM bandwidth is:

$$B_{FM} = 2(\Delta f + f_m) \ . \tag{76}$$

Combining (76) with (75), the following is obtained for the threshold condition:

$$B_{FM} f_m - 2f_m^2 = 0.26\ \omega_n^2 \ . \tag{77}$$

Since both B_{FM} and f_m are involved in (77), a specific example is needed to assess the significance of the result. Suppose that $f_m = B_{FM}/20$. Solving for B_{FM} gives:

$$B_{FM} = 2.4\ \omega_n \tag{78}$$

Comparing this result with $B_{FM} < \omega_n/1.65$ Hz, it is seen that, if the bandwidth of the modulated subcarrier is allowed to increase by a factor of 4 (f_m remaining constant), the PLL will go from a condition of good sideband tracking (10° RMS phase error) to a condition of failure to track the sideband (57° RMS phase error).

A typical range for f_m in relation to B_{FM} for most applications is:

$$\frac{B_{FM}}{30} \leq f_m \leq \frac{B_{FM}}{10} . \tag{79}$$

Clearly, $f_m = B_{FM}/30$ results in the largest bandwidth to loop natural frequency ratio ($B_{FM} = 10.8\ \omega_n$). Typically, the subcarrier FM parameters are given in terms of f_m and Δf; therefore, the no-sideband lock criterion based upon (75) may be expressed as:

$$\Delta f \cdot f_m > 0.13\ \omega_n^2 . \tag{80}$$

A critical no-tracking natural frequency may now be defined by rewriting (80) in the form:

$$\omega_n(\text{no tracking}) \leqq 2.8\ \sqrt{\Delta f \cdot f_m} . \tag{81}$$

As previously stated, the actual loop natural frequency is a function of the amplitude level of the signal being tracked, and, for discrete frequency sidebands, a relationship between the natural frequency prevalent for sideband tracking relative to that for true carrier tracking has been established. Specifically, (69) fixes the no acquisition natural frequency upper limit for discrete sidebands, as well as for FM sidebands for which $2.8\ \sqrt{\Delta f \cdot f_m} \leq \sqrt{\omega_{sw}}$. If the inequality is valid, the FM subcarrier simply cannot be allowed.

Now, suppose from (81) and (69), it is found that $\omega_n(\text{no tracking}) > \omega_n(\text{no acq.})$. Such a relationship may be interpreted to mean that, for a given β, the effective acquisition/tracking signal power that falls within the PLL loop bandwidth is less with the modulation present than if it were to be removed from the subcarrier. Since $\omega_n(\text{no tracking})$ is what determines whether the PLL will acquire and track in the presence of wideband FM of the subcarrier, then a larger β is allowable up to the point that $\omega_n(\text{no tracking})$ is reached.

Combining (70) and (81) results in the equality which establishes the maximum allowable value of β, viz.,

$$\frac{J_1(\beta)}{J_0(\beta)} = 7.84 \frac{\Delta f \cdot f_m}{\omega_{nm}^2} . \qquad (82)$$

Equation (82) is valid up to those values of β for which the maximum carrier suppression criterion is violated. The maximum allowable carrier suppression is taken to be 10 dB, corresponding to β = 1.85 rad. Thus, if (82) portends values of β greater than 1.85 rad, then β must be taken as 1.85 rad.

As an example of all of the above discussion, consider the following parameter values:

$$\Delta f = 2 \text{ kHz}$$
$$f_m = 400 \text{ Hz}$$
$$\omega_{nm} = 3800 \text{ rad/sec}$$
$$f_{sw} = 10 \text{ kHz/sec}.$$

From (81), it is found that ω_n(no tracking) $\leq$ 2500 rad/sec. Now, since ω_n(no tracking) > ω_n(no acq.) = 251 rad/sec [determined using (69)], then the value of β = 0.5° taken to preclude lock onto discrete sidebands may be increased in accord with (82), which gives $J_1(\beta)/J_0(\beta)$ = 0.434 or β = 0.78 rad. This value of β is less than the 1.85 rad allowed maximum which achieves a 10 dB carrier suppression, and is therefore valid.

There is yet one other consideration that must, however, be taken into account. The lock detector must not be allowed to misperform because of the sideband components that appear within its bandwidth. In general, the effects will be akin to increasing the noise into the threshold comparator, manifesting itself as an increased false alarm probability. Intuitively, the false alarm probability should not be allowed to more than double with respect to its receiver minimum operating signal level value. The value of β for which such a false alarm probability is attained depends strongly on the modulating signal characteristics. Thus, at this juncture, a more specific result cannot be established. The conclusion is, however, that the lesser β determined from both the false alarm criterion and that of (82) must prevail.

The situation for modulation form (a) is now examined with the intent to determine how well a PLL tracks a biphase modulated subcarrier

as the data rate is allowed to increase while ω_n remains fixed.

If the data bit stream is unbalanced (i.e., there is, on the average, a preponderance of one bit state), then statistically, there will be a discrete subcarrier component in the resulting subcarrier spectrum, and the loop may be expected to lock irrespective of data rate. Whether, in fact, it does depends upon the nature of the bit stream at the time the sweep acquisition centers the PLL on the relative subcarrier frequency and whether the unbalance is uniformly distributed along the data stream as opposed to occurring only on particular time intervals. If a Manchester type of data modulation is used, there is no unbalance, and residual subcarrier frequency acquisition and tracking is obviated.

As to the situation of balanced data, no analytical or empirical information is available to show when a PLL with fixed ω_n is no longer able to track the subcarrier as a function of increasing R_b. As the data bit period T_b decreases to a value where the transient response to a phase step of π rad no longer approaches the stable null point with small error before the next data transition takes place, then the loop's ability to track the modulation is becoming impaired. This situation might generally be expected to happen as $\omega_n T_b \to 1$. As $\omega_n T_b$ continues to decrease and becomes less than unity, the response to each new transition is more and more dependent upon the past response over the pattern of previous transitions. It is very difficult at this point, however, to be able to state without some experimental insight if the loop is in-lock or whether acquisition might even take place.

A purely speculative criterion might be established between the relative PSK and FM performance, assuming that the loop no-lock conditions occur on a comparative bandwidth basis. Equalizing $\omega_n > 4R_b$ and $B_{FM} < \omega_n/1.65$ Hz to fix a correspondence between R_b and B_{FM}, and taking into account (76) and (79), it may be shown that

$$\omega_n(\text{no tracking}) \leqq R_b \ . \tag{83}$$

This result corresponds exactly with the intuitive reasoning given above. Thus, until further evidence is able to establish otherwise, (83) will be used as the PSK no-lock criterion.*

*This result may also be applied to FSK subcarriers because of their similar spectral characteristics.

As was the situation for FM, if ω_n(no tracking) is found to be greater than ω_n(no acq.), then larger values of β will be allowed according to the relationship:

$$\frac{J_1(\beta)}{J_0(\beta)} = \frac{R_b^2}{\omega_{nm}^2} . \tag{84}$$

Also, the same remarks concerning the false alarm performance of the lock detector that were made with respect to the FM case must also be made concerning the maximum allowable value of β for the PM case.

5.2.3.6 Proper Lock and Demodulation Conditions for Direct Carrier (No Subcarrier) Modulations

This subsection considers the PI acquisition and tracking requirements for direct carrier modulations of the form

$$S(t) = \sqrt{2P} \cos [\omega_0 t + \beta\, m(t)] , \tag{85}$$

where m(t) is a "lowpass" modulating signal, which could be continuous (analog) or discrete (digital). Since carrier phase (rather than frequency) modulation is involved here, the transmission of analog signals is usually avoided because of the rather small linear range of the sinusoidal-characteristic phase detector employed within the receiver. For reasonable linearity, the peak phase deviation of the carrier should be less than 1 rad, severely limiting the amount of transmitter power apportioned to the sidebands. Thus, it is rather unlikely that m(t) will be analog for the payload/PI link under consideration.

Considering then that m(t) = d(t) as defined previously in subsection 5.2.3.4, (85) may be rewritten in the form:

$$S(t) = \sqrt{2P} \cos (\beta) \cos (\omega_0 t) - \sqrt{2P}\, d(t) \sin (\beta) \sin (\omega_0 t) . \tag{86}$$

The left-hand term is the discrete carrier and the right-hand term represents the sidebands. The sideband spectrum is simply the lowpass spectrum of d(t) translated to the carrier frequency.

When d(t) is in the form of aperiodic NRZ data bits at a rate of

R_b bits/sec, the power density spectrum of d(t) is given by:

$$G_d(f) = \frac{2}{R_b} Sa^2\left[\pi \frac{f}{R_b}\right] \tag{87}$$

where $Sa(x) \triangleq Sin(x)/x$ is the sampling function. Note that this spectrum has its maximum value at f = 0 and, therefore, in terms of the modulated carrier, the sideband spectrum is maximum at the carrier frequency.

From the viewpoint of the PI receiver's proper operation with this type of modulated carrier, there are three quantities or performance measures of interest: (a) the discrete carrier level, (b) the loop phase noise component due to that portion of the modulation sidebands that is "tracked" by the loop, and (c) the amount of demodulated data power.

From (86), it is easily seen that the discrete carrier and sideband power components are given by:

$$\begin{aligned} P_c &= P \cos^2(\beta) \\ P_s &= P \sin^2(\beta) \end{aligned} \tag{88}$$

A quantity of interest is the carrier suppression, viz.,

$$\text{Carrier Suppression} \triangleq 10 \log [P_c/P] \ . \tag{89}$$

Typically, for payload/Orbiter link carrier SNR and payload modulation index tolerance considerations, the carrier suppression should not be greater than -10 dB. This then sets the maximum β to 71.5°.

Using linear PLL theory, the loop phase noise due to modulation sideband tracking is given by:

$$\sigma_\phi^2 = \frac{P_s}{P_c} \int_0^\infty G_d(f)|H(f)|^2 \, df \ , \tag{90}$$

where H(f) is the phase transfer function of the PLL. To evaluate (90), it is necessary to specify a particular set of PLL parameters; specifically, the following are chosen:

(1) Second-order loop

(2) Damping factor = $\sqrt{2}/2$

(3) Two-sided loop noise bandwidth, $W_L = 1.06\ \omega_n$.

The transfer function may be obtained from [2]; using (86) and (87) and defining $\eta \triangleq W_L/R_b$, the phase noise expression becomes:

$$\sigma_\phi^2 = \frac{1}{\eta}\tan^2(\beta)\left\{\eta + \frac{3}{4}\left[1 - \exp\left(-\frac{2}{3}\eta\right)\left\{\cos\left(\frac{2}{3}\eta\right) + 3\sin\left(\frac{2}{3}\eta\right)\right\}\right]\right\}. \quad (91)$$

When the data bit rate is much larger than the loop noise bandwidth, i.e., when $R_b >> W_L$ ($\eta<<1$), then:

$$\sigma_\phi^2 \cong \eta\tan^2(\beta) = \left[\frac{W_L}{R_b}\right]\tan^2(\beta) \quad (92)$$

The expression $\sigma_\phi/\tan(\beta)$ is plotted in Figure 22 as a function of η.

The data rate restriction may now be established. Total loop phase jitter is usually comprised of three components arising from (a) additive noise, (b) oscillator instability, and (c) modulation sideband tracking. The RMS value of the phase jitter caused by the additive noise should be less than 15° for a properly designed tracking/demodulation loop and that contributed by oscillator instability will be between 1° and 5°. If the total jitter is to be less than 20°, which represents the upper limit of good engineering practice, the modulation-induced component will have to be 10° or less. Taking, then, $\sigma_\phi = 10°$, together with $W_L = 1460$ Hz (TRW design maximum value at the minimum operating signal level) and $\beta = 1.1$ radian (7 dB carrier suppression), the data rate restriction is established as: $R_b \geq 185$ kbps.

There is a second consideration that gives rise to another restriction on the data stream d(t), that of data transition density. With reference to (85), when d(t) is balanced and has a high transition density, the PLL tracks the mean carrier phase. If, however, the transitions of d(t) cease for a period of time, say $d(t) \equiv 1$, then the PLL could slew to the phase β. This in effect causes the demodulated data waveform to decay to zero, a very undesirable condition. The result is loss of effective data power.

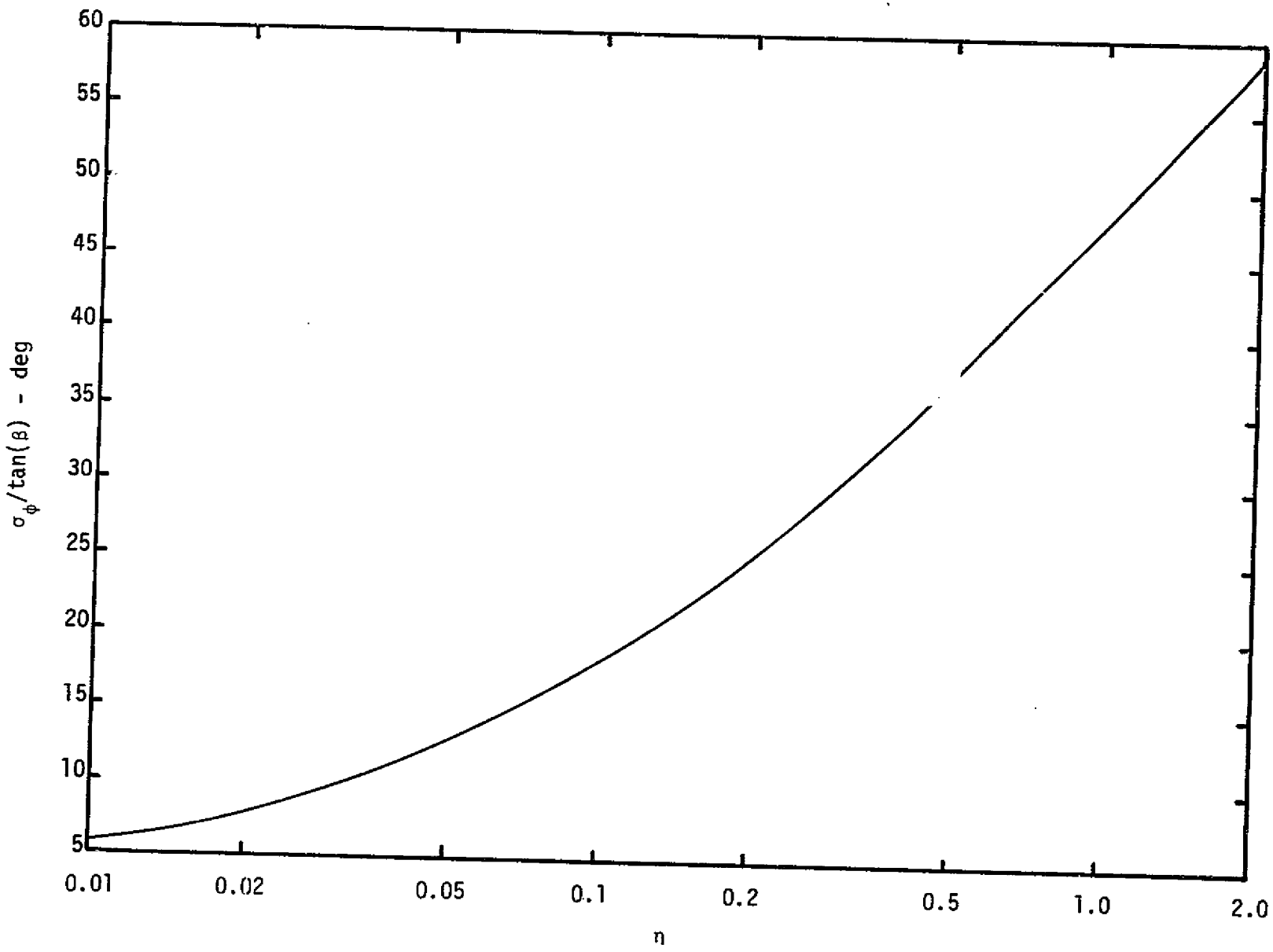

Figure 22. Tracking Loop Phase Noise

The reference phase slewing, $\phi_s(t)$, is given by the expression (damping factor = $\sqrt{2}/2$):

$$\phi_s(t) = \beta \exp\left(-\frac{\sqrt{2}}{2}\omega_n t\right)\left[\cos\left(\sqrt{2}\omega_n t\right) - \frac{1}{2}\sin\left(\sqrt{2}\omega_n t\right)\right] \qquad (93)$$

A reasonable specification is that the maximum data power lost due to demodulation reference slewing be no greater than 0.5 dB for worst-case conditions. This corresponds to a maximum phase slewing of 18° and, for R_b = 185 kbps, the maximum number of transitionless bits allowed to maintain slewing less than 18° is found [using (93)] to be 30 bits.

One way of avoiding the no-transition problem is to Manchester the data bit stream. This changes the power density spectrum of the modulating waveform from that of (87) to:

$$G_d(f) = \frac{2}{R_b}\frac{\sin^4\left[\pi f/2R_b\right]}{\left(\pi f/2R_b\right)^2} \qquad (94)$$

When phase modulated onto the carrier, this spectrum has very little power in the vicinity of the carrier. By comparison with non-Manchestered data, the minimum bit rate restriction for Manchester data for which the tracking loop σ_ϕ = 10° is 1/75 that of non-Manchester data, assuming the condition that $R_b >> W_L$. Thus, the equivalent of equation (91) for Manchester data is:

$$\sigma_\phi^2 = \frac{1}{75}\left(\frac{W_L}{R_b}\right)\tan^2(\beta) \; . \qquad (95)$$

The corresponding lower data rate limit for which σ_ϕ = 10° is R_b = 2.5 kbps.

Clearly, the use of Manchestered data allows for very low data rates for direct carrier modulation. However, at such a rate, false lock potential must again be considered (at 185 kbps and greater, there is no false lock problem). Manchestered data can be viewed as NRZ data modulating a square-wave subcarrier of frequency equal to the bit rate. As such, the no false acquisition conditions of subsection 5.2.3.4 must also be invoked, in particular equation (84), with the modification that $J_1(\beta)/J_0(\beta)$

be replaced by the expression $\frac{1}{2}\tan(\beta)$. This then gives rise to the following Manchester bit rate restriction:

$$R_b \geq \frac{1}{\sqrt{2}}\omega_{nm}\sqrt{\tan(\beta)} \quad . \tag{96}$$

Equation (95) is also rewritten so that:

$$R_b \geq \frac{W_L}{75}\left[\frac{\tan(\beta)}{\sigma_\phi}\right]^2 \tag{97}$$

Therefore, the minimum R_b allowed is taken as the largest value obtained from equations (96) and (97). For the previously assumed parameter values, (96) gives $R_b \geq 3.8$ kbps. Thus, this value governs over 2.5 kbps obtained from (97).

Turning finally to the demodulated data power, P_D, it is calculated by the integral:

$$P_D = P_s \int_0^\infty G_d(f)|1-H(f)|^2\, df \quad . \tag{98}$$

Using the same PLL parameters as above, the result becomes:

$$P_D = \frac{3P_s}{4\eta}\left\{1-\exp\left(-\frac{2}{3}\eta\right)\left[\cos\left(\frac{2}{3}\eta\right)-\sin\left(\frac{2}{3}\eta\right)\right]\right\} \quad . \tag{99}$$

For $R_b >> W_L$, the approximate expression becomes:

$$P_D \simeq P_s\left\{1-W_L/(3R_b)\right\} \quad . \tag{100}$$

Relative to the previous numerical results where $R_b/W_L = 127$, the ratio of demodulated data power to total available data power is $P_D/P_s = 0.997 = -0.01$ dB. This, of course, is a negligible loss.

5.2.3.7 Conclusions and Further Work

The foregoing development has attempted to present a rationale for payload bent-pipe modulation restrictions. A summary of the major restrictions that must be imposed in order to avoid false lock onto sideband components are:

(a) Discrete frequency sideband components must be less than -32 dBc.

(b) Frequency modulated subcarriers by analog signals are allowed subject to constraining FM/PM modulation conditions (81) and (82).

(c) PSK modulated subcarriers by digital data signals are allowed subject to constraining PSK/PM modulation conditions (83) and (84).

(d) Direct PSK modulation of the carrier is allowed with the restriction that the phase modulation index be less than 71.5° or 1.25 rad, and that the PI carrier loop RMS phase noise due to modulation sideband component tracking be no greater than 10°.

(e) For a 1.1 rad carrier deviation, the minimum allowable NRZ bit rate is 185 kbps. The maximum number of sequential transitionless bits is 30.

(f) For a 1.1 rad carrier deviation, the minimum allowable Manchestered bit rate is 3.8 kbps.

The available theory and/or experimental data which gives rise to (a) and (d) above is considerable but by no means complete. On the other hand, the background credence for (b) and (c) is almost nil and the results are quite heuristic. Therefore, it is clear that more work relative to the false acquisition of aperiodically modulated subcarrier sidebands must be accomplished before final criteria and restrictions can be established. Simulation and experimental approaches would appear to offer the best means for obtaining results.

5.2.4 Strawman User's Guideline

A draft of a payload modulations restrictions guideline, based upon the rationale developed in subsection 5.2.3, has been prepared and appears in Appendix C. This guideline is intended as a model which may be used for the preparation of future ICDs or other documents that will be supplied to the payload community. Since the PI design and capability is not yet firm and because additional theoretical and experimental work remains to be done on the development of the restrictions rationale, the numbers supplied in the guideline should be considered as transitory (although many are probably within the "ballpark" of their final values).

5.3 Payload Interrogator Receiver Wideband Output Components as a Function of Modulation Index and Multiple Subcarriers

Payload transponder transmitters usually have the capability to linearly phase modulate the carrier with peak phase deviations up to 2.5 rad. Within the PI receiver, a product type phase detector is employed to phase demodulate the received carrier. Since this type of phase demodulator has a sinusoidal amplitude versus phase characteristic, its operation is not linear relative to the phase modulation of the received signal. It is therefore necessary to determine the level of the demodulated components in proportion to their original phase deviations at the transmitter.

The following derives the expected relative level of the modulation components at the PI receiver output as a function of their peak phase deviation of the carrier. Three cases are considered:

Case I

A single sinusoidal modulation (with application to either a 1.024 MHz or 1.7 MHz subcarrier phase modulating the carrier).

Case II

Two sinusoidal modulations (with application to simultaneous 1.024 MHz and 1.7 MHz subcarriers phase modulating the carrier).

Case III

A sinusoidal plus a "square" type modulation (with application to a sinusoidal subcarrier and a lowpass digital data signal simultaneously phase modulating the carrier). This case is a likely form of a nonstandard bent-pipe class of modulation.

Figure 23 shows a functional model for the payload transmitter (linear phase modulator) and the PI receiver (phase detectors and LPFs). The output of the linear phase modulator is given by the mathematical form:

$$s(t) = \sqrt{2P} \cos \left[\omega_0 t + \theta_1 m_1(t) + \theta_2 m_2(t)\right] , \qquad (101)$$

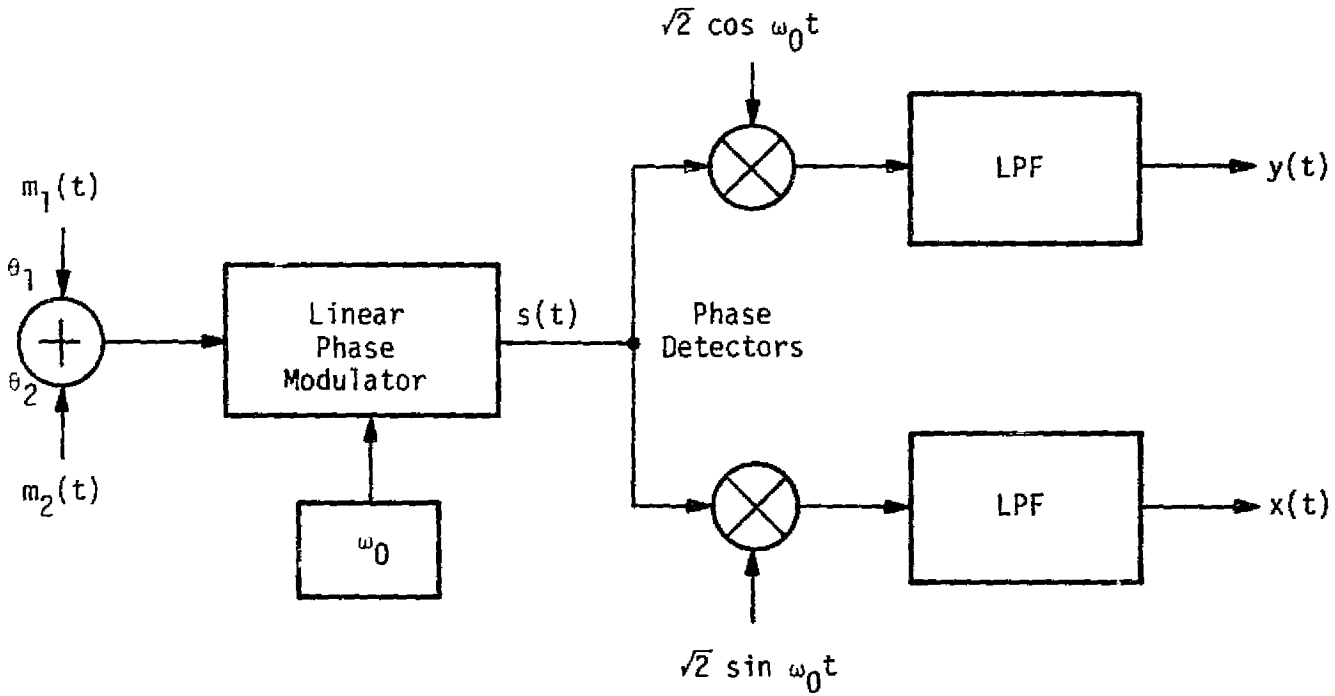

Figure 23. Phase Modulator/Demodulator Model

where:

$m_1(t)$, $m_2(t)$ = modulating functions

θ_1, θ_1 = phase deviations

ω_0 = carrier frequency

P = transmitted power.

By means of trigonometric identities, the LPFs serving to eliminate all $2\omega_0$ terms, it may be easily shown that:

$$x(t) \propto f_1(\theta_1,\theta_2)\, m_1(t) + f_2(\theta_1,\theta_2)\, m_2(t)$$

$$y(t) \propto f_0(\theta_1,\theta_2) \ .$$

Specific developments for the three cases follow.

5.3.1 Analysis of Case I and Case II

The analysis will start with Case II, since it is more general; Case I is simply a special condition. The modulations are defined by:

$$m_1(t) = \sin \omega_1 t \qquad 0.3 \leq \theta_1 \leq 1.2 \ \text{rad}$$

$$m_2(t) = \sin \omega_2 t \qquad 0.3 \leq \theta_2 \leq 1.2 \ \text{rad}$$

where $\omega_1 \neq \omega_2$ and the range of the modulation indices is as shown.

Substituting $m_1(t)$ and $m_2(t)$ into (101) results in:

$$s(t) = \sqrt{2P} \cos \left[\omega_0 t + \theta_1 \sin \omega_1 t + \theta_2 \sin \omega_2 t\right] , \qquad (102)$$

and making use of the cos (a+b) trigonometric identity yields:

$$\begin{aligned} s(t) = \sqrt{2P} \Big\{ & \cos \omega_0 t \left[\cos (\theta_1 \sin \omega_1 t) \cos (\theta_2 \sin \omega_2 t) \right. \\ & \left. - \sin (\theta_1 \sin \omega_1 t) \sin (\theta_2 \sin \omega_2 t)\right] \\ & - \sin \omega_0 t \left[\sin (\theta_1 \sin \omega_1 t) \cos (\theta_2 \sin \omega_2 t) \right. \\ & \left. + \sin (\theta_2 \sin \omega_2 t) \cos (\theta_1 \sin \omega_1 t)\right] \Big\} \ . \end{aligned} \qquad (103)$$

Bessel function series expansions are now applied to the cos (sin) type terms, which produces terms readily identifying the various modulation components.

$$s(t) = \sqrt{2P}\left\{\cos\omega_0 t\left\{\left[J_0(\theta_1) + 2\sum_{\substack{n=2\\ \text{even}}}^{\infty} J_n(\theta_1)\cos n\omega_1 t\right]\left[J_0(\theta_2) + 2\sum_{\substack{n=2\\ \text{even}}}^{\infty} J_n(\theta_2)\cos n\omega_2 t\right]\right.\right.$$
$$\left.\left. - \left[2\sum_{\substack{n=1\\ \text{odd}}}^{\infty} J_n(\theta_1)\sin n\omega_1 t\right]\left[2\sum_{\substack{n=1\\ \text{odd}}}^{\infty} J_n(\theta_2)\sin \omega_2 t\right]\right\}\right.$$
$$- \sin\omega_0 t\left\{\left[2\sum_{\substack{n=1\\ \text{odd}}}^{\infty} J_n(\theta_1)\sin n\omega_1 t\right]\left[J_0(\theta_2) + 2\sum_{\substack{n=2\\ \text{even}}}^{\infty} J_n(\theta_2)\cos n\omega_2 t\right]\right.$$
$$\left.\left. + \left[2\sum_{\substack{n=1\\ \text{odd}}}^{\infty} J_n(\theta_2)\sin n\omega_2 t\right]\left[J_0(\theta_1) + 2\sum_{\substack{n=2\\ \text{even}}}^{\infty} J_n(\theta_1)\cos n\omega_1 t\right]\right\}\right\} \quad (104)$$

Multiplication of (104) by $\sqrt{2}\cos\omega_0 t$ and $\sqrt{2}\sin\omega_0 t$ results in the demodulated terms. Specifically, f_0, f_1, and f_2 are easily recognized as:

$$f_0 = J_0(\theta_1)\, J_0(\theta_2)\,\sqrt{P}$$

$$f_1 = 2\, J_1(\theta_1)\, J_0(\theta_2)\,\sqrt{P}$$

$$f_2 = 2\, J_0(\theta_1)\, J_1(\theta_2)\,\sqrt{P}$$

For Case I,

$$m_1(t) = \sin\omega_1 t \qquad 0.3 \leq \theta_1 \leq 2.0 \text{ rad}$$

$$m_2(t) = 0$$

and the expression for s(t) is easily obtained from (104) as:

$$s(t) = \sqrt{2P}\left\{\cos \omega_0 t \left[J_0(\theta_1) + 2 \sum_{\substack{n=2 \\ \text{even}}}^{\infty} J_n(\theta_1) \cos n\omega_1 t\right]\right.$$

$$\left. - \sin \omega_0 t \left[2 \sum_{\substack{n=1 \\ \text{odd}}}^{\infty} J_n(\theta_1) \sin n\omega_1 t\right]\right\} . \qquad (105)$$

The corresponding amplitude functions are:

$$f_0 = J_0(\theta_1) \sqrt{P}$$

$$f_1 = 2 J_1(\theta_1) \sqrt{P}$$

$$f_2 = 0 .$$

Normalized power levels are now defined according to the relationships:

$$p_0 = \frac{f_0^2}{P}$$

$$p_i = \frac{f_i^2 \overline{m_i^2(t)}}{P} \qquad i = 1,2.$$

These levels for Cases I and II are listed in Table 13. Figures 24 through 27 are plots of the normalized power levels. Note that, because of the symmetrical nature of the modulations for Case II, a single set of curves provides either p_1 or p_2.

5.3.2 Analysis of Case III

The modulations are defined as:

$$m_1(t) = \sin \omega_1 t \qquad 0.3 \leq \theta_1 \leq 1.2 \text{ rad}$$

$$m_2(t) = \text{Sq } \omega_2 t \qquad 0.3 \leq \theta_2 \leq 1.2 \text{ rad}$$

where Sq $\omega_2 t$ is a two-level signal which takes on values +1 or -1, representative of digital data or a square-wave subcarrier.

Table 13. Normalized Demodulated Power Levels

	Case I	Case II	Case III
Carrier Level	$p_0 = J_0^2(\theta_1)$	$p_0 = J_0^2(\theta_1)\, J_0^2(\theta_2)$	$p_0 = J_0^2(\theta_1)\cos^2\theta_2$
Modulation #1 Level	$p_1 = 2\, J_1^2(\theta_1)$	$p_1 = 2\, J_1^2(\theta_1)\, J_0^2(\theta_2)$	$p_1 = 2\, J_1^2(\theta_1)\cos^2\theta_2$
Modulation #2 Level	$p_2 = 0$	$p_2 = 2\, J_0^2(\theta_1)\, J_1^2(\theta_2)$	$p_2 = J_0^2(\theta_1)\sin^2\theta_2$

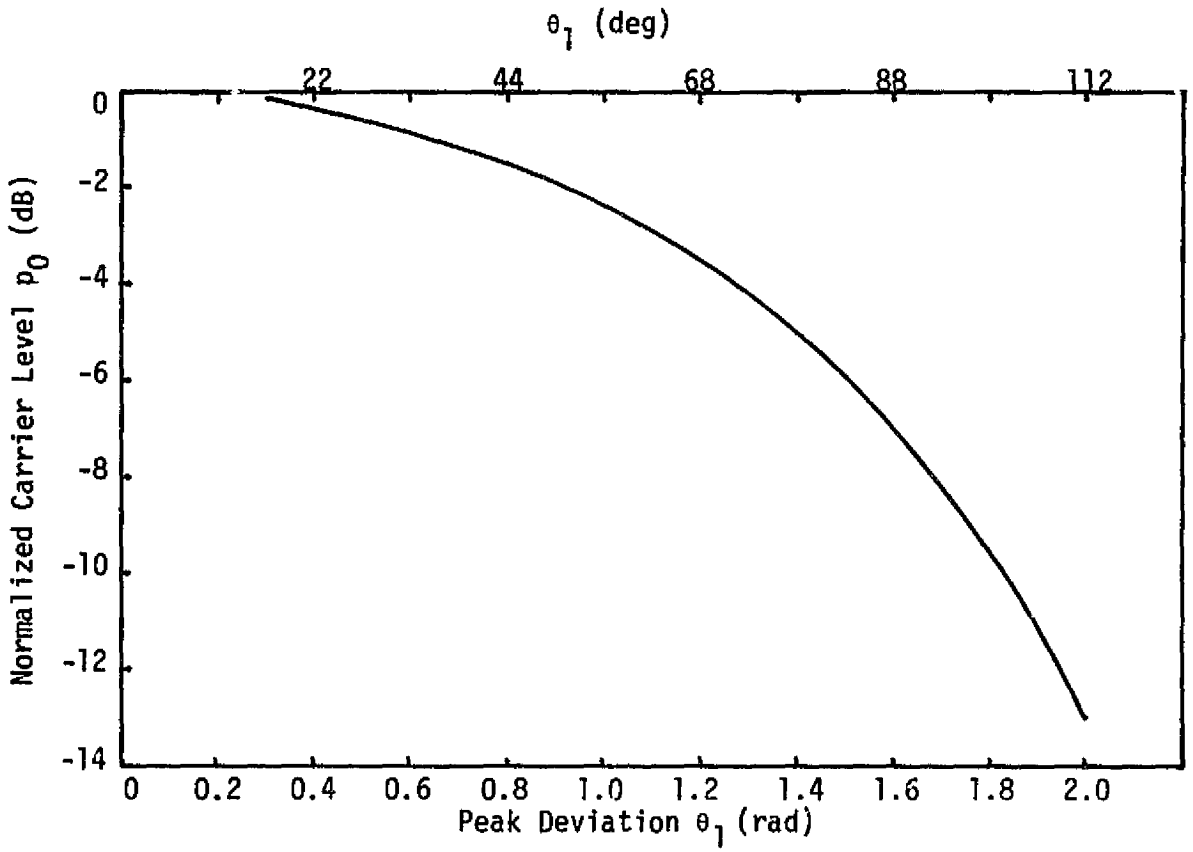

Figure 24. Case I--Carrier Suppression as a Function of Modulation Index

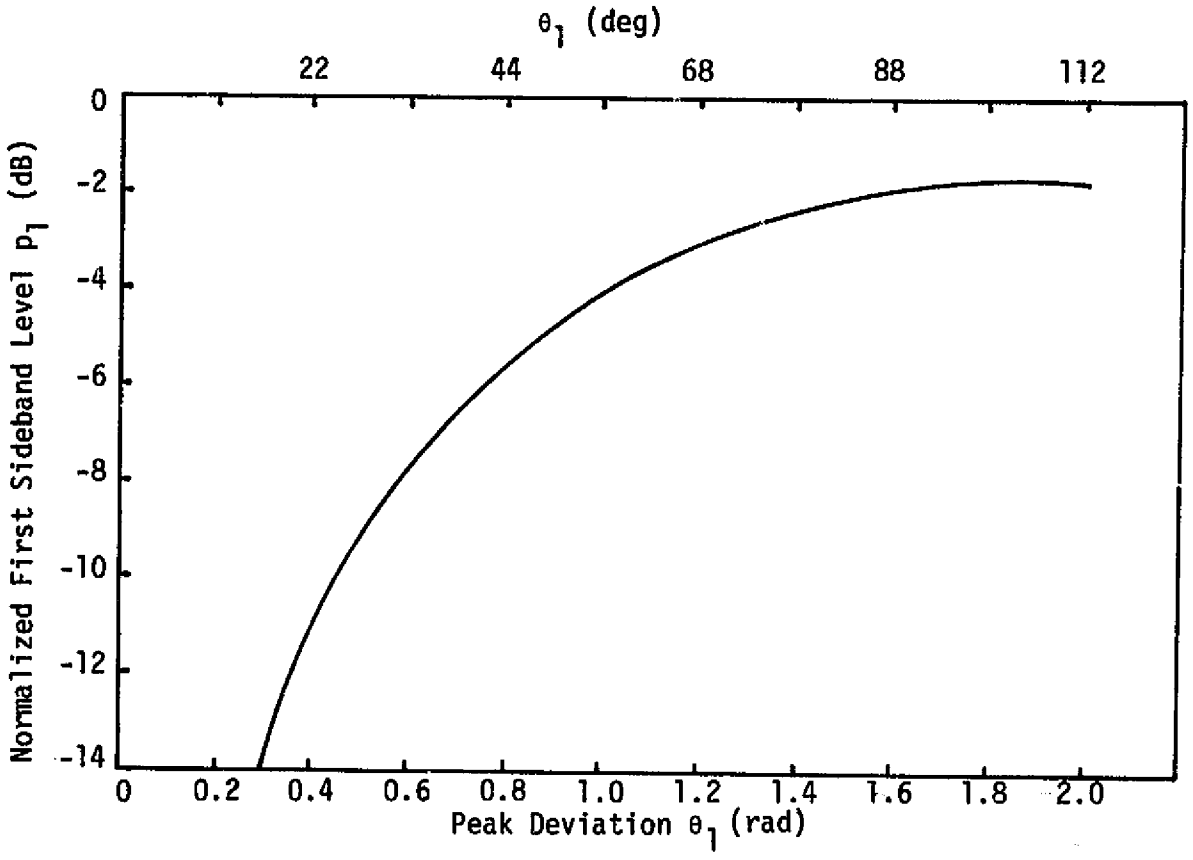

Figure 25. Case I--First Sideband Normalized Power Level as a Function of Modulation Index

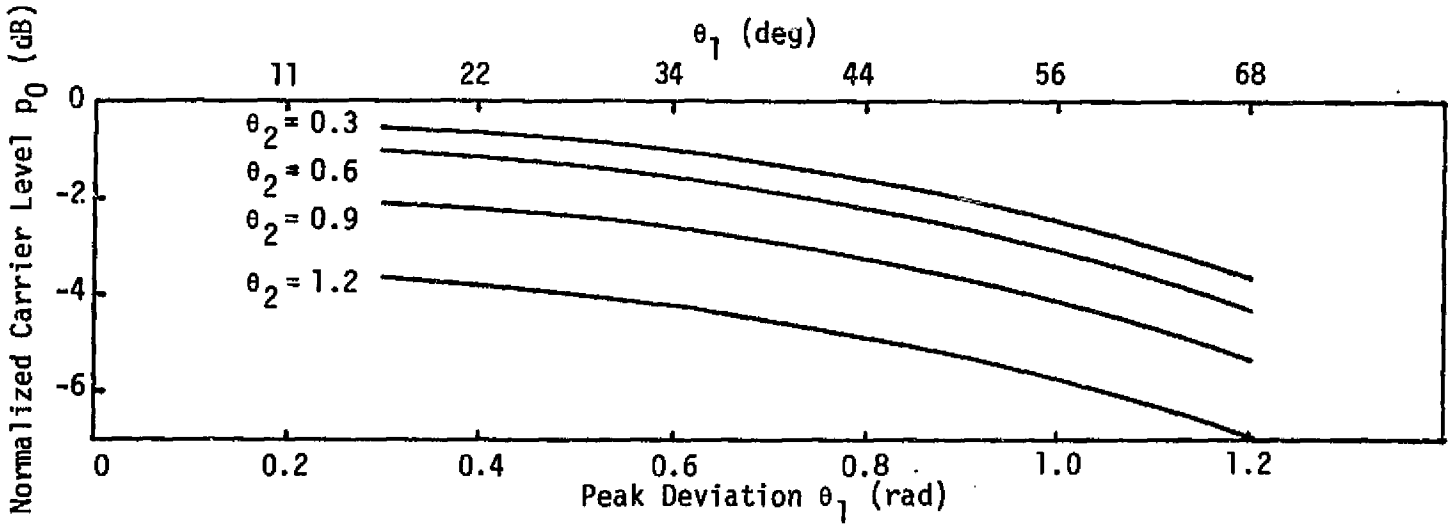

Figure 26. Case II--Carrier Suppression as a Function of Modulation Indices

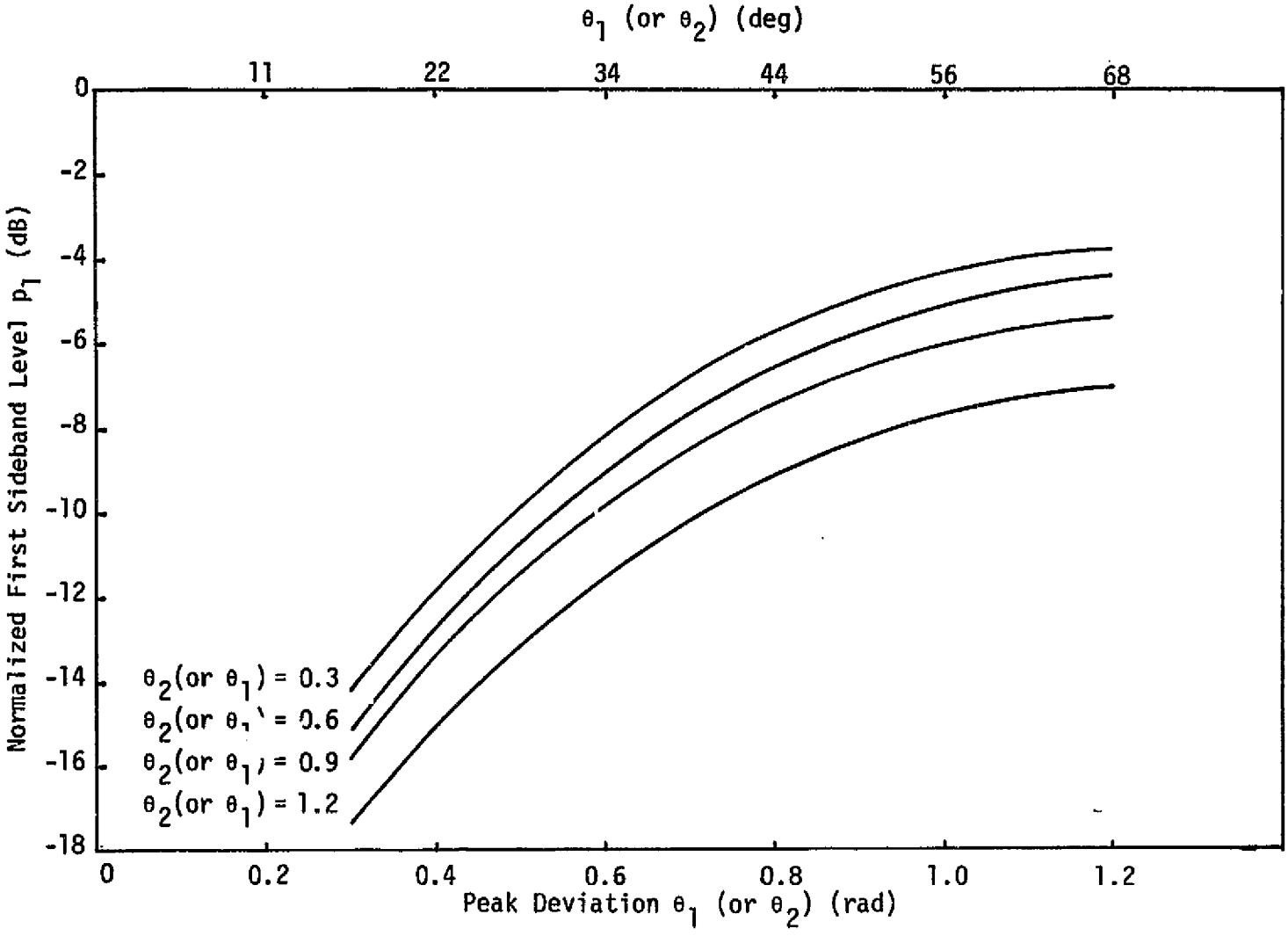

Figure 27. Case II--First Sideband Normalized Power Level as a Function of Modulation Indices

Using the same procedure as for Case II, with appropriate modifications, the expanded equation for s(t) becomes:

$$s(t) = \sqrt{2P}\left[\cos\omega_0 t\left\{\left[J_0(\theta_1) + 2\sum_{\substack{n=2\\ \text{even}}}^{\infty} J_n(\theta_1)\cos n\omega_1 t\right]\cos\theta_2 - 2\sum_{\substack{n=1\\ \text{odd}}}^{\infty} J_n(\theta_1)\sin n\omega_1 t\sin\theta_2\ \mathrm{Sq}\,\omega_2 t\right\} - \sin\omega_0 t\left\{2\sum_{\substack{n=1\\ \text{odd}}}^{\infty} J_n(\theta_1)\sin\omega_1 t\cos\theta_2 + \mathrm{Sq}\,\omega_2 t\sin\theta_2\left[J_0(\theta_1) + 2\sum_{\substack{n=2\\ \text{even}}}^{\infty} J_n(\omega_1)\cos n\omega_1 t\right]\right\}\right] \quad (106)$$

The amplitude functions are:

$$f_0 = J_0(\theta_1)\cos\theta_2\sqrt{P}$$

$$f_1 = 2J_1(\theta_1)\cos\theta_2\sqrt{P}$$

$$f_2 = J_0(\theta_1)\sin\theta_2\sqrt{P}\ .$$

and the normalized power levels are listed in Table 13. Figures 28 through 30 plot the various normalized powers as a function of modulation index.

5.3.3 Conclusions

The results of the analysis, as expressed by (104), (105), and (106), show that the sinusoidal phase demodulator gives rise to harmonics and cross-modulations in addition to the desired outputs. The power coefficients of the components depend on Bessel and cosine functions of the phase modulation indices. Since an ideal linear phase demodulator would simply produce an output of $\theta_1\ m_1(t) + \theta_2\ m_2(t)$, it is clear that the price paid for the use of the easily implemented product type phase detector is a loss of effective modulation signal power to the unwanted terms.

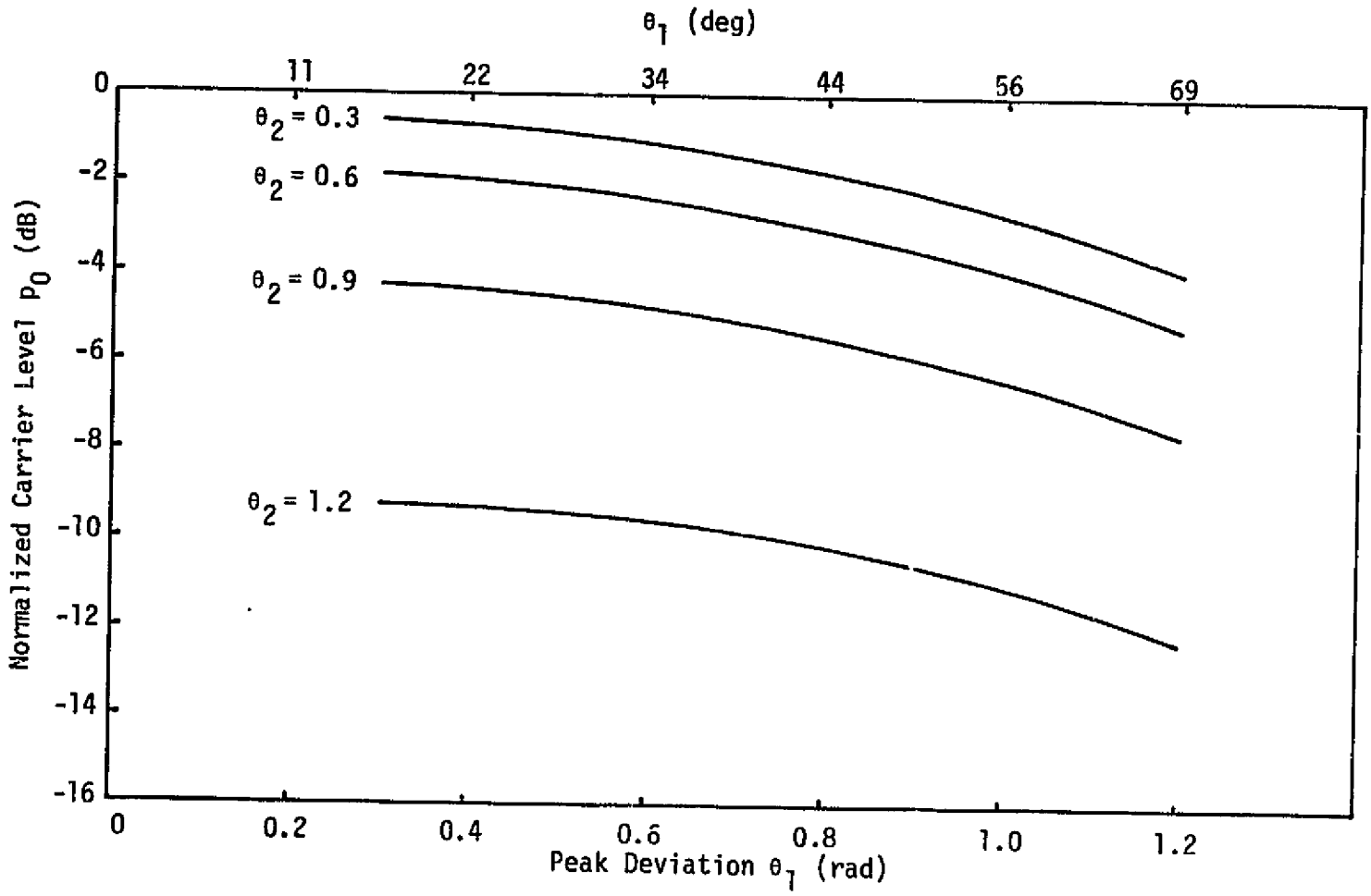

Figure 28. Case III--Carrier Suppression Factor as a Function of Modulation Indices

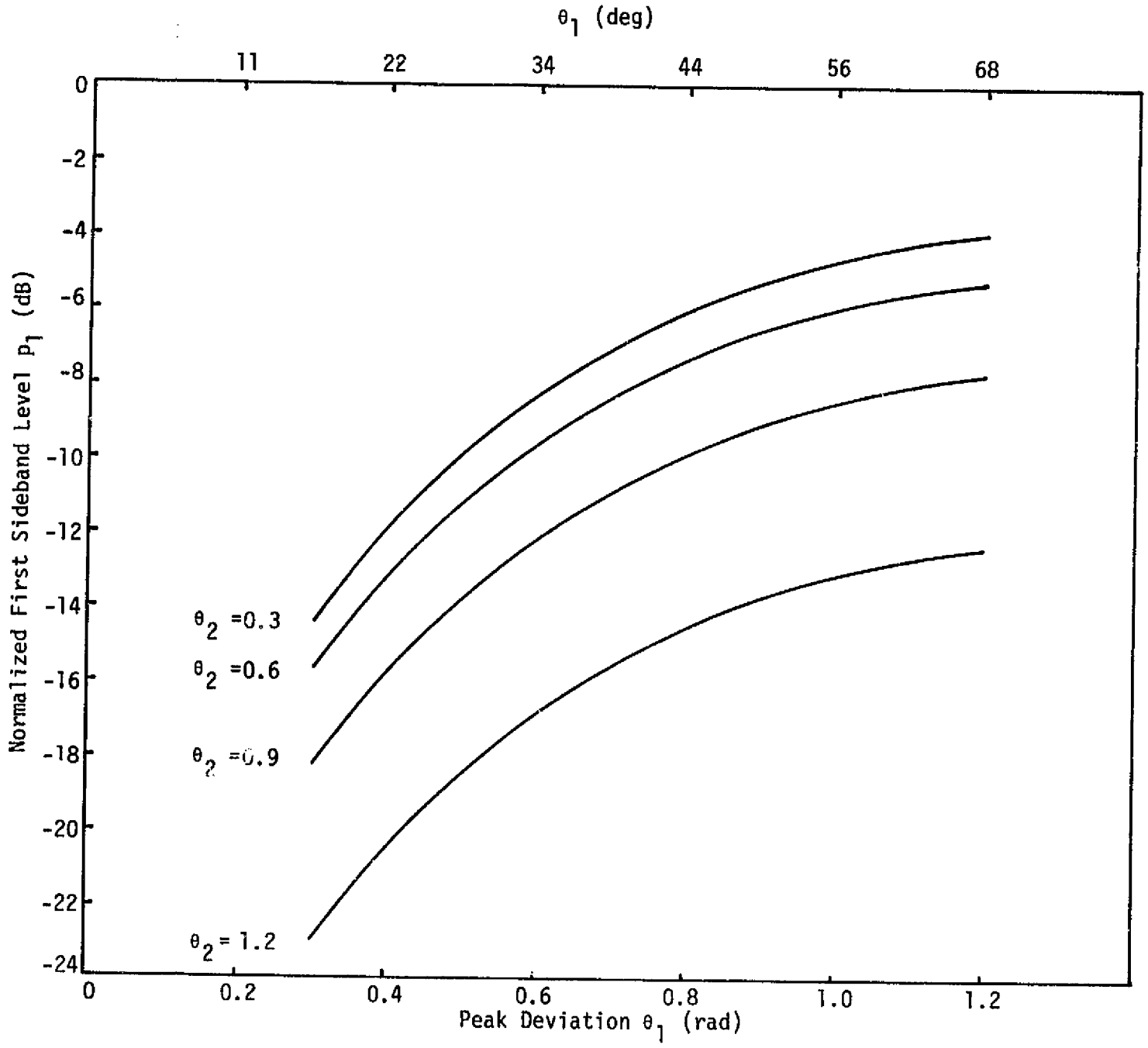

Figure 29. Case III--First Sideband Normalized Power Level for the Sinusoidal Modulation as a Function of Modulation Indices

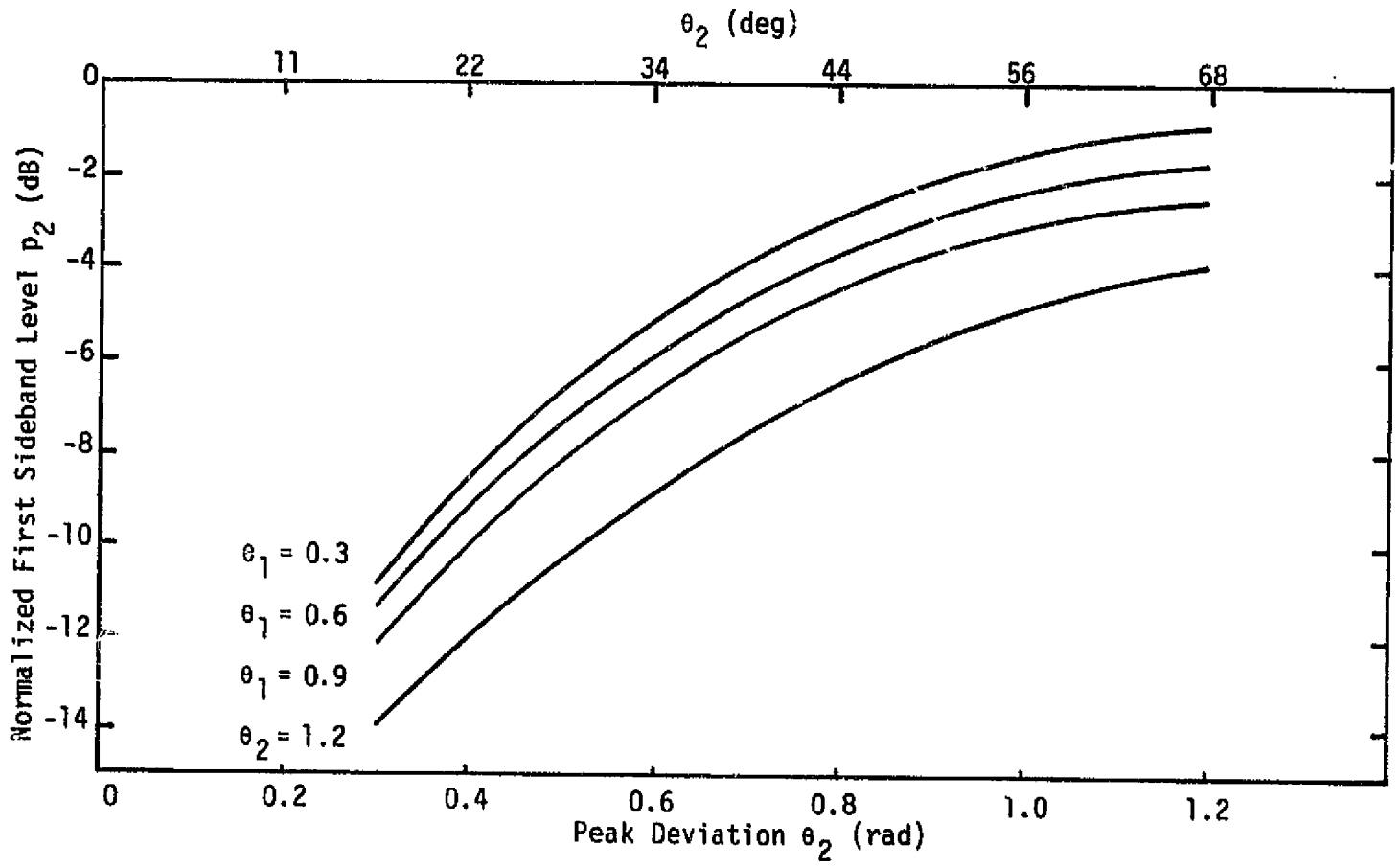

Figure 30. Case III--First Sideband Power Level for the Square Modulation as a Function of Modulation Indices

5.4 Payload Interrogator and Ku-Band Signal Processor Interface Signal Regulation

For nonstandard modulations which cannot be processed by the PSP (or CIU), the output of the PI is transmitted to the ground on what is known as the bent-pipe link. A general description of the bent-pipe link is given in subsection 4.4.1 and the nature of the PI/KuSP interface is summarized in subsection 4.4.2.

The special topic for consideration in the following two subsections is the block labeled "Amplitude Regulator" on Figure 12. In subsection 5.4.1, the optimum performance requirements for the regulator are analyzed, and subsection 5.4.2 discusses a functional breadboard design for the regulator that is under evaluation.

5.4.1 Bent-Pipe Link Wideband Channel FM Drive Requirements

Figure 31 is a diagram of the system model for the bent-pipe link. To the left of the interface line are the payload signal sources, which may be either analog or digital in nature. In particular, the PI receiver generates a number of analog and digital signal types depending upon the modulation waveform and the RF signal level input to the receiver. Signal and noise at the receiver input are summed, and the receiver itself is treated as a perfect demodulator. The noise at the receiver output is taken to be lowpass Gaussian, and the possible signal component waveforms are those listed in Table 10.

At the right of the interface which forms the input to the KuSP, a switch is able to select between the PI output and attached payload signals. The subject FM drive regulator follows, where K is a gain controllable amplifier and Δ is the regulation loop characteristic. Regulator output, in turn, frequency modulates the downlink transmitter, with a modulation sensitivity of D_f (Hz/volt). At the ground station, the receiver is modeled with an additive noise source at its input, followed by the noncoherent frequency discriminator.

The following symbols and expressions are defined:

$r(t)$ = the PI receiver output (signal plus noise)

$n_1(t)$ = the PI receiver noise

S/N_1 = the SNR input to the regulator and frequency modulator

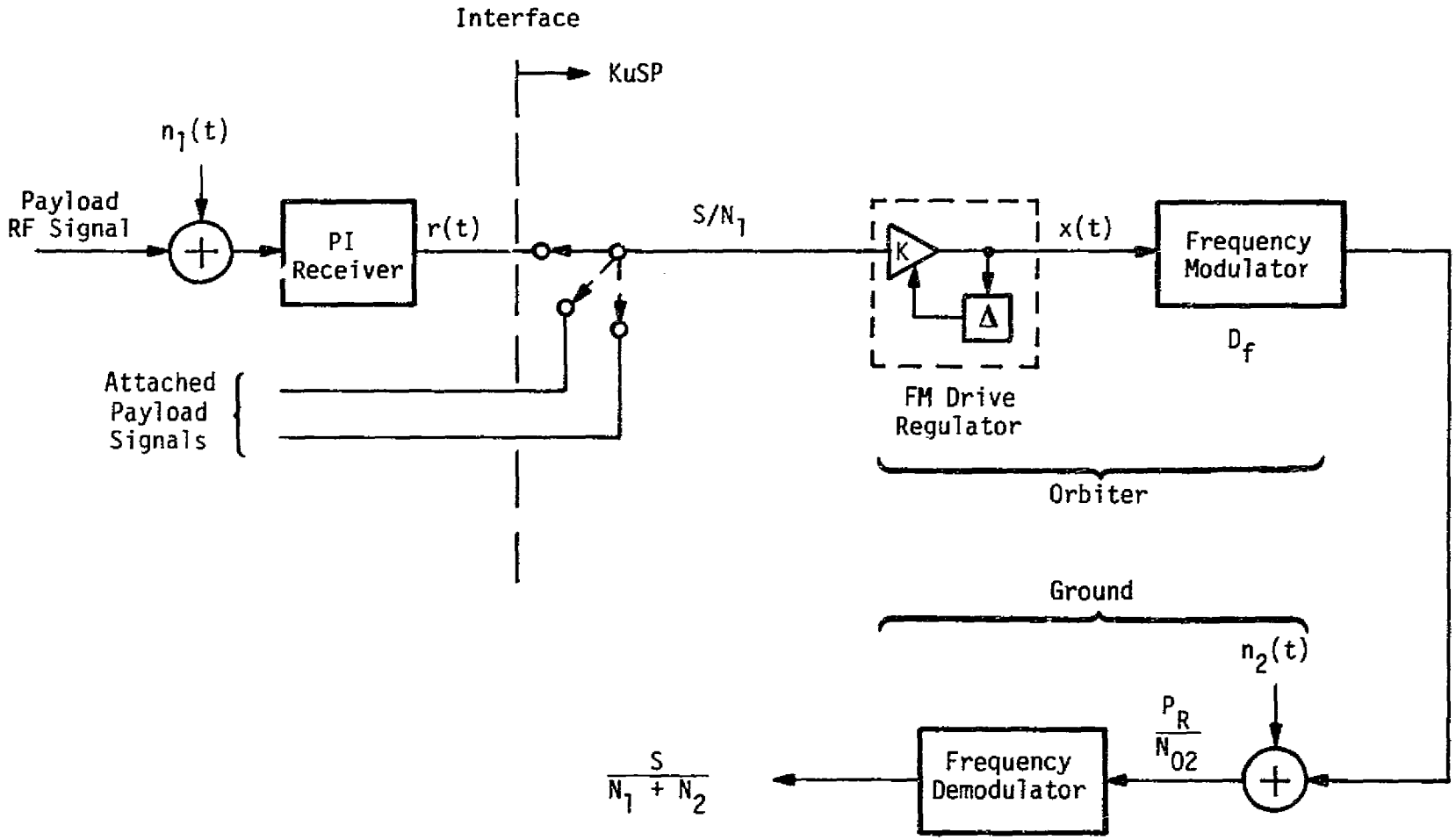

Figure 31. Bent-Pipe System Model

$x(t)$ = the bent-pipe modulating signal

f_m = the noise bandwidth of the modulating signal

$n_2(t)$ = the ground receiver noise

P_R/N_{02} = the carrier power to noise-spectral-density ratio at the input to the FM demodulator

$\frac{S}{N_1+N_2}$ = the useful signal to total-noise ratio at the output of the FM demodulator.

The problem is to determine the best overall characteristic for the FM drive regulator which maximizes $S/(N_1+N_2)$ when S/N_1 is allowed to cover a range from very large SNR to very small SNR. Two specific characteristics are considered: (a) an RMS characteristic which sets $x(t)$ in accord with the RMS value of $r(t)$, and (b) a peak characteristic which sets $x(t)$ in accord with the peak or maximum absolute value of $r(t)$

For the overall system,

$$\frac{S}{N_1+N_2} = \frac{1}{\left(\frac{N_1}{S}\right) + \left(1+\frac{N_1}{S}\right)\left(\frac{N_2}{S+N_1}\right)} \tag{107}$$

where the symbols represent signal and noise powers as previously defined.

For the FM portion of the link:

$$\frac{S+N_1}{N_2} = \left(\frac{P_R}{N_{02}}\right)\left(\frac{3}{f_m{}^3}\right)\left(D_f{}^2\,\overline{x^2(t)}\right) \tag{108}$$

Here the overbar denotes the mean-squared value of $x(t)$.

For educational and comparison purposes, some specific parameter values and ranges are defined as follows:

f_m = 5.5 MHz (assumed noise bandwidth of the PI 4.5 MHz (3 dB) output)

P_R/N_{02} = 90.8 dB (see Table 14)

$D_f|x(t)|_{max}$ = 11 MHz (maximum allowable frequency deviation of the FM transmitter)

Table 14. FM Link Design Control Table

Entry No.	Parameter (Calculation)	Symbol	Units	Nominal Value
1	Total Transmit Power	P_T	dBW	17.0
2	Transmit Circuit Losses	L_{TX}	dB	-3.6
3	Transmit Antenna Gain	G_T	dB	35.4
4	Transmit Pointing Loss	L_{PTX}	dB	-0.7
5	Space Loss, 22,786 nmi f = 15,000 MHz	L_S	dB	-208.5
6	Receive Antenna Gain	G_R	dB	56.2
7	Polarization Loss	L_{POL}	dB	-0.3
8	Receive Pointing Loss	L_{PR}	dB	-0.5
9	Receive Circuit Losses	L_R	dB	-0.3
10	Atmospheric Loss	L_A	dB	-1.0
11	TDRS Loss	L_{TDRS}	dB	-2.0
12	Total Received Power (Σ 1 through 11)	P_R	dBW	-108.3
13	Receiver Noise Density	N_{02}	dBW/Hz	-199.1
14	Received Signal/Noise Density (12 - 13)	P_R/N_{02}	dB	90.8

(This is the maximum or no-margin value)

The PI receiver has a signal dynamic range of 110 dB. Depending upon the payload transmitter modulation index and the PI received signal level, the PI receiver's wideband output SNR (S/N_1) could range from -30 dB to +90 dB in a 5.5 MHz bandwidth.

The FM transmitter deviations produced by the various possible modulating waveforms working with each regulator characteristic are now established. Gaussian noise is selected as the basis for equal performance between the RMS and peak regulators, with the noise peak value taken as three times its RMS value. Defining the RMS value of the modulating waveform, x(t), by σ_x, the RMS deviation, $D_f\ \sigma_x$, for both regulators will be 3.7 MHz. This is also the RMS deviation for all waveforms regulated by the RMS characteristic. On the other hand, the peak regulator maintains the peak value of x(t) (as observed over a reasonable period of time) constant, i.e., $D_f|x(t)|_{max}$ = 11 MHz for all waveforms. Therefore, $D_f\ \sigma_x$ varies with the waveform type. Table 15 summarizes the values of $D_f\ \sigma_x$ for the waveform types and both regulator characteristics.

The FM link performance is now determined to obtain $(S+N_1)/N_2$. Using (108) together with the values in Table 15 and the previously designated parameters (and noting that $\overline{x^2(t)} = \sigma_x^2$), the FM link performance is is calculated. The results appear in Table 16. Note from the table that the values for the peak regulator exceed those for the RMS regulator except for the Gaussian waveform where they are equal (as defined). One immediate practical use for Table 16 is that it gives the end-to-end link performance when N_1 = 0 (i.e., when the PI receiver is operating at very strong received signal levels or when the input to the KuSP is from an attached payload). Clearly, the peak regulator performance is superior, and, for the square waveform (e.g., digital data), it has a 9.4 dB advantage over the RMS regulator.

The presence of measurable noise on the payload to PI link degrades the overall end-to-end link SNR. As an example, let S/N_1 = 20 dB. Using (107), the end-to-end performance measure, $S/(N_1+N_2)$ is calculated and tabulated in Table 17. Comparison with the values of Table 16, which are taken for the situation when N_1 = 0, shows that the presence of the payload to PI link noise degrades all entries. Note also that the peak regulator performance for the square waveform is now only 1.1 dB superior to that for the RMS regulator. This is indicative of the fact that the

Table 15. Values of $D_f\sigma_x$ (MHz)

Waveform	RMS Regulator	Peak Regulator
One Sinusoid	3.7	7.8
Two Sinusoids	3.7	5.5
Three Sinusoids	3.7	4.4
Four Sinusoids	3.7	3.9
Square	3.7	11.0
Gaussian	3.7	3.7

Table 16. FM Link Performance

Waveform	$\frac{S + N_1}{N_2}$ (dB) RMS Regulator	$\frac{S + N_1}{N_2}$ (dB) Peak Regulator
One Sinusoid	24.7	31.1
Two Sinusoids	24.7	28.1
Three Sinusoids	24.7	26.2
Four Sinusoids	24.7	25.1
Square	24.7	34.1
Gaussian	24.7	24.7

This table also gives $S/(N_1 + N_2)$ for $S/N_1 \rightarrow \infty$

Table 17. $S/(N_1 + N_2)$ for $S/N_1 = 20$ dB

Waveform	$\frac{S}{N_1 + N_2}$ (dB)	
	RMS Regulator	Peak Regulator
One Sinusoid	18.7	19.7
Two Sinusoids	18.7	19.4
Three Sinusoids	18.7	19.1
Four Sinusoids	18.7	18.8
Square	18.7	19.8
Gaussian	18.7	18.7

end-to-end channel is payload to PI performance limited. Reference to Table 17, however, shows that the peak regulator still outperforms the RMS regulator and will for any S/N condition.

The conclusions drawn from the above analysis are:

(1) Maximizing the allowable deviation for any of the possible waveforms maximizes the FM link performance.

(2) The peak regulator gives highest performance for all waveforms.

(3) The bent-pipe output SNR will always be less than the FM link performance by itself.

Axiomatix therefore recommends that the KuSP FM drive regulator have a peak characteristic. Design and circuit performance considerations for the peak regulator are covered in the following subsection.

5.4.2 Peak Regulator Design and Functional Breadboard Evaluation

Axiomatix has undertaken to design and evaluate a breadboard peak regulator circuit. The purpose for this activity is threefold:

(1) to demonstrate the simplicity of implementation using readily available integrated circuits;

(2) to show that the loop will be stable and perform to expectations for all input waveforms;

(3) to provide a means to experimentally determine the proper loop response time (i.e., loop bandwidth).

Figure 32 is a functional diagram for the peak regulator loop. The input, V_i, is first passed through a two-pole LPF having a 3 dB frequency of 4.5 MHz. This LPF is really not a part of the loop proper, but is necessary to simulate the output bandwidth characteristics of the PI receiver. Following the LPF is an amplifier whose gain K is voltage controllable by a reference voltage, V_R. Actually, the gain controllable amplifier is operated in a less than unit gain state (i.e., as an attenuator) with a nominal gain (zero loop error) of -24 dB. The +24 dB gain amplifier following therefore compensates for this loss. Nominally, $V_o = V_i$.

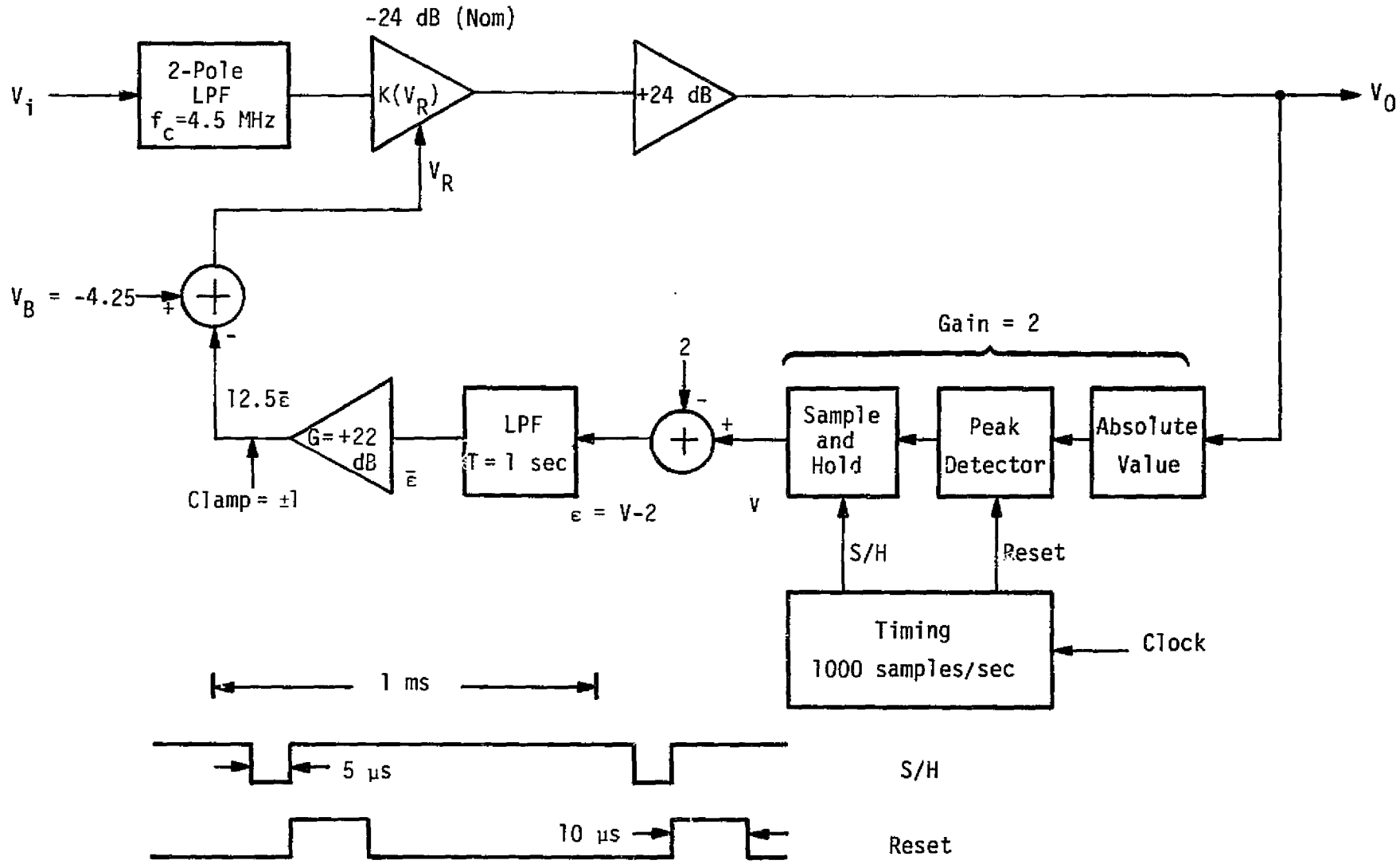

Figure 32. Peak Regulator Loop Functional Diagram

Output of the regulator, V_o, is input to an absolute value circuit which is mechanized in the form of a full-wave linear rectifier. A gated-reset peak detector following the rectifier functions to store or hold the largest voltage peak observed over a 0.99 ms time period. At the end of each 1 ms sample period, the peak value is transferred to a sample-and-hold amplifier where it is retained while the peak detector memory (capacitor) is reset and the next peak detection operation takes place.

Designating the sample-and-hold output by the symbol V, the loop instantaneous error ε is formed by subtracting a 2 volt reference from V. Thus, $\varepsilon = V-2$. An LPF follows (time constant = 1 sec) which averages over a large number of the peak detected error values that may change each 1 ms. The LPF output is denoted by $\bar{\varepsilon}$. Following the LPF is a 22 dB gain amplifier which produces at its output 12.5 $\bar{\varepsilon}$ subject to a maximum constraint of ±1 volt. This constraint is imposed to keep the reference voltage to the gain controllable amplifier within a linear operating range, precluding the possibility of an unstable loop condition. The amplifier voltage reference V_R is formed by offsetting the error 12.5 $\bar{\varepsilon}$ by -4.25 volts.

Operating parameters and the loop regulation characteristic are now presented. The gain controllable amplifier is an RCA type CA3002, and its pertinent gain versus reference voltage plot is shown in Figure 33. An equation of operation for this amplifier may be written as:

$$20 \log [K(V_R)] = -30 - 80 (V_R - 4) .$$

Neglecting the T = 1 sec LPF, the closed-loop equation of operation may be easily derived using ( ) and the relationships indicated on Figure as:

$$V_{op} = V_{ip} \times 10^{100(V_{op}-1)},$$

where V_{op} and V_{ip} are, respectively, the regulator waveform peak output and input voltages. From this equation, it is seen that the regulator will hold the peak output to within ±1% of 1 volt as the input experiences a ±20 dB variation. Table 18 lists some specific input/output voltage values.

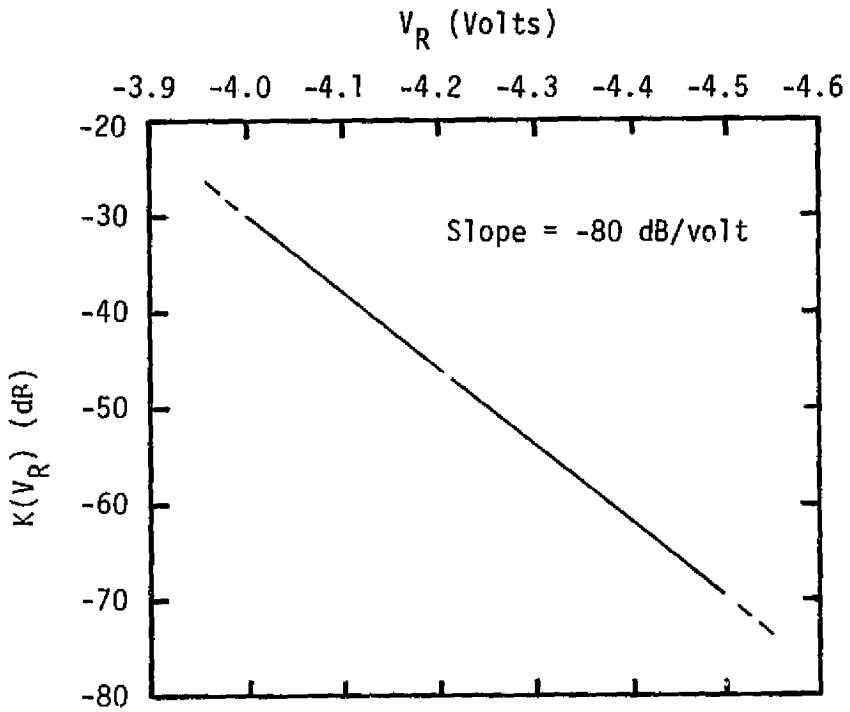

Figure 33. RCA CA3002 Gain versus Reference Voltage Plot

Table 18. Peak Regulator Input and Output Voltages

V_{ip} (volts)	V_{op} (volts)
9.90	0.990
3.14	0.995
1.26	0.999
1.00	1.000
0.79	1.001
0.32	1.005
0.10	1.010

As previously discussed, the peak error sampling rate has been chosen as 1 kHz, and the peak detector averaging time per sample is 0.99 ms. Thus, for any of the waveform shapes considered, where the lowest subcarrier (sinusoid) frequency is expected to be about 30 kHz and random noise occupies the full 5.5 MHz bandwidth, each peak sample should be very close to the true peak value of the waveform. Averaging over a thousand or so error samples also provides the loop with a reasonably rapid response to dynamic input level changes, but is sufficiently long to obviate response to very short signal transients or the possibility of an occasional impulse noise burst due to EMI or other sources. Both the sampling rate and the LPF time constant are changeable in the Axiomatix breadboard, allowing trade-off experiments to be conducted.

Figure 34 is a circuit diagram for the Axiomatix peak regulator breadboard, and Figure 35 shows the companion timing logic circuits. As most of the regulator design is based upon operational amplifier configurations, a correspondence between the circuit diagram and the functional diagram of Figure 32 may be easily established. The amplifiers having the AD prefix are Analog Devices types, and AD583 is the sample/hold amplifier. Block AH0152 is a FET switch used to discharge the peak detector capacitor (100 pf). Clamp for the error voltage amplifier output is provided by the pair of reversed IN457 duo-diode groups. The timing waveforms are produced by monostable multivibrators.

FOLDOUT FRAME

ORIGINAL PAGE IS
OF POOR QUALITY

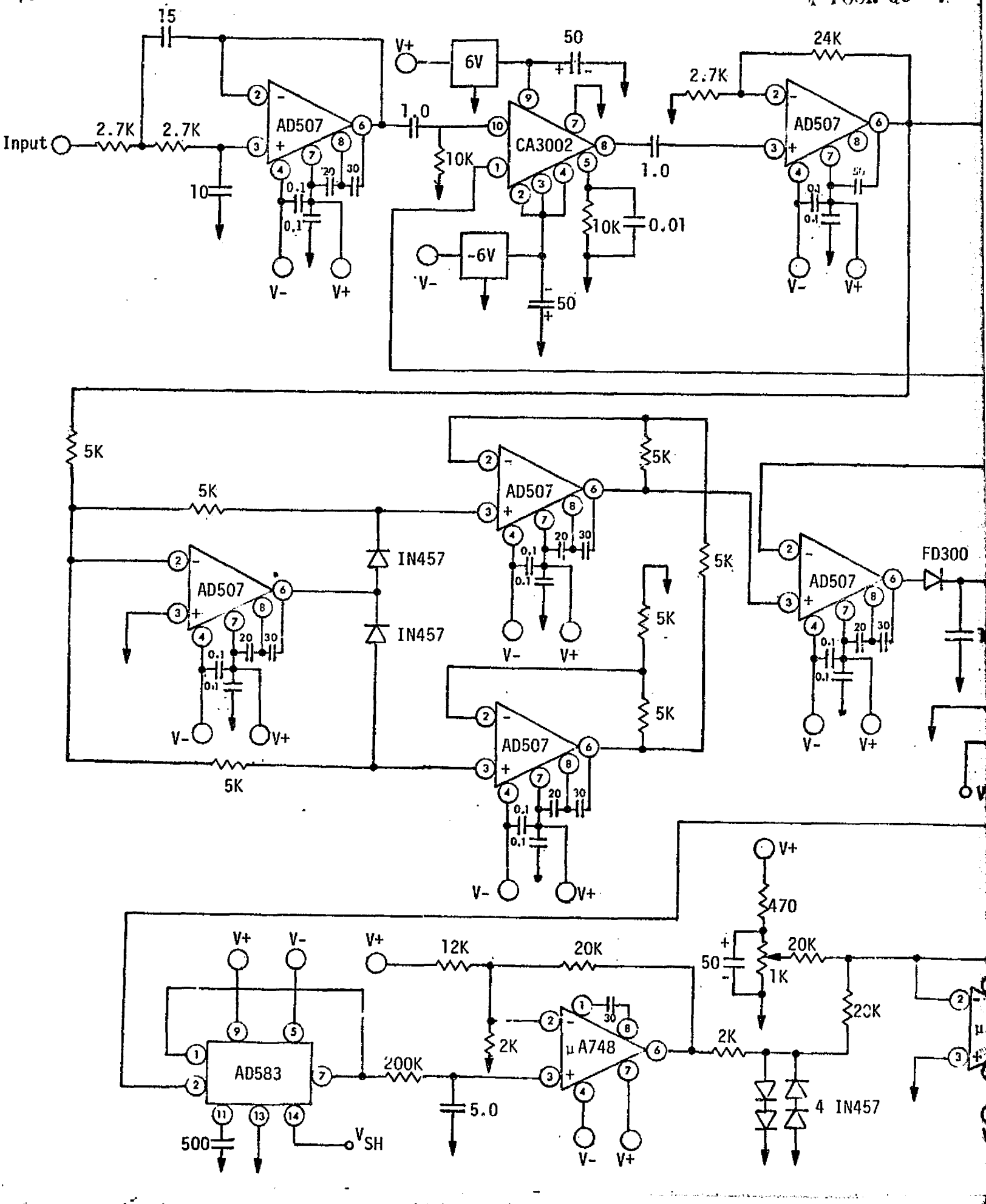

Figure 34. Peak Regulator Circuit Diagram

FOLDOUT FRAME

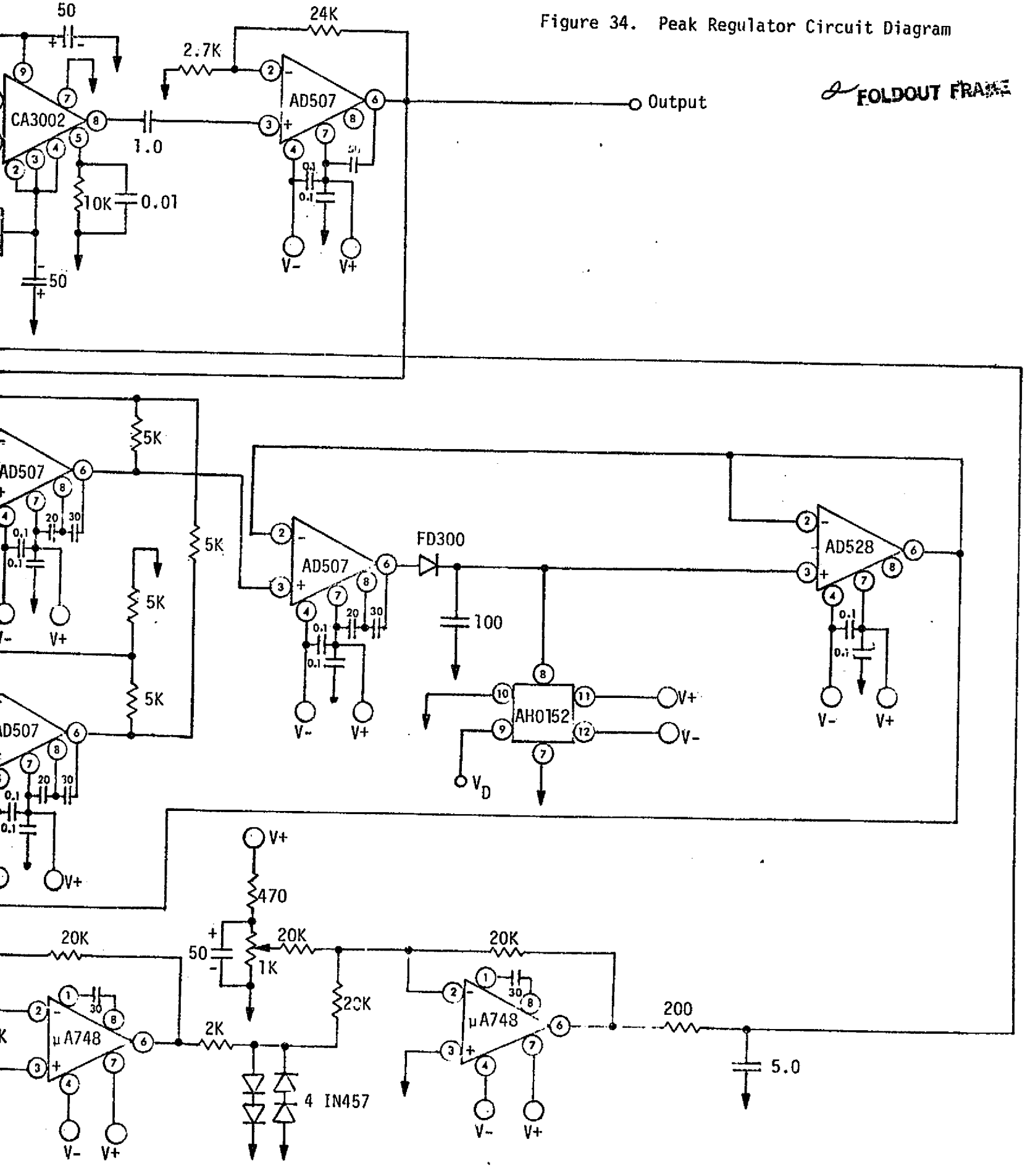

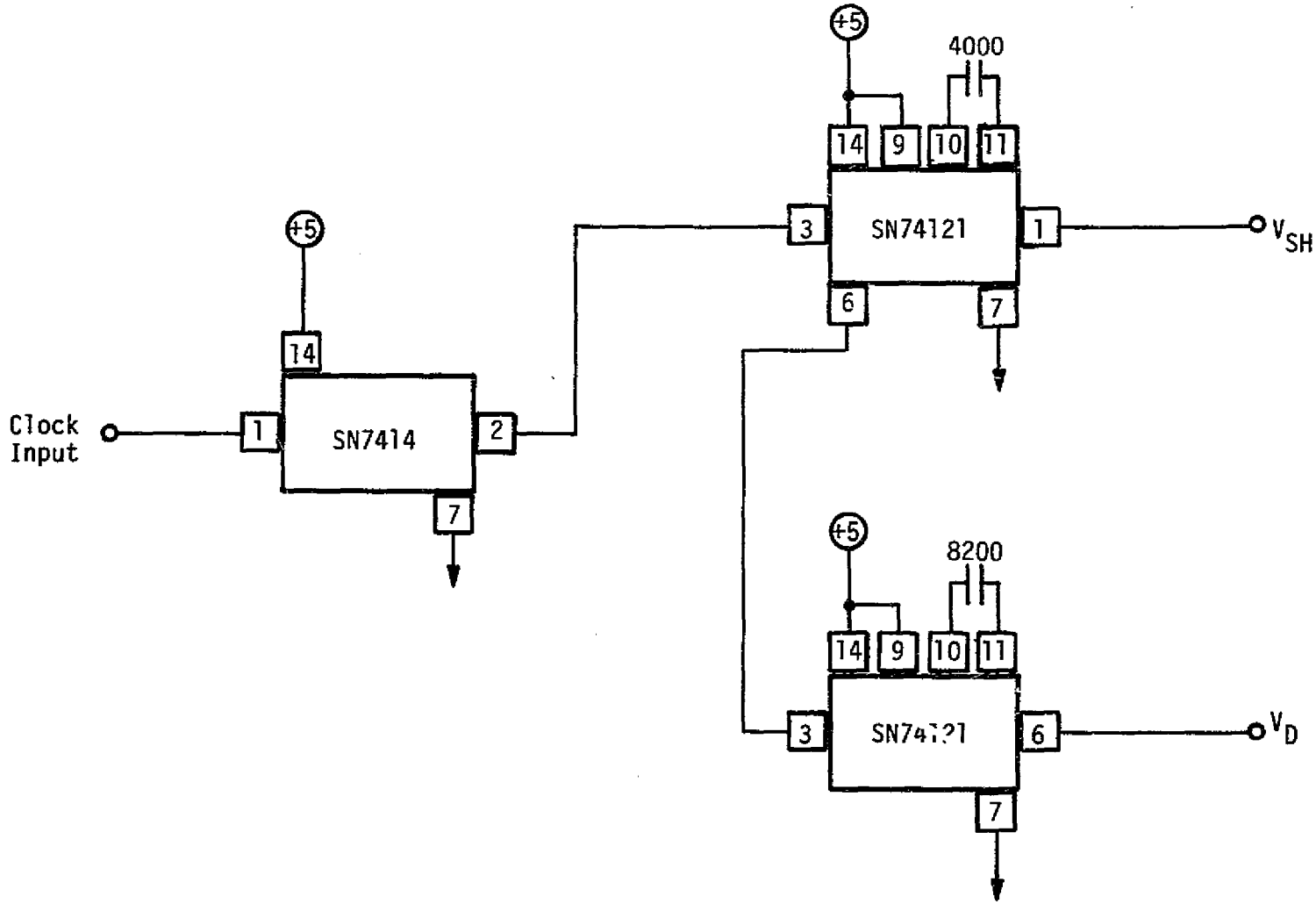

Figure 35. Peak Regulator Timing Logic Diagram

As of the writing of this report, Axiomatix has received delivery of the necessary parts to construct the peak regulator breadboard. The breadboard should be built and tested during the months of March and April, 1979.

6.0 PAYLOAD COMMUNICATION SYSTEM PERFORMANCE ASSESSMENTS

6.1 Payload Interrogator and Payload Signal Processor Combined Performance

From a statistical performance point of view, both the PI and PSP handle and process signals in the presence of noise. If the receiver, subcarrier demodulator, bit synchronizer and data detector were all ideal, a certain maximum level of performance would be expected of the PI/PSP combination. Thus, for a given bit error probability as measured at the output of the PSP, a certain minimum RF signal level would be required at the input to the PI. As an example, consider the following pertinent parameters.

$$P_e = 1 \times 10^{-2}$$

$$R_b = 16{,}000 \text{ bits/sec}$$

$$E_b/N_0 = 4.3 \text{ dB}$$

$$NF = 7.0 \text{ dB} .$$

The expression for the received data power is (parameters in dB):

$$P_d \text{ (dBm)} = \frac{E_b}{N_0} + R_b - (174 - NF) .$$

Substituting the above parameters yields P_d = -120.7 dBm. However, for a carrier modulation index of β = 1.0 radian, Rockwell has specified that the 1×10^{-2} bit error probability occur for a received data power level of -116.4 dBm. This leaves 4.3 dB to account for the combined PI/PSP losses.

The PSP specification allocates a 1.5 dB loss to the PSP (0.6 dB to the subcarrier demodulator and 0.9 dB to the bit synchronizer and detector). This therefore leaves 2.8 dB to be apportioned to the various receiver losses. Actually, the payload transmitter phase modulation index tolerance is included in this allotment, accounting for 0.7 dB when β = 0.9 radian. If, in addition, there is a 0.5 dB tolerance on the receiver NF and a 1.0 dB interference degradation is allowed (as per specification), the remaining receiver loss is but 0.6 dB. This must be

divided between (a) the receiver phase noise effects, (b) wideband phase detector reference phase offset, (c) filtering, and (d) nonlinear effects.

Based upon the PI PLL SNR, the phase noise losses should be no more than 0.1 dB. Filtering may account for about 0.2 dB of loss and nonlinear effects for 0.1 dB. This leaves only 0.2 dB for allocation to demodulation reference phase offset. A 0.2 dB loss corresponds to a phase offset of 12°, which is reasonable for all standard modulation conditions.

With regard to the PSP, TRW has completed a series of tests on the PSP demodulator breadboard to experimentally determine the acquisition and tracking thresholds which appear as TBDs in the Rockwell specification. Based upon a criterion of a fixed minimum input signal level threshold for the PI receiver irrespective of modulation bit rate, the poorest performance for the PSP demodulator can be expected to occur for the highest bit rate of 16 kbps. Therefore, TRW has made the following threshold recommendations for the 16 kbps bit rate:

Tracking Threshold:	44 dB-Hz subcarrier-to-noise density at PSP LRU input. Mean time to lose lock of 10 seconds.
Acquisition Threshold:	45 dB-Hz subcarrier-to-noise density at PSP LRU input. The probability of achieving phase lock in 2 seconds or less shall be at least 0.9.

When the PSP maximum mechanization and operating degradation of 1.5 dB is accounted for, the effective E_b/N_0 tracking threshold becomes 0.5 dB.

Table 19 summarizes the PI and PSP losses.

6.2 Payload to Payload Interrogator Link Performance

The link from the payload to the PI carries telemetry data. In the NASA standard mode, the maximum data rate is 16 kbps. The link from the PI to the payload is the command channel; for the NASA standard mode, the maximum command bit rate is 2 kbps. Tables 8 and 9 of Appendix A are, respectively, typical link budgets (design control tables) for the telemetry and command channels.

Table 19. PI and PSP Losses

Parameter	Loss (dB)
Payload Transmitter β Lower Limit	-0.
PI Noise Figure Tolerance	-0.5
PI Interference Degradation	-1.0
PI Phase Noise Loss	-0.1
PI Demodulation Phase Offset Loss	-0.2
PI Filtering Loss	-0.2
PI Nonlinear Loss	-0.1
PSP Subcarrier Demodulator Loss	-0.6
PSP Bit Synchronizer Loss	-0.9
Total Loss	-4.3

6.3 End-To-End Payload Links

There are a number of possible end-to-end payload communication links. A prime link involves the PI, PSP (or CIU), and Ku-band relay system. This total combination of functional operations is shown in Figures 36 and 37.

The purpose here is to note the complexity of the overall link in terms of signal flow and the sources of noise. Also, a large number of parameters are involved in the determination of the end-to-end link performance. Some design control tables that predict the performance of the links may be found in the report "Users' Handbook For Payload-Shuttle Data Communication", Axiomatix Report No. R7809-4 for NASA Contract NAS 9-15604B, September 27, 1978.

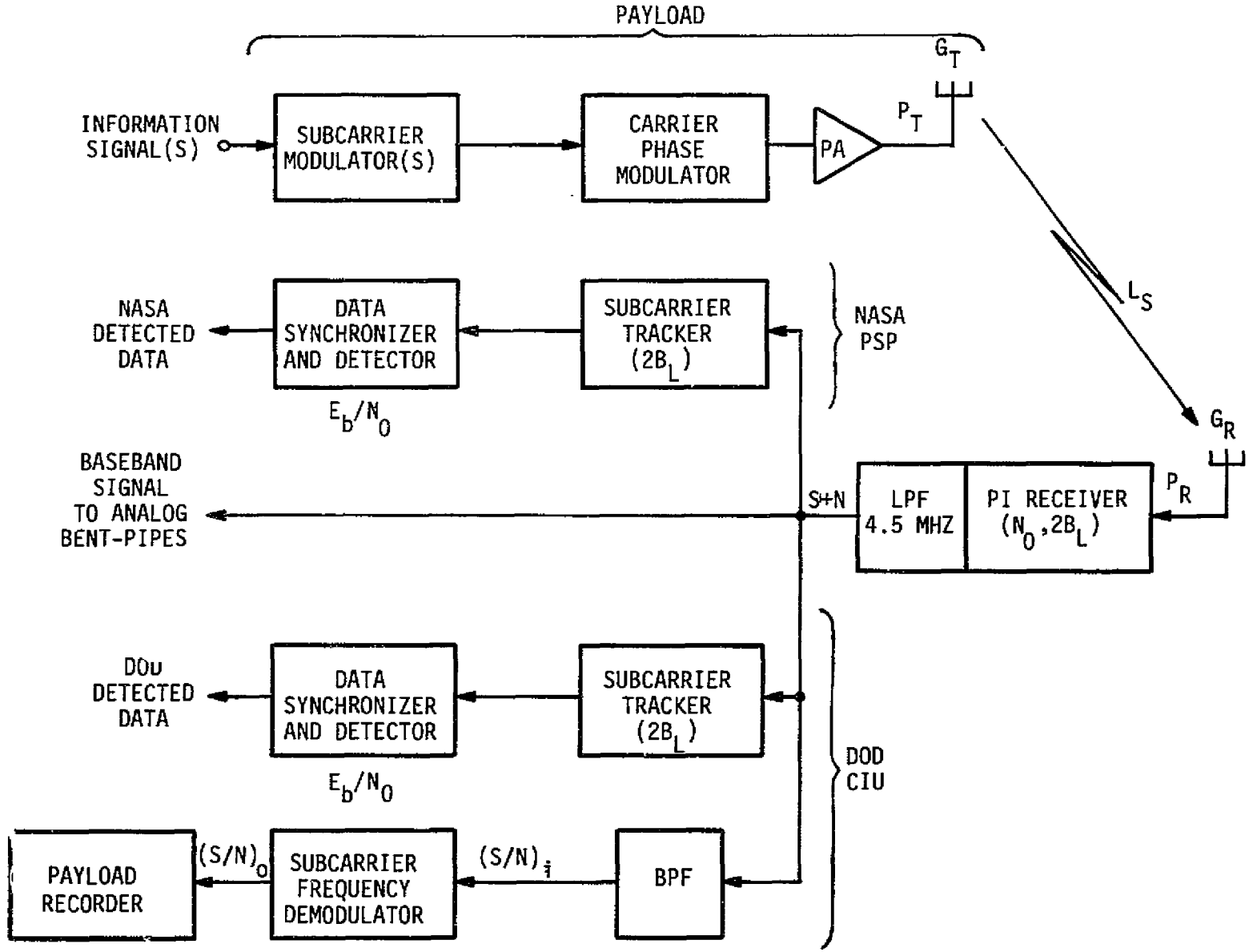

Figure 36. Payload to Orbiter S-Band Link

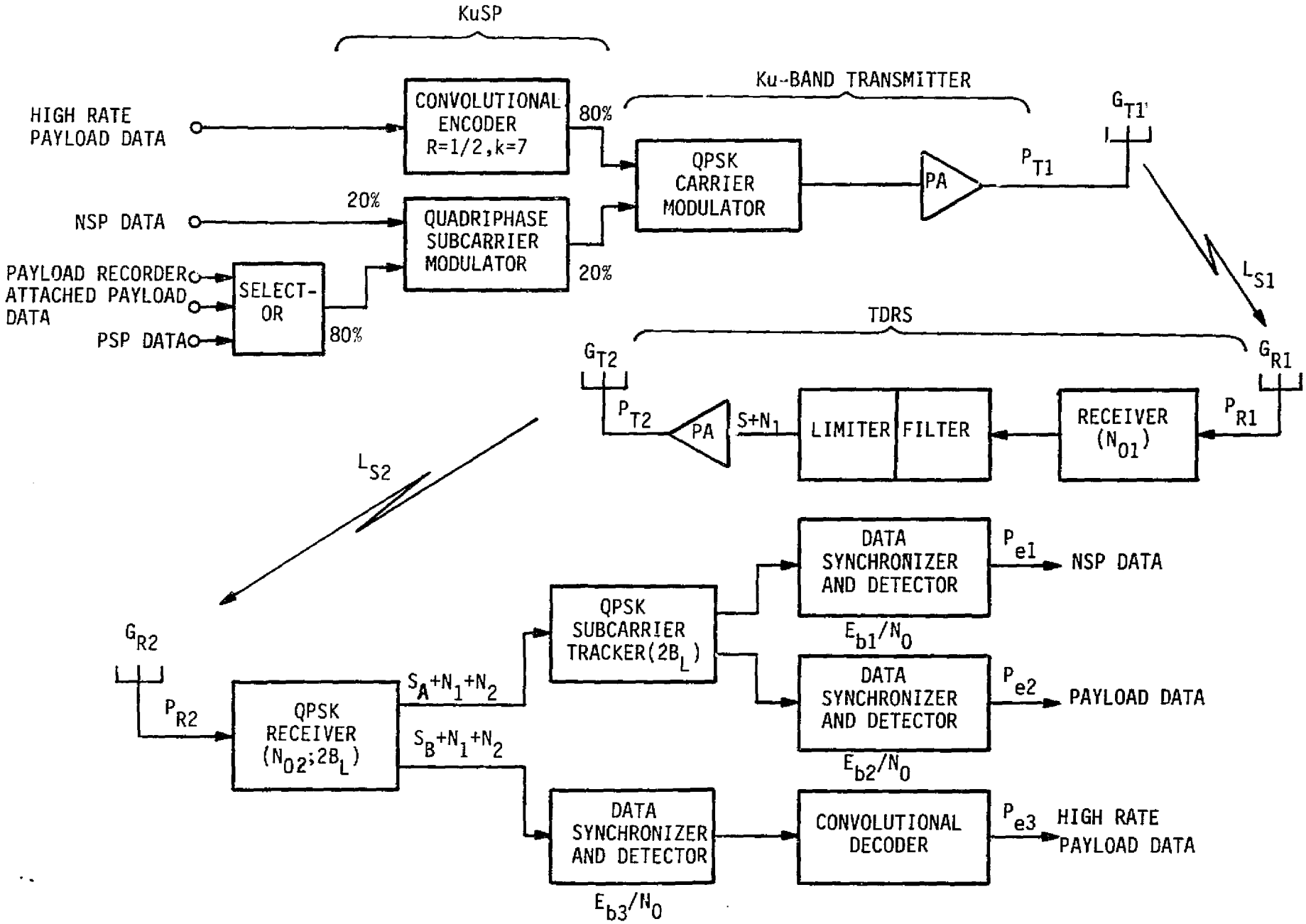

Figure 37. Orbiter to Relay to Ground Ku-Band QPSK Link

7.0 CONCLUSIONS

The overall payload communication system is still evolving. Direct payload interfacing avionic subsystems such as the PI and PSP are only in their conceptual design stages. Other hardware, such as that which makes up the Orbiter-ground S-band and Ku-band links is more fully developed, but is just entering its performance verification testing phase. Thus, it will be some time before all developmental problems are solved and reliable, well understood performance can be documented.

Concerning payload communication system design and performance issues, Table 7 has identified those which are presently unresolved. Others will inevitably arise as a result of near future preliminary design reviews and hardware performance testing. Axiomatix will therefore continue to be involved with all aspects of the maturing payload communication system activity.

Specifically, some of the problems involving the payload avionic equipment capabilities and operating parameters (especially for the PI) that must be resolved in the near term are concerned with:

(1) PI Transmitter Sweep Rates
(2) PI Receiver Sweep Range
(3) PI Receiver Sweep Methodology
(4) PI Receiver Maximum Allowable SPE
(5) PI Transmitter Phase Noise
(6) PI Receiver Wideband Output Characteristics
(7) KuSP Bent-Pipe FM Drive Regulation
(8) PI Receiver Lock Detector Statistics.

In addition, there is the continuing concern over the likelihood of PI receiver false lock, especially to payload nonstandard modulations. Firm trade-offs must be established between augmented PI anti-false-lock capability and payload modulation restrictions. In support of these trade-offs, much analysis and experimental study remains.

The larger system performance assessment must also be detailed. All end-to-end links must be reviewed in-depth, with the parameters being refined and tolerances taken into consideration. More involvement on Axiomatix's part with the various qualification and verification tests is needed. The impact of RFI on performance must be investigated. Clearly,

additional analyses are required to establish good theoretical bases against which test results may be measured.

REFERENCES

1. B. H. Batson. "Special Issue on Space Shuttle Communications and Tracking," IEEE Transactions on Communications, Vol. COM-26, No. 11, Part I, November 1978.

2. A. Blanchard. Phase-Locked Loops, Application to Coherent Receiver Design. John Wiley & Sons, 1976, p. 287.

3. J. C. Springett. "Shuttle Orbiter S-Band Communications Equipment Design Evaluation," Final Report for Contract NAS 9-15514A, Axiomatix Report No. R7901-3, January 20, 1979.

4. "Integrated Source and Channel Encoded Digital Communication System Design Study," Final Report for Contract NAS 9-13467, Axiomatix Report No. R7607-3, July 31, 1976.

5. A. J. Viterbi. "Acquisition and Tracking Behavior of Phase-Locked Loops," JPL External Publication No. 673, Pasadena, California, July 14, 1959.

6. M. K. Simon. "False Lock Performance for the Space Shuttle Orbiter S-Band and Ku-Band Costas Loop Receivers," Axiomatix Report No. R7702-3, February 28, 1977.

7. C. R. Cahn. "Improving Frequency Acquisition of a Costas Loop," IEEE Transactions on Communications, Vol. COM-25, No. 12, December 1977, pp. 1453-1459.

8. J. J. Spilker, Jr., and W. J. Gill. "Demodulation of Angle-Modulated Telemetry Signals," Vol. 2, Report ESD-TR-66-408, Philco-Ford WDL, August 1966, pp. 2-50.

APPENDIX A

IEEE TRANSACTIONS ON COMMUNICATION PAPER "COMMUNICATION WITH SHUTTLE PAYLOADS"

Communication with Shuttle Payloads

JAMES C. SPRINGETT, MEMBER, IEEE, AND SERGEI UDALOV, MEMBER, IEEE

Abstract—One mission of the Shuttle is to place payloads into Earth orbit or on escape trajectories and to recover payloads from Earth orbit. In order to properly deploy and retrieve such payloads, operational and diagnostic communications must take place between the payloads and the Shuttle. The results of such communications, in the form of tracking, commands, and telemetry, will be interpreted both aboard the Shuttle and on the ground. To accommodate a diverse set of payloads for both NASA and DOD programs, multimode avionic equipment dedicated to payload communications is being installed aboard the Shuttle. This equipment, operating at RF and baseband and providing capability for digital and analog signal forms, will furnish all required capabilities to communicate with both attached and detached payloads.

I. INTRODUCTION

THE Shuttle Orbiter is the major element of the Space Transportation System (STS) and the key to future routine space operations. In particular the delivery/recovery of various payloads into/from the space environment is easily effected by carrying them into Earth orbit within the Orbiter's large cargo bay.

Beginning in the early 1980's, nearly all spacecraft launched by the United States and many vehicles transported to Earth orbit for other countries will utilize the Shuttle. Generally, these payloads may be divided into two distinct classes: (1) those which will be separated or become "detached" from the Orbiter and (2) those which will remain "attached" to the Orbiter in the associative surroundings of the cargo bay. Many detached payloads will be transported into geosynchronous or other Earth orbits or placed on deep space trajectories by the Inertial Upper Stage (IUS). Certain detached payloads (known as free-flyers) will simply operate away from the Orbiter in co-orbit, and some of these will be subsequently recovered by the Orbiter for return to the ground. Figure 1 is a rendition of the Orbiter with its cargo bay doors open and a satellite mated with the IUS stowed within the bay.

A versatile standard attached payload is the Spacelab (developed under an international program by the European Space Agency). The Spacelab consists of component assemblies which may be selected and interconnected to make up a desired configuration. Its components consist of a pressurized module with shirtsleeve working environment and various open experiment pallets exposed to the space environment. Figure 2 depicts the Spacelab/Shuttle appearance. For any specific Shuttle flight, the Spacelab hardware may be arranged as a module only, module-plus-pallet, or pallets only.

Manuscript received May 15, 1977; revised June 12, 1978.
The authors are with Axiomatix, Los Angeles, CA 90045.

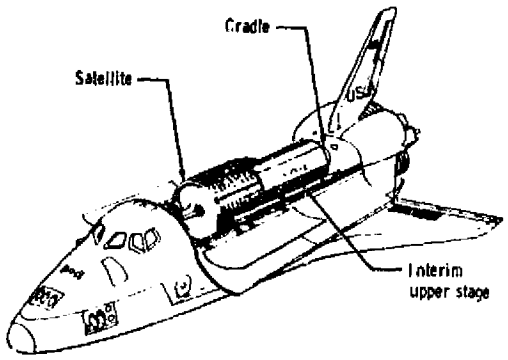

Figure 1. IUS/Satellite Within the Shuttle Cargo Bay

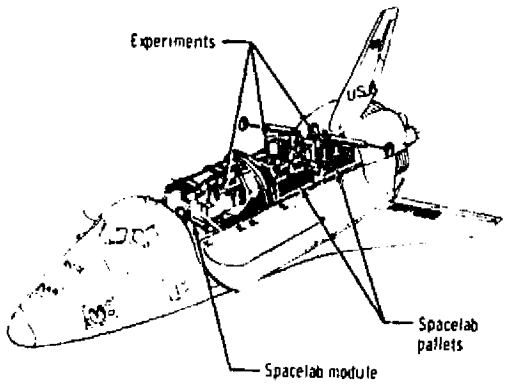

Figure 2. Spacelab System Within the Shuttle Cargo Bay

Key among requirements for payload support are those to communicate between the Orbiter and the payload(s). Generally, attached payloads will be serviced via hardwire links while communications with detached payloads must use RF channels. To provide such capability, a specific set of Shuttle avionic hardware is currently being developed by NASA and industry. It is the purpose of this paper to outline the nature, characteristics, and functional design of these avionic subsystems. In order to acquaint the reader with the entire Shuttle/payload communication system, the salient aspects of typical payload communication requirements and subsystem organization are also discussed.

II. PAYLOAD COMMUNICATION REQUIREMENTS AND SUBSYSTEMS

Whether a payload be attached or detached, a further distinction can be made as to whether it is manned or unmanned. Clearly, the Spacelab, insofar as the pressurized module is con-

0090-6778/78/1100-1584$00.75

cerned, is manned, and its communication requirements are already well established. Detached manned vehicles, on the other hand, are only in the conceptual stages; as a result, their detailed requirements are lacking. The avionic subsystems which will specifically serve manned payloads (especially detached ones) are also less advanced in their development than those intended for use with unmanned payloads. This current state of evolution of unmanned versus manned systems is natural, considering that the unmanned payloads will likely make exclusive use of the STS during the first years of its operational phase. (This is not to imply that the Shuttle itself will be unmanned.) For these reasons, the major topics addressed by this paper are concerned with the unmanned payload communication systems. After reviewing both the payload and Shuttle avionic systems as they pertain to unmanned missions, the manned requirements are briefly examined in Section IV.

The two largest user agencies of the Shuttle as a payload launcher will be NASA and DOD. Other users will be organizations such as COMSAT, private industry, and foreign countries. NASA and DOD payload requirements and subsystem capabilities have predominantly driven the design of the avionic subsystems (especially in terms of the detached payload communication links). Thus, "standard" capabilities have evolved to serve NASA and DOD. Nonstandard conditions have also been provided for, but with generally less operational capability (especially aboard the Orbiter). With all of these qualifications, the specific NASA and DOD unmanned payload requirements and subsystems will now be reviewed.

A. Communication Functions

The model for the ensuing discussion will be a spacecraft that is to be launched on a new trajectory using the IUS.* The spacecraft is mated to the IUS at all times, whether they be jointly attached to the Orbiter in its cargo bay or detached in the near vicinity of the Orbiter (within a radial range of 10 nmi).

Prime requirements to communicate are dictated by the need to perform on-orbit checkout of the IUS and its attached payload. Such checkouts are monitored and controlled by both the Orbiter flight crew and ground control centers. Data to and from (commands and telemetry, respectively) the payload may be generated and displayed within the Shuttle forward cabin area or relayed to ground facilities, usually through the Tracking and Data Relay Satellite System (TDRSS).

In the attached mode for the IUS/spacecraft, all communications are via hardwire links connected through an umbilical with the IUS itself. A versatile signal set capability is allowed for both commands and telemetry and, in most cases, it will be in "standard" forms, which allows it to be fully processed by the avionic equipment. Command data may be in the form of a baseband signal or the data can be modulated onto sinusoidal subcarriers (see further discussion below). Likewise, "standard" telemetry data may be in an NRZ or Manchester serial format or modulated onto subcarriers. All command bit rates are standard, ranging from 7.8125 bits/s to 2000 bits/s in steps of 2, on a 16 kHz subcarrier. Standard telemetry rates range from 250 bits/s to 256 kbits/s in steps of 2. When subcarriers are employed, standard subcarrier frequencies of 1.024 MHz or 1.7 MHz are required. All standard command and telemetry signals are processed by dedicated avionic subsystems aboard the Orbiter, as detailed in Section III.

All nonstandard signals (i.e., those which cannot be fully processed by the avionic equipment) are handled by the Orbiter in what is known as the "bent-pipe" mode. As such, the Orbiter avionic subsystems do not process the signals (i.e., demodulate, detect, demultiplex, etc.) but rather act as "transparent" throughputs. Nonstandard command signals are not allowed. Nonstandard telemetry signals/formats/waveforms, however, are permitted with certain restrictions. The telemetry baseband through-put bandwidth is limited to 4.5 MHz whether the telemetry be digital or analog in nature.

Detached payload communications involve RF links between the Orbiter and the payloads. The payload flight transponder and associated telecommunication subsystems are used for this purpose, just as they are in fulfilling the payload's nominal mission. The only significant difference is that the payload must have a signal (apart from its mission modes, if different) that is Shuttle compatible. Data rates, subcarrier frequencies, etc., are essentially the same as for the attached communications (with a few restrictions as discussed in Section III).

Since there are a large number of possible payload transponder frequency assignments, the Orbiter avionics must be capable of being programmed to all such frequencies. For the detached situation, communication tracking capability is required in addition to the command and telemetry functions. Command and telemetry signals are always in their standard subcarrier formats, with the possible exception of some "bent-pipe" telemetry. Although the IUS and its attached spacecraft may be separately communicated with via the RF links, simultaneous IUS and spacecraft interrogation is not possible using the Orbiter avionics.

The remainder of this section deals with typical NASA and DOD payload communications systems. Both the major operating parameters and a functional description of the relevant subsystems are discussed. An understanding of these subsystems is necessary for comprehension of the overall Orbiter/payload communication capability, as well as the design and operation of the companion Orbiter avionic subsystems delineated in Section III.

B. Payload Transponders

NASA and DOD payload transponders are generically quite similar in terms of their functions and architectures. NASA transponders are standardized, with three mission-oriented types available—deep-space transponders [for use with the Deep Space Network (DSN)], near-Earth transponders [for use with the Spaceflight Tracking and Data Network ground stations (GSTDN)], and TDRSS transponders (for use with the TDRSS or GSTDN)**. DOD transponders interface with the USAF Satellite Control Facility (SCF).

Conspicuous differences between NASA and DOD trans-

* The IUS will be the usual launch vehicle; others, however, are not precluded.

** The Spaceflight Tracking and Data Network (STDN) is comprised of the two major sub-networks, GSTDN and TDRSS.

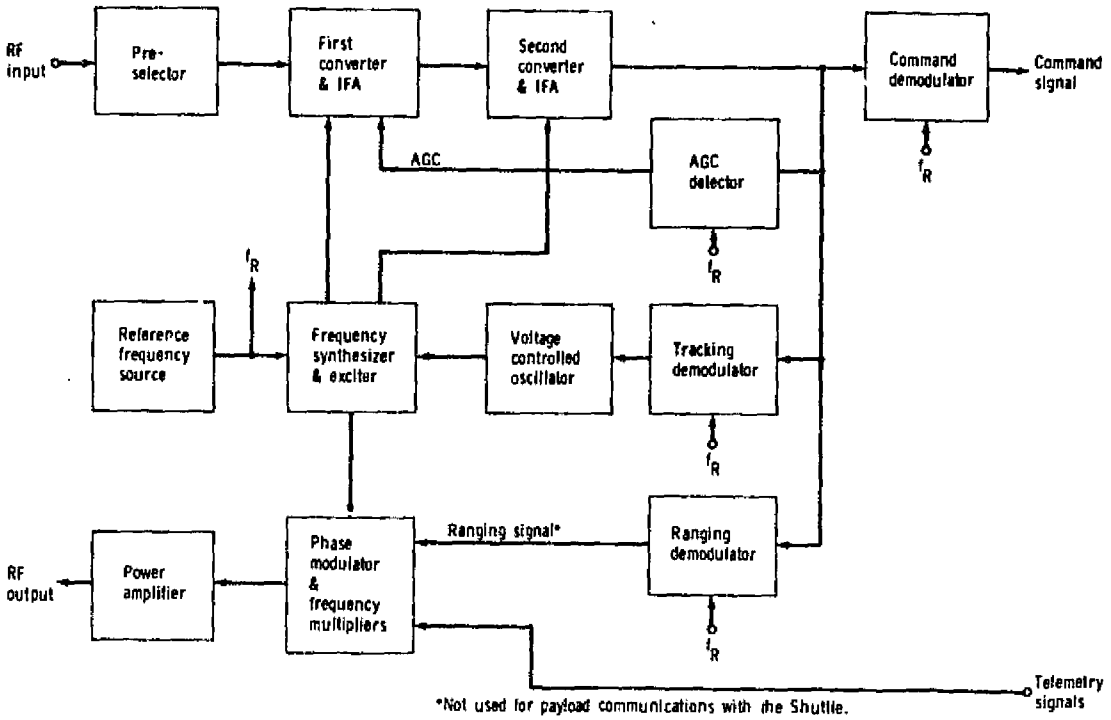

Figure 3. Typical Payload Transponder Diagram

ponders are the forward link frequency bands and transponding ratios. The NASA receive frequency range is *S*-band (2025 MHz to 2120 MHz), while the DOD receive frequency range is *L*-band (1760 MHz to 1840 MHz). The transmitter frequency is related to the receiver frequency by the ratio of integers, called the coherency (or turn-around) ratio. Both the NASA and DOD transmitter frequency ranges are *S*-band (2200 MHz to 2300 MHz). The corresponding coherency ratios are, for NASA, 240/221 and, for DOD, 256/205.

Figure 3 is a block diagram of a typical payload transponder. The forward link RF input is preselected, filtered for the frequency band utilized (*S*-band for NASA and *L*-band for IUS and DOD), and the input is then mixed down to the first IF. Further mixing translates the first IF signal to the second IF, where the output from the second IF amplifier is distributed to four phase detector/demodulator functions.

The carrier tracking loop functions to acquire and track the residual carrier component of the input signal. A second-order tracking loop is employed. Frequency and phase coherence are supplied from the VCO to the synthesizer/exciter where the coherent reference frequencies are derived for the demodulation functions.

AGC is obtained through in-phase demodulation of the residual carrier. The AGC voltage is filtered and applied to the first IF amplifier to control the gain of the receiver. The AGC voltage is also filtered and compared with a threshold to determine whether the carrier tracking loop is in or out of lock.

The command demodulator coherently recovers the command phase modulation from the carrier. Spectral conditioning (in most cases limited to lowpass filtering) is usually provided in the output to the command detector.

Most transponders also have a turnaround ranging capability; there is, however, no plan to make use of such ranging capability with the payload/Shuttle link.

The synthesizer/exciter provides all reference frequencies to the transponder. A reference oscillator supplies standard frequencies to the receiver synthesizer, and coherence is provided by the receiver VCO. Synthesized frequencies are distributed to the receiver mixers and phase detectors and to the transmitter phase modulator through a frequency multiplier.

The phase modulator provides the means of modulating the return link carrier with telemetry and ranging signals. Its output drives the transmitter frequency multiplier, producing the required modulated carrier signal in the *S*-band frequency range.

Finally, the power amplifier raises the modulated *S*-band transmitter signal to the level required by the return link. For near-Earth spacecraft, the power levels may range from a few hundred milliwatts to several watts, while deep-space vehicles employ power levels on the order of 100 W.

Typical transponder operating and performance parameters are indicated in Table 1.

C. Command Detectors

Unlike the payload transponders, NASA and DOD command detectors are quite dissimilar. The NASA command signal format is comprised of a binary serial data bit stream which biphase modulates a subcarrier. Table 2 shows the NASA command performance parameters, and Figure 4 is a diagram of the basic payload command detector functions. The subcarrier demodulator functions to regulate the input signal plus noise amplitude and to recover the command bits from the subcarrier. A data-aided type suppressed subcarrier tracking loop is employed.

TABLE 1
TYPICAL PAYLOAD TRANSPONDER CHARACTERISTICS

Item	Parameter and Range
Receive Frequency Range	
L-Band Frequency (DOD)	1760-1840 MHz
S-Band Frequency (NASA)	2025-2120 MHz
Transmitter Frequency Range	2200-2300 MHz
Tracking Loop Bandwidth	18, 60, 200, or 2000 Hz
Tracking Loop Order	Second
AGC Dynamic Range	100 dB
Command Channel Frequency Response	1 kHz to 130 kHz
Ranging Channel Frequency Response	1 kHz to 1.2 MHz
Noise Figure	5 dB to 8 dB
Transmitter Phase Deviation	Up to 2.5 radians
Transmitter Output Power	200 mW to 5W*

*Up to 200 watts with external power amplifiers

TABLE 2
NASA COMMAND SYSTEM PARAMETERS

Subcarrier Frequency	16 kHz, sinewave
Bit Rates	$2000 \div 2^N$ bps, N = 0,1,2,...,8
E_b/N_0 for $P_e^b = 1\times10^{-5}$	10.5 dB

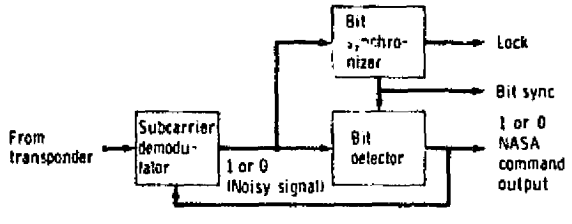

Figure 4. NASA Command Detector

The bit synchronizer is of the digital-data transition tracking loop (DTTL) class and provides accurate bit clock timing to the bit detector. Mechanized as an integrate-and-dump matched filter, the bit detector serves to maximize the signal-to-noise ratio of the noisy input and to make hard "1" and "0" decisions on the received bit stream. The subcarrier demodulator and bit synchronizer also contain a lock detection function which is used as a command stream "validation" indication to the payload command decoder.

The DOD command data are ternary in nature: "1," "0," or "*S*" symbols are transmitted in an FSK manner, each having a discrete subcarrier frequency or tone. Data rate clock (at one-half the symbol rate) in the form of a triangular signal is amplitude modulated onto the tones. Part a of Figure 5 shows the DOD modulation structure. Table 3 lists the general performance parameters, and Part b of Figure 5 shows the payload detector generic functions. The tone demodulator consists of three bandpass filter/envelope detector channels, each centered on one of the symbol tones. Level detection is made by lowpass filtering the demodulator outputs, sampling the LPFs at the proper time, and making a maximum-likelihood decision as to which of the ternary states is being received. Timing for the level detector is obtained by recovering the 1/2 symbol rate AM from the composite tones and detecting its zero crossings. In addition, the amplitude of the AM signal is compared with a threshold to produce a squelch indication which activates/deactivates the command output as a function of signal strength.

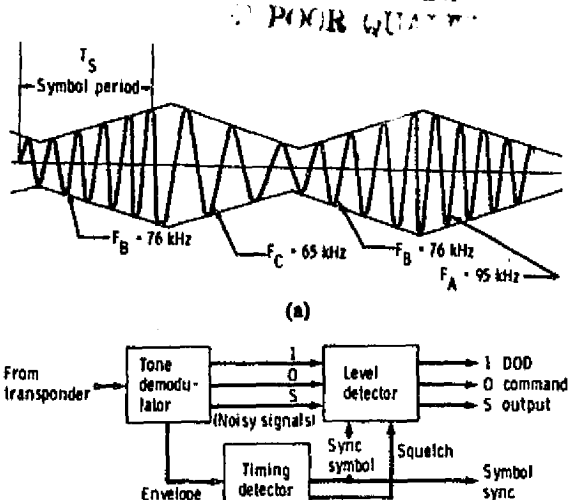

Figure 5. (a) DOD FSK/AM Command Signal Structure (b) DOD Command Detector

TABLE 3
DOD COMMAND SYSTEM PARAMETERS

Signal Tone Frequencies	65 kHz, 76 kHz, 95 kHz
Symbol Rates	1000 or 2000 symbols/second
E_s/N_0 for $P_e^b = 1\times10^{-5}$	-20 dB

TABLE 4
STANDARD PAYLOAD TELEMETRY MODULATION CHARACTERISTICS

Parameter	Parameter/Range	
	PSK Modulation	Frequency Modulation
Subcarrier Frequencies	1.024 MHz or 1.7* MHz	1.7* MHz
Bit Rates or Modulation Response	256,** 128,*† 64,* 32,* 16, 10 8, 4, 2, 1, 0.5,* 0.25* kbps	100 Hz to 200 kHz
Peak Deviation	±π/2 radians	±160 kHz
Output Bandwidth	400 kHz	500 kHz

**DOD only
*1.7 MHz subcarrier only

D. Telemetry Modulation

For the payload/Orbiter communication links, standard digital telemetry is transmitted using biphase modulated subcarriers. In addition, DOD spacecraft-to-Orbiter telemetry may involve the transmission of analog signals in an FM/FM format. Table 4 summarizes the telemetry modulation parameters. All telemetry modulation signals are input to the payload transponder where they are subsequently phase modulated onto the return link carrier.

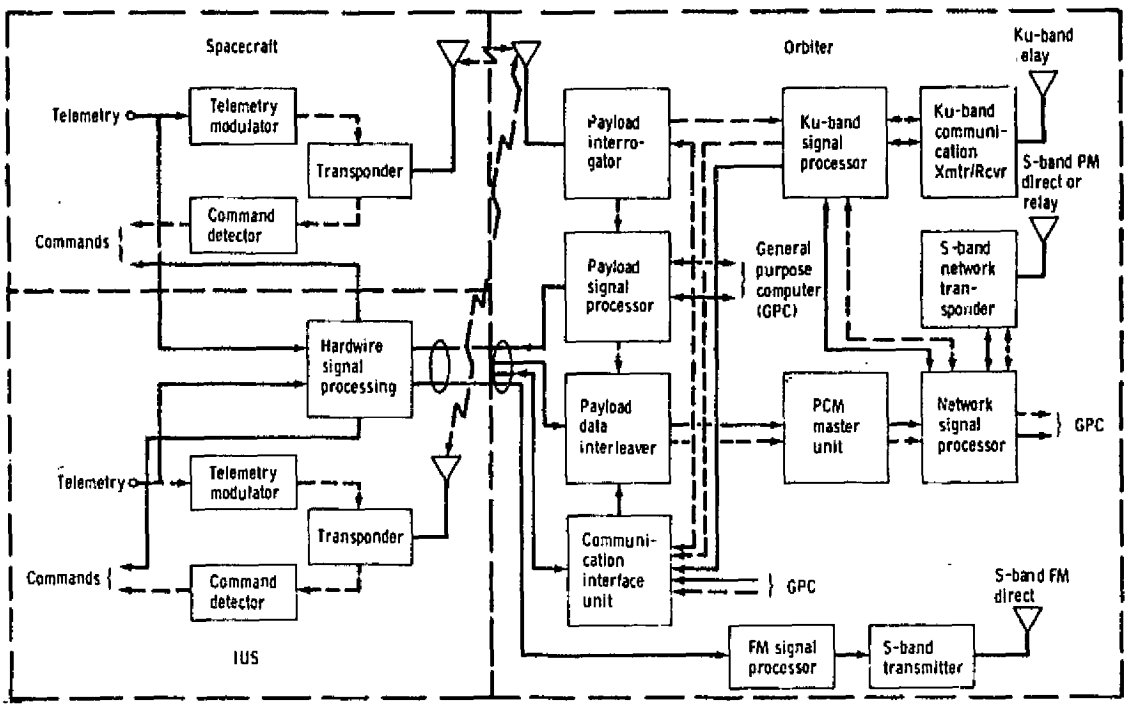

Figure 6. Payload/Orbiter Subsystems and Interfaces

Nonstandard telemetry signals/formats may also be transmitted from the payload to the Orbiter using the *S*-band return link. Such signals can phase modulate the return link carrier subject to certain phase deviation and bandwidth restrictions. A major difference between standard and nonstandard telemetry is that the latter is not specifically processed or displayed within the Shuttle.

III. SHUTTLE AVIONICS EQUIPMENT SERVING PAYLOADS

Figure 6 portrays the major payload communication subsystems, the pertinent Orbiter avionic subsystems, and their respective interfaces. Solid lines indicate signal paths for attached payloads, and dashed lines are the detached payload paths. (Note that the Payload Interrogator cannot communicate with the IUS and Spacecraft simultaneously.)

The Shuttle avionics equipment serving attached and detached payloads can be logically divided into two categories according to function:

(1) Equipment used for payload RF and baseband signal processing functions, and

(2) Equipment used for payload data handling functions.

The functions performed by the equipment in the first category include RF signal transmission and reception, carrier modulation/demodulation, subcarrier modulation/demodulation, and data detection. Equipments in this category are: (a) Payload Interrogator, (b) Payload Signal Processor, (c) Communication Interface Unit, and (d) *Ku*-Band Signal Processor.

The functions of the equipment belonging to the second category emcompass baseband data multiplexing/demultiplexing and encryption/decryption. Major equipments in this category are: (a) Payload Data Interleaver, (b) PCM Master Unit, (c) Network Signal Processor, and (d) various DOD encryptor/decryptor units. (DOD encryption/decryption will not be discussed in this paper.)

A. Payload Interrogator

The function of the Payload Interrogator (PI) is to provide the RF communication link between the Orbiter and detached payloads. For communication with the NASA payloads, the PI operates in conjunction with the Payload Signal Processor (PSP). During DOD missions, the PI is interfaced with the Communication Interface Unit (CIU). Nonstandard (bent-pipe) data received by the PI from either NASA or DOD payloads is delivered to the *Ku*-Band Signal Processor, where it is processed for transmission to the ground via the Shuttle/TDRSS link (see Section D following).

Simultaneous RF transmission and reception is the primary mode of PI operation with both NASA and DOD payloads. The Orbiter-to-payload link carries the commands, while the payload-to-Orbiter link communicates the telemetry data. In addition to this duplex operation, the PI provides for "transmit only" and "receive only" modes of communication with some payloads.

Figure 7 shows the functional block diagram for the Payload Interrogator. The antenna connects to an input/output RF port which is common to the receiver and the transmitter of the PI unit. Because of a requirement to operate the PI simultaneously with the Shuttle/ground *S*-band network transponder which radiates and receives on the same frequency bands, a dual triplexer is employed. The *S*-band network transponder emits a signal at either 2217.5 MHz or 2287.5 MHz; both frequencies thus fall directly into the PI receive band of 2200 MHz to 2300 MHz. Conversely, the payload transmitter, operating either in the 2025-2120 MHz (NASA) or in the 1764-1840 MHz

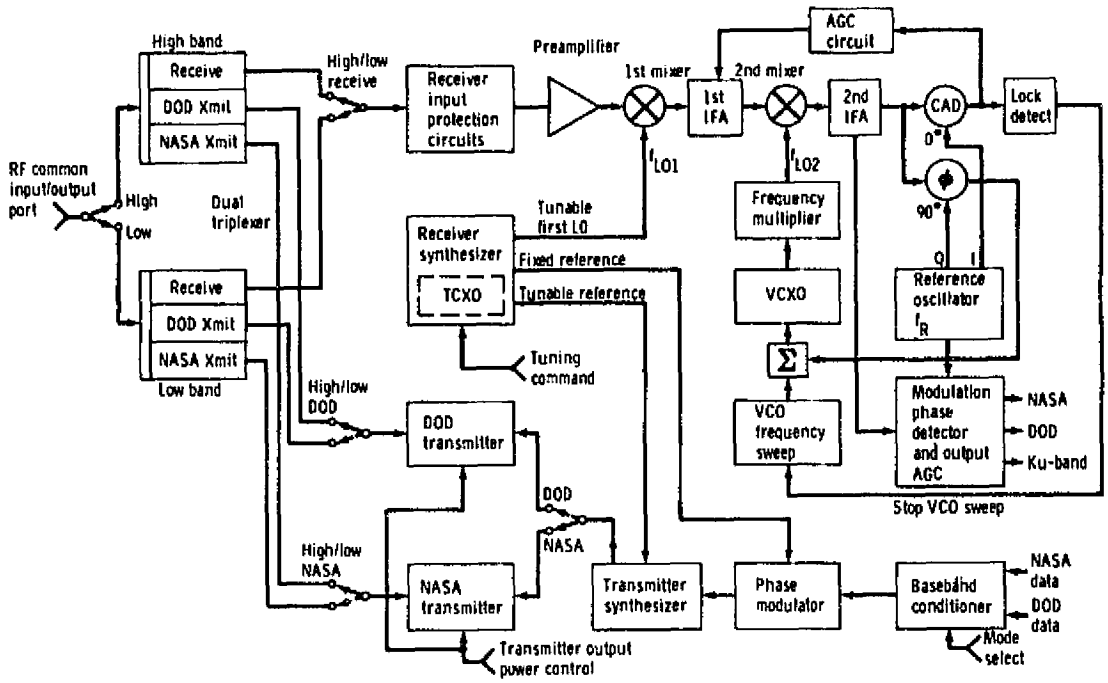

Figure 7. Payload Interrogator Functional Block Diagram

DOD bands, can interfere with uplink signal reception by the *S*-band network transponder receiver. Therefore, by use of the triplexer and by simultaneously operating the PI and network transponder in the mutually exclusive sub-bands, the interference problem is effectively eliminated.

When detached payloads are in the immediate vicinity of the Orbiter, excessive RF power levels may impinge on the interrogator antenna. Thus, the RF preamplifier of the receiver is protected by a combination of sensitivity control attenuators and a diode breakdown limiter. The output of the preamplifier is applied to the first mixer where it is converted to the first IF for amplification and level control. The first local oscillator frequency, f_{LO1}, is tunable and its frequency corresponds with the desired PI receive channel frequency. Except for channel selection, however, f_{LO1} is fixed. Consequently, any unspecified frequency difference between the received payload signal and f_{LO1} will appear within the first IF amplifier and at the input to the second mixer.

The receiver frequency and phase tracking loop begins at the second mixer. As shown in Figure 7, the output of the first IF amplifier is down-converted to the second IF as a result of mixing with a variable second LO frequency, f_{LO2}. The portion of the second IF which involves only the carrier tracking function is narrowband, passing the received signal residual carrier component and excluding the bulk of the sideband frequencies. Demodulation to baseband of the second IF signal is accomplished by mixing with a reference frequency, f_R. The output of the tracking phase detector, after proper filtering, is applied to the control terminals of a VCO which provides the second local oscillator signal, thereby closing the tracking loop. Thus, when phase track is established, f_{LO2} follows frequency changes of the received payload signal.

For the purpose of frequency acquisition, the f_{LO2} may be swept over a ±50 kHz uncertainty region. Sweep is terminated when the output of the coherent amplitude detector (CAD) exceeds a preset threshold, indicating that the carrier tracking loop has attained lock. The output of the CAD also provides the AGC to the first IF amplifier. To accommodate payload-to-Orbiter, received signal level changes due to range variation from about a few feet to 10 nmi, 110 dB of AGC is provided in the first IFA.

A wideband phase detector is used to demodulate the telemetry signals from the carrier. The output of this detector is filtered, envelope level controlled, and buffered for delivery to the PSP, CIU, and *Ku*-Band Signal Processor units.

The PI receiver frequency synthesizer provides the tunable first LO frequency and the corresponding exciter frequency to the transmitter synthesizer. It also delivers a reference signal to the transmitter phase modulator. Baseband NASA or DOD command signals modulate the phase of this reference signal, which is in turn supplied to the transmitter synthesizer where it is upconverted to either the NASA or DOD transmit frequency and applied to the power amplifiers.

For transmitter efficiency optimization, separate NASA and DOD RF power amplifier units are used. Depending on the operating band selected, transmitter output is applied to either the high or low band triplexer. To compensate for varying distances to payloads, each transmitter has three selectable output power levels.

Table 5 summarizes the PI performance characteristics.

B. Payload Signal Processor

The Payload Signal Processor performs the following functions: (1) it modulates NASA payload commands onto a 16 kHz sinusoidal subcarrier and delivers the resultant signal to the PI and the attached payload umbilical, (2) it demodulates

TABLE 5
PAYLOAD INTERROGATOR MAJOR PERFORMANCE PARAMETERS

Item	Parameter and Range
Transmit Frequency Range	
NASA Low Band	2025-2074 MHz
NASA High Band	2074-2120 MHz
DOD Low Band	1763-1804 MHz
DOD High Band	1803-1840 MHz
Transmitter Parameters	
Transmit Power (to antenna)	2.5 mW to 5 watts
Transmitter Phase Deviation Range	Up to 2.5 radians
Transmit Frequency Sweep Range and Rate:	
NASA GSTDN or DOD	±50 kHz at 35 kHz/sec
NASA DSN	±30 kHz at 600 Hz/sec
Receive Frequency Range	
Low Receive	2200-2252 MHz
High Receive	2252-2301 MHz
Receiver Parameters	
Received Signal Range	-122 to -20 dBm
Receiver Bandwidth	5 MHz (3 dB)
Noise Figure	≤ 7 dB
AGC Range	≥110 dB
Tracking Loop Bandwidth ($2B_L$)	2000 Hz
Outputs	
NASA Telemetry to PSP	
Subcarrier	1.024 MHz
Modulation	PSK (π/2)
Data Rate	1 to 16 kbps (in steps of 2)
DOD Telemetry to CIU	
Subcarrier	1.024 MHz and/or 1.7 MHz
Modulation	PSK (π/2) (1.024 MHz and 1.7 MHz subcarrier) FM/FM (1.7 MHz subcarrier)
Data Rates	0.25 to 256 kbps (in steps of 2)
Bent-Pipe to Ku-Band Signal Processor	
Subcarrier Waveform	1.024 MHz or 1.7 MHz subcarrier modulated by payload telemetry
Baseband Waveform	Analog or digital signals up to 4.5 MHz in bandwidth
Inputs	
NASA Commands from PSP	
Subcarrier	16 kHz
Modulation	PSK (π/2)
Data Rate	7.8125 bps to 2 kbps (in steps of 2)
DOD Commands from CIU	
Modulation	Ternary FSK/AM tones (95, 76 and 65 kHz tones)
Data Rate	1 or 2 ksps

the payload telemetry data from the 1.024 MHz subcarrier signal provided by the PI, and (3) it performs bit and frame synchronization of demodulated data and delivers these data and its clock to the Payload Data Interleaver (PDI).

The PSP also transmits status messages to the Orbiter's general purpose computers (GPC's); the status messages allow the GPC's to control and configure the PSP and validate command messages prior to transmission.

The functional block diagram for the PSP is shown in Figure 8. The PSP configuration and payload command data are input to the PSP via a bidirectional serial interface. Transfer of data in either direction is initiated by discrete control signals. Data words 20 bits in length (16 information, 1 parity, 3 synchronization) are transferred across the bidirectional interface at a burst rate of 1 Mbit/s, and the serial words received by the PSP are applied to word validation logic which examines their structure. Failure of the incoming message to pass a validation test results in a request for a repeat of the message from the GPC.

Command data are further processed and validated as to content and the number of command words. The function of the command buffers is to perform data rate conversion from the 1 Mbit/s bursts to one of the selected standard command rates. (See Table 2.) Command rate and format are specified through the configuration message control subunit.

From the message buffers, the command bits are fed via the idle pattern selector and generator to the subcarrier biphase modulator. The idle pattern (which in many cases consists of alternating "ones" and "zeros") precedes the actual command word and is usually also transmitted in lieu of command messages. Subcarrier modulation is biphase NRZ only.

The 1.024 MHz telemetry subcarrier from the PI is applied to the PSK subcarrier demodulator. Since the subcarrier is biphase modulated, a Costas type loop is used to lock onto and track the subcarrier. The resulting demodulated bit stream is input to the bit synchronizer subunit, where a DTTL bit synchronization loop provides timing to an integrate-and-dump matched filter which optimally detects and reclocks the telemetry data.

Detected telemetry bits, together with clock, are input to the frame synchronizer where frame synchronization is obtained for any one of the four NASA standard synchronization words. The frame synchronizer also detects and corrects the data polarity ambiguity caused by the PSK demodulator Costas loop.

From the frame synchronizer, the telemetry data with corrected frame sync words and clock are fed to the PDI. The telemetry detection units also supply appropriate lock signals to the Orbiter's operational instrumentation equipment, thus acting to indicate the presence of valid telemetry.

Table 6 summarizes the PSP salient performance parameters.

C. Communication Interface Unit

The CIU, shown in Figure 9, is the DOD equivalent of the NASA PSP. The major differences are that the CIU (1) handles ternary commands in both baseband and FSK tone formats (2) accepts Orbiter crew-generated commands, (3) permits a larger range of standard telemetry data rates (see Table 4), and (4) is capable of simultaneously handling two subcarrier frequencies.

Ground-generated commands may be received from either the *Ku*-Band Signal Processor or the Network Signal Processor (NSP) (through the GPC/MDM interface). Received as a continuous binary data stream at 128 kbits/s from the *Ku*-Band Signal Processor and 1 Mbit/s bursts from the GPC/MDM, they must be detected and buffered. The binary outputs of the buffers are either a 4 kbits/s or 2 kbits/s which, when converted to the ternary format, become symbol rates of 2 ksymbols/s and 1 ksymbols/s, respectively. The input to the binary-to-ternary converter consists of serial data plus clock (two lines), and the output consists of the "S," "0," and "1" symbols plus clock (four lines).

Crew-generated commands are input through the command generator and verification unit which outputs them in the proper ternary format. A priority selection switch determines whether ground or Orbiter originated commands will be transmitted to the payload. The FSK/AM generator encodes the ternary com-

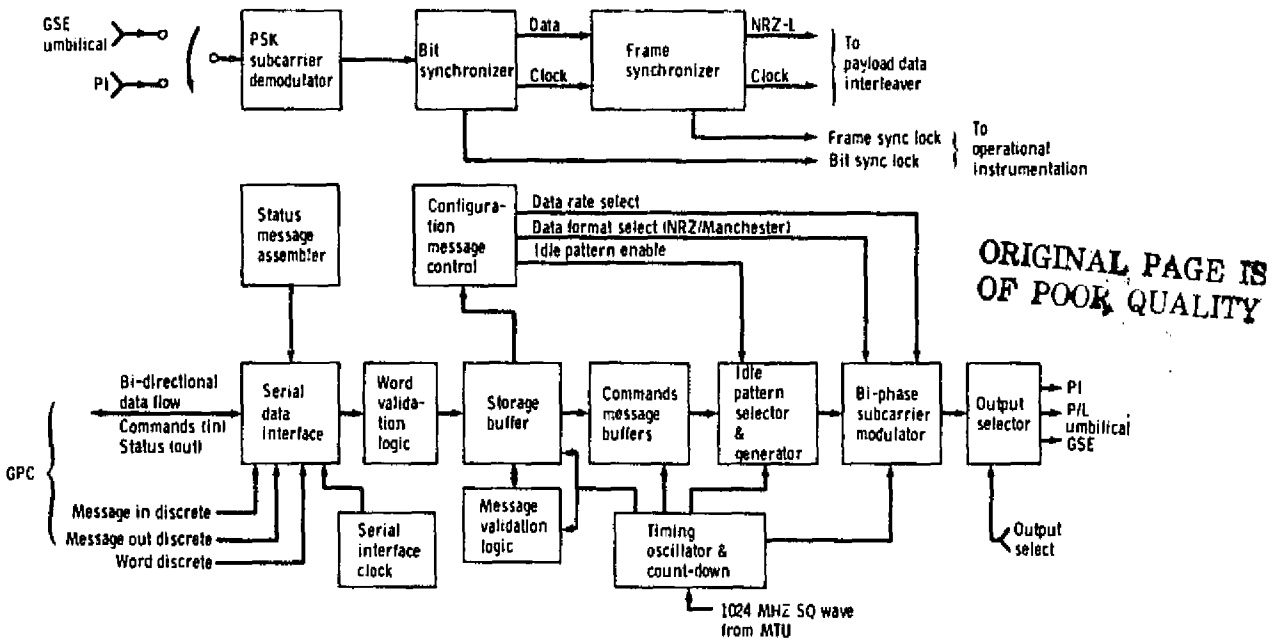

Figure 8. NASA Payload Signal Processor Functional Block Diagram

TABLE 6
PAYLOAD SIGNAL PROCESSOR MAJOR PERFORMANCE PARAMETERS

Item	Parameter and Range
Outputs	
Command Data	
Destination	Payload Interrogator, payload umbilical or ground support equipment
Subcarrier	16 kHz sinusoid
Modulation	PSK (±/2)
Data Rates	7.8125 bps to 2 kbps (in steps of 2)
Formatted Telemetry Data	
Destination	Payload Data Interleaver
Data Rates	1 to 16 kbps
Bits per Word	8
Words per Frame	1024 max
Frame Rate	200 per second max
Frame Sync Word Length	8, 16, 24 or 32 bits
Telemetry Clock	
Destination	Payload Data Interleaver
Rates	1 to 16 kbps (in steps of 2)
Waveform	Squarewave
Format	NRZ
Inputs	
Telemetry	
Source	Payload Interrogator or ground support equipment
Signal	1.024 MHz subcarrier
Modulation	PSK (±/2)
Data Rates	1 to 16 kbps (in steps of 2)
Formats	NRZ or Manchester
Commands and Configuration Message	
Source	General Purpose Computer
Signal	20-bit data burst
Format	Manchester
Rate	1 Mbps
Clock Signal	
Source	Master Timing Unit
Signal	1.024 MHz squarewave

mands into the proper signal for transmission to the payload. Three subcarrier tones of 65 kHz, 76 kHz, and 95 kHz (corresponding respectively to the "*S*," "0," and "1" symbols) are employed in a time-serial manner. The command rate clock, at one-half of the symbol rate and in the form of a triangular wave, is amplitude modulated onto the composite tone stream. Attached payloads may receive either the ternary baseband or tone command signals from the CIU

Figure 9 shows that there is one PI and four hardline telemetry inputs to the CIU. The modulated subcarrier characteristics are indicated in Table 4. All subcarrier inputs are routed through an input selector to the two PSK demodulators. These PSK demodulators are similar to that used in the PSP. The FM discriminator demodulates the analog baseband signal from its 1.7 MHz subcarrier (see Table 4), which is in turn sent to the *Ku*-Band Signal Processor to be handled as "bent-pipe" telemetry. All demodulated/detected and hardline telemetry is routed to the selector/multiplexer where it is partially demultiplexed and sorted for reformatting to the PDI and where the command verification data from the payload is extracted for the command generator and verification unit.

Table 7 lists the major CIU performance specifications.

D. Bent-Pipe Signal Handling

To accommodate payloads whose telemetry formats are not compatible with standard data rates and subcarrier frequencies, "bent-pipe" modes of operation are provided within the Shuttle's avionic equipment. Several signal paths acting as "transparent throughputs" are available for both digital and analog signals.

Digital data streams at rates higher than 64 kbits/s (which therefore cannot be handled by the PDI) may directly enter the *Ku*-Band Signal Processor where they may be (1) QPSK modulated onto an 8.5 MHz subcarrier, (2) QPSK modulated onto the *Ku*-band carrier (e.g., 50 Mbits/s Spacelab data), or

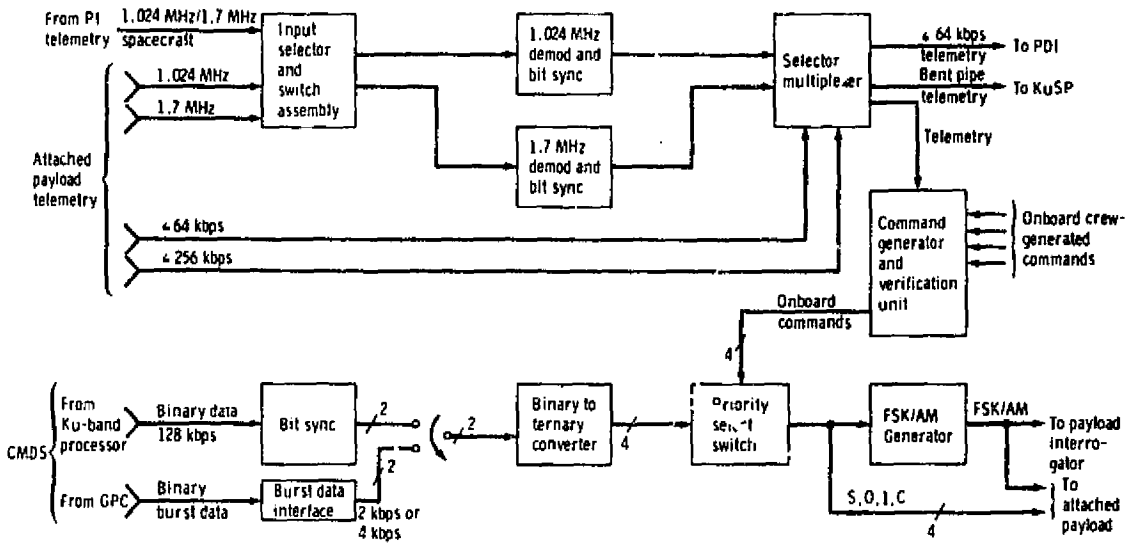

Figure 9. Communication Interface Unit for DOD Payloads

TABLE 7
COMMUNICATION INTERFACE UNIT MAJOR PERFORMANCE PARAMETERS

Item	Parameter and Range
Outputs	
FSK/AM Commands	
Destination	Payload Interrogator or attached payload
Modulation	FSK/AM tones
Data Rate	1 or 2 ksps
Ternary Commands	
Destination	Attached payload
Signal Form	Two-level 4-line signaling
Telemetry	
Destination	Payload Data Interleaver and Ku-Band Processor
Signal Form	NRZ
Data Rate	Up to 64 kbps to PDI, up to 256 kbps to Ku-Band Processor
Inputs	
Detached Payload Telemetry	
Source	Payload Interrogator
Subcarrier	1.024 MHz and/or 1.7 MHz
Modulation	PSK (1.024 MHz and 1.7 MHz subcarrier) FM/FM (1.7 MHz subcarrier)
Data Rates	0.25 to 2[illegible] kbps (in steps of 2)
Attached Payload Telmetry	
Source	Payload umbilical
Subcarrier	1.024 MHz and/or 1.7 MHz
Modulation	[illegible] FM/FM (1.7 MHz subcarrier)
On-Board Commands	
Source	Crew inputs
Ground Generated Commands	
Source 1	Ku-band Processor
Input Data Rate	128 kbps
Source 2	Network Signal Processor (general purpose computer)
Input Data Rate	1 Mbps bursts

(3) frequency modulated onto the *Ku*-band carrier. Detection and processing of all such data occur at ground stations.

Analog signals may take one of two paths. If they are in the form of a modulated subcarrier and do not have significant frequency components above 2 MHz, they may be hard-limited (i.e., a two-level or one-bit-quantized waveform produced) and treated as "digital" signals by the 8.5 MHz subcarrier QPSK modulator. On the other hand, if the analog signal is baseband in nature on the frequency range 0 Hz*** to 4.5 MHz, it may be transmitted via the *Ku*-band link utilizing FM. Again, all processing is accomplished on the ground.

IV. MANNED PAYLOAD SUPPORT FUNCTIONS

It was previously mentioned in Section II that some aspects of communication between the Orbiter and manned payloads are less advanced, both in terms of definition and of hardware development.

In addition to command, telemetry, and tracking, three additional capabilities are required for manned payloads—voice, video, and caution-warning.

A piece of avionic equipment known as the Audio Central Control Unit (ACCU) functions as the audio interface between the payloads and other applicable avionic units. For attached payloads, six two-way (talk/listen) duplex analog audio channels will be provided. Audio bandwidth is 3 kHz, and 60 dB or more of interchannel isolation is specified. For detached payloads, no voice capability is currently planned.

Presently, video links only between the Orbiter and attached payloads are planned. For this capability, used to monitor cargo bay and Spacelab activities, an EIA standard 525 line, interlaced 30 frames/s system will be employed. Interfaces have been established with both the *S*-Band FM Signal Processor

*** The lower frequency limit is 1 kHz for direct modulation (i.e., no subcarrier) of the payload *S*-band transmitter, due to PI receiver carrier loop sideband component tracking in a bandwidth of 2 kHz about the carrier.

TABLE 8
TYPICAL NASA OR DOD PAYLOAD-TO-ORBITER TELEMETRY LINK MARGIN CALCULATION FOR ONE PSK SUBCARRIER

	Parameter	Nominal Value
1)	Payload Transmitter EIRP (P_{tx} = 2 watts, G_{tx} = 0 dB, L_{RF} = 2 dB)	+1.0 dBW
2)	Space Loss at 10 nmi (f_{tx} = 2300 MHz)	-125.0 dB
3a)	Interrogator Receiver Antenna Gain	+2.5 dB
3b)	Interrogator RF Cable Loss	-6.0 dB
4)	Total Received Power (Sum 1 through 3)	-127.5 dBW
5)	Noise Spectral Density, N_0 (Noise Figure = 7 dB)	-197.0 dBW/Hz
6)	Receiver Power/Noise Spectral Density (Sum 4 and 5)	+69.5 dB-Hz
7)	Modulation Loss (β = 1.0 radian)	-4.1 dB
8)	Bit Rate Bandwidth (10 log 16 kbps)	+42.0 dB-bps
9)	Signal-to-Noise Ratio in Bit Rate Bandwidth (6 minus 8 plus 7)	+23.4 dB
10)	Required E_b/N_0 for Bit Error Rate = 10^{-5} (Includes 2 dB implementation losses)	+11.6 dB
11)	Link Margin (9 minus 10)	+11.8 dB

TABLE 9
TYPICAL ORBITER-TO-PAYLOAD COMMAND LINK MARGIN CALCULATION

	Parameter	Nominal Value NASA	Nominal Value DOD
1)	Interrogator Transmitter EIRP (P_{tx} = 5 watts, G_{tx} = +2.5 dB, L_{RF} = -6 dB)	+3.5 dBW	+3.5 dBW
2)	Space Loss at 10 nmi	-124.2 dB (2100 MHz)	-122.9 dB (1800 MHz)
3)	Payload Receiver Antenna Gain	0 dB	0 dB
4)	Payload Receiver RF Losses	-2 dB	-2 dB
5)	Total Received Power (Sum 1 through 4)	-122.7 dBW	-121.4 dBW
6)	Noise Spectral Density, N_0 (Noise Figure = 7 dB)	-197.0 dBW/Hz	-197.0 dBW/Hz
7)	Received Power/Noise Spectral Density (Sum 5 and 6)	+74.3 dB-Hz	+75.6 dB-Hz
8)	Modulation Loss (β = 1.0 radian)	-4.1 dB	-4.1 dB**
9)	Bit Rate Bandwidth (10 log 2 kbps)	+33.0 dB-Hz	+33.0 dB-bps
10)	Required E_b/N_0 for Bit Error Rate 10^{-5} (Including all implementation losses)	+11.6 dB	+20.0 dB
11)	Link Margin (7 plus 8 minus 9 and 10)	+25.6 dB	+18.5 dB

*L_{RF} is the cable loss

**Modulation loss for DOD transmission may be greater due to lower value of β = 0.3 (Modulation loss = -13.6 dB) which is employed for some applications. The link margin is reduced accordingly.

and the *Ku*-Band Signal Processor so that such video signals can be transferred to ground control centers.

Finally, caution and warning (C&W) capability is needed to alert flight personnel to payload anomalies requiring action. Dedicated C&W channel capabilities are planned only for attached payloads. For detached payloads, the C&W signals must be handled as an integral part of the normal telemetry stream. Hardline C&W signals may be either analog or digital in nature. On the Orbiter side of the interface, light and audio annunciators are used to alert the crew for trouble or out-of-tolerance conditions.

V. SHUTTLE/PAYLOAD COMMUNICATION LINK POWER BUDGET

A quantitative example† of the Shuttle/Payload communication link performance is provided by Tables 8 and 9. These tables show the power budgets for the telemetry (payload-to-Orbiter) and the command (Orbiter-to-payload) links, respectively. For the telemetry link, a common sample calculation is presented based on the selection of the same subcarrier frequency (1.024 MHz) and PSK telemetry rate (16 kbits/s) for both the NASA and the DOD modes. From the link margins shown in Table 8, it is evident that at 16 kbits/s a good margin exists for this link with a 2 W payload transmitter. Positive margin also exists even if the telemetry rate is increased up to 64 kbits/s, as may be the case with some of the DOD payloads. Higher data rates, however, may require an increase in the payload transmitter output power. Also, as shown in Table 9, relatively good margins are indicated for the Orbiter-to-payload command link operating in both NASA and DOD modes. As shown, these margins are available at the maximum command rate of 2 kbits/s.

The antenna gain of 0 dB for the payload end of the link is conservative. This gain, however, is typical of the wide angle antennas required for a near hemispherical coverage characterizing the Shuttle/payload communication link.

† All parameters are for illustrative purposes and are based upon preliminary specifications and initial design capability. They do not necessarily represent the operational Shuttle system performance.

VI. SUMMARY

When the Space Shuttle is used as a transportation vehicle to place/retrieve various payloads into/from Earth orbit, communications are required between the Shuttle and the payload to perform on-orbit checkout and to perform experiments. In order to accommodate the prime functions of command and telemetry, a number of payload dedicated Shuttle avionic systems are being developed. Able to communicate with attached payloads via "hardlines" and with detached payloads over an *S*-band RF link, the Shuttle hardware performs all of the necessary functions: carrier modulation/demodulation, subcarrier modulation/demodulation, detection, data multiplexing/demultiplexing, and data encryption/decryption. For most payloads, the data and signal formats must conform to the avionic system "standards." However, provision is also made to handle nonstandard signals via a "bent-pipe" channel. The results of all such communications are transmitted and received between the Shuttle and the ground, and selected data are both generated and displayed aboard the Shuttle.

BIBLIOGRAPHY

1. Batson, B. H.; Teasdale, W. E.; and Huth, G. K., "Payload Data Processing for the Space Shuttle Program," *NTC'77 Conference Record*, Vol. 2, Los Angeles, December 1977.

2. Bacinsky, R., and Wolverton, C., "*S*-Band Communications and Tracking Equipment," *NTC'77 Conference Record*, Vol. 2, Los Angeles, December 1977.
3. Batson, B. H., and Moorehead, R. W., "The Space Shuttle Orbiter Telecommunication System," *IEEE Communications Society Digest of News*, Vol. 14, No. 3, May 1976
4. Batson, B. H., and Johnson, J. H., "Space Shuttle Communications and Tracking System," *ITC Conference Record*, Los Angeles, October 1974.
5. "Space Shuttle System Payload Accommodations," Level II Program Definition and Requirements, NASA Document JSC 07700, Vol. XIV, Rev. D, Houston, Texas, November 26, 1975.
6. *Space Transportation System User Handbook*, NASA JSC, July 1977.

★

James C. Springett (M'77) received the B.S.E.E. and M.S.E.E. degrees from Washington University, St. Louis, MO, in 1958 and 1960, respectively.

From 1959 to 1977, he was with the Jet Propulsion Laboratory in Pasadena, CA, where he was responsible for research and development of advanced communication system techniques for use on planetary spacecraft and earth satellites. Since joining Axiomatix, Marina del Rey, CA, in 1977, he has been involved with system design analysis for Shuttle/payloads and the development of various spread-spectrum systems. Mr. Springett concurrently holds the position of Coordinator of Electrical Engineering at West Coast University, Los Angeles. His specializations include synchronization, modulation, detection, nonlinear methods, sampled data techniques, and digital processing.

Sergei Udalov (S'57-M'58) received the B.S. degree in Engineering from the University of California at Los Angeles in 1957 and the M.S.E.E. degree from the University of Southern California, Los Angeles, in 1962.

From 1957 to 1960, he was employed by Hoffman Electronics Corporation, Los Angeles, as a radio receiver design engineer. From 1960 to 1962, he was with Gilfillan Corporation, Los Angeles, where he carried out design of radar receiving and signal processing equipment. From 1962 to 1974, he was a staff engineer at Magnavox Research Laboratories, Torrance, CA, where he specialized in spread spectrum applications to communications and radar systems, digital voice and data modem design, and radar transponder research and development. In 1974, he joined Axiomatix, Marina del Rey, CA, where he has been extensively involved with systems design analysis of the *Ku*-Band Integrated Radar and Communication equipment for the Space Shuttle and the *S*-Band Payload Interrogator subsystem. His major interests include analysis and design of communication and radar systems, modem techniques and digital processing applications.

APPENDIX B

1978 INTERNATIONAL TELEMETERING CONFERENCE PAPER PRESENTATION VIEWGRAPHS

SPACE SHUTTLE PAYLOAD COMMUNICATION LINKS

JAMES C. SPRINGETT
SERGEI UDALOV

NOVEMBER 15, 1978

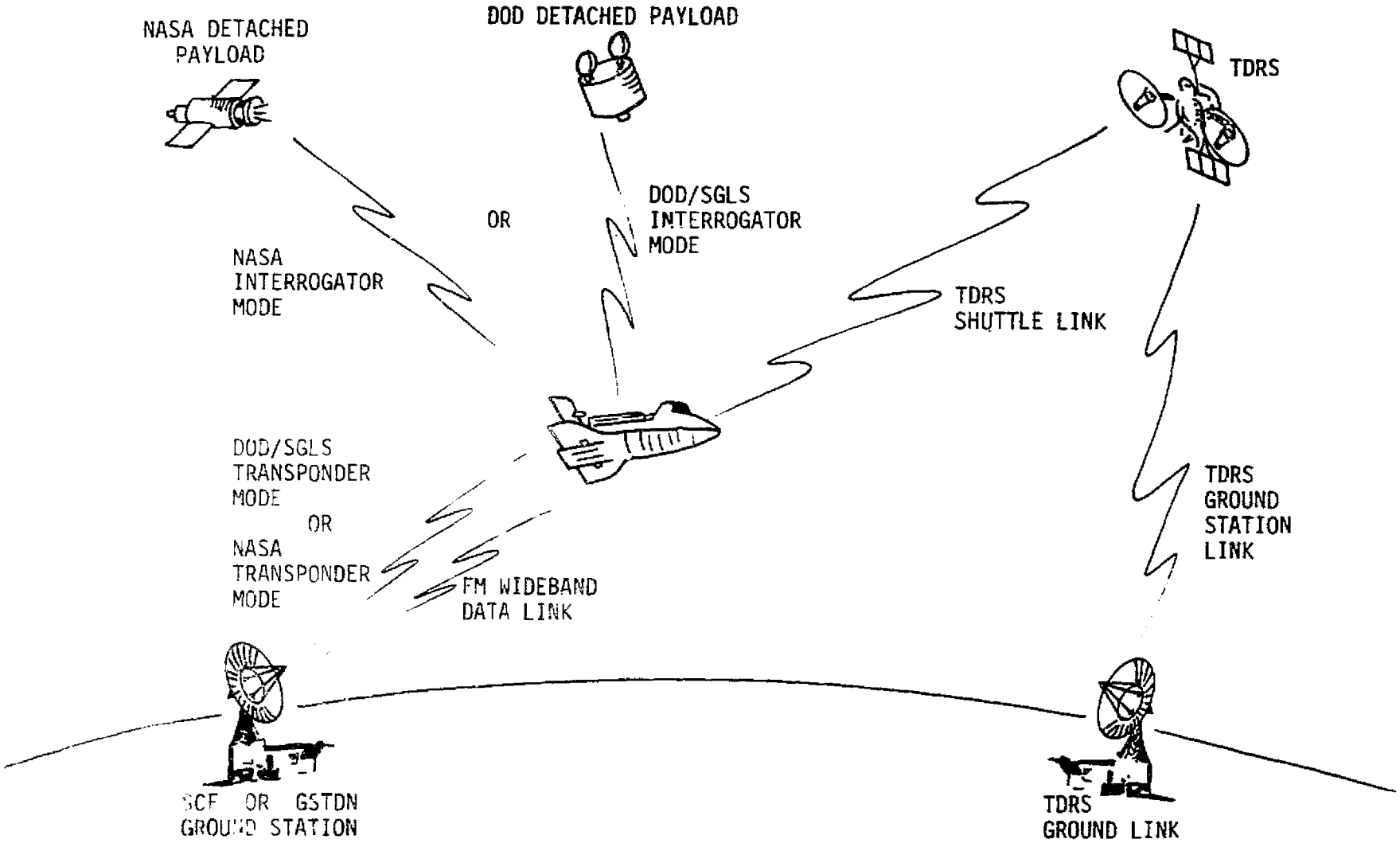

Payload Communication Links Overview

ATTACHED AND DETACHED PAYLOADS

- ATTACHED PAYLOADS (WITHIN THE ORBITER'S CARGO BAY) COMMUNICATE WITH THE SHUTTLE AVIONIC SUBSYSTEMS VIA CABLE INTERFACES (HARDLINE).

- DETACHED PAYLOADS (OUTSIDE THE ORBITER'S CARGO BAY TO A RANGE OF 10 NMI) COMMUNICATE WITH THE ORBITER'S PAYLOAD INTERROGATOR (PI) AT S-BAND.

TYPES OF INFORMATION/DATA

Telemetry (Return Links) -

- Digital (250 bps to 50 bps)
- Analog (4.5 MHz Lowpass Bandwidth)

Command (Forward Links) -

- NASA Standard Command ($2000 \div 2^N$ bps : N = 0, 1,...,8)
- DOD/SGLS Command (2000 bps or 1000 bps)
- High Rate (128 kbps)

Standard Conditions - Data conforms to fixed formats, bit rates, modulation types, and subcarrier frequencies.

Non-standard Conditions - Other than standard but subject to certain constraints.

PAYLOAD COMMUNICATION LINKS SUMMARY

		ATTACHED PAYLOADS	DETACHED PAYLOADS	STANDARD CAPABILITIES	NON-STANDARD CAPABILITIES
S-BAND	PSK DIRECT	X	X	X	
S-BAND	PSK RELAY	X	X	X	
S-BAND	FM DIRECT[1]	X		X	X
KU-BAND	QPSK RELAY	X	X	X	
KU-BAND	FM RELAY[2]	X	X		X

[1] RETURN LINK TELEMETRY ONLY.

[2] KNOWN AS THE BENT-PIPE.

Orbiter Avionic Subsystems and Functions

Subsystem Name	Acronym	INTERNAL FUNCTIONS									
		Carrier Modulation	Carrier Tracking & Demodulation	Subcarrier Demodulation	Data Synchronization & Detection	Command Modulation Generation	Data Stream Multiplexing	Data Stream Demultiplexing	Data Validity Check	Data Buffering & Rate Change	Data Decoding
Payload Interrogator	PI	X	X								
NASA Payload Signal Processor	PSP			X	X	X			X	X	X
DOD Communication Interface Unit	CIU			X	X	X	X		X	X	X
S-Band Network Transponder	-	X	X								
Payload Data Interleaver	PDI						X				
Network Signal Processor	NSP				X		X	X		X	X
Ku-Band Transmitter & Receiver	-	X	X								
Ku-Band Signal Processor	KuSP				X		X	X		X	X
Multiplexer/ Demultiplexer General Purpose Computer	MDM GPC						X	X	X		X

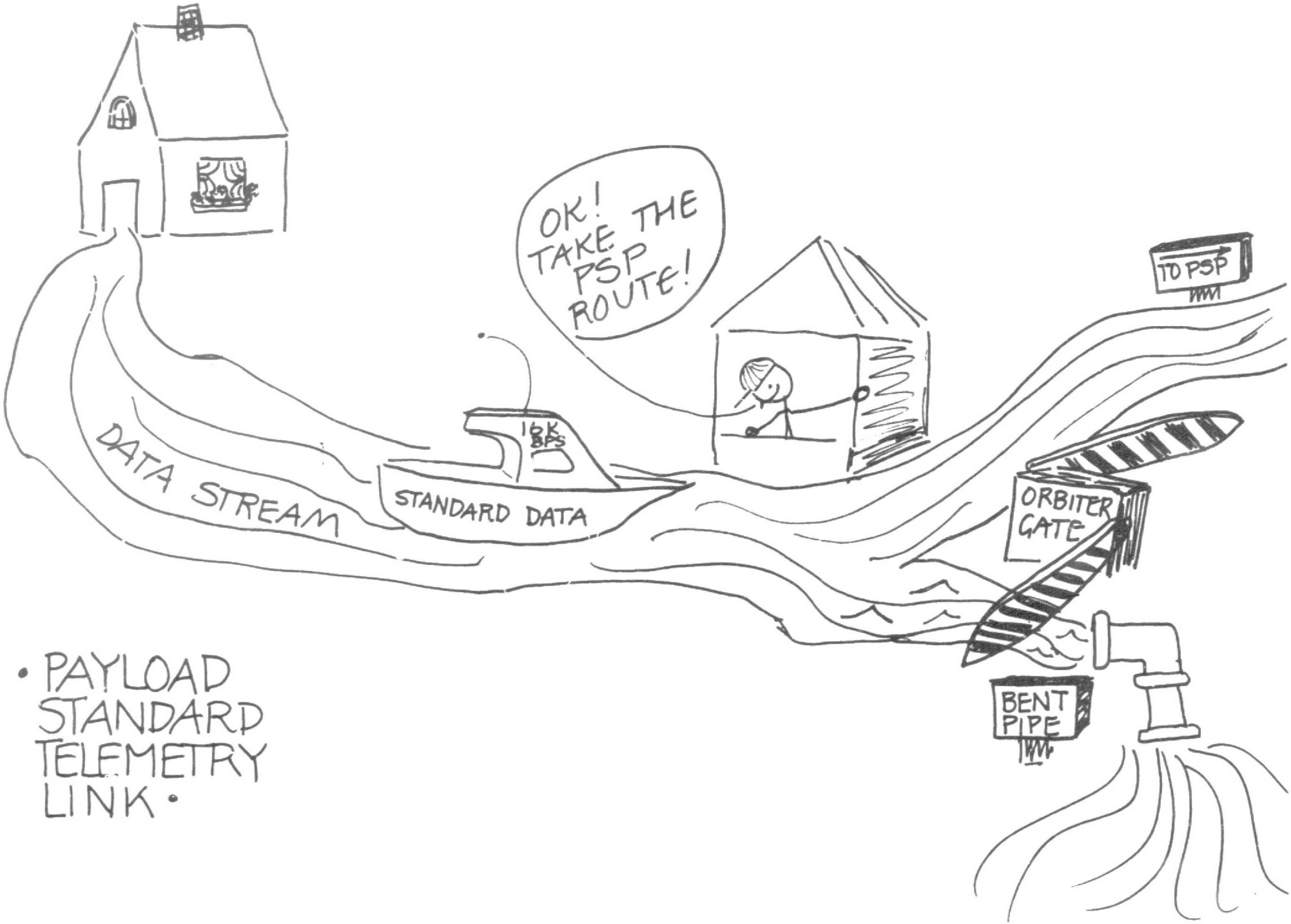

- PAYLOAD STANDARD TELEMETRY LINK -

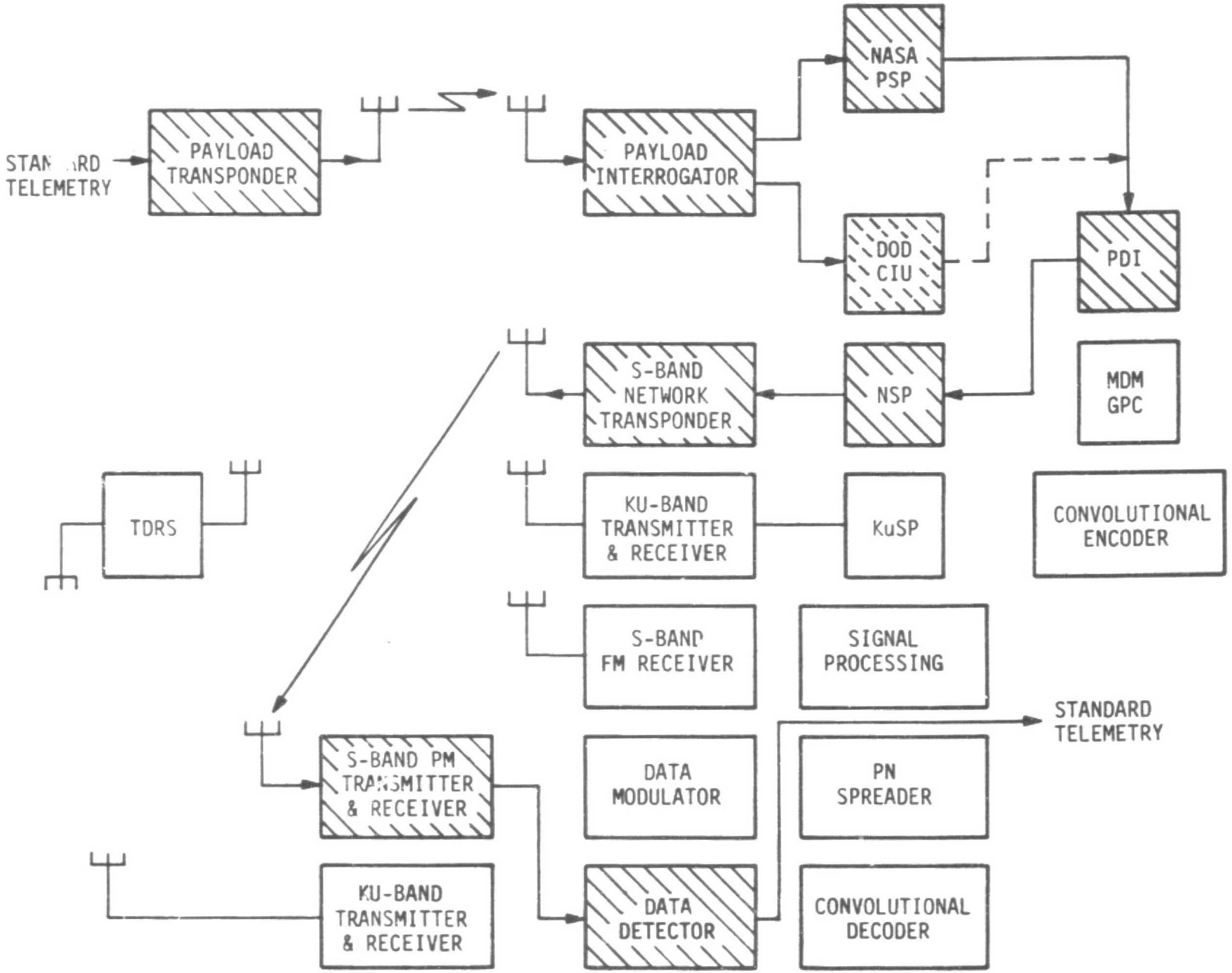

Detached Payload Standard Telemetry S-Band Direct Link

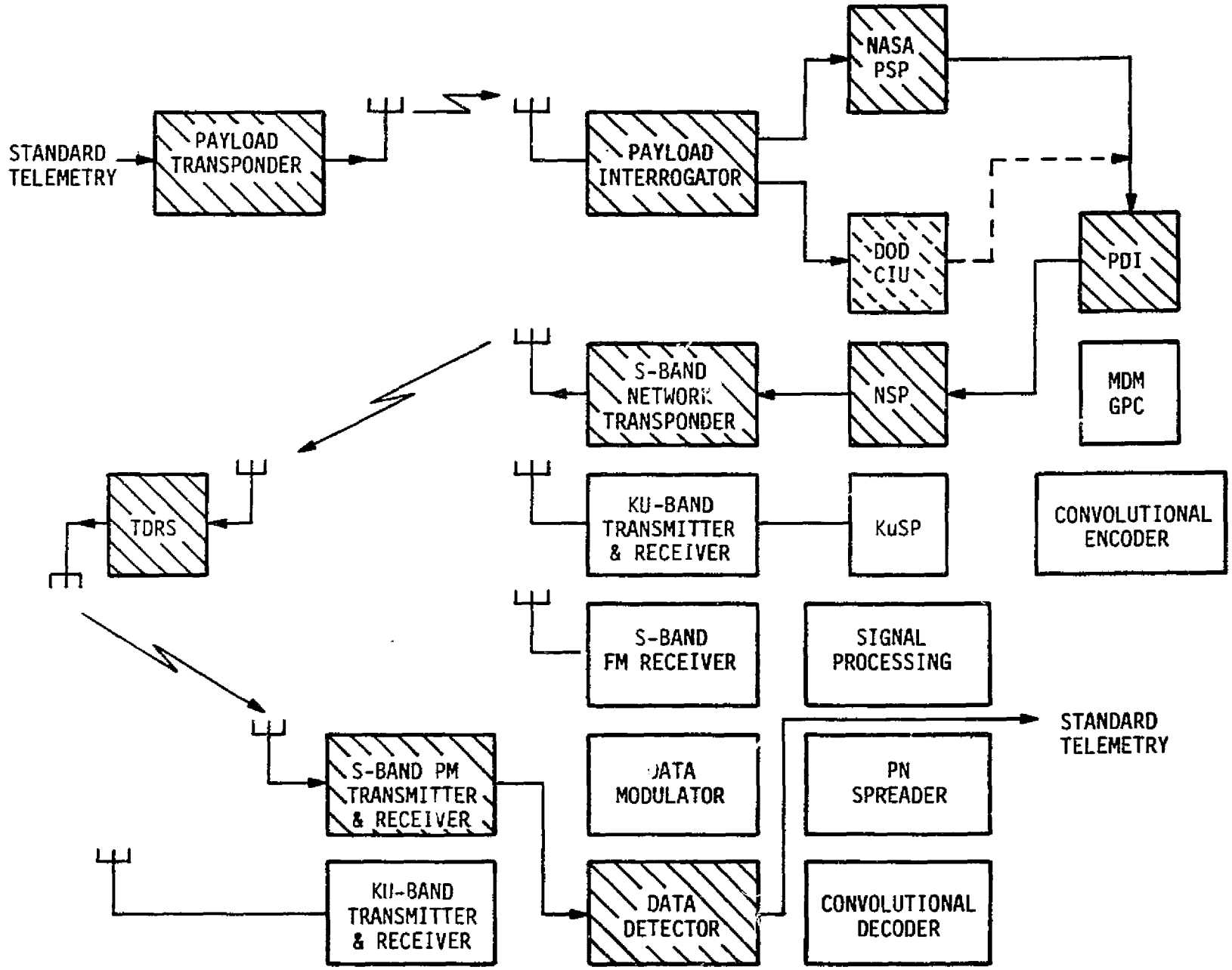

Detached Payload Standard Telemetry S-Band Relay Link

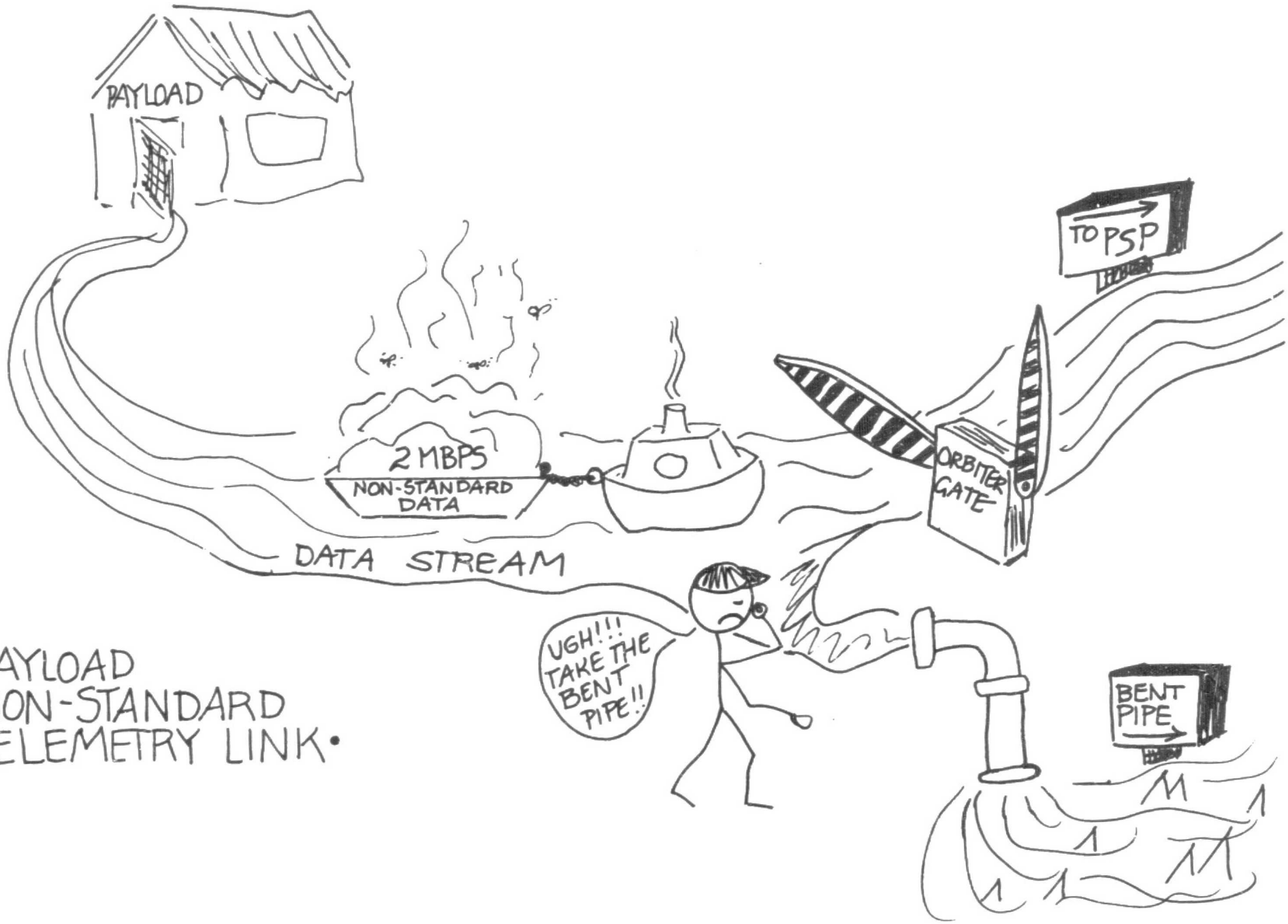

- PAYLOAD NON-STANDARD TELEMETRY LINK.

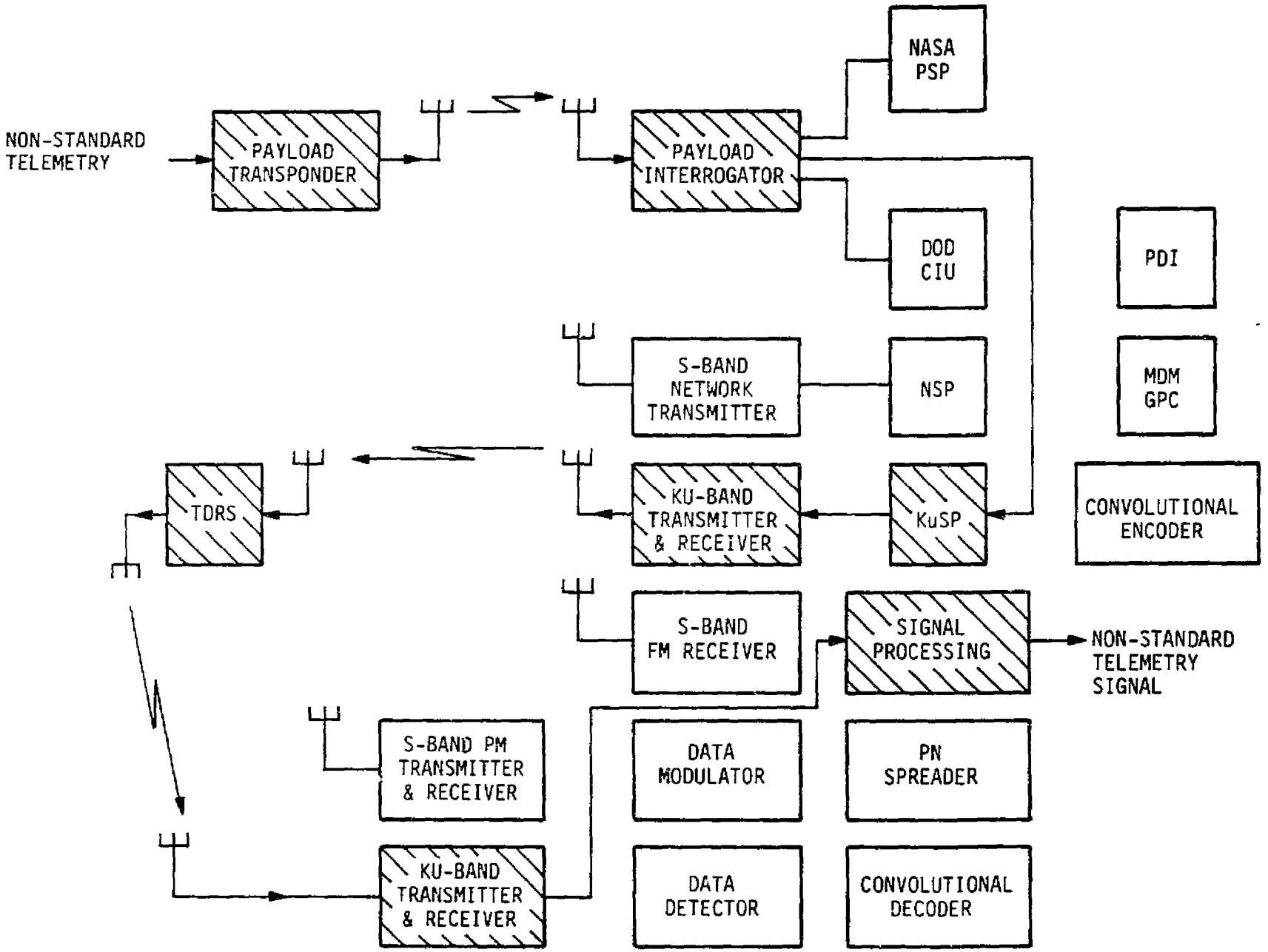

Detached Payload Non-Standard Telemetry Bent-Pipe Link

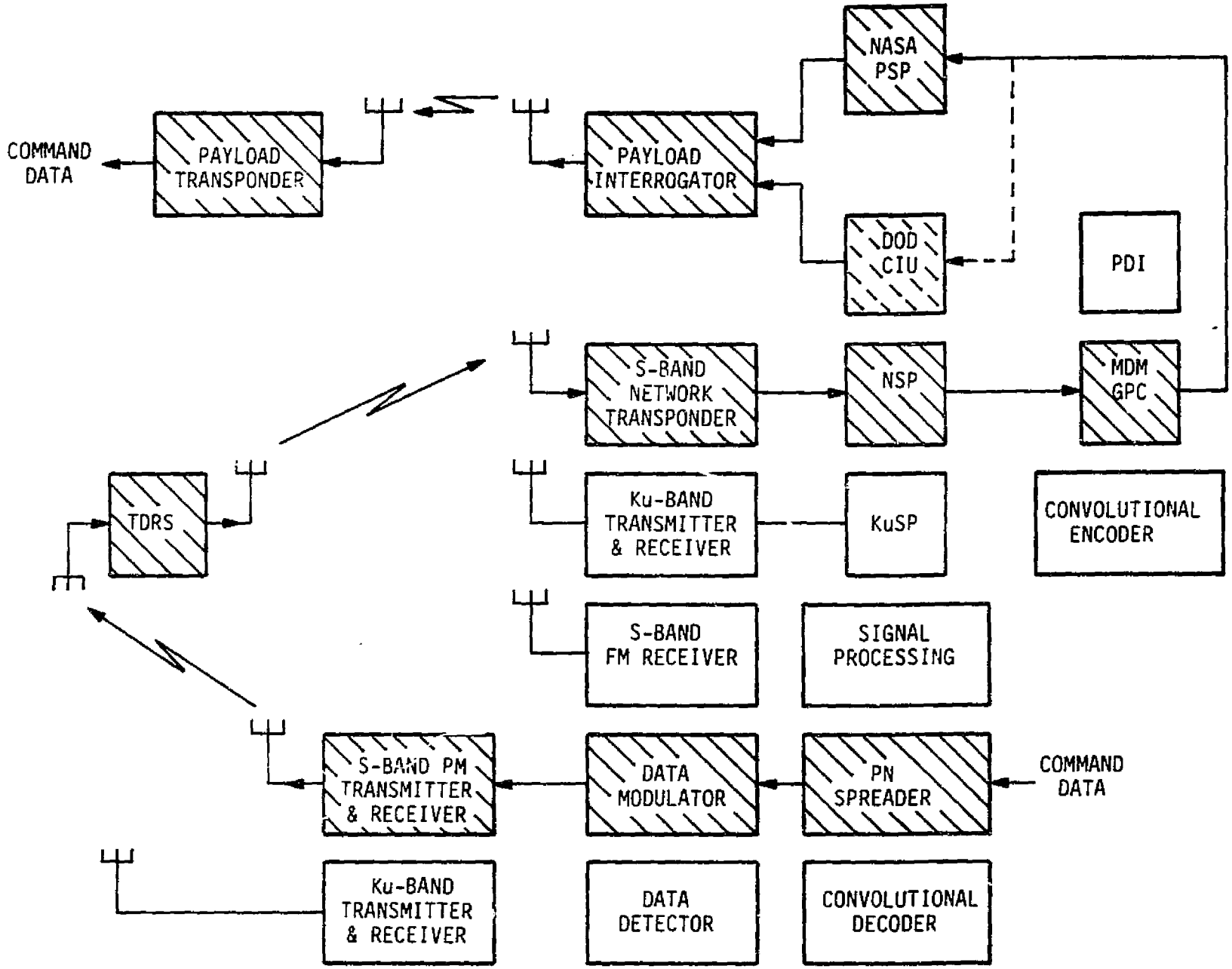

Detached Payload Command S-Band Relay Link

APPENDIX C

USER'S GUIDELINE FOR NONSTANDARD MODULATION FORMATS INPUT TO THE SHUTTLE PAYLOAD INTERROGATOR RECEIVER

USER'S GUIDELINE FOR NONSTANDARD MODULATION FORMATS INPUT TO THE SHUTTLE PAYLOAD INTERROGATOR RECEIVER

Revision 1

February 1979

1.0 PAYLOAD INTERROGATOR (PI) RECEIVER CAPABILITIES AND PARAMETERS

1.1 Type of Receiver

The PI receiver utilizes a discrete carrier phase-locked tracking loop, a coherent amplitude lock detector, and a wideband phase detector as the demodulator for modulation recovery.

1.2 Carrier Tracking Loop Bandwidth

The nominal tracking loop bandwidth, W_L, of 1200 Hz (two-sided) is designed to occur at a discrete carrier signal level (in the high sensitivity mode) of -124 dBm. As the received signal level increases to its maximum allowable value, the tracking loop bandwidth increases to approximately 1460 Hz (carrier loop in-lock and coherent AGC functioning). When the carrier loop is out-of-lock, noncoherent AGC regulation of receiver gain is employed. For maximum signal levels, the tracking loop natural frequency is on the order of 3800 radians/sec.

1.3 Post-Demodulation Lowpass Bandwidth

The post-demodulation 3 dB lowpass frequency is 4.5 MHz. The post-demodulation 3 dB highpass frequency is 200 Hz.

1.4 Carrier Swept-Frequency Acquisition

The PI receiver tracking loop VCO is linearly frequency swept at a rate of 10 kHz/sec such that the receiver searches ±85 kHz about its nominal frequency in order to obtain carrier lock. Modulation sidebands within a ±200 kHz frequency range about the carrier must be such that receiver false-lock to sidebands is precluded.

2.0 GENERAL PAYLOAD TRANSMITTER MODULATION CRITERIA

2.1 Allowable Modulations

Phase modulation (PM) of the carrier is the only allowable type of modulation. Frequency modulation (FM) and amplitude modulation (AM) of the carrier are not permitted. Quadriphase and spread spectrum modulations are also not allowed.

2.2 Maximum Carrier Suppression

The maximum allowable carrier suppression due to the composite of all phase modulating sources shall not exceed 10 dB.

2.3 Subcarrier Modulation

When subcarriers are employed, they may be either phase or frequency modulated. Amplitude modulated subcarriers are not permitted. Restrictions on the use of subcarriers are given under 3.2 and 3.3.

2.4 Direct Carrier Modulation by Baseband Signals

Direct carrier modulation by analog type baseband signals is not allowed. Direct carrier modulation by digital type baseband signals is allowed, subject to the restrictions given under 3.4.

3.0 SPECIFIC NONSTANDARD MODULATION RESTRICTIONS

3.1 Discrete Frequency Component Sideband Levels

Carrier phase modulation by periodic signals (sinusoids, square-waves, etc) is not permitted. No incidental and/or spurious discrete frequency component sideband levels shall be greater than -32 dBc on a frequency range of ±200 kHz about the carrier frequency.

3.2 Frequency Modulated Subcarriers

3.2.1 Analog Modulations

No analog signal frequency modulated subcarrier, on a frequency range of ±200 kHz about the carrier frequency, shall be allowed to phase modulate the carrier if the inequality

$$f_m \Delta f > 8 \times 10^3 \qquad \text{(C-1)}$$

is violated, where f_m is the bandwidth or maximum frequency of the baseband analog signal in Hz and Δf is the peak frequency deviation of the subcarrier in Hz. Provided that the inequality (C-1) is satisfied, the maximum allowable carrier phase modulation index, β, by the frequency modulated sinusoidal subcarrier shall be the lesser of 1.85 rad (106°), or the β which satisfies the relationship:

$$J_1(\beta)/J_0(\beta) = 5.43 \times 10^{-7} f_m \Delta f, \qquad \text{(C-2)}$$

or the β which results in a lock detector false alarm probability greater than 1×10^{-4} when the lock detector bandwidth is centered on the FM subcarrier (i.e., on either relative subcarrier frequency sideband of the carrier). The value of β in (C-2) may be determined with the aid of Figure C-1.

3.2.2 Digital Modulations

No frequency-shift-keyed (FSK) subcarrier, on a frequency range of ±200 kHz about the carrier frequency, shall be allowed to phase modulate the carrier if the inequality

$$R_b > 2.5 \times 10^2 , \qquad \text{(C-3)}$$

is violated, where R_b is the data bit rate (bps). Provided that the inequality (C-3) is satisfied, the maximum allowable carrier phase modulation index, β, by the FSK modulated sinusoidal subcarrier shall be the lesser of 1.85 rad (106°), or the β which satisfies the relationship

$$J_1(\beta)/J_0(\beta) \leq 6.9 \times 10^{-8} (R_b)^2 \qquad \text{(C-4)}$$

or the β which results in a lock detector false alarm probability greater than 1×10^{-4} when the lock detector bandwidth is centered on the FM subcarrier. The value of β in (C-4) may be determined with the aid of Figure C-1.

3.3 Phase Modulated Subcarriers

3.3.1 Analog Modulations

Phase modulation of subcarriers by analog baseband signals is not recommended due to inefficiency. As a result, no such modulations are expected, and no guidelines have been developed.

3.3.2 Digital Modulations

No phase-shift-keyed (PSK) subcarrier, on a frequency range of ±200 kHz about the carrier frequency, shall be allowed to phase modulate the carrier if the inequality

$$R_b > 2.5 \times 10^2 \qquad \text{(C-5)}$$

is violated, where R_b is the data bit rate (bps). Provided that the inequality (C-5) is satisfied, the maximum allowable carrier phase modulation index, β, by the PSK modulated sinusoidal subcarrier shall be the lesser of 1.85 rad (106°), or the β which satisfies the relationship

$$J_1(\beta)/J_0(\beta) \leq 6.9 \times 10^{-8}(R_b)^2 \ , \qquad \text{(C-6)}$$

or the β which results in a lock detector false alarm probability greater than 1×10^{-4} when the lock detector bandwidth is centered on the FM subcarrier. The value of β in (C-6) may be determined with the aid of Figure C-1.

3.4 Direct Carrier Modulations

3.4.1 Analog Modulations

Direct phase modulation of the carrier by an analog baseband signal is not recommended due to inefficiency. As no such modulations are expected, no guidelines have been developed.

3.4.2 Digital Modulations

The criterion for the minimum allowable bit rate is based upon a carrier tracking loop RMS phase noise component due to modulation sidebands tracking of 10° or less. The allowable NRZ bit rate must therefore satisfy the following inequality:

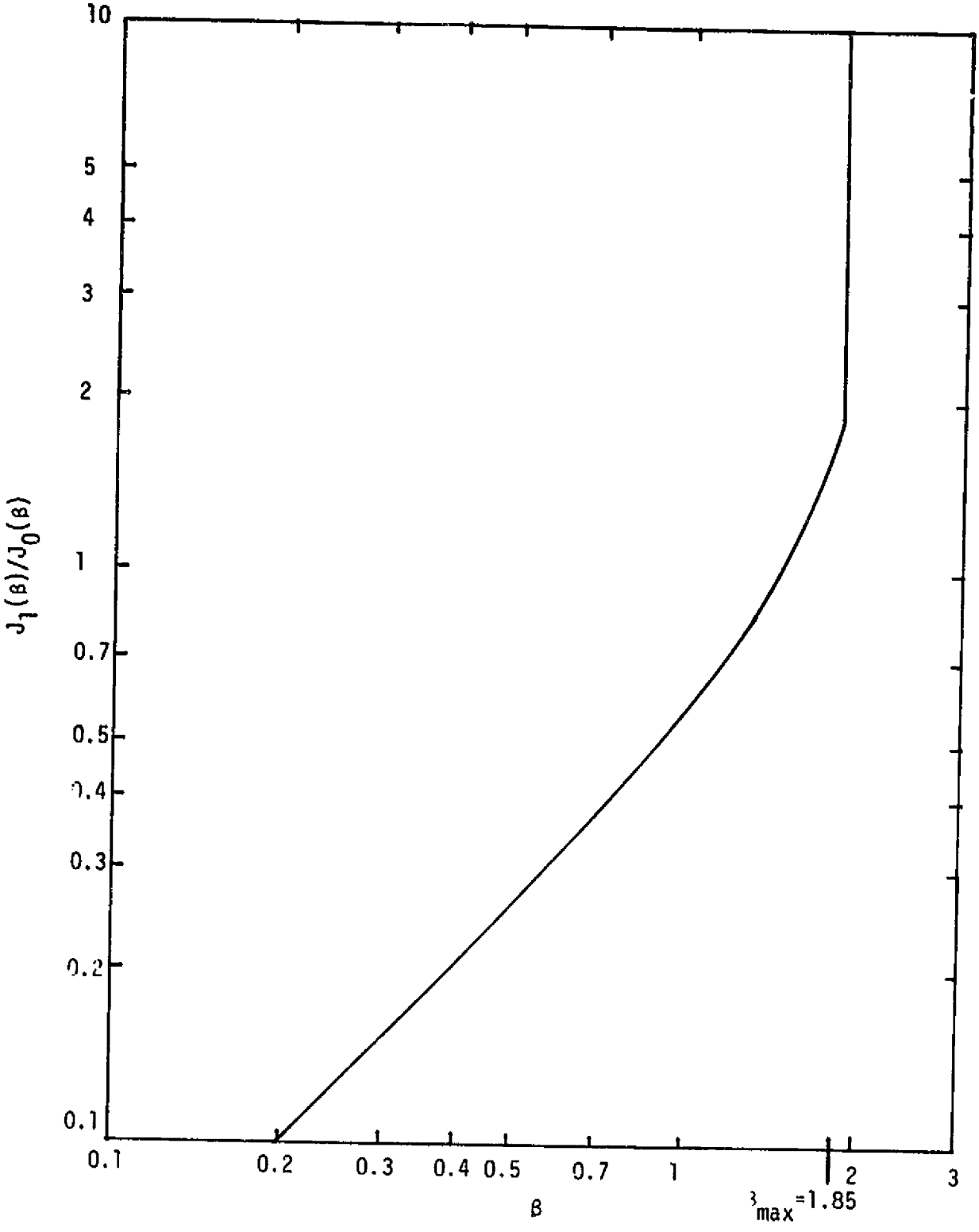

Figure C-1. Curve Used for Determination of Modulation Index

$$R_b > 4.8 \times 10^4 \tan^2(\beta) \ , \qquad \text{(C-7)}$$

where the numerical coefficient is based upon the carrier tracking loop maximum in-lock bandwidth,* and β is the carrier phase deviation ($\beta \leq 71.5°$).

In order to keep carrier loop phase slewing to less than 18° during a string of transitionless data bits, the maximum number of such bits shall be:

$$\text{Maximum No. of Bits Without Transition} = 1.65 \times 10^{-4} R_b \qquad \text{(C-8)}$$

This transitionless period must be followed by a reasonable number of transitions in such a pattern that the slewing error is negated within a period of bits equal to five times the transitionless period.

To avoid the problem of bit slewing, Manchestering of the bits is recommended. Given Manchestered bits, condition (C-7) is no longer applicable, and the minimum bit rate allowed is the larger bit rate calculated from (C-9) and (C-10).

$$R_b \geq 640 \tan^2(\beta). \qquad \text{(C-9)}$$

$$R_b \geq 2.7 \times 10^3 \sqrt{\tan(\beta)} \ . \qquad \text{(C-10)}$$

Maximum modulation index β for all digital modulations shall not exceed 71.5° or 1.25 rad.

*See Paragraph 1.2.